ADAPTIVE SIGNAL PROCESSING FOR DIGITAL COMMUNICATION

OVER DISPERSIVE UNKNOWN CHANNELS

ADAPTIVE SIGNAL PROCESSING FOR DIGITAL COMMUNICATION

OVER DISPERSIVE UNKNOWN CHANNELS

By

JON WEI MARK, B.A.Sc., M.Eng.

A Thesis

Submitted to the Faculty of Graduate Studies

in Partial Fulfilment of the Requirements

for the Degree

Doctor of Philosophy

McMaster University

August 1970

DOCTOR OF PHILOSOPHY (1970)   McMaster University
(Electrical Engineering)   Hamilton, Ontario

TITLE: Adaptive Signal Processing For Digital Communication Over
         Dispersive Unknown Channels

AUTHOR: Jon Wei Mark, B.A.Sc. (University of Toronto, 1962)
                        M.Eng. (McMaster University, 1968)

SUPERVISOR: Professor S.S. Haykim

NUMBER OF PAGES: xiv, 230

SCOPE AND CONTENTS:

An adaptive signal processing technique for improved reception

of pulse amplitude-modulated (PAM) communication signals in the presence

of intersymbol interference and additive noise has been introduced. A

mechanism, consisting of a carrier regeneration scheme and a coherent

phase acquisition decision logic, for the synchronous demodulation of

AM signals has been proposed and its feasibility demonstrated. An

adaptive signal processor, designed to combat the simultaneous effects

of intersymbol interference and additive noise, has been developed using

an adaptive recursive filter and an adaptive recursive equalizer

connected in cascade.

A capability for the adaptive equalizer to track its own frame

of reference has been introduced. Computer simulation has indicated

that the latter feature permits stable operation of the adaptive

recursive equalizer in the absence of any stability constraint, thereby

providing faster convergence than presently known equalizers.

ABSTRACT

The problem of communication would have been trivial if the
channel through which the signal must propagate were ideal, that is,
an all pass system with a linear phase response. In practice, channels
are non-ideal; imperfections in the physical channel, such as time-
dispersion and frequency-dispersion, are the results of signal
dependent distortions. In addition, upon reception the signal is
further corrupted by the inevitable presence of additive random noise.
Time dispersion causes successive pulses to overlap, thereby creating a
phenonemon which has been termed 'intersymbol interference'. Frequency
dispersion causes the received signal spectrum to vary both in amplitude
and phase. Unless these channel imperfections are taken into account
in the design of the communication system, the rate of data transmission
can be limited by the physical channel. Also, the presence of additive
noise poses further limitations on the ultimate performance of the
system.

This thesis is concerned with adaptive signal processing
techniques for digital communication through dispersive unknown channels.
The research undertaken has been principally aimed at the analytical
derivations of an adaptive recursive filter and an adaptive recursive
equalizer, and the simulations of overall binary communication systems,
taking into account dispersive effects as well as random noise.

Computer simulation tests have indicated that the new adaptive
equalizer exhibits a much more robust operation capability and improved

system performance than the conventional adaptive equalizer. This study

has indicated that adaptive signal processing is a viable technique

upon which a reliable communications system may be designed.

ACKNOWLEDGEMENTS

TABLE OF CONTENTS

LIST OF ILLUSTRATIONS

LIST OF ILLUSTRATIONS (cont'd)

LIST OF ILLUSTRATIONS (cont'd)

LIST OF ILLUSTRATIONS (cont'd)

LIST OF TABLES

NOMENCLATURE

Symbol	Definition
*	superscript, scalar estimate
c	superscript, complex conjugate
t	superscript, matrix transpose
+	superscript, complex conjugate transpose
^	overhead, estimate in orthogonal projection
~	overhead, error in orthogonal projection
∪	overhead, error in scalar estimate
—	overbar, ensemble average
-	underbar, a vector quantity
$E\{\cdot\}$	statistical expectation
$\{a_i\}$	information sequence
N	length of sequence
$a(t)$	modulating signal
T_0	baud length (digit duration)
T_s	pulse separation
T	duration of one sequence
$s(t,\{a_i\})$	transmitted signal
C	channel matrix
$c(\tau,\xi)$	channel impulse response
L	(half) time spread
B	(half) frequency spread
ω_0	carrier frequency

NOMENCLATURE (cont'd)

<u>Symbol</u>   <u>Definition</u>

δ delay rate

ω_d doppler frequency

$\underline{m}$ channel output vector

$\underline{n}$ additive noise vector

d   subscript, determinstic component

r   subscript, random component

$\underline{m}_d$ deterministic channel output

$\underline{m}_r$ random channel output

a_n^* estimate of a_n

$\bar{n}$ subscript, iteration time

G   gain matrix of recursive filter

$\underline{W}$ weight vector in the non-recursive equalizer

$\{W_{n,i}(a)\}$ the set of weights in estimation loop

$\{W_{n,i}(x)\}$ the set of weights in learning loop

$\{b_{n,i}\}$ the set of weights in recursive equalizer

$K(i,j)$ second-order moment matrix

$P(n|i)$ covariance matrix of error in orthogonal projection

α gradient constant for reference tap

β gradient constant for learning loop

γ gradient constant for recursive loop

P_e or $P(e|d_n)$ probability of error per binary symbol

SNR_{in} input signal-to-noise ratio

NOMENCLATURE (cont'd)

<u>Symbol</u>   <u>Definition</u>

SNR_o output signal-to-noise ratio

SIR_{cd} signal-to-interference ratio at output of
                             correlation decoder

CHAPTER 1

INTRODUCTION

1.1 Outline of the Problem

Communication theory deals with the study of systems for trans-
mitting information or data from one point to another. Examples of
point-to-point communications which we may mention are the telephone
line, the ionospheric links and the tropospheric scatters, etc., while
examples of two-way communications are active radar and sonar systems.
Except for some fundamental differences in the transmission media, such
as the frequency and phase characteristics, the theory and techniques
behind the design of a reliable communications system for all above
mentioned situations are essentially the same. A general block diagram
for visualizing the behaviour of a communications system is given in
Figure 1.1. Neither the physical channel nor the background noise is
at the system designer's disposal. The 'Black Box' denoted 'Signal
Processor', however, is to be optimized in order to combat background
noise as well as distortions arising from imperfections in the physical
channel, such that the input to the channel decoder is a 'good' estimate
of the output of the channel encoder.

Communication systems usually employ some type of signal
modulation, e.g., A.M., F.M., P.M., etc. That is, a low frequency wave-
form, which contains the information, is modulated onto a high frequency
carrier, which serves to carry the signal energy to distant points. In
digital communication systems pulse modulation is normally employed,
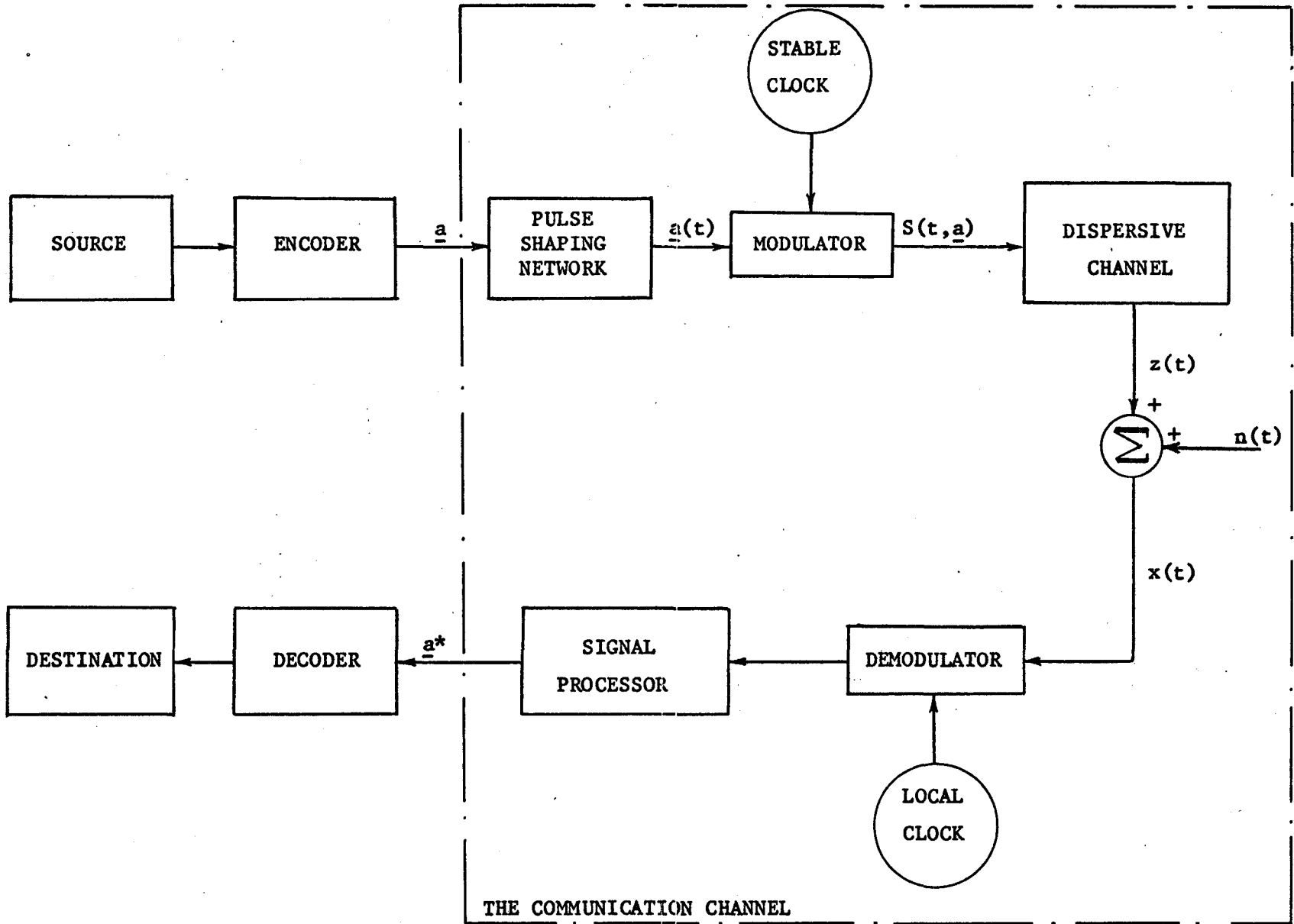
Figure 1.1   A Digital Communications Link

that is, the transmitted waveforms may be amplitude, frequency, phase, duration or position modulated by the information. The resulting systems are known as Pulse Amplitude Modulation (PAM), Pulse Frequency Modulation (PFM), Pulse Phase Modulation (PPM), Pulse Duration Modulation (PDM), or Pulse Position Modulation (PPM).

Physical channels are essentially bandlimited or time-limited, both of which distort the transmitted signals. A channel which is essentially band-limited possesses a finite response time, so that when a signal is transmitted through such a channel, it increases the duration of the signal. This characteristic is commonly referred to as 'multipath spread' or 'time dispersion'. The time-limiting effect is fundamentally a time variation in the frequency spectrum of the signal, that is, an aging effect in both amplitude and phase characteristics. This phenomenon is commonly referred to as 'Doppler spread' or 'frequency dispersion'. The combined effect of these two forms of distortion may be considered as slow fading. A third ill-effect is characterized by the so-called 'random channel scattering', in which the signal is almost totally mutilated[†]. The output of a 'random scattered channel', as the term implies, is random and has a form of wide-band noise which is signal dependent. In a practical situation the received signals are further corrupted by a signal independent random additive noise, so that the problem of accurate reception is further compounded.

[†] In this thesis 'random channel scattering' is defined to constitute rapid fading or highly dispersive effects both in time and in frequency.

A consequence of time dispersion is that successive pulses which have become lengthened by the channel tend to overlap if the transmission rate is high enough, causing what is termed 'intersymbol interference'. At high data rates such that the guard spaces between adjacent pulses are short compared to the response time of the channel, intersymbol interference becomes a limiting factor on the performance of the system. An obvious approach to combat the effect of intersymbol interference is to transmit data at such a rate that the guard spaces between adjacent pulses are comparable to or longer than the finite response time of the channel. However, such an approach will severely limit the efficiency of the transmitter.

A consequence of frequency dispersion is that, in order to achieve 'good' performance, the receiver is required to be a time-varying system. That is, the impulse response of the receiver needs to be adjusted periodically, hence the term 'adaptive' is used.

In general the limiting factors on the performance of a communications system are intersymbol interference, time-variational effects, random channel scattering effects, and background noise. The first three types of distortions are signal dependent, while the last one is signal independent. Because of the inherent signal dependent characteristics in the distortions, the performance of a communications system cannot be improved by an increase in transmitter power. The limiting effects of signal dependent distortions may be appreciated by examining Figure 1.2 which shows a plot of probability of error vs signal-to-(additive) noise ratio[†]in a digital communication system. Figure 1.2

[†] See pages 27 and 125 for definition
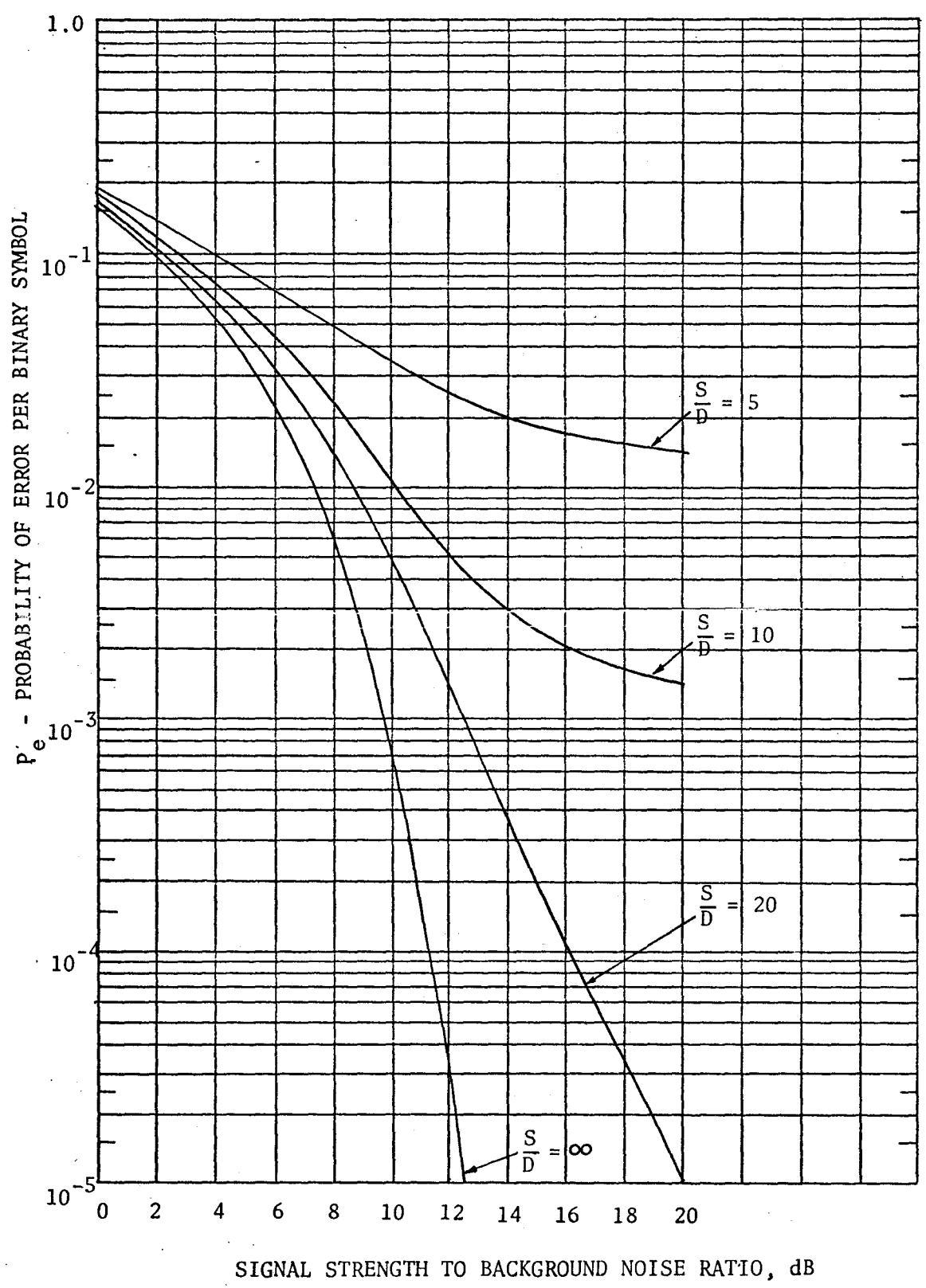
Figure 1.2 Error Probabilities for Matched Filter Receiver
Showing the Limiting Effects of Signal Distortions

was plotted using data from TABLE II-1. This diagram clearly indicates that the performance of the system cannot be improved merely by increasing the signal strength.

1.2 History of the Problem

The perturbations which arise from the transmission media are inherently statistical in nature, i.e., the perturbing mechanisms, noise and distortions, are usually random. Recognition of the inherently statistical nature of communication sources and channels has led to the evolution of a mathematical theory of communications. One approach is based on information theoretic concepts as introduced by Shannon (1948); the other approach is statistical communication theory as introduced by Wiener (1942). Information theory deals only with mathematical models and not with physical sources or physical channels. The theory places emphasis on probability and algebraic theories; it is primarily con-cerned with the encoder and the decoder. Thus information theory is concerned with coding sequence of symbols produced by a discrete source so that the sequence may be recognized and accurately reproduced at the decoder even though the information has been transmitted through a noisy channel. Shannon has shown that, as long as the rate of data transmission is less than channel capacity, there is no limit to the reliability with which information may be transmitted over a communication channel. On the other hand, statistical communication theory deals with physical sources and physical channels. It is concerned with the problem of how to extract the transmitted signal from the noisy received signal,

in an optimum fashion, in some statistical sense. Thus, both information theory and statistical communication theory are complementary and vital to the design of reliable communication systems.

Ideally, the signal or data arriving at the destination should be identical to that leaving the source. This would only be possible if the physical channel were an all-pass system with a linear phase response, and the background noise is identically zero, conditions which are never realized in practice. If the physical channel were ideal and the background noise were white Gaussian, then from an information theory viewpoint, for transmission rates smaller than channel capacity, the probability of error upon reception can be made arbitrarily small by appropriate signal encoding. On the other hand, from the statistical communication theory viewpoint, for such a channel the matched filter would be the optimum receiver (North, 1943).

Noise or distortion may be grossly defined as that which masks the identity of the signal. If P_e represents the probability that an error occurs, then $(1 - P_e)$ represents the probability of correct reception. In digital communications, with all code symbols equally likely, the optimum system is that which minimizes the probability of error, P_e, or equivalently, maximizes the probability of correct reception, $(1 - P_e)$. The quantity $(1 - P_e)$ is known as the a posteriori probability of a transmitted symbol, a, given $\{x|a\}$ has been received. Thus, a minimum probability of error criterion is equivalent to a maximum a posteriori criterion. On the other hand, when a priori knowledge is lacking the criterion to be used is a maximum likelihood one.

As mentioned above, when additive noise is the only limiting factor in a communications system, matched filtering is optimum. The matched filter is identical with a correlation receiver in that they are mathematically the same. A simple derivation of the matched filter is given in Appendix A. It is shown there that, in the case of white Gaussian noise, with $p(t)$ denoting the transmitted pulse, $c(t)$ the channel impulse response, and $q(t)$ the channel output, we find that the impulse response of the matched filter is given by

$$h_o(t) = q(-t) .\tag{1.1}$$

With E_p denoting the transmitted signal energy, N_o the one-sided noise spectral density, and C^2 the power gain of a non-distorting channel, the signal-to-noise ratio at the output is given by

$$(S/N)_o = \frac{2E_p C^2}{N_o}\tag{1.2}$$

independent of the input pulse shape. A matched filter is thus a linear receiver that maximizes the signal-to-noise ratio; it gives optimum performance provided the random processes are stationary and the channel is non-distorting. In the presence of channel distortion and non-stationary noise (such as the signal dependent random channel scattered noise) the matched filter is no longer the optimum receiver.

In the presence of nonstationary noise and time-varying dispersive effects, for optimum reception it is mandatory that the receiver should possess time-varying properties in order to maintain 'good' performance. The receiver should be capable of simultaneously

rejecting wide-band noise (or extracting the desired signal) and compensating for time-dispersion of the transmitted signal (i.e., combatting intersymbol interference). A process which enables the extraction of a signal from noise is termed 'filtering'; that which is designed to combat intersymbol interference is termed 'equalizerion'.

The design of optimum filters can be attained via either a frequency-domain optimization (Wiener, 1942; Zadeh and Ragazzini, 1950, 1952) or a time-domain optimization approach (Kalman, 1960; Kalman and Bucy, 1961). A Wiener filter derived using a frequency-domain approach if often optimized with respect to a particular set of parameter values and is, therefore, a non-iterative device. In the presence of non-stationary disturbances, such a filter may not be optimum for all situations. On the other hand, the Kalman-Bucy filter is iterative in nature; it seeks to minimize the covariance matrix of the errors inherent in the estimation process. In so doing it lacks dynamic range, i.e., the Kalman-Bucy filter is not capable of tracking a time-varying signal.

When there is no noise present and the channel is linear, then a network whose transfer function is the inverse of that of the physical channel will provide an overall system that has an all-pass transfer function. Under this condition the system is said to be exactly equalized and the network is called an equalizer. Thus, an equalizer has a frequency response which is such that, when connected in cascade with

the physical channel, the overall amplitude response over the frequency range is constant, and the phase response is linear over the frequency band of interest.

Intersymbol interference can be caused by (1) the presence of multiple paths (multipath effects), (2) the differential delays existing at different frequencies, and (3) the finite bandwidth of the physical channel. Equalization and intersymbol interference reduction has been an active area of research for many years. One approach used has been the construction of 'inverse' networks (Di Toro, 1964, 1965, 1968). Another approach has been referred to as 'time-domain equalization' (Gorog, 1965; Lucky, 1965, 1966; Gersho, 1969). While the 'inverse' channel approach relies upon a knowledge of the frequency spectrum, the latter approach relies upon a knowledge of the received signal waveform. A third approach, which is closely related to 'time-domain equalization', has been referred to as 'sampled-data compensation' (Coll, 1966; Coll and George, 1965; George, 1965; George and Coll, 1965).

Mostly, studies on intersymbol interference reduction have been made in the absence of noise or with restrictive assumptions and con-straints. (Aein and Hancock, 1963; Di Toro, 1964, 1965, 1968; Lucky, 1965, 1966.) The problem of receiving time-dispersed pulses in station-ary noise has also received much attention. (Coll, 1966; Coll and George, 1965; George, 1965; George and Coll, 1965; Tufts, 1961, 1962, 1963, 1965.)

1.3 Scope of the Thesis

This thesis is concerned with improved techniques for the reception of amplitude or biphase modulated pulse communications signals in the presence of intersymbol interference, time-variational distortion, random channel scattered wide-band noise, and random additive noise. From an information theory viewpoint the subsystems connected in cascade between the encoder and the decoder (see Figure 1.1), that is, the pulse shaping network, the physical channel and the signal processor, may be treated as the 'communications channel'. The objective of this research is to make the 'communications channel' approximate to an ideal one, that is, an all-pass system with a linear phase response. This ideal condition is to be approached by forcing the signal processor, which is a cascade connection of a filter and an equalizer, to approximate an inverse transfer function to that of the physical channel. This is to be done adaptively, that is, each subsystem treats all others in cascade connection preceding it as the unknown environment and attempts to adapt itself to any environmental changes. The physical channel is assumed to be linear. Also, the signal processor shall be maintained a linear one. The performance of the overall adaptive system is evaluated by digital computer simulations.

CHAPTER 2

DIGITAL COMMUNICATION TECHNIQUES

2.1 Introduction

Generally speaking the design of a reliable communication system
can be divided into the following categories: the transmitter design,
the channel characterization, and the receiver design. A communications
system is functionally depicted in Figure 1.1. While the design parameters
for a transmitter and those for a receiver are often at the designer's
disposal, the characteristics of the physical channel are controlled by
nature. The design problem of reliable communication systems as defined
in section 1.1 is, therefore, a game of war between man and nature. In
order to achieve any degree of success it is necessary to have a clear
understanding of the characteristics of the channel. Failing this the
system designer often resorts to mathematical modelling of the channel
behaviour and the communications problem becomes a guessing game. That
is, the channel characteristics are random variables which can be approx-
imated only in some statistical sense.

Channel modelling has been an area of active studies for many
years; yet there have been no results available which are general enough
such that the system designer can use the information directly. Thus,
channel characterization for a particular application necessarily takes
into consideration physical insights. The channel characterization
appropriate for this research is considered in the next Chapter. The
remaining Chapters of this thesis are concerned with making the

'communication channel' to approximate an ideal system, as defined in section 1.2. At this juncture we assume that intersymbol interference, i.e., dispersive effects, is absent and centre our discussions on the factors influencing the design of a reliable communication system under such conditions. In this respect we shall not concentrate any effort on designing signals capable of combatting dispersive effects. Suffice it to say that a non-dispersive channel and white gaussian background noise with a one-sided spectral density of N_o watts/Hz are assumed. The communications system of Figure 1.1 then reduces to that given in Figure 2.1, where the channel is now characterized by a fading parameter, $\gamma(t,\tau)$, and a doppler parameter, ω_d, contained in $e^{-j\omega_d\tau}$. The communications problem now reduces to the one analyzed by Mark (1968). There, the main concern in the design of a reliable communications system was to develop techniques to cope with the fading parameter and the doppler frequency, ω_d. An approximate scheme was developed to track the input carrier. In this Chapter we derive a mechanism for tracking the input carrier to permit synchronous demodulation.

In the case of point-to-point communications, one wishes to recover the transmitted data with little or no distortion. In this situation, a criterion to be used may be one of minimizing the probability of error. The properties inherent in the codes can be utilized to devise suitable decoders to permit minimization of the probability of error. In the case of signal detection, the objective is to recognize whether or not a target is present and to obtain information with respect to its velocity and its relative location. In this case
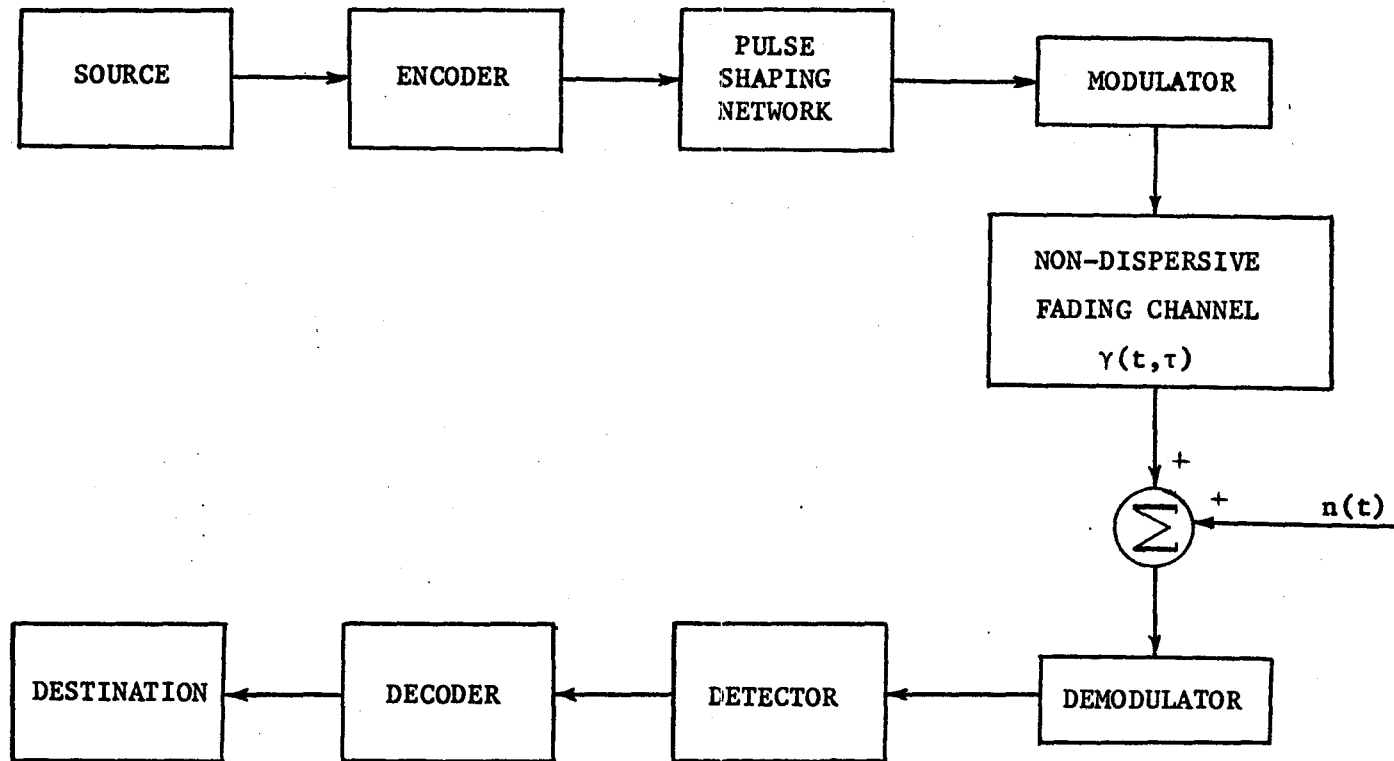
Figure 2.1   Communication Over A Non-dispersive Channel

the probability of error is still a suitable criterion for system design;
however, the properties of the codes may be utilized such that the signal-
to-noise ratio may be defined over the entire signal duration. This is
the so-called pulse compression technique commonly employed in the design
of active radar and sonar systems. For the present we are mainly con-
cerned with waveform generation and waveform processing.

2.2 Waveform Representation

Signal representation is well described in the literature (see,
for example, Balakrishnan, 1968). As stated in section 1.1 the trans-
mission of a signal to distant points requires modulation of the low-
pass information waveform onto a high frequency carrier. Reception of
a signal, in turn, requires demodulation to recover the low-pass
information waveform. Thus, the basic components of a transmitter are a
pulse shaping network and a modulator; those of a receiver are a de-
modulator and a detector, as depicted in Figure 2.1. The pulse shaping
network is basically a mechanism which transforms the discrete symbols
at the encoder output into L_2 functions, that is, finite energy
functions such as $a(t)$ for which $\int |a(t)|^2 \, dt < \infty$. (Vulikh, 1963)

In this thesis we consider only PAM systems. The discussion is
also applicable to a biphase modulated system which is mathematically
equivalent to a double sideband suppressed carrier amplitude modulated
system. Without loss of generality, let $\{a_i\}$ be a set of m-ary symbols
at the output of the encoder, as depicted in Figure 2.2. The binary
information sequence enters the encoder at a rate of R bits/sec while

BINARY
INFORMATION
SEQUENCE
$\{\xi_i\}$
   →   ENCODER   →   m-ary
MESSAGE
SEQUENCE
$\{a_i\}$
   →   PULSE
SHAPING
NETWORK
f(t)
   →   m-ary
L_2 FUNCTIONS
$\{a_i(t)\}$
   →   MODULATOR   →   TRANSMITTED
SIGNAL
$s(t,\{a_i\})$
   →
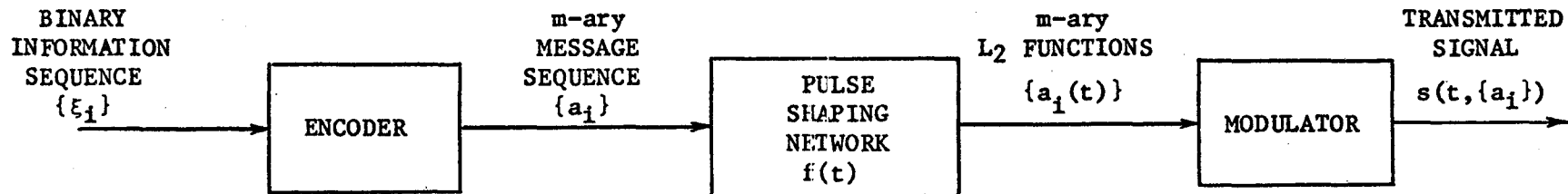
SEQUENCES:

INFORMATION AT ENCODER INPUT $\xi_1, \xi_2, \ldots \xi_i = (0,1)$ R BITS PER SEC.

ENCODER OUTPUT $a_1, a_2, \ldots a_i = (1, 2,\ldots, m)$ r SYMBOLS PER SEC.

PULSE SHAPING NETWORK OUTPUT $a_1(t), a_2(t - \frac{1}{r}), a_3(t - \frac{2}{r}), \ldots$

MODULATOR OUTPUT $s_1(t, a_1), s_2(t - \frac{1}{r}, a_2), s_3(t - \frac{2}{r}, a_3), \ldots$

Figure 2.2   Waveform Generation

the m-ary sequence leaves the encoder at a rate of r symbols/sec. The
rate of inflow equals that of out-going information when

$$m^r = 2^R$$

or

$$r = R/\log_2 m .\qquad(2.1)$$

The encoder will introduce redundancy when $r > R/\log_2 m$. We note that
each a_i is a function of L information bits, where L is often called the
constraint length, in information bits, of the encoder. For binary
signaling, when no redundancy has been introduced, m = 2 and r = R.
r and L are primarily the design parameters for the encoder.

Assuming the set $\{a_i\}$ to be statistically independent, that is,
$E\{a_i a_j\} = \delta_{ij}$, where δ_{ij} is the Kronecker delta, we may represent the
output of the pulse shaping network corresponding to the ith symbol by

$$a_i(t) = a_i \, f(t - iT_s)\qquad(2.2)$$

where f(t) is the impulse response of the pulse shaping network, and
T_s is the pulse separation, so that the rate is $r = 1/T_s$. The impulse
response of the pulse shaping network is assumed to have an effective
memory of T_0 seconds. The signal representation of equation (2.2) has
the following interpretation: The pulse corresponding to the ith symbol
has its centre of gravity located at the time iT_s and has a finite value
lasting for a nominal duration of T_0 seconds. The overall output of the
pulse shaping network can then be represented by

$$a(t) = \sum_{i=1}^{N} a_i \, f(t - iT_s)\qquad(2.3)$$

where N is the code length given by $N \geqslant L/\log_2 m$. Obviously, L should be chosen to be much greater than $\log_2 m$.

Whether the transmitted signal $a(t)$ retains the statistical independence of the set $\{a_i\}$ depends on the function $f(t)$. This condition is maintained if

(i) $f(t) \equiv 0$ for t lying outside the interval $[0, T_o]$

and

(ii) $T_o \leqslant T_s$.

Typical examples for the function $f(t)$ and its autocorrelation function $\phi_f(t)$ are the following (Papoulis, 1962):

(1)   The rectangular pulse:

$$f(t) = \begin{cases} 1 , & -T_o/2 \leqslant t \leqslant T_o/2 \\ \\ 0 , & |t| > T_o/2 \end{cases} \qquad (2.4)$$

$$\phi_f(t) = \begin{cases} \dfrac{1}{T_o} (1 - |t|/T_o) , & |t| \leqslant T_o \\ \\ 0 , & |t| > T_o \end{cases} \qquad (2.5)$$

(2)   The raised cosine pulse:

$$f(t) = \begin{cases} \dfrac{1}{2} (1 + \cos \dfrac{\pi t}{T_o}), & -T_o \leqslant t \leqslant T_o \\ \\ 0 , & |t| > T_o \end{cases} \qquad (2.6)$$

$$\phi_f(t) = \begin{cases} \dfrac{3}{4} T_o [\{ \dfrac{2T_o - t}{3T_o} \}\{1 + \dfrac{1}{2} \cos \dfrac{\pi t}{T_o} \} + \dfrac{1}{2\pi} \sin \dfrac{\pi t}{T_o}], & |t| \leqslant 2T_o \\ \\ 0 , & |t| > 2T_o \end{cases} \qquad (2.7)$$

(3) The Gaussian Pulse:

$$f(t) = e^{-Bt^2} \tag{2.8}$$

$$\phi_f(t) = \sqrt{\frac{\pi}{2B}}\, e^{-\frac{1}{2}Bt^2} \tag{2.9}$$

(4) The RC filtered rectangular pulse:

$$f(t) = \begin{cases} 1 - e^{-Bt}, & 0 \leqslant t \leqslant T_o \\ (e^{BT_o} - 1)e^{-BT}, & T_o \leqslant t \end{cases} \tag{2.10}$$

$$\phi_f(t) = \begin{cases} T_o[1 - \dfrac{t}{T_o} + \dfrac{e^{-BT_o}}{2BT_o}(e^{Bt} - e^{-Bt}) - \dfrac{e^{-Bt}}{BT_o}], & t \leqslant T_o \\ \dfrac{1}{2B}e^{-Bt}(e^{BT_o} + e^{-BT_o} - 2), & t > T_o \end{cases} \tag{2.11}$$

and   (5) The exponential pulse:

$$f(t) = \begin{cases} e^{-Bt}, & t \geqslant 0 \\ 0, & t < 0 \end{cases} \tag{2.12}$$

$$\phi_f(t) = \frac{1}{2B}e^{-B|t|}, \tag{2.13}$$

where B is the effective bandwidth of the pulse shaping network and T_o is the time constant of the RC filter.

The autocorrelation functions given by equations (2.5), (2.7), (2.9), (2.11) and (2.13) are in essence the coherent components of the outputs of matched filter receivers, as given in Appendix A. The waveforms and their autocorrelation functions for the above examples are sketched in Figure 2.3. It is noted that the exponential pulse, and,
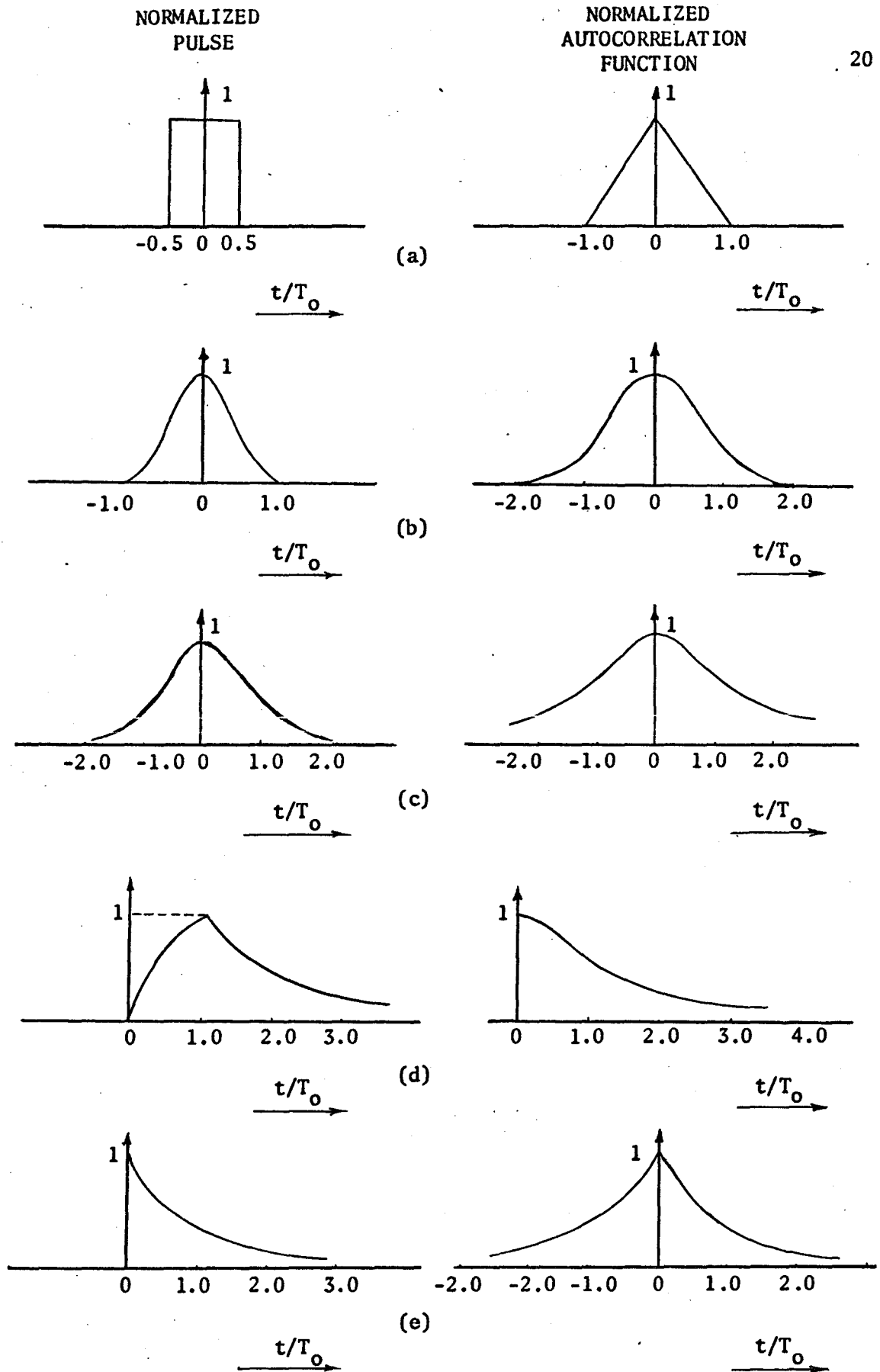
Figure 2.3   Pulses and their Autocorrelation Functions
              (a) Rectangular Pulse, (b) Raised Cosine Pulse,
              (c) Gaussian Pulse, (d) RC filtered rectangular
              pulse, (e) Exponential Pulse

to some degree, the RC filtered rectangular pulse, is all 'tails'. There-fore, if the impulse response of the pulse shaping network is prescribed by either (4) or (5) above, the resulting waveform, $a(t)$, will contain intersymbol interference at transmission time. An appropriate choice for the function $f(t)$ is then either a rectangular response, a raised cosine response, or a Gaussian response. If the encoder output sequence is binary, that is, $m = 2$, we may maintain the a_i's to be equally likely. Moreover, for maximum transmitter efficiency, we require that

$$\int |a_i(t)|^2 dt = E_b \tag{2.14}$$

for all i, where E_b is the bit energy. That is, the signals are equi-probable equal energy signals. Maintaining the statistical independence inherent in the set $\{a_i\}$ implies that the functions $a_i(t)$ are orthogonal, i.e.,

$$\int a_i(t) \, a_j(t) \, dt = E_b \, \delta_{ij} . \tag{2.15}$$

For non-orthogonal functions, we have

$$\int a_i(t) \, a_j(t) \, dt = \rho E_b, \; i \neq j , \tag{2.16}$$

again assuming equal-energy signals. Here ρ is the correlation coefficient between the signals $a_i(t)$ and $a_j(t)$.

The basic reception problem is to find the optimum way to distinguish between either of two waveforms $a_i(t)$ and $a_j(t)$, each defined over the bit interval T_o sec in length. The same interval is used for processing at the receiver.

To deal with the reception problem in terms of error probabilities, it is necessary to transform the L_2 functions into discrete symbols. Since the signals are defined over the interval $0 \leqslant t \leqslant T_o$, we can expand each in terms of an orthonormal series:

$$a_i(t) = \sum_{k=1}^{\infty} a_{ki} \, \phi_k(t), \qquad i = 1, 2, \ldots, m \qquad (2.17)$$

with the coefficients given by

$$a_{ki} = \int_{0}^{T_o} a_i(t) \, \phi_k(t) \, dt, \qquad i = 1, 2, \ldots, m \qquad (2.18)$$

and orthonormality implying

$$\int_{0}^{T_o} \phi_k(t) \, \phi_j(t) = \delta_{kj}, \qquad (2.19)$$

where δ_{kj} is the Kronecker delta. Likewise, the noise n(t) can also be expanded in terms of an orthonormal series:

$$n(t) = \sum_{k=1}^{\infty} n_k \, \phi_k(t) \, dt \qquad (2.20)$$

with

$$n_k = \int_{0}^{T_o} n(t) \, \phi_k(t) \, dt \, . \qquad (2.21)$$

For n(t) Gaussian, the coefficients, n_k are also Gaussian. For white Gaussian noise with a one-sided spectral density of N_o watts/Hz, the probability density of each coefficient is given by

$$p(n_k) = \frac{e^{-n_k^2/N_o}}{\sqrt{\pi N_o}} \, . \qquad (2.22)$$

2.3 Probability of Error

Using matched filter reception the decision rule when $a_1(t)$ is transmitted can be shown to be (see, for example, Schwartz, Bennett and Stein, 1966)

$$\int_0^{T_o} r(t) \, a_1(t) \, dt + b_1 > \int_0^{T_o} r(t) \, a_j(t) \, dt + b_j \qquad (2.23)$$

for $j = 2, \ldots, m$. Here $r(t)$ is the received signal and b_j is a constant bias given by

$$b_j = \frac{N_o}{2} \ln P_j - \frac{E_j}{2} \qquad (2.24)$$

with $E_j = \int_0^{T_o} a_j^2(t)dt$, the energy in the jth signal, and

P_j = the a priori probability of the jth signal.

For equal-energy signaling, $E_j = E_b$ for all j; the probability of correct decision is given by

$$P_c = \text{Prob}[a_1 + E_b(1 - \rho) > a_2, a_3, \ldots, a_m]$$

$$= \frac{1}{\sqrt{2\pi}} \int_{-\infty}^{\infty} e^{-y^2/2} [1 - Q(\sqrt{\frac{2E_b(1-\rho)}{N_o}} + y)]^{m-1}dy \quad , \qquad (2.25)$$

where

$$Q(d) \overset{\Delta}{=} \frac{1}{\sqrt{2\pi}} \int_d^{\infty} e^{-y^2/2} \, dy \, . \qquad (2.26)$$

Now, following Nuttall (1962), we note that

$$\int_0^{T_o} [\sum_{i=1}^{m} a_i(t)]^2 \, dt \geq 0 \, .$$

Expanding, we get

$$\int_0^T [\sum_{i=1}^m a_i(t)][\sum_{j=1}^m a_j(t)]\, dt = mE_b + m(\sum_{j=2}^m \int_0^{T_o} a_1 a_j\, dt$$

$$= mE_b + m(m-1)\rho E_b \geq 0. \qquad (2.27)$$

From the above we get

$$1 \geq \rho \geq -\frac{1}{m-1} \qquad (2.28)$$

The probability of error is given by

$$P_e = 1 - P_c\ .$$

For binary signaling with equal-energy signals

$$P_c = \frac{1}{\sqrt{2\pi}} \int_{-\infty}^{\infty} e^{-y^2/2}\, [1 - Q(\sqrt{\frac{2E_b(1-\rho)}{N_o}} + y)]\, dy \qquad (2.29)$$

and

$$P_e = Q(\sqrt{\frac{E_b(1-\rho)}{N_o}}) = Q(\sqrt{\frac{\alpha^2(1-\rho)}{2}}) \qquad (2.30)$$

where $\alpha^2 = 2E_b/N_o$ is the signal-to-noise power ratio. $Q(d)$ and, therefore, P_e is a monotonically decreasing function of the argument d. We note that the function $Q(d)$ is related to the error function erf(d) by

$$Q(d) = \frac{1}{2}[1 - \text{erf}(d/2)],$$

where

$$\text{erf}(d) = \frac{2}{\sqrt{\pi}} \int_0^d e^{-x^2}\, dx\ .$$

In the case of receiving a signal with a random phase, the probability of error is then a function of both the amplitude and the phase. The joint probability density function is given by (see, for example, Helstrom, 1968)

$$q(\alpha,r) = r \exp[-\tfrac{1}{2}(r^2 + \alpha^2)] \, I_0(\alpha r) \qquad (2.31)$$

where

$$I_0(x) \triangleq \frac{1}{2\pi} \int_0^{2\pi} e^{x\cos\theta} \, d\theta \qquad (2.32)$$

is the zero-order modified Bessel function of the first kind. The function represented by equation (2.31) is called the 'non-central Rayleigh' or the 'Rician' density function. It describes the distribution of the distance from a point in a plane to the origin when the Cartesian coordinates of the point are independent Gaussian random variables of unit variance and expected values equal to $\alpha\cos\theta$ and $\alpha\sin\theta$, where θ is an arbitrary angle. The complementary cumulative distribution

$$Q(\alpha,\beta) = P_r(r > \beta) = \int_\beta^\infty q(\alpha,r)dr$$

$$= \int_\beta^\infty r \exp[-\tfrac{1}{2}(r^2+\alpha^2)] I_0(\alpha r)dr \qquad (2.33)$$

is known as Marcum's Q-function (Marcum, 1960) of two arguments. It is readily seen that

$$Q(0,\beta) = \exp(-\beta^2/2),$$

$$Q(\alpha,0) = 1 \ .$$

The probability of detection is effectively given by the Q-function of equation (2.33), where β is the threshold and α is the signal-to-noise voltage ratio. For equiprobable equal energy m-ary signals the probability of error can be shown to be (Reiger, 1958)

$$P_e = 1 - \int_0^\infty r(1 - e^{-r^2/2})^{m-1} e^{-(r^2+\alpha^2)/2} I_0(\alpha r) dr$$

$$= \frac{1}{m} \sum_{k=2}^m (-1)^k \binom{m}{k} e^{-(k-1)\alpha^2/2k} \qquad (2.34a)$$

Replacing α^2 by $\alpha^2(1-\rho)$, where ρ is the correlation coefficient given by the inequality (2.28), we may rewrite (2.34a) as:

$$P_e = \frac{1}{m} \sum_{k=2}^m (-1)^k \binom{m}{k} e^{-(k-1)\alpha^2(1-\rho)/2k} . \qquad (2.34b)$$

For binary signaling, that is, m = 2, the above probability of error expression reduces to

$$P_e = \frac{1}{2} e^{-\frac{\alpha^2(1-\rho)}{4}} \qquad (2.35)$$

with

$$-1 \leqslant \rho \leqslant 1 .$$

Equation (2.35) states that for binary signaling, the maximum value of P_e is $\frac{1}{2}$. This occurs when $\rho = 1$, i.e., when the signals are completely correlated. Thus, this observation is intuitively satisfying.

In Chapter 3 we will derive an expression for the signal-to-interference ratio. At this juncture we may define the signal-to-interference ratio as follows:

$$(S/I) = \frac{\text{signal power}}{\text{distortion} + \text{mean square noise power}}$$

where distortion is signal dependent. Symbolically, S/I may be written as

$$(S/I) = \frac{s^2}{d^2 + \sigma_n^2}$$

where

$$s^2/\sigma_n^2 = 2E_s/N_o = S/N \text{ is the signal-to-additive noise ratio,}$$

and

$$d^2/\sigma_n^2 = D/N \text{ is the distortion-to-additive noise ratio.}$$

Then we may rewrite S/I as

$$(S/I) = \left(\frac{S}{N}\right)\left[\frac{1}{D/N + 1}\right].$$

The factor inside the square brackets is always less then unity. An increase in signal strength will increase (S/N); but, by the same token (D/N) will also be increased. Assuming the distortion has a Gaussian distribution, we may replace α^2 by (S/I) in the probability of error expressions given in this section. The probabilities of error for matched filter reception of binary antipodal signals are calculated and tabulated in TABLE II-1. The results of TABLE II-1 have been plotted in Figure 1.2.

TABLE II-1   Probability of Error vs SNR with S/D as Parameter for a

Matched Filter Receiver

SNR dB	Probability of Error, P_e			
	No Distortion	S/D = 20	S/D = 10	S/D = 5
0	1.587×10^{-1}	1.636×10^{-1}	1.685×10^{-1}	1.814×10^{-1}
3	7.899×10^{-2}	8.815×10^{-2}	9.681×10^{-2}	1.293×10^{-1}
6	2.276×10^{-2}	3.438×10^{-2}	4.457×10^{-2}	6.813×10^{-2}
8	6.039×10^{-3}	1.427×10^{-2}	2.386×10^{-2}	4.846×10^{-2}
10	7.906×10^{-4}	4.940×10^{-3}	1.321×10^{-2}	3.399×10^{-2}
12	3.289×10^{-5}	1.490×10^{-3}	5.087×10^{-3}	2.559×10^{-2}
16		1.218×10^{-4}	2.118×10^{-3}	1.765×10^{-2}
20		1.028×10^{-5}	1.309×10^{-3}	1.463×10^{-2}

2.4 Synchronous Demodulation

The motion of scatters in the propagation paths introduces, among other things, a discrete frequency drift termed the doppler frequency. Consider the reception of an amplitude modulated signal that has propagated through such a channel. In the absence of noise we may represent the received signal by

$$r(t) = 2\,a(t - \tau(t))\,\cos[\omega_0(t - \tau(t)) + \phi] \qquad (2.36)$$

where

$a(t)$ is the low frequency modulating signal,

ω_0 is the transmitted carrier frequency,

ϕ is the phase deviation, and

$\tau(t)$ is the range delay.

The range delay may be written as

$$\tau(t) = \tau_0 + \delta t$$

where

τ_0 = nominal delay, and

δ = the delay rate.

The product of delay rate and carrier frequency gives rise to the doppler frequency, i.e.,

$$\omega_d = \delta\omega_0 \ .$$

Since the nominal delay, τ_0, is merely a time translation, we may re-write equation (2.36) as follows:

$$r(t) = 2a(t - \delta t)\,\cos[(\omega_0 - \delta\omega_0)t + \phi]$$

$$= 2a(t - \delta t)\,\cos[(\omega_0 - \omega_d)t + \phi] \qquad (2.37)$$

The objective is to recover the modulating signal, $a(t)$, which is possible   if   the demodulation is conducted synchronously. The following analysis leads to a synchronous demodulation scheme which is based on the quadrature demodulation technique.

Consider first multiplying the received signal by $2\cos(\omega t+\theta)$ and applying low-pass filtering; thus

$$u_c(t) = a(t - \delta t)[\cos(\phi - \theta)\cos(\omega_r - \omega)t$$
$$- \sin(\phi - \theta)\sin(\omega_r - \omega)t] \qquad (2.38)$$

where

$$\omega_r = \omega_o - \omega_d .$$

Inspection of equation (2.38) shows that

(i)   If $\omega = \omega_r$, i.e., frequency synchronization is attained, equation (2.38) reduces to

$$u_c(t) = a(t - \delta t)\cos(\phi - \theta) \qquad (2.39)$$

(ii)   If $\theta = \phi$, i.e., phase synchronization is attained, then (2.38) reduces to

$$u_c(t) = a(t - \delta t)\cos(\omega_r - \omega)t \qquad (2.40)$$

(iii)   If $\omega = \omega_r$ and $\theta = \phi$, i.e., both frequency and phase synchronizations are attained, then (2.38) becomes

$$u_c(t) = a(t - \delta t) . \qquad (2.41)$$

Equation (2.41) represents an optimum coherent recovery of the modulating signal. To achieve this we propose to acquire frequency and phase synchronizations separately.

Suppose next we multiply the received signal, r(t), by

2sin($\omega t + \theta$) and apply low-pass filtering; we thus get

$$u_s(t) = a(t - \delta t)[\sin(\phi - \theta)\cos(\omega_r - \omega)t$$
$$- \cos(\phi - \theta)\sin(\omega_r - \omega)t] . \qquad (2.42)$$

When we have frequency synchronization, equation (2.42) reduces to

$$u_s(t) = a(t - \delta t)\sin(\phi - \theta) . \qquad (2.43)$$

The signals $u_c(t)$ and $u_s(t)$ represented,respectively, by equations (2.39)
and (2.43) are projections of a vector with amplitude $a(t - \delta t)$ and
phase angle ($\phi - \theta$) onto orthogonal axes. Detection based on either
$u_c(t)$ or $u_s(t)$ is known as non-coherent detection. To attain the
performance of coherent detection both $u_c(t)$ and $u_s(t)$ are needed. In
other words, the detected signal should be independent of the phase
difference. Since $u_c(t)$ and $u_s(t)$ are quadrature signals, we may apply
the following decision rules:

Decision Rule 1: Squaring and summing the signals $u_c(t)$ and $u_s(t)$, we
get
$$u_c^2(t) + u_s^2(t) = [a(t - \delta t)]^2 .$$

This decision rule is nonlinear. However, as we normally desire to
maintain system linearity, decision rule (1) is not appropriate. For
instance, if $a(t)$ were a coded signal, application of the above
decision rule would destroy the properties of the code.

Decision Rule 2: Assuming $a(t)$ to be positive, the quadrature signals
$u_c(t)$ and $u_s(t)$ may be combined as follows:

(a) If $\mathrm{sgn}[u_c(t)] = \mathrm{sgn}[u_s(t)]$ = a positive quantity, the phase difference $(\phi - \theta)$ lies in the first quadrant, then

$$u(t) = u_c(t) + u_s(t) \quad .$$

$$= a(t)[\cos(\phi - \theta) + \sin(\phi - \theta)] \; . \qquad (2.44)$$

(b) If $\mathrm{sgn}[u_c(t)]$ is negative and $\mathrm{sgn}[u_s(t)]$ is positive, then $(\phi - \theta)$ lies in the 2nd quadrant and

$$u(t) = u_s(t) - u_c(t)$$

$$= a(t - \delta t)[\sin(\phi - \theta) + \cos(\phi - \theta)] \; . \qquad (2.45)$$

(c) If $\mathrm{sgn}[u_c(t)] = \mathrm{sgn}[u_s(t)]$ = a negative quantity, the phase difference $(\phi - \theta)$ lies in the third quadrant, then

$$u(t) = -u_c(t) - u_s(t)$$

$$= a(t)[+\cos(\phi - \theta) + \sin(\phi - \theta)] \; . \qquad (2.46)$$

(d) If $\mathrm{sgn}[u_c(t)]$ is positive and $\mathrm{sgn}[u_c(t)]$ is negative, $(\phi - \theta)$ lies in the 4th quadrant, then

$$u(t) = u_c(t) - u_s(t)$$

$$= a(t - \delta t)[\cos(\phi - \theta) + \sin(\phi - \theta)] \; . \qquad (2.47)$$

Consider the case $(\phi - \theta)$ lying in the first quadrant; we have

(i) as $(\phi - \theta) \to 0$, $\cos(\phi - \theta) \to 1$ and $\sin(\phi - \theta) \to 0$,

(ii) as $(\phi - \theta) \to 90^o$, $\cos(\phi - \theta) \to 0$ and $\sin(\phi - \theta) \to 1$, and

(iii) the algebraic sum of $\cos(\phi - \theta) + \sin(\phi - \theta)$ reaches a maximum value of $\sqrt{2}$ at $(\phi - \theta) = 45^{O}$.

Likewise, the bracketed quantities of equations (2.45), (2.46) and (2.47) are always positive lying in the interval $[1, \sqrt{2}]$, as illustrated graphically in Figure 2.4. An implementation of decision rule 2 is shown diagrammatically in Figure 2.5. We note that the output, u(t), of the decision circuit of Figure 2.5 differs from $a(t - \delta t)$ by at most a constant multiplier k, where $1 \leqslant k \leqslant \sqrt{2}$.

Having outlined a detection procedure that is independent of the phase difference, $(\phi - \theta)$, we turn our attention to devising a means of tracking the carrier frequency. Assuming the information inherent in the received signal has been removed by means of a band-pass (hard) limiter, a bandpass squarer, and a frequency divider connected in cascade (Mark, 1968), then we may represent the signal component of the output of the frequency divider by

$$r'(t) = 2A\cos(\omega_r t + \psi) \qquad (2.48)$$

where

A is a constant, and

ψ is phase deviation.

Multiplying r'(t) by $\cos \omega t$ and $\sin \omega t$ separately and applying low-pass filtering to each product, we get, respectively,

$$v_c(t) = A \cos[(\omega_r - \omega)t + \psi] \qquad (2.49)$$

and

$$v_s(t) = A \sin[(\omega_r - \omega)t + \psi] . \qquad (2.50)$$
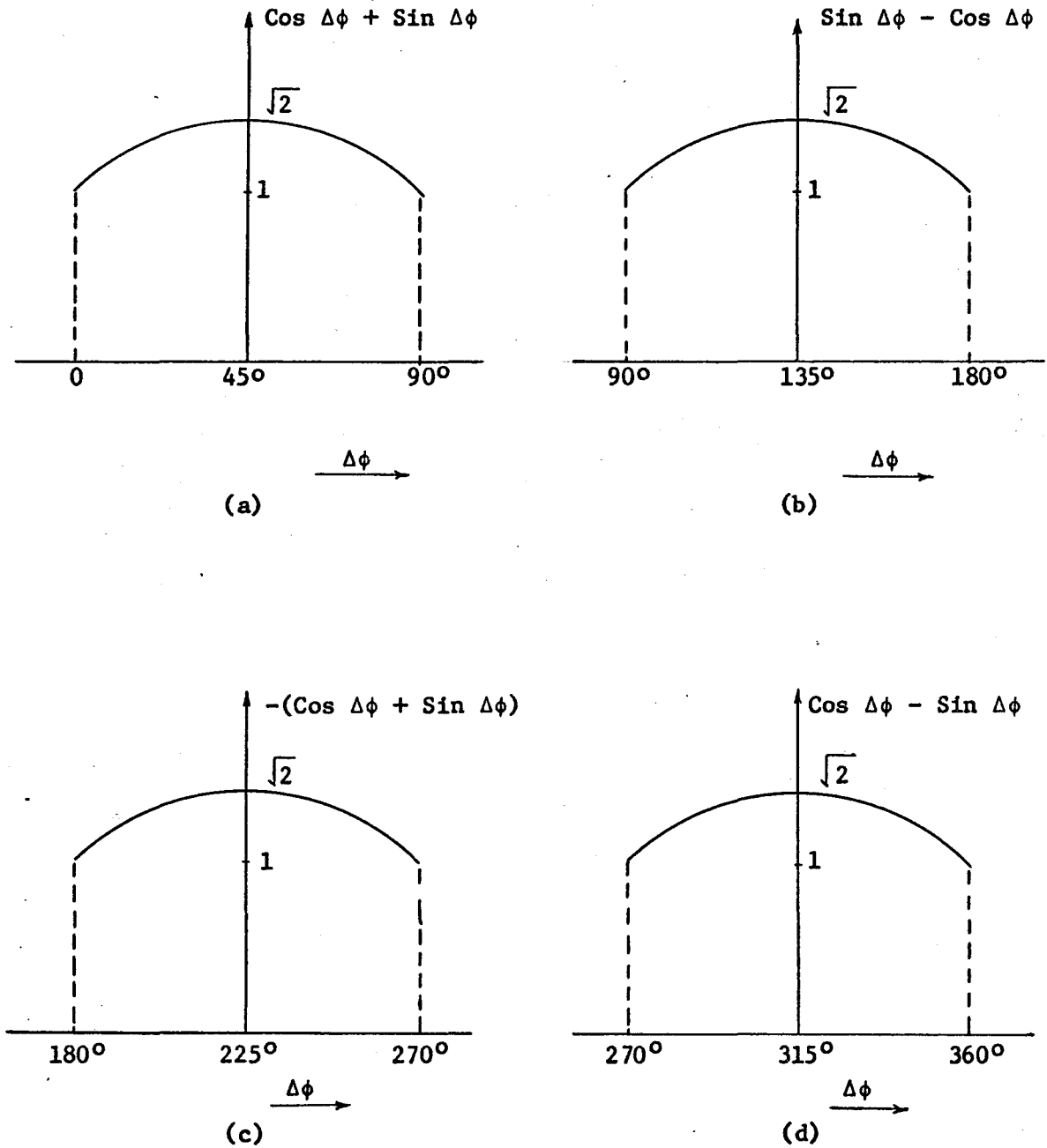
Figure 2.4   Techniques for Combining the Quadrature Signals
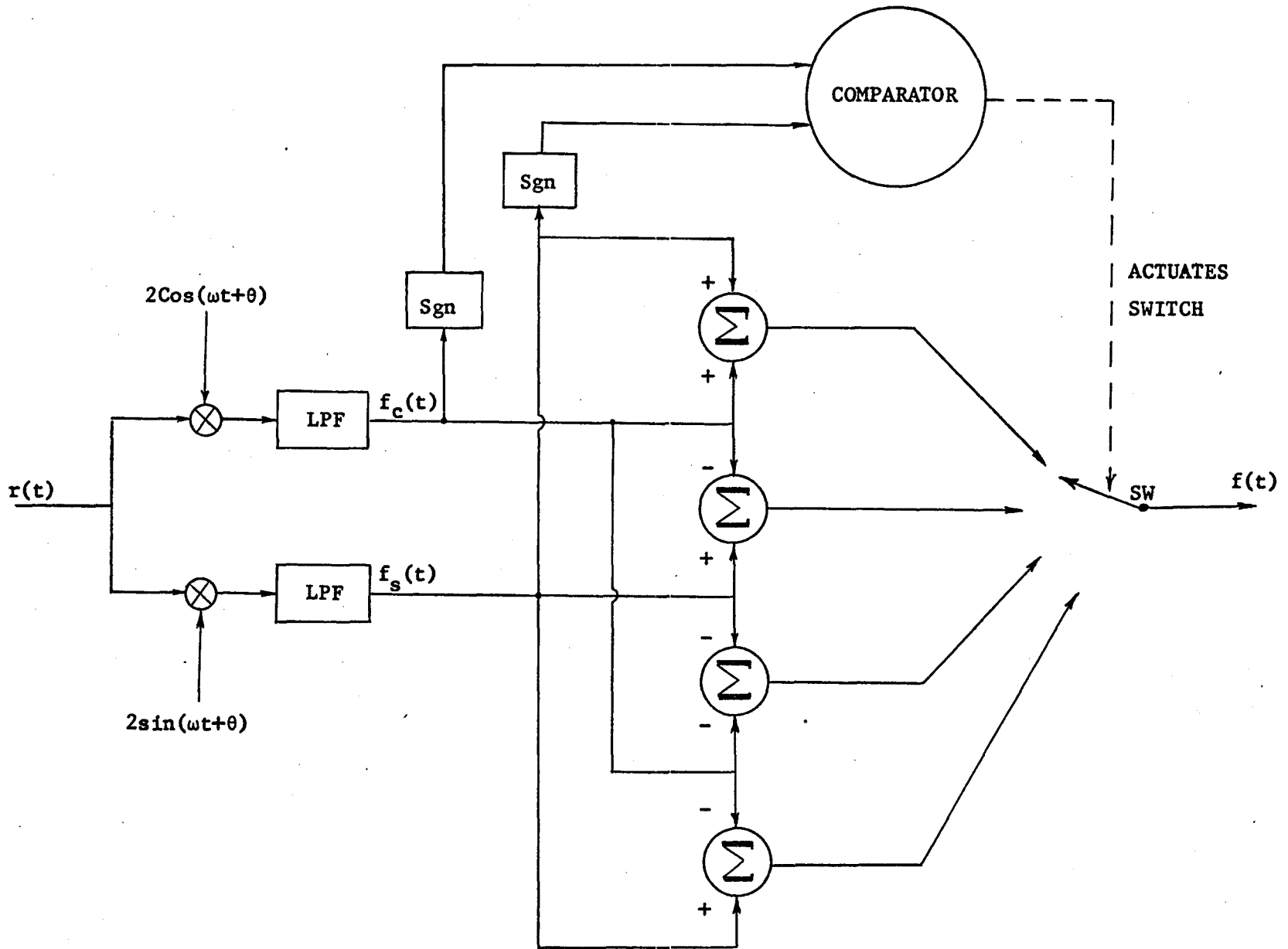
Figure 2.5   A Decision Logic For Combining the Quadrature Signals

35

Multiplying $v_c(t)$ and $v_s(t)$ together and applying low-pass filtering, we get

$$V(t) = \frac{A^2}{2} \sin[2(\omega_r - \omega)t + 2\psi] \ . \tag{2.51}$$

$V(t)$ can be used as a control signal to actuate a VCO in a manner similar to that used by Costas (1956). The output of the VCO is a sinusoidal wave at frequency ω. In addition, the VCO output can be used again to heterodyne with the quadrature signals, $v_c(t)$ and $v_s(t)$, to regenerate the signal component as follows:

$$v_c(t) \cos\omega t - v_s(t) \sin\omega t = A\{\cos[(\omega_r - \omega)t + \psi]\cos\omega t$$

$$-\sin[(\omega_r - \omega)t + \psi]\sin\omega t\}$$

$$= A \cos(\omega_r t + \psi)$$

$$= v(t) \ .$$

The double heterodyning process is functionally given in Figure 2.6. At first sight this exercise of double heterodyning appears to be futile as the output appears to be a reproduction of the input. However, the double heterodyning system behaves as a narrow band-pass filter which rejects noise, so that the regenerated signal is much cleaner than that at the input.

The bandpass limiter and the bandpass squarer mentioned above can be shown to have the following properties:

(i) The bandpass limiter (Davenport, 1953)

$$\alpha_o \approx \frac{\pi}{4} \alpha_i \qquad \text{for } \alpha_i \to 0$$

$$\alpha_o \approx 2\alpha_i \qquad \text{for } \alpha_i \to \infty$$
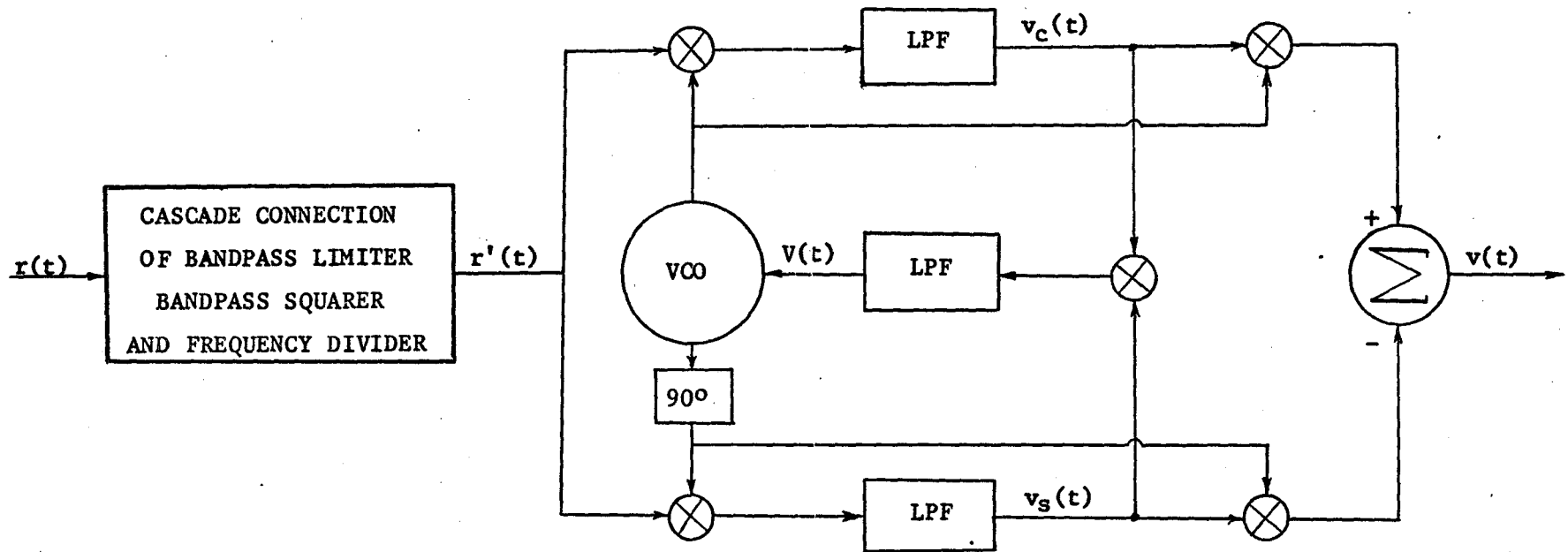
Figure 2.6   Carrier Regeneration Scheme

(ii) The bandpass squarer (Davenport and Root, 1958; Mark, 1968)

$$\alpha_o \propto \alpha_i^2 \qquad \text{for } \alpha_i \to 0$$

$$\alpha_o \propto \alpha_i \qquad \text{for } \alpha_i \to \infty$$

where α_i and α_o are, respectively, the input and output signal-to-noise ratio.

The overall synchronous demodulation system is obtained by combining the carrier regeneration scheme (Figure 2.6) with the coherent phase decision logic (Figure 2.5) as depicted in Figure 2.7.

2.5 Computer Simulation Results

Monte Carlo simulation of the adaptive communications system is given in Appendix H. Here we present a demonstration of the synchronous demodulation scheme described in the preceding section. The waveforms shown in Figures 2.8 through 2.11 are for the case of binary antipodal signaling through a dispersive channel with impulse response shown in Figure 2.9a. Figure 2.8 shows the biphase modulation process; Figure 2.9 shows the case of +14 dB signal-to-additive noise ratio; Figure 2.10 shows the case of +6 dB signal-to-additive noise ratio; while Figure 2.11 shows the case of -3.5 dB signal-to-additive noise ratio. At this juncture we have anticipated the use of the recursive adaptive filter to be derived in Chapter 4. The results of Figures 2.9 through 2.11 clearly demonstrate the feasibility of the synchronous demodulation scheme described in the preceding section.
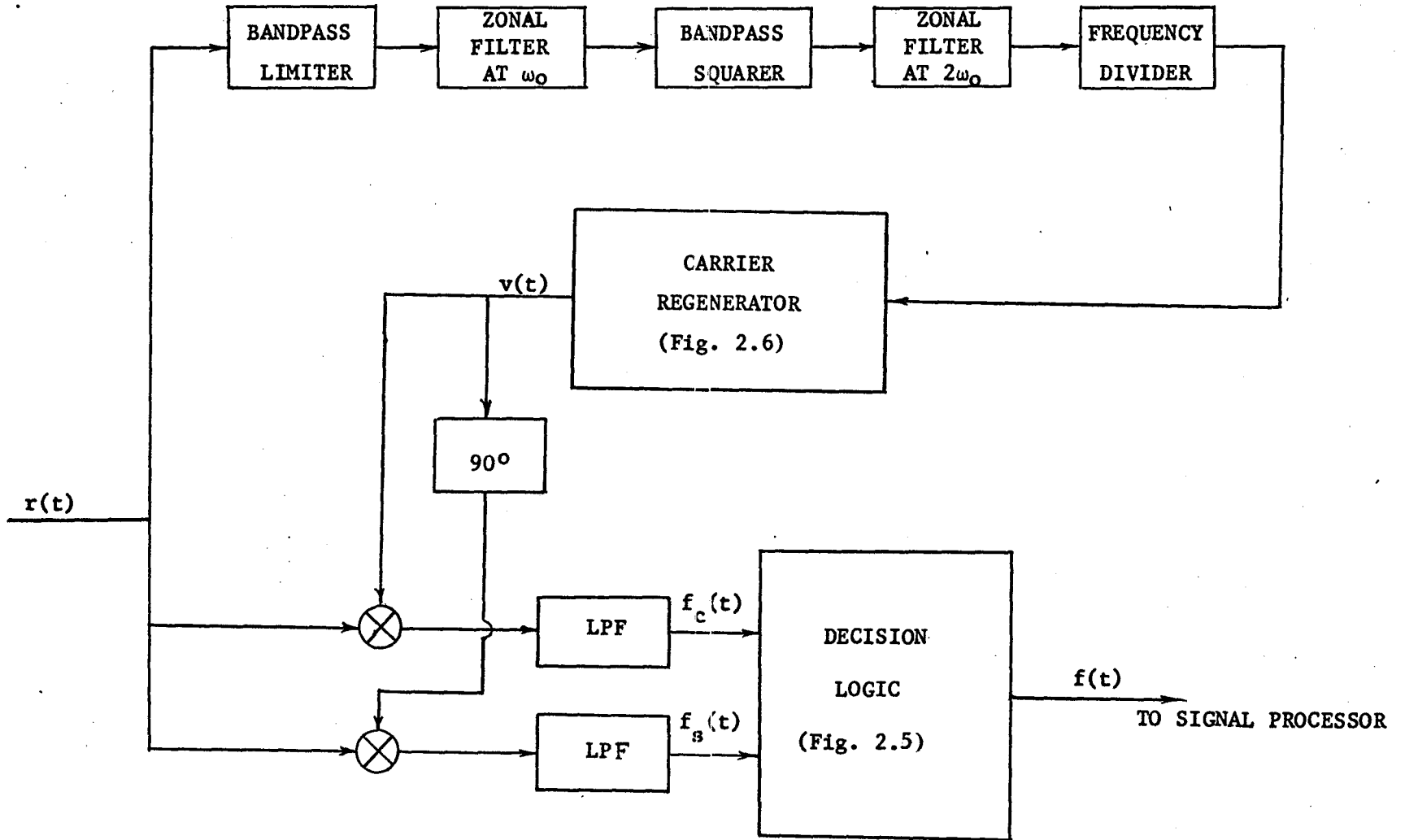
Figure 2.7   Synchronous Demodulation Scheme For AM Systems

2.6 Summary

In this chapter we have presented some relevant techniques for digital communications over non-dispersive, non-fading channels. We considered the problem of signal representation and system performance analysis in terms of probability of error at the receiver. In addition, we have proposed and demonstrated the feasibility of a synchronous demodulation scheme to facilitate coherent reception.
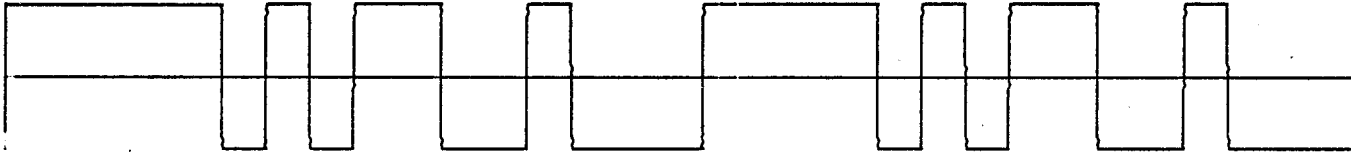
(a) 31-DIGIT BINARY M-SEQUENCE MODULATING WAVEFORM
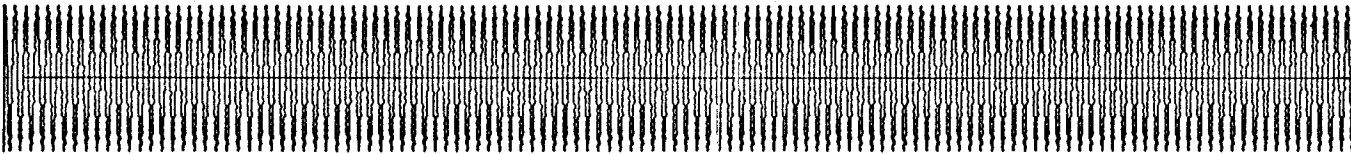
(b) HIGH FREQUENCY CARRIER
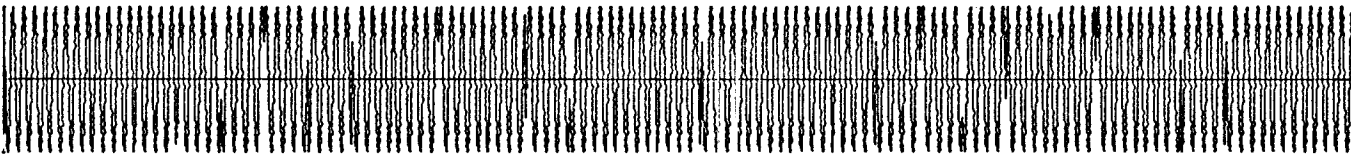
(c) PHASE REVERSAL MODULATED SIGNAL

Figure 2.8 Binary Antipodal Signaling Waveforms
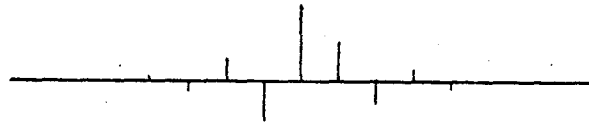
(a)   CHANNEL IMPULSE RESPONSE
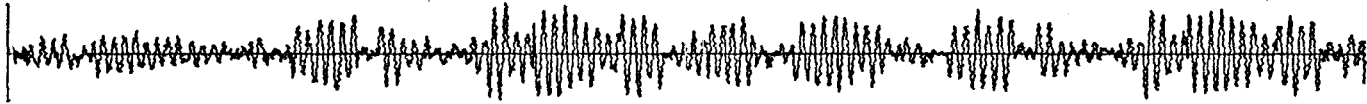
(b)   RECEIVED SIGNAL AT +14 dB SIGNAL-TO-ADDITIVE NOISE RATIO
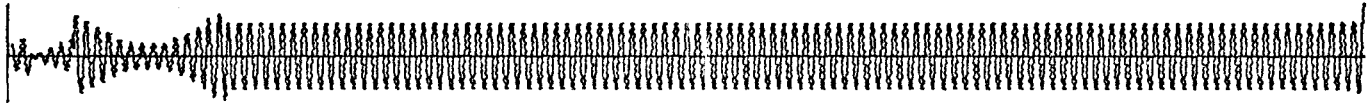
(c)   REGENERATED CARRIER
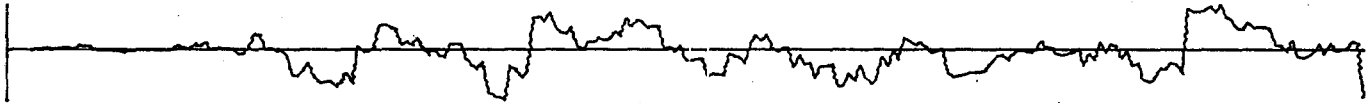
(d)   DECISION LOGIC OUTPUT
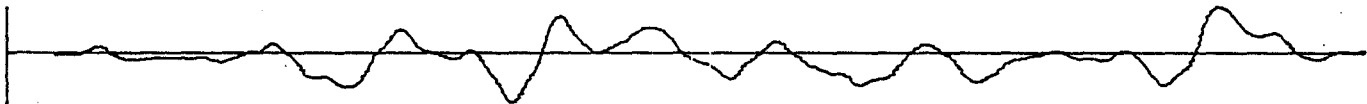
(e)   RECURSIVE FILTER OUTPUT

Figure 2.9   Synchronous Demodulation Waveforms (+14 dB SNR)

42
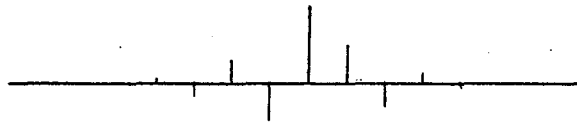
(a) CHANNEL IMPULSE RESPONSE

(b) RECEIVED SIGNAL AT +6 dB SIGNAL-TO-ADDITIVE NOISE RATIO

(c) REGENERATED CARRIER

(d) DECISION LOGIC OUTPUT
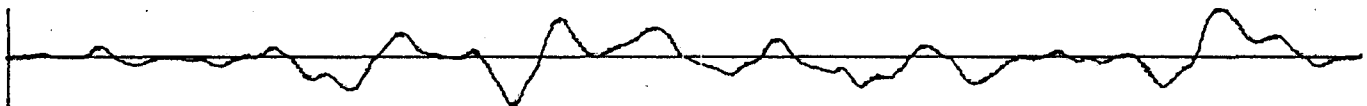
(e) RECURSIVE FILTER OUTPUT

Figure 2.10 Synchronous Demodulation Waveforms (+6 dB SNR)

43

(a)   RECEIVED SIGNAL AT -3.5 dB SIGNAL-TO-ADDITIVE NOISE RATIO

(b)   REGENERATED CARRIER
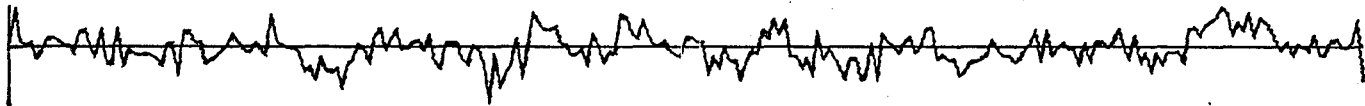
(c)   DECISION LOGIC OUTPUT
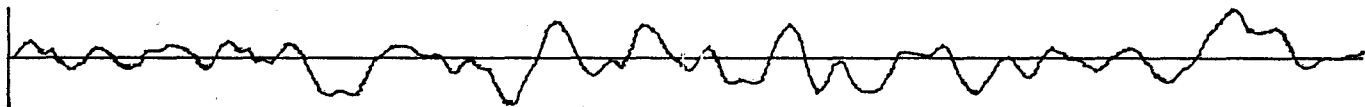
(d)   RECURSIVE FILTER OUTPUT

Figure 2.11   Synchronous Demodulation Waveforms (-3.5 dB SNR)

CHAPTER 3

COMMUNICATION OVER DISPERSIVE CHANNELS

3.1 Channel Characterization

As stated in section 2.1 knowledge of the channel characteristics
is vital to the design of a reliable communication system. In general,
the communication channel is uncontrollable. There has been a tremendous
interest in channel modelling; the most fervent researchers in this field
have been Bello, Kailath, Pierce, Price and Turin (see bibliography).
The work of these investigators in the field has recently been collated
and published by Kennedy (1969).

A statistical model of the channel is given in Appendix B,
where the macroscopic effect of the channel is described in terms of a
'channel scattering function', $\sigma(\tau,f)$. Time and frequency variations
may be studied by considering the delay scattering function, $\sigma(\tau)$, and
the doppler scattering function, $\sigma(f)$, separately, where[†]

$$\sigma(\tau) = \int \sigma(\tau,f)df,$$

and

$$\sigma(f) = \int \sigma(\tau,f)d\tau.$$

The scattering functions $\sigma(\tau,f)$, $\sigma(\tau)$ and $\sigma(f)$ are depicted in Figure 3.1.

[†]Unless otherwise indicated all integrations are from $-\infty$ to $+\infty$.
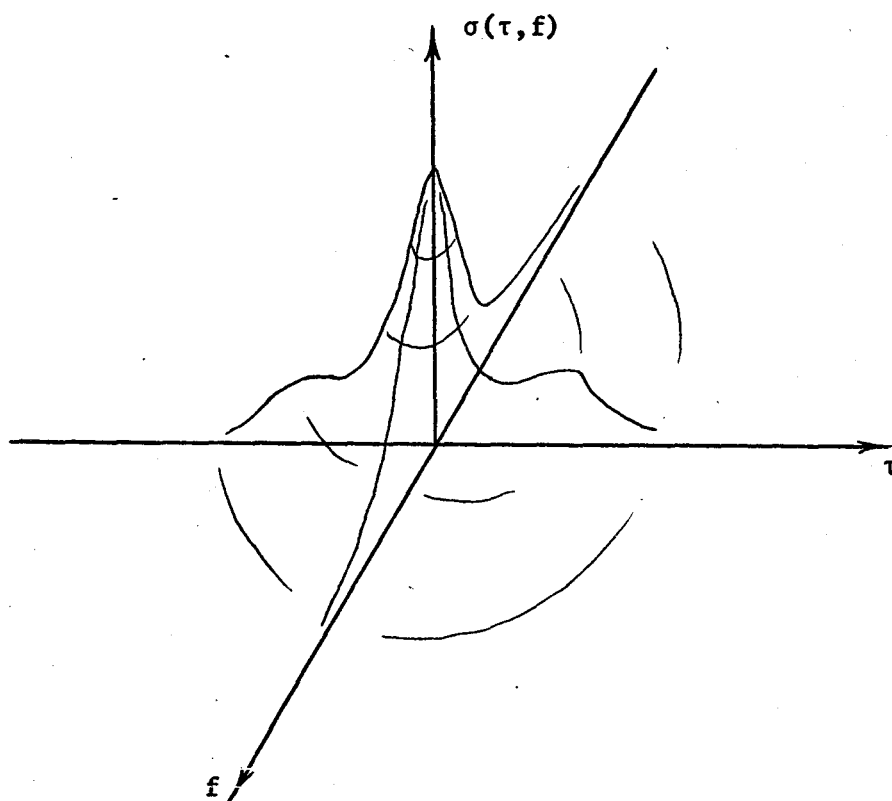
(a)
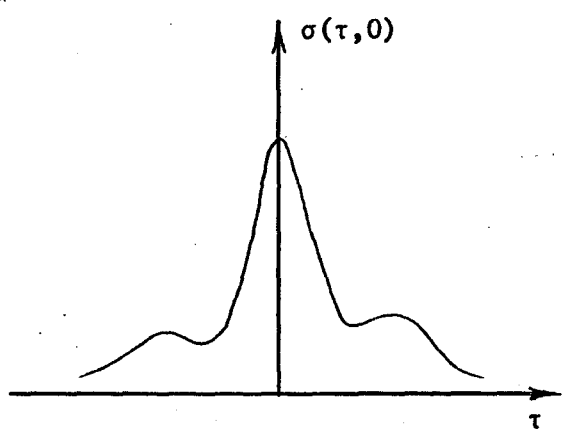
(b)
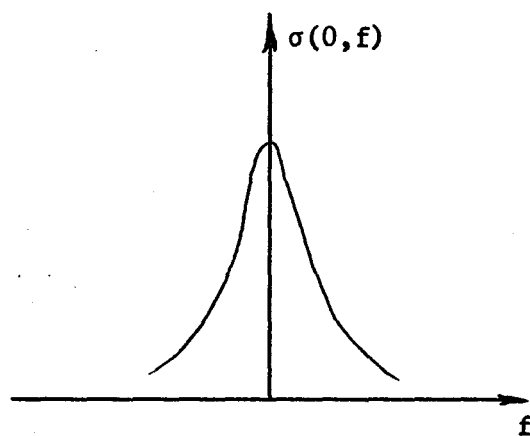
(c)

Figure 3.1 . Graphical Representation of the Scattering Function

Since the scattering function is an average power gain representation, however, it is not a flexible model for the studies of adaptive systems. A more appropriate model is the delay line model with the channel impulse response represented by $c(t,\xi)\delta(t-iT_s)$, where $c(t,\xi)$ is a continuum, $\delta(t-iT_s)$ is a unit sampling pulse, T_s is the sampling interval, and ξ is the time delay due to random multipaths. The rate of change of ξ gives a measure of the frequency instability. We note that as $i \to \infty$ and $T_s \to 0$ simultaneously, $c(t,\xi)\delta(t-iT_s) \to c(t,\xi)$. The delay line model is depicted in Figure 3.2.

Consider exciting the complex channel by a real bandpass signal as illustrated in Figure 3.3, where $a(t)$ is the modulating signal and $c(t,\xi)$ is the time-varying complex impulse response of the channel. The channel output is then given by the convolution integral:

$$z(t) = \int 2\text{Re}[a(t-\xi)e^{j\omega_0(t-\xi)}]c(t,\xi)e^{j\omega_0\xi}\,d\xi$$

$$= \int 2\text{Re}[a(t-\xi)e^{j\omega_0(t-\xi)}]\text{Re}[c(t,\xi)e^{j\omega_0\xi}]\,d\xi$$

$$+ j\int 2\text{Re}[a(t-\xi)e^{j\omega_0(t-\xi)}]\text{Im}[c(t,\xi)e^{j\omega_0\xi}]\,d\xi \qquad (3.1)$$

Using equations (B.1) and (B.3) in (3.1), we get

$$z(t) = \int \text{Re}[a(t-\xi)c^c(t,\xi)e^{j\omega_0(t-2\xi)}]\,d\xi$$

$$+ \int \text{Re}[a(t-\xi)c(t,\xi)e^{j\omega_0 t}]\,d\xi$$

$$+ j\int \text{Im}[a(t,\xi)c(t,\xi)e^{j\omega_0 t}]\,d\xi \quad - j\int \text{Im}[a(t-\xi)c^c(t,\xi)e^{j\omega_0(t-2\xi)}]\,d\xi$$
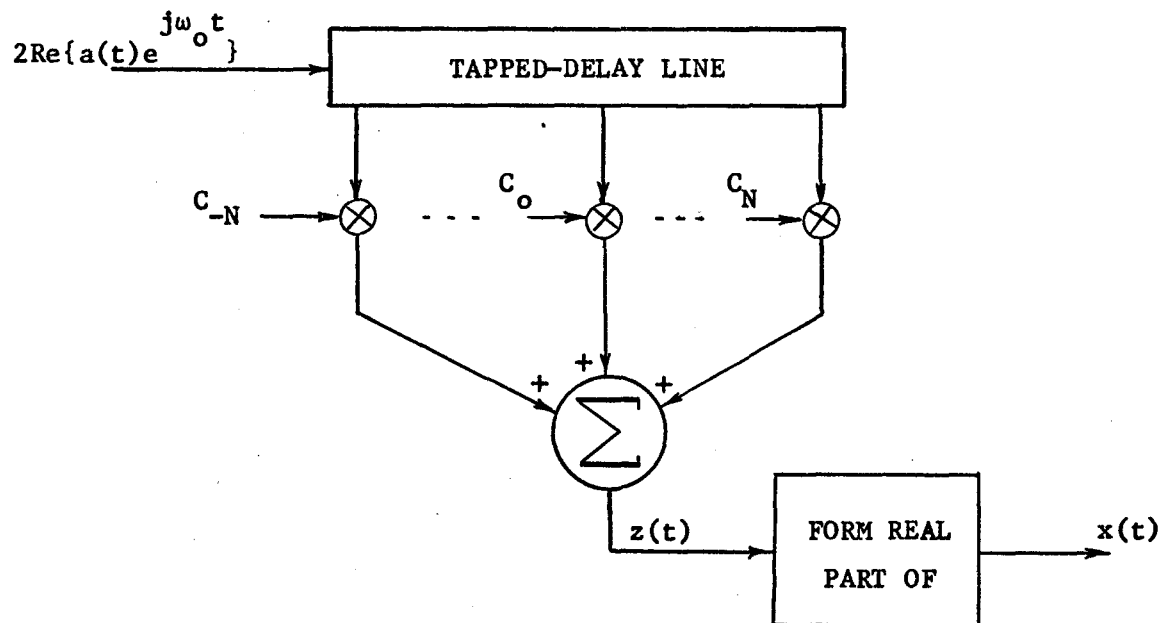
Figure 3.2   Tapped–delay Line Model
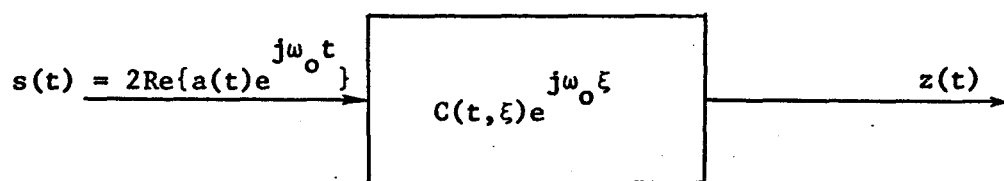
Figure 3.3   Symbolic Representation of Complex Channel Response

$$z(t) = \int a(t-\xi)c(t,\xi)e^{j\omega_0 t} d\xi + \int a(t-\xi)c(t,\xi)e^{-j\omega_0(t-2\xi)} d\xi \quad (3.2)$$

where the superscript c denotes complex conjugate. Carrying out the integration the second term on the right-hand-side of equation (3.2) vanishes, leaving

$$z(t) = e^{j\omega_0 t} \int a(t-\xi)c(t,\xi)d\xi$$

$$= u(t) \, e^{j\omega_0 t} \quad (3.3)$$

where

$$u(t) = \int a(t-\xi)c(t,\xi)d\xi \quad (3.4)$$

is the complex envelope of the channel output. That is to say, the complex envelope of the channel output is obtained by convolving the modulating signal with the complex channel impulse response. By affecting the transformation $\xi \rightarrow \tau + \tau_0$, where τ_0 is the 'mean' multipath delay, the channel output may be written as

$$u(t) = \int a(t-\tau_0-\tau)c(t,\tau+\tau_0)d\tau \quad . \quad (3.5)$$

If $a(t)$ is deterministic, then the nth order derivative $\dfrac{d^n}{dt^n} a(t)$ exists. A series expansion of $a(t-\tau_0-\tau)$ about the 'mean' multipath delay, τ_0, may be made to yield

$$a(t-\tau_0-\tau) = \sum_{n=0}^{\infty} \frac{1}{n!} \frac{d^n}{dt^n} a(t-\tau_0)(-\tau)^n \quad . \quad (3.6)$$

Substituting (3.6) in (3.5), we get

$$u(t) = \sum_{n=0}^{\infty} \frac{1}{n!} \int (-\tau)^n c(t,\tau_0+\tau)d\tau \frac{d^n a(t-\tau_0)}{dt^n} \tag{3.7}$$

or

$$u(t) = \sum_{n=0}^{\infty} \frac{1}{n!} \Gamma_n(t) \frac{d^n a(t-\tau_0)}{dt^n} \quad , \tag{3.8}$$

where

$$\Gamma_n(t) = \int (-\tau)^n c(t,\tau_0+\tau)d\tau \quad . \tag{3.9}$$

The degree of selective fading is then given by the terms in equation (3.8), i.e.,

$$\Gamma_0(t)\, a(t-\tau_0) \rightarrow \text{flat fading,}$$

$$\Gamma_1(t) \frac{d\, a(t-\tau_0)}{dt} \rightarrow \text{linear or deep fading,}$$

etc.

A selective fading channel can thus be modelled by superposing terms expressed by equation (3.8), i.e., many branches connected in parallel preceded by the 'mean' multipath delay. Considering only the first two terms in the series expansion of equation (3.8), a time-variant selectively fading channel model may be depicted as shown in Figure 3.4.

The integral, $\Gamma_n(t)$, of equation (3.9) represents the channel behaviour. The 'mean' multipath delay may be optimized by minimizing the energy contribution from the linear fading branch of Figure 3.4 as follows: From equation (3.8) the mean squared value of the flat fading term is given by

$$\overline{|\Gamma_0|^2} = \iint \overline{c(t,\tau)\, c(t,\xi)}\, d\tau\, d\xi$$

$$= \iint R_c(\tau,\xi)d\tau\, d\xi \tag{3.10}$$

where $R_c(\tau,\xi)$ is the correlation function of the channel impulse response, and the over bar denotes ensemble average. The mean square value of the linear fading term is given by

$$\overline{|\Gamma_1|^2} = \overline{\int (\tau-\tau_0)c(t,\tau+\tau_0)d\tau \int (\xi-\tau_0)c(t,\xi+\tau_0)d\xi}$$

$$= \iint (\xi-\tau_0)(\tau-\tau_0) \, R_c(\tau,\xi)d\tau \, d\xi \quad . \tag{3.11}$$

The cross-talk between the flat and the linear fading branches is given by

$$\overline{|\Gamma_0\Gamma_1|} = \iint (\tau-\tau_0) \, R_c(\tau,\xi)d\tau \quad d\xi \quad . \tag{3.12}$$

Our objective is to minimize $\overline{|\Gamma_1|^2}$ with respect to the 'mean' multipath delay, τ_0, as follows:

$$\frac{\partial}{\partial\tau_0}\overline{|\Gamma_1|^2} = \iint - (\xi+\tau) \, R_c(\tau,\xi)d\tau d\xi + 2\tau_0 \iint R_c(\tau,\xi)d\tau \, d\xi$$

$$= 0 \quad ,$$

from which we obtain

$$\tau_0 = \frac{1}{2} \frac{\iint (\xi+\tau) \, R_c(\tau,\xi)d\tau \, d\xi}{\iint R_c(\tau,\xi)d\tau \, d\xi} \quad . \tag{3.13}$$

The second order derivative is given by

$$\frac{\partial^2}{\partial\tau_0^2}\overline{|\Gamma_1|^2} = 2 \iint R_c(\tau,\xi)d\tau \, d\xi$$

$$> 0$$

since $R_c(\tau,\xi)$ is a positive definite covariance kernel.
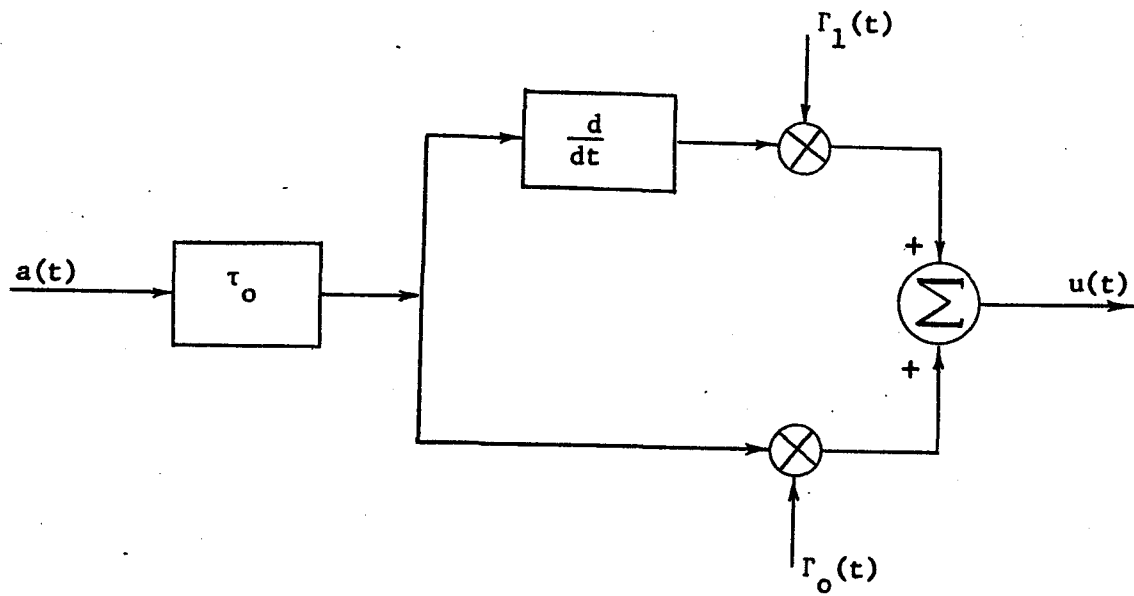
Figure 3.4   A First Order Selectively-Fading Channel Model
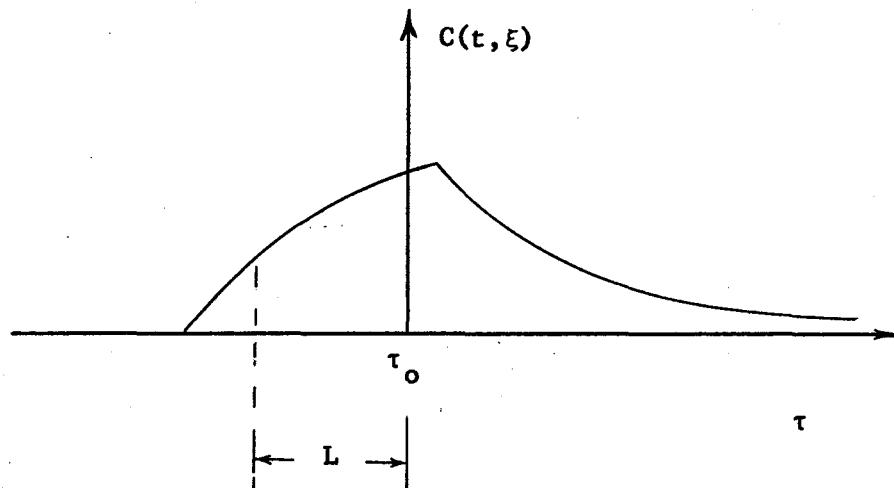
Figure 3.5   Illustration of Time Spread

Thus, the first derivative of $\overline{|\Gamma_1|}^2$ with respect to τ_0, in fact, yields a minimum. For the particular value of τ_0 chosen we have

$$\overline{|\Gamma_0 \Gamma_1|} = \frac{1}{2} \iint (\tau - \xi)\, R_c(\tau, \xi)\, d\tau\, d\xi\ , \tag{3.14}$$

The denominator of the right member of equation (3.13) is just the mean square value of the flat fading term given by equation (3.10). If $R_c(\tau, \xi)$ is viewed as a mass with respect to the τ-axis, then, τ_0, as given by equation (3.13), is the centre of mass (the first moment). The radius of gyration (the second moment) about the centre of mass is then given by

$$L' = \left[\frac{\iint (\xi + \tau - \tau_0)^2\, R_c(\tau, \xi)\, d\tau\, d\xi}{\iint R_c(\tau, \xi)\, d\tau\, d\xi} \right]^{\frac{1}{2}} \tag{3.15}$$

where L' is a measure of (half) time spread as illustrated in Figure 3.5. We introduce a two dimensional Fourier transform to describe the power spectrum in terms of two frequency variables by

$$\Phi_c(f, \nu) = \iint R_c(\tau, \xi) e^{-j2\pi(f\tau + \nu\xi)}\, d\tau\, d\xi\ . \tag{3.16}$$

Taking into account the time and frequency duality, it can be shown that the centre of mass with respect to the f-axis is given by

$$\bar{f} = \frac{1}{2} \frac{\iint f\, \Phi_c(f, \nu)\, df\, d\nu}{\iint \Phi_c(f, \nu)\, df\, d\nu} \tag{3.17}$$

and the radius of gyration is given by

$$
B' = \left[\frac{\iint (f+\nu-\bar{f})^2 \, \Phi_c(f,\nu)\, df \, d\nu}{\iint \Phi_c(f,\nu)\, df \, d\nu} \right]^{\frac{1}{2}} . \tag{3.18}
$$

B' is a measure of the (half) doppler spread. If the channel impulse response is a bandwidth restricted time-invariant system, then equation (3.15) is an adequate representation for time spread. In this case the second argument in $R_c(\tau,\xi)$ is superfluous.

The time-variant transfer function of the channel is given by the Fourier transform of the channel impulse response:

$$
C(\nu,t) = \int c(t,\xi) e^{-j2\pi\nu\xi} \, d\xi . \tag{3.19}
$$

A time-frequency correlation function may thus be defined as (Bello, 1969)

$$
R(\tau,f) = \overline{C^c(\nu,t)C(\nu+f,\ t+\tau)}
$$

$$
= \int R_c(\tau,\xi) e^{-j2\pi f\xi} \, d\xi \tag{3.20}
$$

The time-frequency correlation function defined by equation (3.20) is both conceptually and practically pleasing from a linear systems analysis viewpoint. $R(\tau,f)$ exhibits similar properties as the scattering function, $\sigma(\tau,f)$, derived on a statistical basis in Appendix B. Corresponding to the delay scattering function we may define a delay correlation function by

$$
R(\tau) \overset{\Delta}{=} \int R(\tau,f) \, df \tag{3.21}
$$

and a doppler correlation function by

$$R(f) \triangleq \int R(\tau, f) d\tau \ . \tag{3.22}$$

Replacing $R_c(\tau, \xi)$ by $R(\tau)$ and $\Phi_c(f, \nu)$ by $R(f)$ in equations (3.15) and (3.18), we get, respectively,

$$L = \left[\frac{\int (\tau - \tau_0)^2 R(\tau) d\tau}{\int R(\tau) d\tau} \right]^{\frac{1}{2}} \tag{3.23}$$

and

$$B = \left[\frac{\int (f - \bar{f})^2 R(f) \ df}{\int R(f) \ df} \right]^{\frac{1}{2}} \ , \tag{3.24}$$

where

$$\tau_0 = \frac{1}{2} \left[\frac{\int \tau \ R(\tau) \ d\tau}{\int R(\tau) \ d\tau} \right]$$

and

$$\bar{f} = \frac{1}{2} \left[\frac{\int f \ R(f) \ df}{\int R(f) \ df} \right] \ .$$

The parameter L is a measure of the (half) time spread; it is equivalent to L'. The parameter B is a measure of the (half) doppler spread; it is equivalent to B'.

3.2 Channel Distortion Characteristics

Suppose the transmitted signal, as suggested in Figure 3.3, is

$$s(t) = 2Re\{a(t)e^{j\omega_0 t}\} \quad , \tag{3.25}$$

where the envelope function $a(t)$ has a baud length T_0, or an effective bandwidth $W=1/T_0$. As suggested in section 2.2, the signal duration is given by $T=NT_0$, where N is the code length, i.e., the number of information symbols contained in $a(t)$. A measure of time dispersion, which we call the dispersion number, is given either by

$$(i) \quad \eta_1 = \frac{L}{T_s} \quad , \quad \text{for } T_0 < T_s$$

where T_s is the pulse separation, or

$$(ii) \quad \eta_2 = \frac{L}{T_0} = WL \quad , \quad \text{for } T_0 \geqslant T_s \quad .$$

If measurements made at the sampling instants suffice, then the dispersion number becomes

$$\eta_1 = \left\lceil \frac{L}{T_s} \right\rceil$$

or

$$\eta_2 = \left\lceil \frac{L}{T_0} \right\rceil = \left\lceil WL \right\rceil \tag{3.26}$$

where $\lceil \cdot \rceil$ denotes the largest integer of. We use the largest integer because L is the radius of gyration and the tail ends of the channel impulse response may also cause distortion. From the transmitter efficiency point of view the transmitted intelligence, $a(t)$, will at

least have $T_o = T_s$. Henceforth, wherever we refer to time dispersion we mean η as represented by equation (3.26). Distortions, termed inter-symbol interference, will arise when $\eta \geqslant 1$. Intersymbol interference becomes increasingly pronounced as η becomes large. For $\eta > N$, the code length, the distortion becomes so severe that the entire signal may have been dispersed or mutilated. From the frequency domain point of view, when L is large compared to the signal duration T, the spectral bandwidth of the channel, given by 1/L, is so narrow compared to the signal bandwidth, that very little signal energy passes through. If the signal processor has a transfer function which is inverse to the physical channel transfer function, then the physical channel and the signal processor connected in cascade will behave as an 'equalized channel' or an all pass filter. The derivation of such a mechanism is the topic of Chapter 5.

In section 3.1, the doppler spread, as derived from the time-frequency duality principle, has been termed frequency dispersion. The aging process, both in amplitude and phase of the channel impulse response, may selectively alter certain time segments of the transmitted signal. This phenomenon is actually the manifestation of frequency dispersion. In what follows, the effect of doppler will be considered as primarily a discrete shift on the carrier frequency. The doppler spread will be considered as the manifestation of phase aging. The gross effect of frequency dispersion will be compensated for by making the impulse response of the signal processor a time-varying one.

3.3 Problem Formulation

Thus far, we have characterized the channel in terms of time-
dispersion (source of intersymbol interference) and frequency dispersion
(slow time variations). In addition, if the channel exhibits very
rapid fluctuations (compared to the data rate), then the output signal
from such a branch of the channel may be totally mutilated such that any
possibility for the recovery of the signal may not exist. Our channel
model will have three parallel branches: a rapid fluctuating random
branch which almost completely mutilates the transmitted signal; a time-
invariant branch, and a slow fluctuation branch. The random as well as
the slow fluctuation branches have amplitude and phase distributions
given by equations (B.20) and (B.21), respectively. The difference
between these two components lies in their rate of fluctuation. Rapid
fluctuations give rise to an effective doppler spread much wider than
the signal bandwidth, i.e., B>>W, so that the output from the random
branch has high harmonic contents (hence the term wide-band signal
dependent noise). On the other hand, slow fluctuations are such that
over the observation interval the phase and amplitude characteristics
have not changed very much, i.e., B<1/T, so that any changes on the
signal are tractable. In our model, then, both the time-invariant and
the slow-fluctuation components of the channel impulse response have
finite memories whereas the random component has essentially zero
memory (as compared to the baud length). Since signals propagating
through both the time-invariant and the slow-fluctuation branches are
subject to similar distortions, we lump these together to reduce the

channel model to two branches in parallel, that is, a deterministic and a random branch. The composite channel has been termed a Rician channel which may be described by the probability density functions given by equations (B.23), (B.24) and (B.25).

For reasons of compactness in presentation, we will formulate our communications problem in Hilbert space notations (see Appendix C). Specifically we let the channel be excited by a (baseband) signal vector $\underline{\alpha}$, where $\underline{\alpha}$ is given by the linear mapping

$$\underline{\alpha} = F\underline{a} \qquad (3.27)$$

where

$\underline{a}$ is an s dimension information column vector,

F is an sxs pulse shaping matrix, and

$\underline{\alpha}$ is an s dimensional signal column vector.

.The channel response at the nth instant may be written as

$$\underline{m}(n) = C^{c}(n)\ \underline{\alpha}(n) \qquad (3.28)$$

where

$\underline{m}$ is an s dimensional column vector, and

C is an sxs channel matrix.

We assume that the channel matrix C is decomposable into a deterministic and a random component as follows:

$$C = C_d + C_r \quad . \qquad (3.29)$$

where C_d is deterministic and C_r is random. Substituting equation (3.29) in (3.28), we get

$$\underline{m}(n) = C_d^C(n) \; \underline{\alpha}(n) \; + \; C_r^C(n) \; \underline{\alpha}(n) \quad . \tag{3.30}$$

Substituting equation (3.27) in (3.30), we get

$$
\begin{aligned}
\underline{m}(n) &= C_d^C(n)F(n)\underline{a}(n) + C_r^C(n)F(n)\underline{a}(n) \\
&= H_d(n)\underline{a}(n) \; + \; H_r(n)\underline{a}(n) \\
&= \underline{m}_d(n) \; + \; \underline{m}_r(n) \tag{3.31}
\end{aligned}
$$

where

$$H_d(n) = C_d^C(n)F(n) \quad \text{is a deterministic linear mapping}$$

and

$$H_r(n) = C_r^C(n)F(n) \quad \text{is a stochastic linear mapping.}$$

The information inherent in the output of the deterministic component may be recovered accurately whereas that which is implicit in the random component is not recoverable accurately. The output of the channel is further corrupted by an additive noise vector, $\underline{n}$, so that the received signal is given by

$$\underline{u}(n) = D(n)[\underline{m}(n) \; + \; \underline{n}(n)] \tag{3.32}$$

where D is a linear mapping.

Thus far in this section, all signal vectors employed have been baseband signals. In practice the baseband signal is modulated onto a

carrier before transmission. From the analytical viewpoint, it serves

our purpose better by modulating the overall channel output vector onto

a carrier prior to reception as follows:

$$\underline{x}(n) = Re\{V^c(n) \; \underline{u}(n)\} \tag{3.33}$$

where $V(n)$ is a linear mapping. We contend that provided $\underline{u}(n)$ implicitly

contains noise as well as time and frequency distortions, there is no

loss of generality in employing the above treatment of signal modulation.

As an example we consider functions in the L_2 space and let

$$v(t) = e^{j\omega_o t}$$

so that we have, corresponding to equation (3.33),

$$x(t) = Re[u(t) \; e^{j\omega_o t}] \; . \tag{3.34}$$

We note that

$$[v(t)]^{-1} = e^{-j\omega_o t} = v^c(t) \; . \tag{3.35}$$

Our communication model represented by the set of equations (3.28) to

(3.33) is depicted in Figure 3.6, where the double lines denote signal

flow of vector valued quantities.

3.4 Signal-To-Interference Ratio

The problem of receiving signals emerging from fading dispersive

channels will be centred around the communication model characterized in

the preceding section. The receiver design problem is divided into four
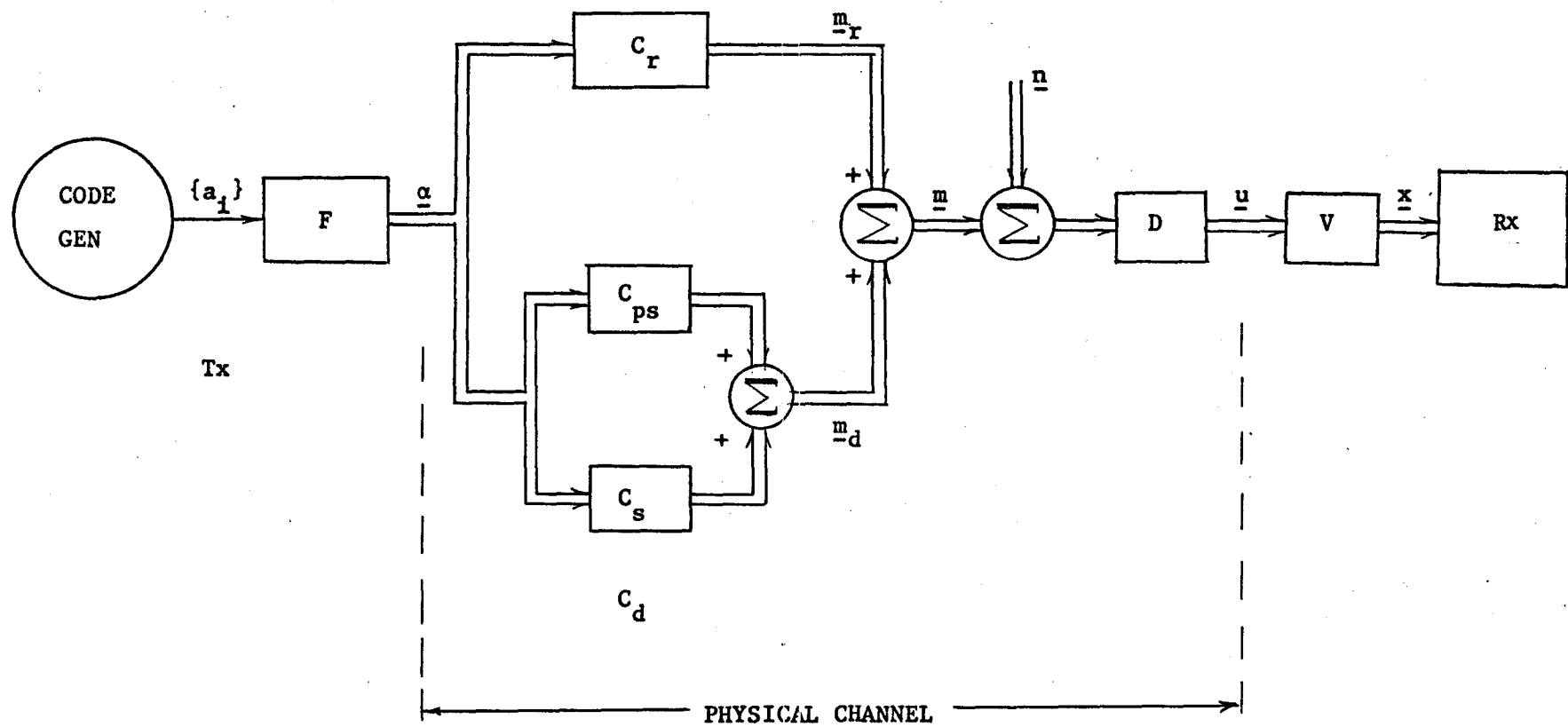
Figure 3.6   Proposed Channel Model

sub-sections (see Figure 1.1), namely,

     (1)   synchronous demodulation,

     (2)   filtering of wide-band noise,

     (3)   equalization of time and frequency dispersions, and

     (4)   signal decoding.

If the first three of the above are optimized such that the input to the decoder is a 'good' estimate of the encoder output, then decoding becomes a trivial problem. In this thesis our main interest lies in evolving a synchronous receiver for the reception of PAM signals. The synchronous receiver includes primarily a synchronous demodulator, an adaptive filter and an adaptive equalizer. The synchronous demodulator has been derived in section 2.5; the adaptive filter and the adaptive equalizer will be derived in Chapters 4 and 5, respectively. In this section we demonstrate the need for signal processing.

Using equation (3.31) in (3.32), we get

$$\underline{u}(n) = D(n)\ H_d(n)\ \underline{a}(n)\ +\ D(n)\ H_r(n)\ \underline{a}(n)\ +\ n(n)$$

$$=\ \underline{u}_d(n)\ +\ \underline{u}_r(n) \tag{3.36}$$

where

$$\underline{u}_d(n)\ =\ D(n)\ H_d(n)\ \underline{a}(n)$$

and

$$\underline{u}_r(n)\ =\ D(n)\ H_r(n)\ \underline{a}(n)\ +\ n(n)\ .$$

The observed vector would be mainly distorted by dispersive effects if

the covariance matrix, $Cov[\underline{u}_r] = E[\underline{u}_r \underline{u}_r^t]$ is a null matrix. Our first objective in optimizing signal acquisition is, therefore, to minimize $Cov[\underline{u}_r]$. With respect to the deterministic and the random components of the channel output we make the following assumptions:

(i) Since the channel is assumed to be linear, $\underline{u}_d$ is given by a superposition of deterministic quantities (as defined in section 3.3). Hence, $\underline{u}_d$ may be treated as a deterministic quantity as opposed to the random component $\underline{u}_r$.

(ii) In the space U where the inner products are defined by $E[u_1 u_2]$, u_1, $u_2 \in U$, $\underline{u}_d$ and $\underline{u}_r$ are uncorrelated under the expectation operator $E[\cdot]$. Since $E[\underline{u}_r] = \underline{0}$, $\underline{u}_d$ and $\underline{u}_r$ are statistically independent.

On the basis that superposition applies we may consider the transmission of an isolated pulse. Let the energy of the input taken at the sampling instant be given by $E_a = E[a^2] = a^2$. The energy contribution from the deterministic component is given by

E_d = sums of elements along all diagonals of $E[\underline{u}_d \underline{u}_d^t]$

   = trace of $E[\underline{u}_d \underline{u}_d^t]$ + sums of elements of all off principal

   diagonals of $E[\underline{u}_d \underline{u}_d^t]$.

In expanded form,

$$E_d = \sum_i \sum_j E[\underline{u}_{d,i}\, \underline{u}_{d,j}]$$

$$= \sum_i \sum_j h_{d,i}\, h_{d,j}\, E[a_i\, a_j]$$

$$= E_a\, h_{d,o}^2 + \sum_{\substack{i \ j \\ j=i \neq 0}} h_{d,i}\, h_{d,j}\, E[a_i\, a_j] \qquad (3.37)$$

where

$$h_{d,i} = \sum_{j \epsilon J} f_j \, c_{d,i-j} \; .$$

Since we are considering the transmission of an isolated pulse, each sample of the channel impulse response is excited by the same information symbol a. Thus the factor $E\{a_i a_j\}$ in the second term of equation (3.37) may be taken to be $E[a^2] = E_a$, so that we may express E_d as the sum of the coherent signal energy and intersymbol interference as shown by

$$E_d = E_a h_{d,o}^2 + E_a \sum_i \sum_j h_{d,i} h_{d,j} \qquad (3.38)$$
$$i=j\neq 0$$

The energy contribution from the random component is given by

$$E_r = \text{sums of all diagonals of } E[\underline{u}_r \underline{u}_r]$$

$$= \sum_i \sum_j E[(h_{r,i} a_i + n_i)(h_{r,j} a_j + n_j)]$$

$$= \sum_i \sum_j E[h_{r,i} h_{r,j} a_i a_j + h_{r,i} a_i n_j + h_{r,j} a_j n_i + n_i n_j]$$

where

$$h_{r,i} = \sum_j f_j c_{r,i-j} \quad \cdot$$

For zero mean $\{n_i\}$ which is statistically independent of $\{a_i\}$ the above reduces to

$$E_r = \sum_i \sum_j E[h_{r,i} h_{r,j} a_i a_j + n_i n_j]$$

$$= \sum_i \sum_j E[h_{r,i} h_{r,j} a_i a_j] + \sum_i \sum_j E[n_i n_j] \qquad (3.39)$$

$$= \left(\begin{array}{c} \text{mean square energy of} \\ \text{signal dependent noise} \end{array} \right) + \left(\begin{array}{c} \text{mean square energy of} \\ \text{signal independent noise} \end{array} \right)$$

The signal-to-interference ratio at the observation point is then given by

$$(S/I)_{ob} = \frac{\text{coherent signal energy}}{\text{Total Interferences}} \qquad (3.40)$$

where total interferences include energy due to intersymbol interference, signal dependent noise and signal independent additive noise. Using equations (3.38) and (3.39) in (3.40) and assuming $\{h_{r,i}\}$ and $\{a_i\}$ are statistically independent, we get

$$(S/I)_{ob} = \frac{h_{d,o}^2 E_a}{E_a \sum\limits_{\substack{i,j \\ i=j\neq 0}} h_{d,i} h_{d,j} + E_a \sum\limits_{i} \sum\limits_{j} E[h_{r,i} h_{r,j}] + \sum\limits_{i} \sum\limits_{j} E[n_i n_j]}$$

$$= \frac{h_{d,o}^2}{\sum\limits_{\substack{i,j \\ i=j\neq 0}} h_{d,i} h_{d,j} + \sum\limits_{i} \sum\limits_{j} E[h_{r,i} h_{r,j}] + \sum\limits_{i} \sum\limits_{j} E[n_i n_j]/E_a} \qquad (3.41)$$

For $h_{d,o}$ normalized to unity equation (3.41) becomes

$$(S/I)_{ob} = \frac{1}{\sum\limits_{\substack{i,j \\ i=j\neq 0}} h_{d,i} h_{d,j} + \sum\limits_{i} \sum\limits_{j} E[h_{r,i} h_{r,j}] + \sum\limits_{i} \sum\limits_{j} E[n_i n_j]/E_a} \qquad (3.42)$$

If we further assume the $\{h_{r,i}\}$ and the $\{n_i\}$ are themselves statistically independent, then equation (3.42) reduces to

$$(S/I)_{ob} = \frac{1}{\sum\limits_{\substack{i \ j \\ i=j\neq 0}} h_{d,i} h_{d,j} + \sigma_r^2 + \sigma_n^2/E_a} \qquad (3.43)$$

where

$$\sigma_r^2 = \sum_i E[h_{r,i}^2]$$

and

$$\sigma_n^2 = \sum_i E[n_i^2] \quad .$$

3.5 Summary

In this chapter we have derived mathematical expressions for a measure of time as well as frequency spread. The time spread, L, and the frequency spread, B, provide a conceptual feel for the amount of distortions arising from the fading dispersive channels.

The characterization of the 'communications channel' in terms of a deterministic and a random component paves the way to the derivations of an adaptive filter and an adaptive equalizer in Chapters 4 and 5, respectively. The signal-to-interference ratio given by equation (3.42) or (3.43) clearly demonstrates the need for filtration and equalization.

CHAPTER 4

DERIVATION OF AN ADAPTIVE FILTER

4.1 Introduction

In section 3.3 we characterized the physical channel in terms of a deterministic and a random branch. The output of the deterministic branch contains the recoverable signal, which has been perturbed mainly by distortions. The output of the random branch is essentially wideband signal dependent noise. In addition, the channel output is further corrupted by additive Gaussian noise. Accurate recovery of the transmitted signal requires firstly, the extraction of the deterministic branch output from the received signal and secondly, compensations for signal distortions. In this Chapter we are mainly concerned with the signal extraction or filtering problem.

In keeping with the channel model formulation of section 3.3, the derivation in this Chapter is carried out in the abstract Vector Space concept as defined in Appendix C. The projection theorem and the decomposition theorem given in this Appendix are the main tools employed in the derivation of the recursive filter. The recursive filter is made to operate adaptively via the incorporation of a gradient technique. It is shown that for certain types of signaling (modulation) the adaptive filter behaves as a synchronous demodulator-estimator device. In this case the demodulation action is characteristically similar to a phase-locked loop.

68

4.2 Objective and Criterion

Our objective is to find a best linear estimate of the vector $\underline{m}_d$. By the projection theorem the optimal linear estimate is just the projection of $\underline{m}_d(n)$ onto a linear manifold of dimension n. The error is given by the component of $\underline{m}_d(n)$ which is orthogonal to the linear manifold $\underline{u}_n \in U$. We then have, by the projection theorem,

$$\underline{m}_d(n) = \hat{\underline{m}}(n) + \tilde{\underline{m}}(n) \tag{4.1}$$

where $\hat{\underline{m}}$ is an estimate of $\underline{m}_d$, and

$\tilde{\underline{m}}$ with covariance matrix $E\{\tilde{\underline{m}}\ \tilde{\underline{m}}^+\}$ defines the error in the estimate. Based on the projection theorem the optimal estimate is just the conditional mean:

$$\hat{\underline{m}}(j|i) = E\{\underline{m}_d(j)|\underline{u}_1,\ldots,\underline{u}_i\} \tag{4.2}$$

Using the conditional notations, equation (4.1) may be re-arranged as

$$\tilde{\underline{m}}(j|i) = \underline{m}_d(j) - \hat{\underline{m}}(j|i) \tag{4.3}$$

where $\hat{\underline{m}}(j|i)$ is shorthand for the jth instant and in an i dimensional linear manifold. In words, $\hat{\underline{m}}(j|i)$ represents the best estimate of the state vector $\underline{m}_d(j)$ at the discrete time j given all the available observables $\underline{u}_1,\ldots,\underline{u}_i$, up to time i. The quantity $\tilde{\underline{m}}(j|i)$ defines the error in the best linear estimate $\hat{\underline{m}}(j|i)$ at the discrete time j. Thus, by the projection theorem

$$\underline{m}_d(n) = \hat{\underline{m}}(n|n-1) + \tilde{\underline{m}}(n|n-1) \tag{4.4}$$

Definition:

The covariance matrix which reflects the uncertainty of the best estimate $\hat{\underline{m}}(n|n)$ is defined as:

$$P(n|n) = E\{\tilde{\underline{m}}(n|n)\ \tilde{\underline{m}}^+(n|n)\} \qquad (4.5)$$

where the superscript + denotes the complex conjugate transpose. With the exception of the principal diagonal, all other elements of the covariance matrix are, in general, complex quantities. In our optimization problem, we use the

Criterion:

An optimal estimate, which is the conditional mean, can be found by minimizing the trace of the covariance matrix (the mean square energy) of equation (4.5). The trace operator offers the following

Identity:

If $\underline{u}$ and $\underline{v}$ are two vectors and A is a matrix, then

$$\underline{u}^t A \underline{v} = tr\{\underline{v} \cdot \underline{u}^t A\} \qquad (4.6)$$

where tr{·} denotes the trace operation of a matrix, i.e., sum of the principal diagonal elements of the matrix, and t denotes the matrix transpose.

4.3 Derivation of a Recursive Filter

We stated in section 4.2 that the best linear estimate is given by the conditional mean. Application of the conditional expectation operator $E\{\cdot|\underline{x}_1,\ldots,\underline{x}_n\}$ to equation (4.4) yields the following:

$$\hat{\underline{m}}(n|n) = E\{\underline{m}_d(n)|\underline{x}_1,\ldots,\underline{x}_n\}$$

$$= \hat{\underline{m}}(n|n-1) + E\{\tilde{\hat{\underline{m}}}(n|n-1)|\underline{x}_1,\ldots,\underline{x}_n\} \qquad (4.7)$$

Again applying the operator $E\{\cdot|\underline{x}_1,\ldots,\underline{x}_{n-1}\}$ to both sides of equation (4.4), we get

$$\hat{\underline{m}}(n|n-1) = \hat{\underline{m}}(n|n-1) + E\{\tilde{\underline{m}}(n|n-1)|\underline{x}_1,\ldots,\underline{x}_{n-1}\} \quad . \qquad (4.8)$$

From equation (4.8) we get the identity

$$E\{\tilde{\underline{m}}(n|n-1)|\underline{x}_1,\ldots,\underline{x}_{n-1}\} \equiv \underline{0} \quad . \qquad (4.9)$$

Let $G(n,i)$ be a gain matrix which contains past statistics of the observables up to time $(i - 2)$. It is then permissible to write

$$E\{\underline{m}_d(n|i-1)|\underline{x}_1,\ldots,\underline{x}_{i-1}\} = G^c(n,i)\,\underline{x}(i|i-1) \qquad (4.10)$$

where the superscript c denotes the complex conjugate. Through the introduction of the gain matrix $G(n,i)$, we can state that past statistics are not being abandoned but are being propagated. This statement will be substantiated subsequently when we make the computation of $G(n,n)$ adaptive. The conditional estimate at time n conditioned on the observables up to time $(n-1)$ is obtained by summing equation (4.10) over all i up to $i=n-1$:

$$E\{\underline{m}_d(n|n-1)|\underline{x}_1,\ldots,\underline{x}_{n-1}\} = \sum_{i=1}^{n-1} E\{\underline{m}_d(n|i-1)|\underline{x}_1,\ldots,\underline{x}_{i-1}\}$$

$$= \sum_{i=1}^{n-1} G^c(n,i)\,\underline{x}(i|i-1) \qquad (4.11)$$

By the projection theorem, we have

$$E\{\underline{m}_d(n|n-1)|\underline{x}_1,\ldots,\underline{x}_{n-1}\} = E\{[\hat{\underline{m}}(n|n-1) + \tilde{\underline{m}}(n|n-1)]|\underline{x}_1,\ldots,\underline{x}_{n-1}\}$$

$$\ldots(4.12)$$

and

$$\underline{x}(i|i-1) = \hat{\underline{x}}(i|i-1) + \tilde{\underline{x}}(i|i-1) \quad . \tag{4.13}$$

Using (4.12) and (4.13) in (4.11), we get

$$E\{[\hat{\underline{m}}(n|n-1) + \tilde{\underline{m}}(n|n-1)]|\underline{x}_1,\ldots,\underline{x}_{n-1}\} = \sum_{i=1}^{n-1} G^c(n,i)[\hat{\underline{x}}(i|i-1) + \tilde{\underline{x}}(i|i-1)]$$

$$\ldots(4.14)$$

Application of the decomposition theorem to equation (4.14) yields

$$E\{\hat{\underline{m}}(n|n-1)|\underline{x}_1,\ldots,\underline{x}_{n-1}\} = \sum_{i=1}^{n-1} G^c(n,i)\, \hat{\underline{x}}(i|i-1) \quad , \tag{4.15}$$

and

$$E\{\tilde{\underline{m}}(n|n-1)|\underline{x}_1,\ldots,\underline{x}_{n-1}\} = \sum_{i=1}^{n-1} G^c(n,i)\, \tilde{\underline{x}}(i|i-1) \quad . \tag{4.16}$$

From equations (4.9) and (4.16) it therefore follows that

$$\sum_{i=1}^{n-1} G^c(n,i)\, \tilde{\underline{x}}(i|i-1) = \underline{0} \quad . \tag{4.17}$$

Consider advancing the time one step so that the observable under consideration is $\underline{x}_n$ at time n and the latest estimate is $\hat{\underline{m}}(n|n-1)$ based on the observation up to time (n-1). The conditional error arising from the latest estimate, given $\underline{x}_n$ as the observation vector, is

$$E\{\tilde{\underline{m}}(n|n-1)|\underline{x}_1,\ldots,\underline{x}_n\} = \sum_{i=1}^{n} G^c(n,i)\, \tilde{\underline{x}}(i|i-1) \tag{4.18}$$

Since equation (4.17) must hold for all $\underline{x}_1,\ldots,\underline{x}_{n-1}$ and since $\tilde{\underline{x}}(i|i-1)\neq 0$,

for all i, we have $G(n,i)=0$ for $i < n$. Equation (4.18) becomes

$$E\{\tilde{\underline{m}}(n|n-1)|\underline{x}_1,\ldots,\underline{x}_n\} = G^c(n,n)\ \tilde{\underline{x}}(n|n-1) \quad . \tag{4.19}$$

Equation (4.19) holds because $G(n,n)$ has been declared to contain past information. Substituting equation (4.19) in (4.7), we get the recursive form

$$\hat{\underline{m}}(n|n) = \hat{\underline{m}}(n|n-1) + G^c(n,n)\ \tilde{\underline{x}}(n|n-1) \quad . \tag{4.20}$$

But

$$\hat{\underline{m}}(n|n) = \underline{m}_d(n) - \tilde{\underline{m}}(n|n) \tag{4.21}$$

and

$$\hat{\underline{m}}(n|n-1) = \underline{m}_d(n) - \tilde{\underline{m}}(n|n-1) \quad . \tag{4.22}$$

Using (4.21) and (4.22) in (4.20) we get

$$\tilde{\underline{m}}(n|n) = \tilde{\underline{m}}(n|n-1) - G^c(n,n)\ \tilde{\underline{x}}(n|n-1)$$

$$= \tilde{\underline{m}}(n|n-1) - G^c(n,n)\ V^c(n)\ \tilde{\underline{u}}(n|n-1) \tag{4.23}$$

where (from section 3.3)

$$\underline{x}(n) = V^c(n)\ \underline{u}(n) \quad .$$

Also,

$$\underline{u}(n) = D(n)\ [\underline{m}_d(n) + \underline{m}_r(n) + \underline{n}(n)] \quad .$$

Applying the projection and the decomposition theorems to the above, we have

$$\tilde{\underline{u}}(n|n-1) = D(n)[\tilde{\underline{m}}(n|n-1) + \underline{m}_r(n|n-1) + \underline{n}(n|n-1)] \quad , \tag{4.24}$$

where $\tilde{\underline{m}}(n|n-1)$ is the error associated with the estimation process,

$\underline{m}_r(n|n-1)$ is the random component of the channel output, and

$\underline{n}(n|n-1)$ is the additive noise vector.

To facilitate the derivation in the sequel, we make the following assumption:

$\tilde{\underline{m}}$, $\underline{m}_r$ and $\underline{n}$ are zero mean random vectors which are statistically independent of each other.

Substituting equation (4.24) in (4.23), we get

$$\tilde{\underline{m}}(n|n) = \tilde{\underline{m}}(n|n-1) - G^c(n,n) \ V^c(n) \ D^c(n)$$

$$\cdot [\tilde{\underline{m}}(n|n-1) + \underline{m}_r(n|n-1) + \underline{n}(n|n-1)] \qquad (4.25)$$

Substituting equation (4.25) into the definition of covariance matrix (4.5) and using the above assumption, we get

$$P(n|n) = E\{[\tilde{\underline{m}}(n|n-1) - G^c(n,n) \ V^c(n) \ D^c(n) \ [\tilde{\underline{m}}(n|n-1)$$

$$+ \ \underline{m}_r(n|n-1) + \underline{n}(n|n-1)]] \cdot [\tilde{\underline{m}}(n|n-1)$$

$$- G^c(n,n) \ V^c(n) \ D^c(n) \ [\tilde{\underline{m}}(n|n-1) + \underline{m}_r(n|n-1) + \underline{n}(n|n-1)]]^\dagger\}$$

which simplifies to

$$P(n|n) = P(n|n-1) - G^c(n,n) \ V^c(n) \ D^c(n) \ P(n|n-1)$$

$$- P(n|n-1) \ [G(n,n) \ V(n) \ D(n)]^t$$

$$+ G^c(n,n) \ V^c(n) \ D^c(n) \ [P(n|n-1) + K_{\underline{m}}(n|n-1) + K_{\underline{n}}(n|n-1)]$$

$$\cdot [G(n,n) \ V(n) \ D(n)]^t \qquad (4.26)$$

where $K_{\underline{m}}(n|n-1) = E\{\underline{m}_r(n|n-1) \cdot \underline{m}_r^+(n|n-1)\}$, and

$$K_{\underline{n}}(n|n-1) = E\{\underline{n}\ (n|n-1) \cdot \underline{n}^+(n|n-1)\} \ .$$

The covariance matrices appearing in equation (4.26) are:

   (i) $P(n|n-1)$, due to error in the estimate.

   (ii) $K_{\underline{m}}(n|n-1)$, due to multiplicative noise.

   (iii) $K_{\underline{n}}(n|n-1)$, due to additive noise.

The covariance equation (4.26) may be re-arranged to assume a recursive form:

$$P(n|n) = [I - G(n,n)\ V(n)\ D(n)]^c\ P(n|n-1)$$

$$\cdot [I - G(n,n)\ V(n)\ D(n)]^t$$

$$+[G(n,n)V(n)D(n)]^c[K_{\underline{m}}(n|n-1) + K_{\underline{n}}(n|n-1)][G(n,n)V(n)D(n)]^t$$

$$\text{. . . (4.27)}$$

The gain matrix, $G(n,n)$, is derived in Appendix D with the principal result given by equation (D.15), which is repeated below as equation (4.28):

$$G(n,n)=P(n|n-1)[V(n)D(n)[P(n|n-1) + K_{\underline{m}}(n|n-1) + K_{\underline{n}}(n|n-1)]]^{-1}$$

$$\text{. . . (4.28)}$$

By the projection theorem

$$\tilde{\underline{x}}(n|n-1) = \underline{x}(n) - \hat{\underline{x}}(n|n-1) \ .$$

But,

$$\hat{\underline{x}}(n|n-1) = V^c(n)\ \hat{\underline{u}}(n|n-1)$$

$$= V^c(n)\ D^c(n)\ \hat{\underline{m}}(n|n-1) \ .$$

Therefore,

$$\tilde{x}(n|n-1) = \underline{x}(n) - V^c(n) \; D^c(n) \; \hat{\underline{m}}(n|n-1) \; . \tag{4.29}$$

Substituting equation (4.29) in (4.20), we get

$$\hat{\underline{m}}(n|n) = \hat{\underline{m}}(n|n-1) + G^c(n,n)[\underline{x}(n) - V^c(n)D^c(n) \; \hat{\underline{m}}(n|n-1)] \; . \tag{4.30}$$

Equation (4.30) is a recursive formula for the conditional estimate, which has the appearance of the Kalman-Bucy filter (Kalman, 1960; Kalman and Bucy, 1961). In the Kalman-Bucy filter the gain matrix is computed from the formula given by an equation of the form of (4.28), where the covariance matrices $K_{\underline{m}}(n|n-1)$ and $K_{\underline{n}}(n|n-1)$ are assumed known quantities. In other words, the derivation of the Kalman-Bucy filter is facilitated through the assumption that the process is Gauss-Markov. In our derivation we did not make such an assumption, but assert that the gain matrix, G(n,n), takes account of past statistics. G(n,n) will not be computed from equation (4.28) but rather, (4.28) will be modified so that the gain matrix is adjusted adaptively. The recursive algorithm of equation (4.30) is depicted in Figure 4.1 where the double lines denote vector valued quantities.

4.3.1 Performance of the (Non-adaptive) Recursive Algorithm

The set of equations (4.30), (4.28) and (4.27) which form the recursive conditional estimator relies on the fact that the covariance matrices $K_{\underline{m}}$ and $K_{\underline{n}}$ are known. To start the iteration an initial value of the estimate, $\hat{\underline{m}}(1|0)$, together with the associated covariance matrix,
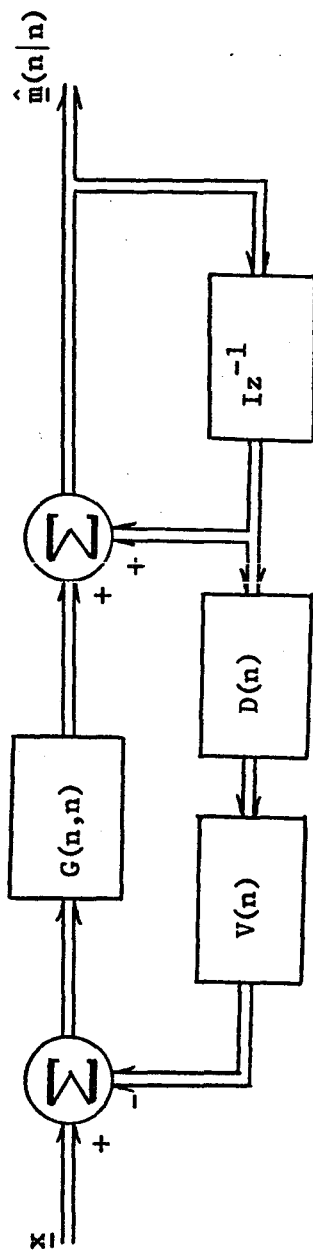
Figure 4.1   The Recursive Filter

$P(1|0)$, are assumed. Consider the vectors $\underline{m}_d$ and $\hat{\underline{m}}(1|0)$ as points belonging to a signal space Ω. Since the covariance matrix $P(1|0)$ reflects the uncertainty about the estimate $\hat{\underline{m}}(1|0)$, let S be a hyper-sphere with radius equal to $\sqrt{tr[P(1|0)]}$ which encloses the point $\hat{\underline{m}}(1|0)$. As the estimate $\hat{\underline{m}}(n|n)$ moves closer to the true value $\underline{m}_d$ the radius of the hypersphere shrinks. We assert that

Lemma 1:

The estimate $\hat{\underline{m}}(n|n)$ will converge to the true value $\underline{m}_d$ with probability 1 if and only if $\underline{m}_d \; \epsilon \; S$ throughout the range of n.

Proof:

By the projection theorem

$$\underline{m}_d = \hat{\underline{m}} + \tilde{\underline{m}} \; .$$

By the triangle inequality

$$||\underline{m}_d|| \leq ||\hat{\underline{m}}|| + ||\tilde{\underline{m}}|| \; .$$

But

$$\sqrt{tr[P(n|n-1)]} = ||\tilde{\underline{m}}||$$

Therefore, $\underline{m}_d$ is always an interior point of S. In the limit as $\tilde{\underline{m}} \to \underline{0}, \hat{\underline{m}} \to \underline{m}_d$. Suppose we define the subspace S as a feasible region. Convergence is assured if and only if the true value $\underline{m}_d$ is interior to the feasible region.

To examine the convergence properties of the (non-adaptive) recursive algorithm, we consider a one dimensional baseband case, where

we have advanced one step in time. Let

(i) $p(1|0)$ be the initial value of the covariance,

(ii) $p(1|1)$ be the next covariance to be estimated,

(iii)   k be the total covariance of multiplicative and additive
         noise,

(iv) $g(1,1)$ be the gain factor, and

(v) $v(1) = 1$ (for the received signal to be at baseband).

From equation (4.28) we have

$$g(1,1) = \frac{p(1|0)}{p(1|0) + k}$$

From equation (4.27) we have

$$p(1|1) = p(1|0)(1 - \frac{p(1|0)}{p(1|0)+k})^2 + (\frac{p(1|0)}{p(1|0)+k})^2 . k.$$

Simplifying, we get

$$p(1|1) = \frac{p(1|0)k}{p(1|0)+k} < p(1|0) .$$

Thus, the covariance is decreasing with time. With the covariance k being

constant, the gain factor also decreases with time. Provided Lemma 1 is

satisfied, the estimate approaches the true value so that the updating

component of the recursive algorithm becomes less important after each

iteration. Eventually when $P(n|n) \rightarrow 0$, the estimate $\hat{\underline{m}}(n|n) \rightarrow \underline{m}_d$.

Although it is satisfying to note that the recursive algorithm

converges with probability 1, under favourable conditions governed by

Lemma 1, its application is feasible only if $\underline{m}_d$ remains time-invariant

throughout the observation interval. For a train of rectangular pulses free from intersymbol interference, $\underline{m}_d$ remains constant only within a duration T_o, where T_o is the information symbol duration. It is imperative, therefore, that convergence should be attained within a fraction of T_o seconds. In order for the estimator to track $\underline{m}_d$, every time $\underline{m}_d$ assumes a new value the estimation process must be restarted such that $\underline{m}_d$ is an interior point to a hypersphere with radius $\sqrt{\text{tr}[P(n|n-1)]}$, at the instant of time n. That is, the covariance matrix $P(n|n)$ cannot be a strictly monotonically decreasing function throughout the observation interval, otherwise the recursive estimation process will diverge. In section 4.4 we propose an adaptive realization of the recursive filter to permit tracking of a time-variant signal.

4.4 Adaptive Implementation of the Recursive Filter

As stated in the preceding section the recursive filter re-presented by equations (4.30), (4.28) and (4.27) requires a knowledge of the covariance matrices $K_m(n|n-1)$ and $K_n(n|n-1)$. Moreover, this recursive filter has absolute convergent property. If the signal is time varying, the filter as it stands, cannot track the time-varying signal. That is, in the presence of time varying signals the recursive algorithm diverges. To make the filter a tracking one we must sacrifice absolute convergence, at the same time we have to compute the covariance matrices K_m, K_n and $P(n|n)$ during each iteration cycle, or at least every L iteration cycles, where L is the updating period. Computation of covariance matrices is diffucult if not impossible. It becomes

necessary to devise techniques whereby the necessity to compute covariance matrices is avoided.

In this section we assume the received signal has been successfully demodulated (by means of synchronous demodulation, section 2.5), i.e., the input signal is at baseband. Then in equation (4.30) the matrix V(n) becomes an identity matrix and the signal vector $\underline{x}$ becomes the baseband signal vector $\underline{u}$. To simplify notation, we assume further that the input signal is real. This assumption entails no loss of generality since a complex variable is equivalent to two real variables in quadrature. The estimator represented by equation (4.30) becomes

$$\hat{\underline{m}}(n|n) = \hat{\underline{m}}(n|n-1) + G(n,n)[\underline{u}(n) - D(n) \hat{\underline{m}}(n|n-1)] \qquad (4.31)$$

where

$$G(n,n) = P(n|n-1)[D(n)[P(n|n-1) + K_{\underline{m}}(n|n-1) + K_{\underline{n}}(n|n-1)]]^{-1}. \qquad (4.32)$$

Let

$$\underline{b}(n|n-1) = G(n,n)[\underline{u}(n) - D(n) \hat{\underline{m}}(n|n-1)]$$

be a vector. Then the corresponding time function b(t) is given by

$$\underline{b}(t) = \int_{\Gamma} g(t,\tau)[\underline{u}(\tau) - \int_{\Gamma} d(y) \underline{m}(\tau-y)dy]d\tau \qquad (4.33)$$

where Γ is specified by the reciprocal of the signal bandwidth. Substituting equation (4.33) into (4.31) we have

$$\hat{\underline{m}}_{n}(t) = \hat{\underline{m}}_{n-1}(t) + \int_{\Gamma} g_{n}(t,\tau)[\underline{u}_{n}(\tau) - \int_{\Gamma} d(y) \hat{\underline{m}}_{n-1}(\tau-y)dy]d\tau \qquad (4.34)$$

where the subscript n denotes the iteration cycle. In discrete form (4.34) becomes

$$\hat{m}_{n,j} = \hat{m}_{(n-1),j} + \sum_{i=1}^{M} g_{n,ij} (u_{n,i} - \sum_{k=1}^{M} d_k \hat{m}_{(n-1),ki}) \, , \qquad (4.35)$$

$$j=1,\ldots,M$$

where

$$M = \lceil \Gamma/T_s \rceil \, ,$$

T_s = the sampling period, and

$\lceil \cdot \rceil$ denotes integer part of.

Consider the case where the observed signal is a scalar. The channel model and its dual is depicted in Figure 4.2. We then have

$$\underline{u} \rightarrow u, \quad D \rightarrow \underline{d} \text{ and } G \rightarrow \underline{g} \quad ,$$

where

$$u = \underline{d}^t [\underline{m} + \underline{n}]$$

$$= \underline{d}^t \underline{m}_d + \underline{d}^t \underline{m}_r + \underline{d}^t \underline{n}$$

$$= m_d + m_r + n \quad .$$

Equation (4.35) reduces to

$$\hat{m}_{n,j} = \hat{m}_{(n-1),j} + g_{n,j} (u_n - \sum_{i=1}^{M} d_i \hat{m}_{(n-1),i}) \quad . \qquad (4.36)$$

Also, we have

$$m_d = \underline{d}^t \underline{m}_d$$

$$= \underline{d}^t (\hat{\underline{m}} + \tilde{\underline{m}})$$

$$= m^* + \overset{v}{m} \, , \qquad (4.37)$$

where

$$m_n^* = \underline{d}^t \hat{\underline{m}}$$
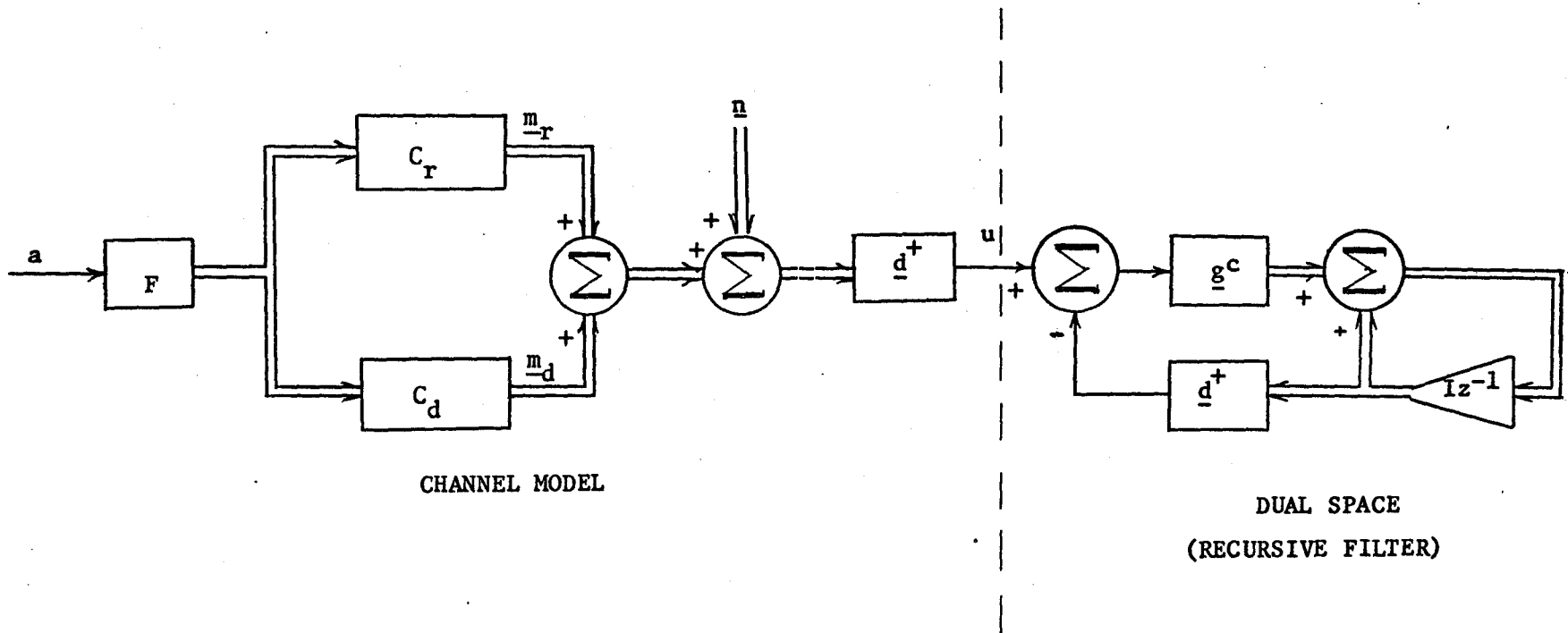
Figure 4.2   Reception of a Scalar Quantity by Recursive Filtering

$$= \sum_{i=1}^{M} d_i \hat{m}_{n,i}$$

$$= m^*_{n-1} + \sum_{j=1}^{M} d_j \, g_{n,j} (u_n - m^*_{n-1}) \tag{4.38}$$

is the scalar estimate, and

$$\overset{\lor}{m} = \underline{d}^t \, \underline{\tilde{m}} \tag{4.39}$$

is the error in making the estimate. The recursive filter given by equations (4.31) and (4.32) may then be optimized by minimizing the mean square error defined by

$$e \overset{\Delta}{=} E\{(m_d - m^*_n)^2\} \tag{4.40}$$

where m_d and m^*_n are given by (4.37) and (4.38), respectively. Substituting (4.38) and (4.39) in (4.40), we get

$$e = \overline{m_d^2} - \overline{2m_d m^*_n} + \overline{[m^*_n]^2}$$

$$= m_d^2 - \overline{2m_d[m^*_{n-1} + \sum_j d_j g_{n,j}(u_n - m^*_{n-1})]}$$

$$+ \overline{[m^*_{n-1} + \sum_j d_j g_{n,j}(u_n - m^*_{n-1})]^2}$$

$$= \overline{m_d^2} - \overline{2m_d m^*_{n-1}} - \overline{2\sum_j d_j g_{n,j}(m_d - m^*_{n-1})(u_n - m^*_{n-1})}$$

$$+ \overline{[m^*_{n-1}]^2} + \sum_j \sum_i d_j d_i g_{n,j} g_{n,i} \overline{(u_n - m^*_{n-1})_j (u_n - m^*_{n-1})_i} \tag{4.41}$$

where the over bar denotes ensemble average. We note that

$$u_n - m^*_{n-1} = \overset{\lor}{m}_{n-1} + m_r + n \ ,$$

$$m_d - m^*_{n-1} = \overset{\lor}{m}_{n-1} \ ,$$

and that $\overset{\cup}{m}_{n-1}$, m_r, and n are zero mean statistically independent random variables. Using the above information in equation (4.41), the mean square error is given by

$$e = \overline{m_d^2} - \overline{2m_d m^*_{n-1}} - 2\underset{j}{\Sigma} d_j g_{n,j} p(j,i)$$

$$+ \overline{[m^*_{n-1}]^2} + \underset{j}{\Sigma} \underset{i}{\Sigma} d_j d_i g_{n,j} g_{n,i} [p(j,i) + k_m(j,i) + k_n(j,i)] \qquad (4.42)$$

where

$$p(j,i) = E\{\overset{\cup}{m}_{(n-1),j} \overset{\cup}{m}_{(n-1),i}\} \text{ is the error covariance,}$$

$$k_m(j,i) = E\{m_{rj} m_{ri}\} \text{ is the covariance of the random component}$$
$$\text{of the channel output, and}$$

$$k_n(j,i) = E\{n_j n_i\} \text{ is the covariance of the additive noise.}$$

The mean square error represented by equation (4.42) is a minimum when

$$\frac{\partial e}{\partial g_{n,j}} = 0$$

and

$$\frac{\partial^2 e}{\partial g_{n,j} \ \partial g_{n,i}} > 0 \quad .$$

Taking the first pratial derivative, we get

$$\frac{\partial e}{\partial g_{n,j}} = -2d_j p(j,i) + 2\underset{i}{\Sigma} d_j d_i g_{n,i} [p(j,i) + k_m(j,i) + k_n(j,i)] . \qquad (4.43)$$

Equating the right member of (4.43) to zero, we get

$$p(j,i) = \underset{i}{\Sigma} d_i g_{n,i} [p(j,i) + k_m(j,i) + k_n(j,i)] . \qquad (4.44)$$

In vector notation (4.44) becomes

$$P(n|n-1) = \underline{g} \; \underline{d}^t [P(n|n-1) + K_{\underline{m}}(n|n-1) + K_{\underline{n}}(n|n-1)] \; . \tag{4.45}$$

Now, if the observed signal is a vector valued quantity, then

$$\underline{g} \rightarrow G \quad \text{and} \quad \underline{d} \rightarrow D,$$

and (4.45) becomes

$$G(n,n) = P(n|n-1)[D(n) \; [P(n|n-1) + K_{\underline{m}}(n|n-1) + K_{\underline{n}}(n|n-1)]]^{-1} \; ,$$

which is equation (4.32). We thus have demonstrated that the optimality of the recursive filter given by equations (4.31) and (4.32) is maintained, yet the gain function may be optimized through application of the minimum mean square error criterion. Taking the second order partial derivative yields

$$\frac{\partial^2 e}{\partial g_{n,j} \; \partial g_{n,i}} = 2d_j d_i [p(j,i) + k_m(j,i) + k_n(j,i)] > 0 \; ,$$

since the covariance matrices are positive definite, as shown in Appendix E. The gradient of the mean square error, e, with respect to the filter gain is given by equation (4.43). In terms of scalar variables, (4.43) becomes

$$\frac{\partial e}{\partial g_{n,j}} = -2 \; d_j [E\{\overset{\vee}{m}(u_n - m^*_{n-1})\} - \sum_{i=1}^{M} d_i g_{n,i} E\{(u_n - m^*_{n-1})^2\}]$$

$$= -2d_j [E\{[m_d - m^*_{n-1} - \sum_i d_i g_{n,i}(u_n - m^*_{n-1})](u_n - m^*_{n-1})\}]$$

$$= -2d_j [E\{(m_d - m^*_n)(u_n - m^*_{n-1})\}]$$

$$= -2d_j [E\{\overset{\vee}{m}_n(u_n - m^*_{n-1})\}] \quad , \tag{4.46}$$

where

$$\overset{\cup}{m} = m_d - m^* .$$

Equation (4.46) is the gradient of the error surface as a function of the gain vector $\underline{g}$. Because of the quadratic form of the error, the error surface is convex and hence has a unique minimum. The gain, $g_{n,j}$, may then be approximated by an iterative formula of the form

$$
\begin{aligned}
g_{n+1,j} &= g_{n,j} + \frac{\alpha'}{2} \frac{\partial e}{\partial g_{n,j}} \\
&= g_{n,j} - \alpha' \, d_j E\{\overset{\cup}{m}_n (u_n - m^*_{n-1})_j \} \\
&= g_{n,j} - \alpha_j \, E\{\overset{\cup}{m}_n (u_n - m^*_{n-1})_j \} .
\end{aligned}
\tag{4.47}
$$

The adaptive filter as represented by equations (4.38) and (4.47) is shown in Figure 4.3,[†] where α_j is taken to be constant for all j and the ensemble average has been approximated by a time average. In the case of passive detection where one does not know what decision to make, we may modify (4.47) through application of the following linear estimation procedures (Wilks, 1962):

    (1) m^* is a linear combination of the set $\{\hat{m}_j\}$, i.e.,

$$m^* = d_1 \hat{m}_1 + d_2 \hat{m}_2 + \ldots + d_M \hat{m}_M$$

for a finite population of size M.

    (2) m^* is a sample mean of the set $\{\hat{m}_j\}$ if

$$d_1 + d_2 + \ldots + d_M = 1 .$$

[†] Throughout this thesis the symbol $\longrightarrow \boxed{\Sigma} \longrightarrow$ denotes accumulation.

(3) Since $\overset{\cup}{m}$ has zero mean value, m* is also an unbiased estimator of the true value, m_d. The variance of the unbiased estimate has a unique minimum which occurs for

$$d_1 = d_2 = \ldots = d_M = 1/M \ .$$

(4) The random variable $\hat{m}_j$ is an unbiased estimate of the sample mean m*, i.e., $E\{\hat{m}_j\} = E\{m*\}$. Hence $\tilde{m}_j$ is an unbiased estimate of $\overset{\cup}{m}$.

(5) Using procedures (1) to (4), we may make the approximation

$$\tilde{m}_j \doteq m* - \hat{m}_j$$

(6) We replace $\overset{\cup}{m}$ in equation (4.47) by its unbiased estimate $\tilde{m}_j$.

(7) The d_j's are now constants of equal value; we incorporate these into the scalar constant α' and write $\alpha = \alpha' d_j$.

(8) Since the time average is an unbiased estimate of the ensemble average, we replace $E\{\cdot\}$ by $\frac{1}{K} \sum\limits_{i=n-K}^{n} (\cdot)_i$.

Procedures (1) to (8) enable (4.47) to be written as

$$g_{n+1,j} = g_{n,j} - \alpha \frac{1}{K} \sum_{i=n-K}^{n} [\tilde{m}_{n,j} (u_n - m*_{n-1})_j]_i \qquad (4.48)$$

The recursive formula of equation (4.38) together with (4.48) form the adaptive filter which is depicted in Figure 4.4. The convergence properties of the gain formula are described in Appendix F.1.
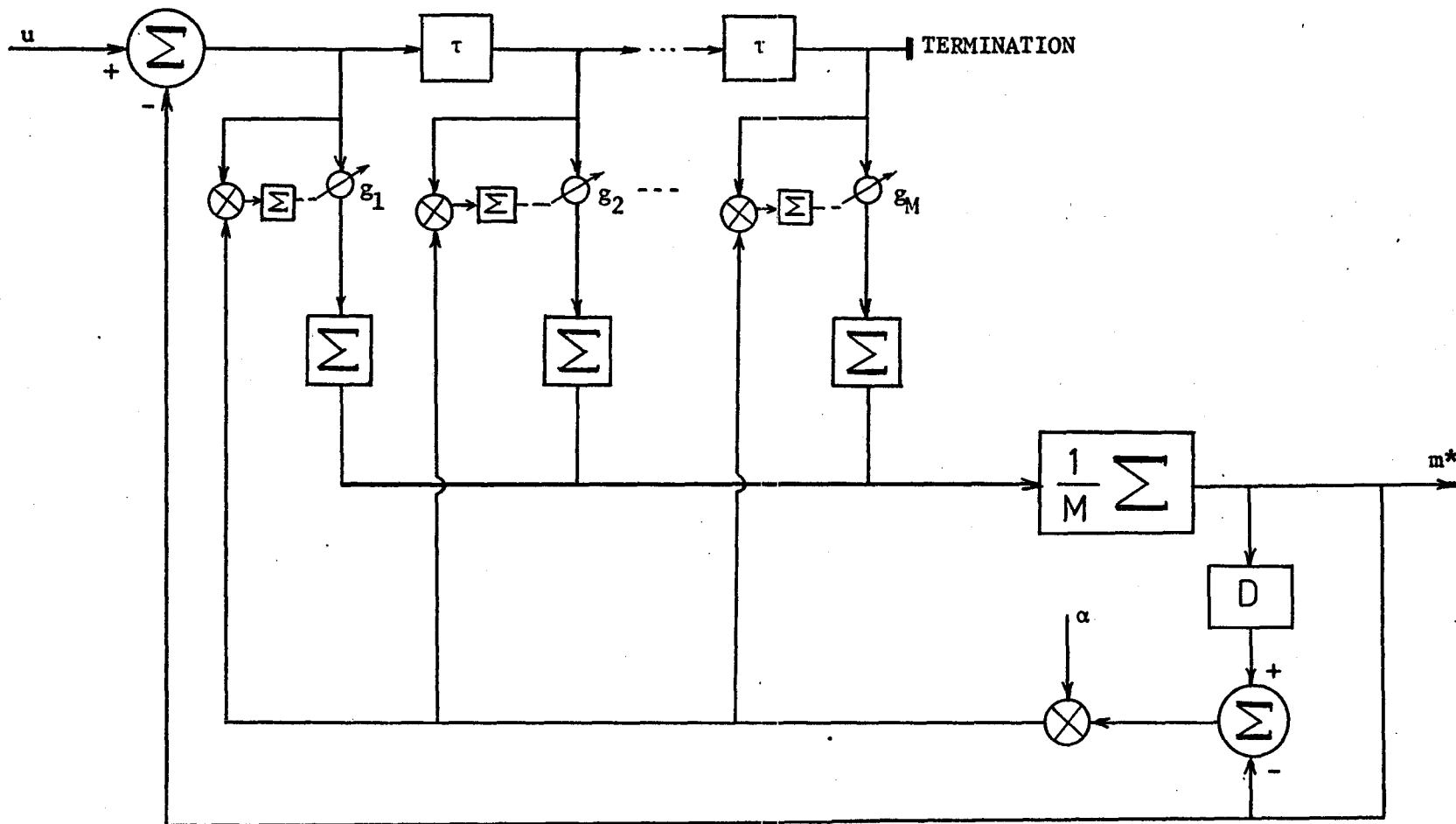
Figure 4.3   Decision Directed Implementation of the
Adaptive Recursive Filter with $d_1 = \ldots = d_M = \frac{1}{M}$
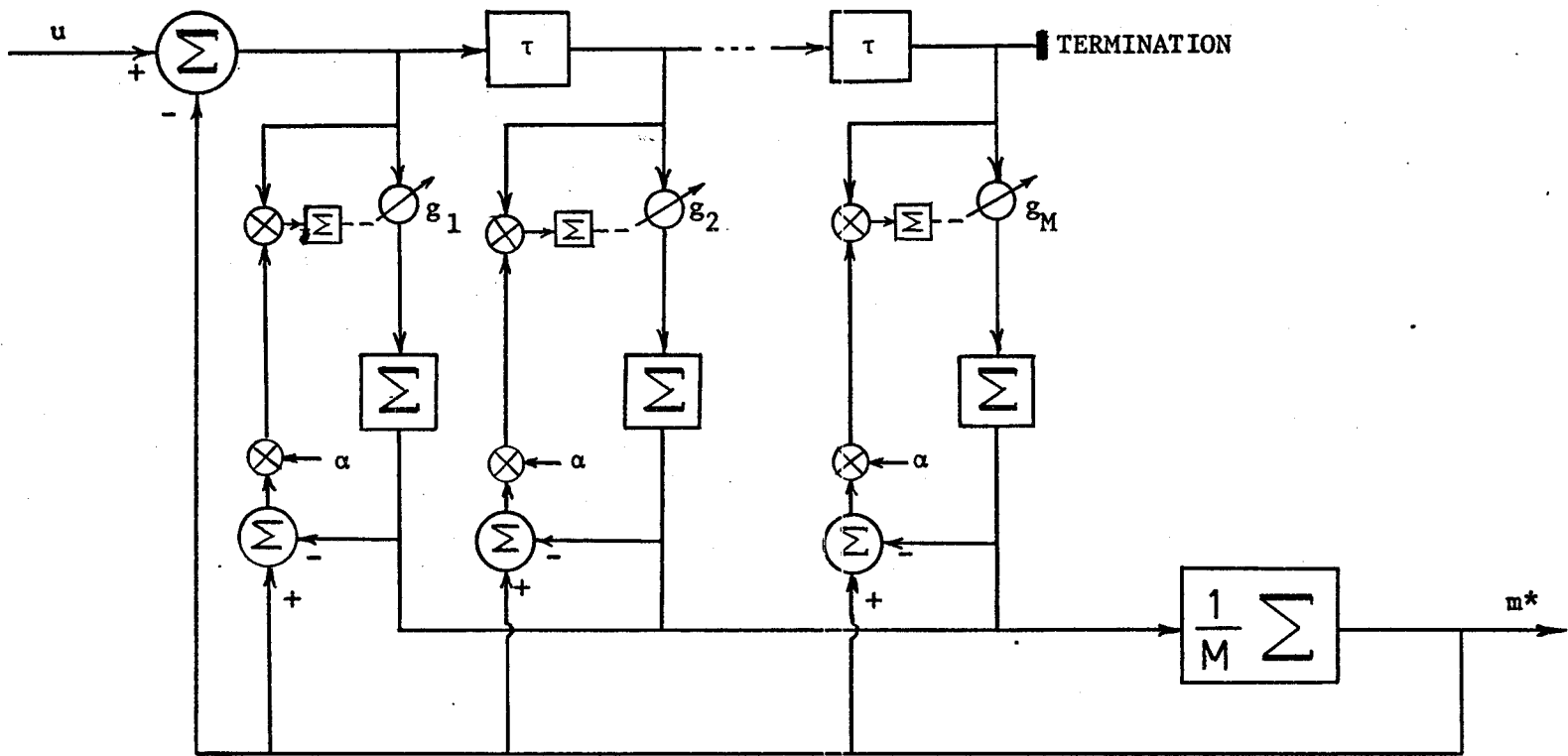
Figure 4.4   An Alternative Form of the Adaptive Recursive Filter

4.5 Reception of Bandpass Signals

Consider the reception of a scalar bandpass signal, $x(t)$. The recursive formula of (4.30) becomes

$$\hat{\underline{m}}(n|n) = \hat{\underline{m}}(n|n-1) + \underline{g}(n,n)[x(n) - v^c(n)\ \underline{d}^+(n)\ \hat{\underline{m}}(n|n-1)] \qquad (4.49)$$

The gain formula of (4.28) may be modified to become

$$\underline{g}(n,n) = v^c(n)[P(n|n-1)[P(n|n-1) + K_m(n|n-1) + \underline{K}_n(n|n-1)]^{-1}]\underline{d}$$

$$= v^c(n)\ \underline{g}'(n,n) \qquad (4.50)$$

where $v(n)$ is a scalar quantity which contains the carrier frequency

(see section 3.3), and

$\underline{g}' = [P(n|n-1)[P(n|n-1) + K_m(n|n-1) + K_n(n|n-1)]^{-1}]\underline{d}$ is the

gain vector of the low-pass network.

From section 3.3 we have

$$x(n) = v^c(n)\underline{d}^+(n)\hat{\underline{m}}(n) = v^c(n)m*(n)\ .$$

Therefore

$$v^c(n) = \frac{\partial \hat{x}(n)}{\partial\ m*(n)}\ . \qquad (4.51)$$

The receiver represented by equations (4.49), (4.50) and (4.51) is depicted in Figure 4.5 in terms of complex valued quantities. A practical realization, suggested by the technique employed in section 2.4, is depicted in Figure 4.6. The receiver described in this section has the remnants of a synchronous demodulator-estimator device, where the demodulation action is characteristically similar to a phase-locked
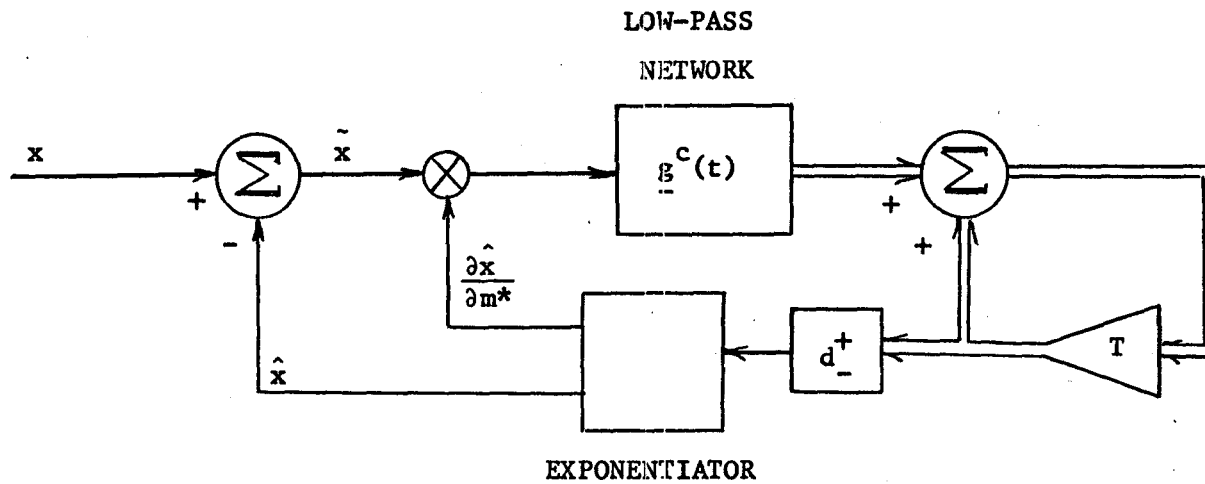
Figure 4.5   Recursive Filter for Bandpass Signals
(A Demodulator-Estimator Device)

Figure 4.3 or 4.4
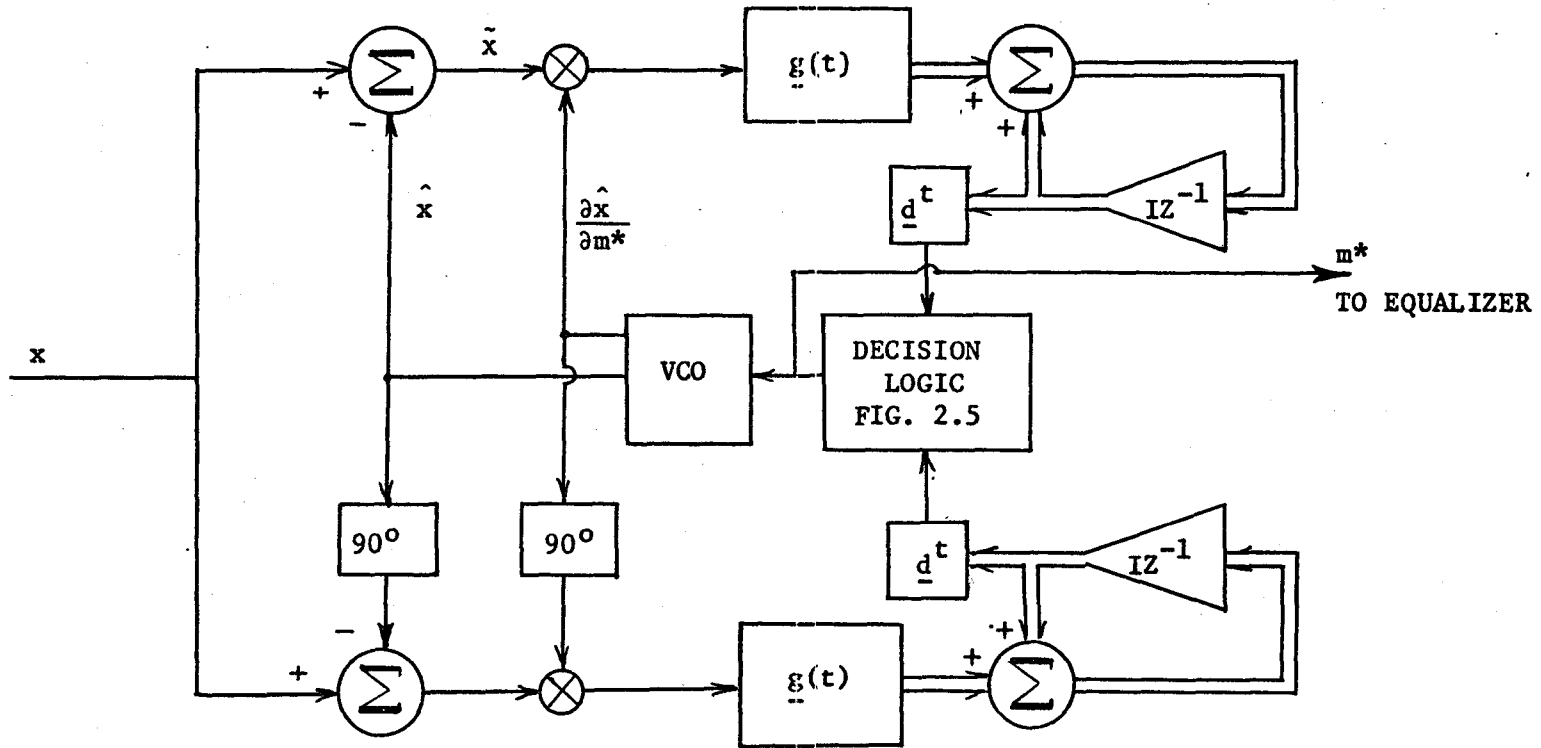
Figure 4.6   Possible Mechanization of the Demodulator-Estimator Receiver

loop. The mechanization of the low-pass network has been described in the preceding section.

4.6 Summary

The adaptive filter derived in this Chapter has the following properties:

(1)   The filter is optimum in that it is a linear conditional estimator.

(2)   The gains are functions of the second order moment statistics of the observed process.   In this way statistical information is built into the gain function.

(3)   The adaptive filter seeks to unscramble the mean value.   If intersymbol interference corrupting the pulse is completely random, then the adaptive filter can smooth out certain intersymbol interference effects.   However, the problem of combatting intersymbol interference is the subject of the next Chapter.

CHAPTER 5

A GENERAL FORMULATION OF THE ADAPTIVE EQUALIZER

5.1 Introduction

Intersymbol interference resulting from time-dispersion may
be minimized by means of time-domain equalization. The various forms
of non-recursive adaptive equalizers that have been proposed (Lucky,
1966; Proakis and Miller, 1969) thus far for digital communication
systems have been formulated with an assumed frame of reference (e.g.,
the centre tap denoting present time in the transversal filter implemen-
tation). The equalizer itself does not, however, know that such a frame
of reference exists. In the formulation described in this Chapter a
means of tracking the frame of reference is explicitly built into the
non-recursive adaptive equalizer.

A recursive adaptive equalizer is derived through the application
of a sufficient stability constraint. The best adaptive equalizer is
shown to be a cascade connection of a non-recursive section and a recursive
section. An unconstrained recursive equalizer is also proposed. The
unconstrained recursive adaptive equalizer is simpler to implement than
the constrained one. It is shown in Chapter 6 that because of the
capability for the complete equalizer to track its own frame of reference,
instability may not be a problem. Moreover, the unconstrained recursive
equalizer offers faster convergence.

In the usual operation of a digital communications receiver the
output of the adaptive filter derived in Chapter 4 is the input to the

95

adaptive equalizer formulated in this Chapter. In Chapter 4 we used the

symbol m* to represent the adaptive filter output, where the asterisk

denotes the estimate. In this Chapter we also employ the asterisk to

denote the estimate. To avoid any confusion which may arise in reading

this Chapter we let x represent the input to the equalizer, while bearing

in mind that when the adaptive filter and the equalizer are connected in

cascade, m* and x represent the same physical quantity at the input to

the equalizer. The use of x to represent the equalizer input serves the

following purpose: The equalizer may be viewed as a system by itself,

not necessarily as a member of a chain of subsystems. This Chapter may

be read without reference to the preceding Chapters. In what follows

the terms 'weights' and 'tap gains' are being used synonymously.

5.2 Statement of the Equalization Problem

Consider a real time series $\{x_j | a\}$, where the $\{x_j\}$ is the set

of observables and a is the desired parameter to be estimated. The

objective is to operate on $\{x_j\}$ in order to produce an estimate, a^*, such

that the mean square error between the desired parameter and the estimate

is a minimum.

Suppose now a dispersive channel is excited by a unit impulse.

The normalized channel response is a train of pulses, with $x_0 = 1$, as

illustrated in Figure 5.1. The subset $\{x_j\}$, $j \neq 0$, constitutes the source

of intersymbol interference. If the set $\{x_j\}$ spans the entire space X,

then the total energy in the space X is constant. Conservation of energy

imposes the requirement that any attempt to operate on the set $\{x_j\}$ to
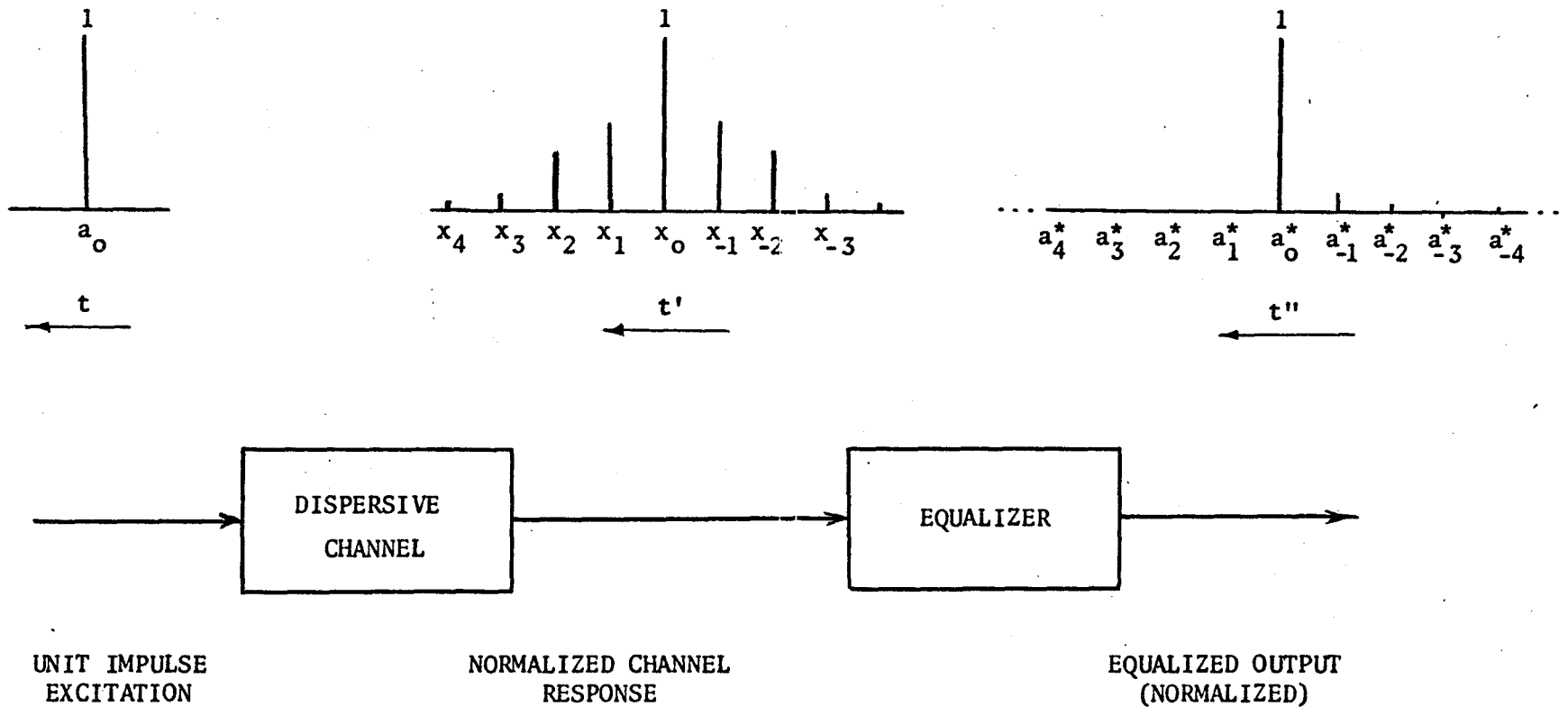
Figure 5.1 A Simple Illustration of Time Dispersion

97

recover a_0 is merely an attempt to re-allocate the energy distribution. The objective is to redistribute the energy in the received signal such that the sample at the reference point in the estimate, a_0^*, is maximized in favour of all others. This process is known as equalization. The values of the smeared sidelobes at the equalizer output, $\{a_n^*\}$, $n \neq 0$, approach zero as the memory of the equalizer approaches infinity in both positive and negative directions with respect to the frame of reference. If, therefore, the equalizer has finite memory, it cannot be expected to exactly reproduce the desired parameter, a_0. In designing the equalizer the objective is to minimize the error between the desired parameter, a_0, and its estimate, a_0^*.

When the channel is time-varying, as often is the case in practice, it is desirable for the equalizer to be time-varying too, that is, adaptive. However, in making the equalizer adaptive a frame of reference needs to be identified and tracked at all times in order to maintain synchronization. The adaptive equalization algorithm to be described in section 5.3 incorporates such a feature.

5.3 Derivation of the Non-recursive Adaptive Equalizer

Before proceeding to derive the structure of the equalizer, we wish to make two definitions:

(1)   A process which permits the extraction of a parameter implicit in the set of observables shall be referred to as an estimation process. For example, an operation on a time series $\{x_j|a\}$, where $\{x_j\}$ is the set of observables and a is the parameter to

be estimated, is an estimation process.

(2)   A process which permits a member of a set to be approximated

by a linear combination of all other members in the same set

is referred to as a linear learning process.

Suppose the equalizer has a finite memory of 2M + 1 cells with

a set of weights $\{W_j(a)\}$, j = -M,..., -1, 0, 1,..., M. The point j = 0

is to be chosen as frame of reference, normally referred to as the

'present time'. The set $\{a_n\}$ implicit in the observables are the desired

parameters. In accordance with definition (1) the set $\{W_j(a)\}$ are,

therefore, weights in an estimation process. An estimate of a_n at the

n^{th} iteration is given by a linear combination of the set of observables

$\{x_j\}$, that is,

$$a_n^{*'} = \sum_{j=-M}^{M} W_{n,j}(a)x_{n-j} \qquad (5.1)$$

where * denotes estimate and the prime is used to distinguish the estimate

given by equation (5.1) from an augmented estimate to be introduced later.

Equation (5.1) is a truncated form of the convolution sum,

which constitutes the basis of a conventional equalizer. The error at

the nth iteration cycle is defined as:

$$e_n \triangleq a_n - a_n^* \quad .$$

An optimum set of weights $\{W_j(a)\}$ is to be found by minimizing the mean

square error:

$$E\{e_n^2\} = E\{a_n - a_n^{*'})^2\} \quad . \qquad (5.2)$$

Substituting equation (5.1) in (5.2), we obtain

$$E\{e_n^2\} = E\{a_n^2\} - 2 \sum_{j=-M}^{M} W_{n,j}(a) \, K(x_{n-j}, \, a_n)$$

$$+ \sum_{i=-M}^{M} \sum_{j=-M}^{M} W_{n,i}(a) \, W_{n,j}(a) \, K(x_{n-j}, \, x_{n-i}) \qquad (5.3)$$

where

$$K(x_{n-j}, \, a_n) \equiv E(x_{n-j} \, a_n)$$

and

$$K(x_{n-j}, \, x_{n-i}) \equiv E(x_{n-j} \, x_{n-i})$$

are second-order moments. The mean square error is a quadratic function of the weights $\{W_j(a)\}$ and hence possesses a global minimum. From calculus of variations, it is known that a minimum will be attained when the following conditions are simultaneously satisfied:

(i) $\qquad \dfrac{\partial}{\partial W_{n,j}(a)} \quad E\{e_n^2\} = 0,$

(ii) $\qquad \dfrac{\partial^2}{\partial W_{n,j}(a) \, \partial W_{n,i}(a)} \, E\{e_n^2\} > 0.$

Taking the first partial derivative yields

$$\dfrac{\partial}{\partial W_{n,j}(a)} \, E\{e_n^2\} = 2 \sum_{i=-M}^{M} W_{n,i}(a) \, K(x_{n-j}, \, x_{n-i}) - 2K(x_{n-j}, \, a_n)$$

Using condition (i) yields $\qquad\qquad\qquad\qquad$ . . . (5.4)

$$K(x_{n-j}, \, a_n) = \sum_{i=-M}^{M} W_{n,i}(a) \, K(x_{n-j}, \, x_{n-i}), \; j=-M,\ldots,-1,0,1,\ldots,M$$

$\qquad\qquad\qquad\qquad\qquad\qquad\qquad\qquad\qquad$ . . . (5.5)

Equation (5.5) is recognized to be a Wiener-Hopf like equation. The stationary point thus reached is indeed a minimum, since the second partial derivative has the value

$$\frac{\partial^2}{\partial W_{n,j}(a)\ W_{n,i}(a)}\ E\{e_n^2\} = 2K(x_{n-j},\ x_{n-i}) > 0$$

and since the second-order moment matrix, $[K(x_{n-j},\ x_{n-i})]$, is positive definite (see Appendix E).

The conventional equalizer based on equation (5.1) is non-optimum in that it lacks the ability to track its own frame of reference. To overcome this limitation, we introduce an augmented estimate of the form:

$$a_n^* = a_n^{*'} + f(x_n,\ x_n^*) , \tag{5.6}$$

where $f(x_n,\ x_n^*)$ is an auxiliary function, x_n is the chosen frame of reference and x_n^* is an approximation of x_n as obtained by a learning process (see definition (2)). Let

$$f(x_n,\ x_n^*) = \sum_{j=-M}^{M} \delta W_{n,j}(a)\ x_{n-j} , \tag{5.7}$$

that is, we allow the auxiliary function to be a linear combination of the input data such that the coefficients are increments, $\delta W_j(a)$, in the weights of the conventional equalizer. Using equation (5.7) in (5.6) the augmented estimate becomes

$$a_n^* = \sum_{j=-M}^{M} W_{n,j}(a)\ x_{n-j} + \sum_{j=-M}^{M} W_{n,j}(a)\ x_{n-j} = \sum_{i=-M}^{M} W_{n+1,j}(a)\ x_{n-j}$$

$$\ldots (5.8)$$

Equation (5.8) represents a non-causal system in that, at the nth iteration, it requires a knowledge of the weights belonging to the $(n+1)^{th}$ iteration. In the sequel, we attempt to overcome the non-causal difficulty by incorporating a learning feature in the structure of the equalizer. It thus turns out that the learning algorithm provides a self-synchronizing capability for the overall equalizer structure.

Following a procedure similar to that used in deriving equation (5.5) the set of weights, $\{W_{n+1,j}(a)\}$, can be shown to be optimum if they are solutions of the set of $2M + 1$ equations:

$$K(x_{n-j}, a_n) = \sum_{i=-M}^{M} W_{n+1,i}(a) \, K(x_{n-j}, x_{n-i}), \quad j=-M,\ldots,-1,0,1,\ldots,M$$

$$\ldots \quad (5.9)$$

Equating the right-hand-sides of equations (5.5) and (5.9), we have

$$\sum_{i=-M}^{M} W_{n,i}(a) \, K(x_{n-j}, x_{n-i}) = \sum_{i=-M}^{M} W_{n+1,i}(a) \, K(x_{n-j}, x_{n-i}) \, .$$

$$\ldots \quad (5.10)$$

Re-arranging equation (5.10), we have

$$\delta W_{n,0}(a) \, K(x_{n-j}, x_n) = \sum_{\substack{i=-M \\ i \neq 0}}^{M} K(x_{n-j}, x_{n-i})(W_{n,i}(a) - W_{n+1,i}(a))$$

or

$$K(x_{n-j}, x_n) = \sum_{\substack{i=-M \\ i \neq 0}}^{M} K(x_{n-j}, x_{n-i}) \, \frac{W_{n,i}(a) - W_{n+1,i}(a)}{\delta W_{n,0}(a)}$$

$$j=-M,\ldots,-1,1,\ldots,M \quad . \quad (5.11)$$

The left-hand-side of equation (5.11) is a second-order moment, or a correlation, of the input data set with the reference sample. Thus,

equation (5.11) indicates that in order to realize the augmented estimate of equation (5.6), the system requires an approximation of x_n by a learning process as described earlier (see definition 2). Let $\{W_{n,j}(x_n)\}$, $j = -L, \ldots, -1, 1, \ldots, L$ be a set of weights. For $L = M$, x_n^* is representable by

$$x_n^* \triangleq \sum_{\substack{j=-M \\ j \neq 0}}^{M} W_{n,j}(x_n)\, x_{n-j} \qquad (5.12)$$

The weights $\{W_{n,j}(x_n)\}$ are optimum if they are solution of the set

$$K(x_{n-j}, x_n) = \sum_{\substack{i=-M \\ i \neq 0}}^{M} K(x_{n-j}, x_{n-i})\, W_{n,i}(x_n), \quad j=-M,\ldots,-1,1,\ldots,M \qquad \ldots (5.13)$$

Equating the right-hand-sides of equations (5.11) and (5.3), we get

$$W_{n,i}(x_n) = \frac{W_{n,i}(a) - W_{n+1,i}(a)}{\delta W_{n,0}(a)}, \quad i=-M,\ldots,-1,\,1,\ldots,M \qquad (5.14)$$

Equation (5.14) may be re-arranged to yield

$$W_{n+1,i}(a) - W_{n,i}(a) + \delta W_{n,0}(a)\, W_{n,i}(x_n) = 0 \qquad (5.15a)$$

or

$$W_{n+1,i}(a) = W_{n,i}(a) - \delta W_{n,0}(a)\, W_{n,i}(x_n), \quad i=-M,\ldots,-1,1,\ldots,M \qquad \ldots (5.15b)$$

Substituting equation (5.15b) into equation (5.8), the augmented estimate becomes

$$a_n^* = \sum_{j=-M}^{M} W_{n,j}(a)\, x_{n-j} + \delta W_{n,0}(a)\, x_n - \delta W_{n,0}(a) \sum_{\substack{j=-M \\ j \neq 0}}^{M} W_{n,j}(x_n) x_{n-j} \qquad \ldots (5.16)$$

The summation in the last term on the right-hand-side of equation (5.16) is recognized to the right-hand-side of equation (5.12). Therefore, we may write

$$a_n^* = \sum_{j=-M}^{M} W_{n,j}(a) x_j + \delta W_{n,0}(a) (x_{n,0} - x_{n,0}^*) \qquad (5.17)$$

Equation (5.17) together with equations (5.12) and (5.15) constitute the basis of the new equalization algorithm. Although equation (5.17) represents the optimum structure, $\delta W_{n,0}(a)$ is not available, since, in a causal system, output must follow input. To make the structure of (5.17) realizable, we use $\delta W_{n-1,0}(a)$ in lieu of $\delta W_{n,0}(a)$, thereby relinquishing a certain degree of optimality.

From equation (5.15) we see that

$$\delta W_{n,i}(a) = -\delta W_{n,0}(a) \, W_{n,i}(x_n), \quad i=-M,\ldots,-1,\, 1,\ldots,M \qquad (5.18)$$

That is, the increments in the weights $\{W_{n,i}(a)\}$, $i \neq 0$, are direct functions of the increment in $W_{n,0}(a)$ and the weights of the learning loop. It is in this way that the overall equalizer structure is provided with a self-synchronizing capability.

5.4 Recursive Algorithm for the Weighting Functions

The Wiener-Hopf like equations (5.5) and (5.13) are rather difficult to solve. An alternative approach is to use the iterative formula:

$$\underline{W}_{n+1} = \underline{W}_n + \frac{\beta}{2} \underline{P}_n \qquad (5.19)$$

where β is a (small) scalar constant chosen to escalate the optimization

process, and $\underline{p}_n$ is a direction (gradient) vector. With appropriate

designation for a weight vector, a recursive formula for the set of

weights in the learning loop may be written as:

$$W_{n+1,j}(x_n) = W_{n,j}(x_n) + \frac{\beta}{2} p_{n,j}, \quad j=-M,\ldots,-1,1,\ldots,M \qquad (5.20)$$

where

$$p_{n,j} = \frac{\partial \eta_n^2}{\partial W_{n,j}(x_n)} = -2E(\eta_n x_{n-j}), \qquad (5.21)$$

$$\eta_n = x_n - x_n^*.$$

Substituting equation (5.21) in (5.20), we get

$$W_{n+1,j}(x_n) = W_{n,j}(x_n) - \beta E(\eta_n \, x_{n-j}), \quad j=-M,\ldots,-1,1,\ldots,M \qquad (5.22)$$

Similarly, an iterative formula for the weight at the reference point in

the estimation loop is given by

$$W_{n+1,0}(a) = W_{n,0}(a) + \frac{\alpha}{2} q_{n,0}, \qquad (5.23)$$

where

$$q_{n,0} = \frac{\partial e_n^2}{\partial W_{n,0}(a)} = -2E(e_n x_n) \qquad (5.24)$$

$$e_n = a_n - a_n^* = a_n - \left(\sum_{j=-M}^{M} W_{n,j}(a)x_j + \delta W_{n,0}(a)\eta_n \right). \qquad (5.24a)$$

Use of equation (5.24) in (5.23) gives

$$W_{n+1,0}(a) = W_{n,0}(a) - \alpha E(e_n x_n) \qquad (5.25)$$

The recursive formulae of equations (5.22) and (5.25) together with equation

(5.15) provide the adaptive structure for the equalizer as represented by equation (5.17). The recursive algorithms of equations (5.22) and (5.25) require expectation computations explicitly. This poses some difficulty in a physical implementation. However a sample mean may be used as an unbiased estimate of the expected value. Hence, for the purpose of implementation, equations (5.22) and (5.25) may be modified, respectively, as follows:

$$W_{n+1,j}(x_n) = W_{n,j}(x_n) - \beta \frac{1}{K} \sum_{k=n-K}^{n} n_k \, x_{k-j} \; ,$$

$$n \geqslant K,$$

$$j = -M,\ldots,-1,1,\ldots,M \qquad (5.26)$$

$$W_{n+1,0}(\alpha) = W_{n,0}(\alpha) - \alpha \frac{1}{K} \sum_{k=n-K}^{n} e_k \, x_k \; ,$$

$$n \geqslant K \qquad (5.27)$$

A functional block diagram of the modified non-recursive adaptive equalizer, as prescribed by equations (5.17), (5.12), (5.15), (5.26) and (5.27), is shown in Figure 5.2. The convergence properties of the new equalizer is described in Appendix F.

5.5 Recursive Equalization

5.5.1 Constrained Optimization

The unit-impulse response of a dispersive channel may be represented, in z-transform notation, as

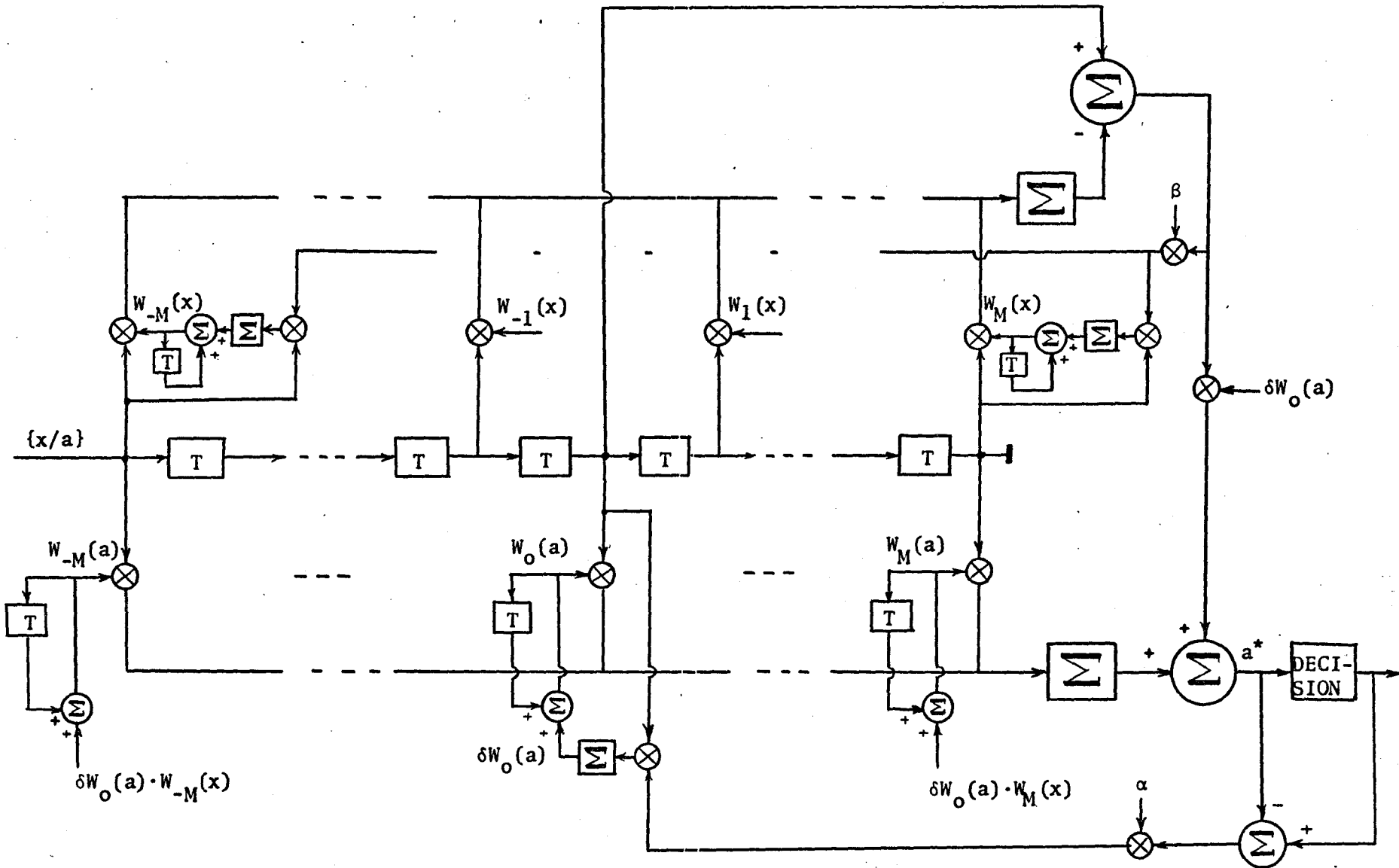$$I(z) = \sum_{i=-N}^{N} x_i \, z^{-i} \qquad (5.28)$$

Figure 5.2 The Modified Non-recursive Adaptive Equalizer

or, equivalently,

$$I(z) = \sum_{i=1}^{N} x_{-i} z^i + x_0 + \sum_{i=1}^{N} x_i z^{-1} \qquad (5.29)$$

where $i = 0$ is chosen as the frame of reference with $x_0 = 1$, and N is the maximum dispersion. The term $\sum_{i=1}^{N} x_{-i} z^i$ represents the past data, while $\sum_{i=1}^{N} x_i z^{-i}$ represents future data. To equalize the effect of $\sum_{i=1}^{N} x_{-i} z^i$ we are required to use a non-recursive section, while to equalize the effect of $\sum_{i=1}^{N} x_i z^{-i}$ we may use a recursive section with a finite number of elements, (which is equivalent to a non-recursive section of infinite memory). Thus, the discrete transfer function of the desired equalizer may, in general, be written in the form:
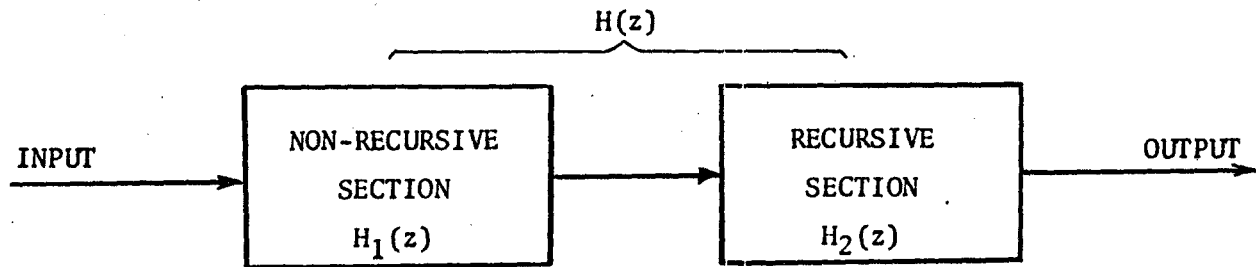
$$H(z) = \frac{\sum_{i\epsilon I} W_i z^{-i}}{1 + \sum_{j\epsilon J} b_j z^{-j}} \qquad (5.30)$$

where $I + J = 2M + 1$, that is, the number of memory cells in the overall equalizer is precisely the same as before. We may rewrite equation (5.30) as

$$H(z) = (\sum_{i\epsilon I} W_i z^{-1}) \cdot (\frac{1}{1 + \sum_{j\epsilon J} b_j z^{-j}}) = H_1(z) \cdot H_2(z) \qquad (5.31)$$

that is, we may realize the $H(z)$ as a cascade of a non-recursive, $H_1(z)$, and a recursive, $H_2(z)$, section, as depicted in Figure 5.3a. In Figure 5.3b we have shown an implementation of the overall structure using tapped delay lines.

Austin (1967) has used a similar idea, but with an entirely different interpretation. The present formulation differs from Austin's

$H(z)$

INPUT → | NON-RECURSIVE SECTION $H_1(z)$ | → | RECURSIVE SECTION $H_2(z)$ | → OUTPUT

(a)

INPUT

$\delta W_o(a)$

OUTPUT

NON-RECURSIVE SECTION

RECURSIVE SECTION
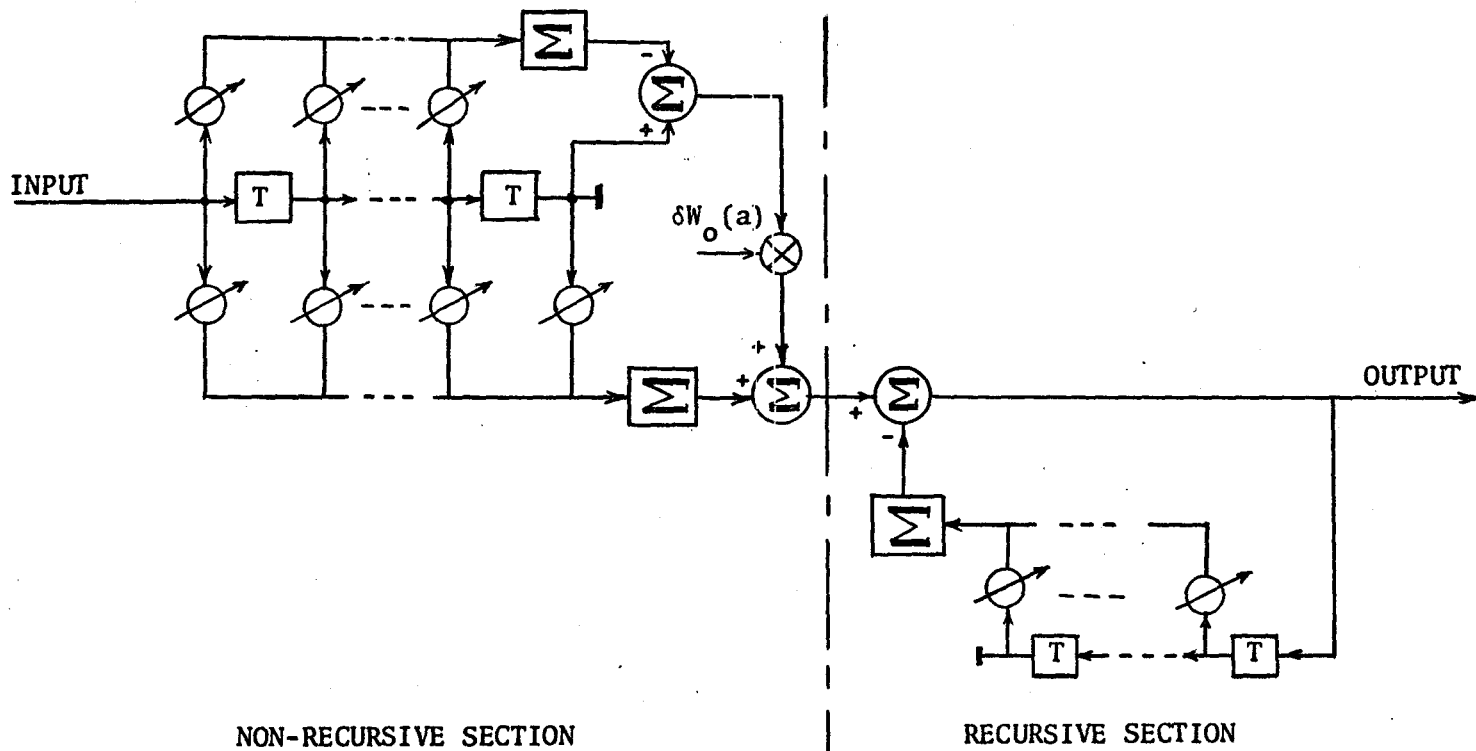
(b)

Figure 5.3   A Complete Adaptive Equalizer - (a) Cascade Connection
(b) Tapped-delay Line Implementation

work in at least two respects:

(i)   Austin deals with known channels and his system is non-adaptive. In our case the channel is unknown and the resultant equalizer is adaptive.

(ii)   Austin makes a decision on the equalized output and feeds back the decision in his recursive loop, assuming the decision made is correct; in so doing he incorporates a nonlinearity in the recursive loop. In our case we do not require the use of a nonlinear element within the recursive loop; stability of the system is assured through application of an appropriate constraint.

The non-recursive component of the overall equalizer of Figure 5.3 has been dealt with in section 5.3. There, we introduce a learning feature so that the structure of the equalizer is provided with a capability for tracking its own frame of reference. The frame of reference, that is, the $i = 0$ tap, is always contained in the non-recursive section. Assuming the system has attained adaptation, we may consider the output of the non-recursive section as given effectively by the first term of equation (5.17). We may, therefore, consider the non-recursive section as having, effectively, a discrete transfer function given by

$$H_1(z) = \sum_{i \epsilon I} W_i z^{-i} \tag{5.32}$$

The z-transform of the output sequence of the non-recursive section is obtained by multiplying equations (5.29) and (5.32):

$$Y(z) = I(z) \, H_1(z)$$

$$= \sum_{j=1}^{K} y_{-j} z^j + y_0 + \sum_{j=1}^{N} y_j z^{-j} \qquad (5.33)$$

where

$$K + N + 1 = 2M + 1,$$

or

$$K = 2M - N,$$

and

$$y_0 = 1.$$

The convolution of an input sequence with the system impulse response is illustrated in Figure 5.4, where the frame of reference has been chosen to be that tap which is nearest the recursive section. From Figure 5.4, we see that the y_{-j}'s, j positive, are small, while the y_j's, j positive, are essentially the same as the initial dispersions x_i, i positive.

The output of the non-recursive section is further equalized by the recursive section, which is designed to minimize the effect of $\sum_{j=1}^{N} y_j z^{-j}$. To do this the recursive section only needs N elements, so that the non-recursive section can be allotted $2M - N$ degrees of freedom for equalizing past data, that is, data preceding the $i = 0$ point.

From Appendix G, a sufficient but not necessary condition for the recursive section, represented by

$$H_2(z) = \frac{1}{1 + \sum_{j=1}^{N} b_j z^{-j}} \qquad (5.34)$$

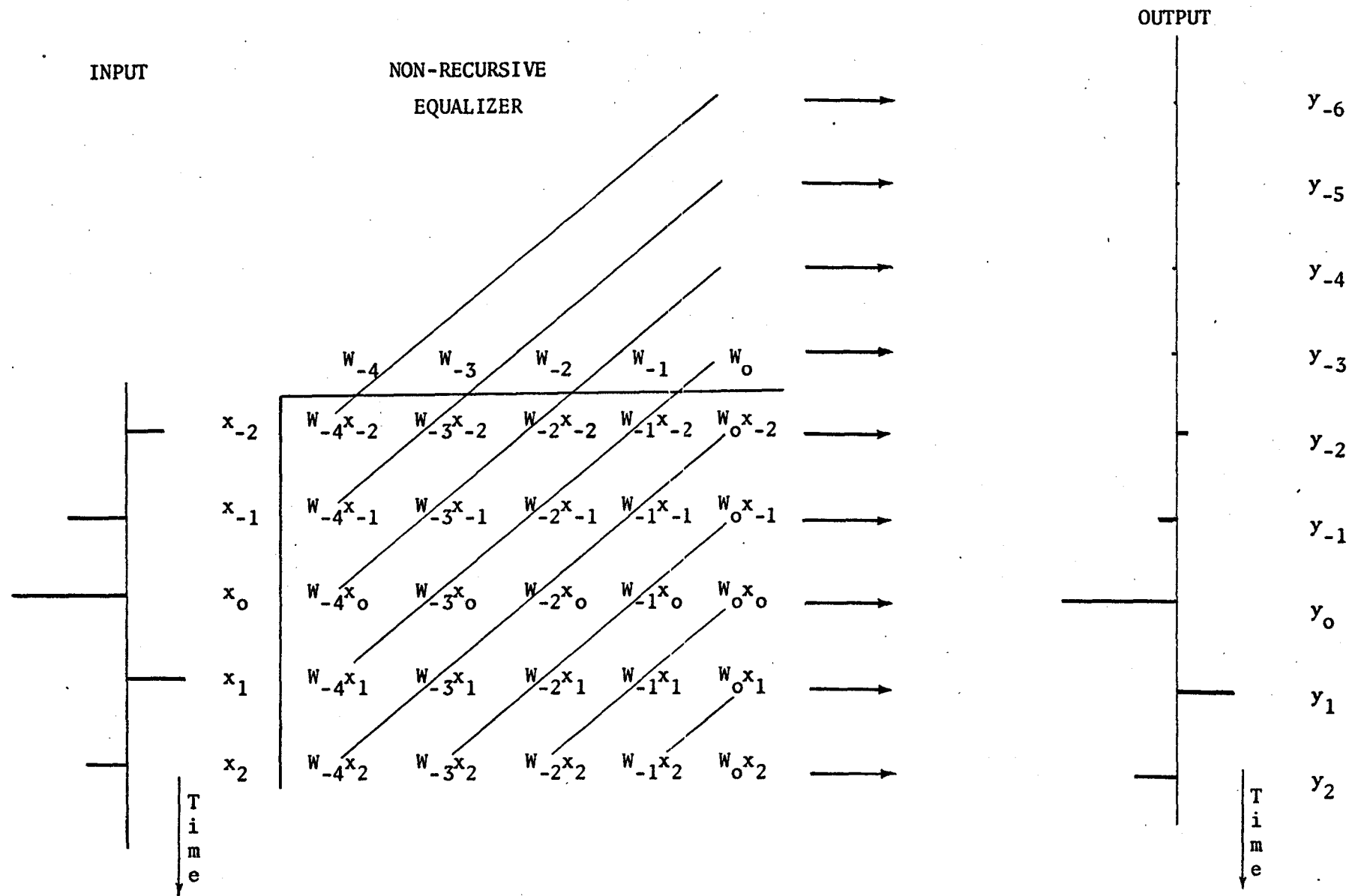to be stable is that the following inequality constraint be satisfied:

Figure 5.4   A Convolution Map for Two Sequences

$$\sum_{j=1}^{N} |b_j| < 1 \quad .$$ (5.35)

For optimum equalization of the term $\sum_{j=1}^{N} y_j z^{-i}$, we require that

$$H_2(z) \left[1 + \sum_{j=1}^{N} y_j z^{-i} \right] = 1$$

or

$$H_2(z) = \cfrac{1}{1 + \sum_{j=1}^{N} y_j z^{-i}} \quad .$$

If

$$\sum_{j=1}^{N} |y_j| < 1,$$ (5.36)

then clearly the system can provide exact equalization and yet be stable. If, however, the condition (5.36) is not satisfied, the system represented by equation (5.34) will operate in a sub-optimum manner. However, through appropriate selection for the frame of reference, one could make

$$\sum_{j=1}^{N} |y_j| < 1 \quad .$$

The output of the recursive section is given by

$$a_n^* = y_n - \sum_{i=1}^{N} b_i a_{n-i}^* \quad .$$ (5.37)

In the absence of a reference sequence, we will use a decision directed approach to implement the adaptive algorithm. Letting the decisions be $\{a_n\}$, the error at the nth iteration cycle is

$$e_n = a_n - a_n^* = a_n - y_n + \sum_{i=1}^{N} b_i a_{n-i}^* \quad .$$

The criterion for optimization is one of minimizing the mean square error

subject to the constraint of inequality (5.35). The objective function is thus

$$G = E\{e_n^2\} + \lambda \sum_{i=1}^{N} |b_{n,i}| \qquad (5.38)$$

where λ is the Lagrange multiplier, and

$$E\{e_n^2\} = E\{(a_n - y_n)^2\} + 2 \sum_{i=1}^{N} b_{n,i} E\{(a_n - y_n)a_{n-i}^*\}$$

$$+ \sum_{i,j=1}^{N} b_{n,i} b_{n,j} E\{a_{n-i}^* \ a_{n-j}^*\} \ . \qquad (5.39)$$

For a minimum to occur, we must satisfy conditions (i) and (ii) of section 5.3. Taking the first partial derivative of G with respect to $b_{n,i}$, we obtain

$$\frac{\partial G}{\partial b_{n,i}} = 2E\{(a_n - y_n)a_{n-i}^*\} + 2 \sum_j b_{n,j} E(a_{n-i}^* \ a_{n-j}^*) + \lambda Sgnb_{n,j}$$

$$\quad . \ . \ . \ (5.40)$$

We will choose λ so that $E\{e_n^2\}$ is a minimum and $\sum_{i=1}^{N} |b_i| < 1$. Equating the right-hand-side of equation (5.40) to zero and using the result in equation (5.39), we obtain

$$E\{e_n^2\} = E\{(a_n - y_n)^2\} + \{\sum_{j=1}^{N} b_{n,j} E(a_n - y_n)a_{n-j}^*\} - \frac{\lambda}{2} \sum_{j=1}^{N} |b_{n,j}|$$

$$\quad . \ . \ . \ (5.41)$$

In the absence of the constraint of inequality (5.35) the minimum mean square error is given by the first two terms on the right-hand-side of equation (5.41). We choose a λ such that

$$\frac{\lambda}{2} \sum_{j=1}^{N} |b_{n,j}| > 0 \ ,$$

so that the constrained minimum is smaller than the unconstrained minimum. This can be done by introducing a slack variable r, 0 < r < 1, such that the following identity holds:

$$E\{(a_n - y_n)^2\} + \sum_{j=1}^{N} E\{(a_n - y_n)a_{n-j}^*\} - \frac{\lambda}{2} \sum_{j=1}^{N} |b_{n,j}|$$

$$\equiv r[E\{(a_n - y_n)^2\} + \sum_{j=1}^{N} b_{n,j} E\{(a_n - y_n)a_{n-j}^*\}] .$$

The above equation can be re-arranged to yield

$$\frac{\lambda}{2} \sum_{j=1}^{N} |b_{n,j}| = (1 - r)[E\{(a_n - y_n)^2\} + \sum_{j=1}^{N} b_{n,j} E\{(a_n - y_n)a_{n-j}^*\}] .$$

$$. . . (5.42)$$

With respect to equation (5.42), we make the following interesting observations:

(i) $(1 - r) < 1$, since $0 < r < 1$

(ii) $\sum_{j=1}^{N} |b_{n,j}| < 1$, inequality (5.35)

(iii)   choose λ for which $\sum_{j=1}^{N} |b_{n,j}| = (1 - r)$.

Observation (iii) enables equation (5.42) to be written explicitly as

$$\lambda = 2[E(a_n - y_n)^2 + \sum_{j=1}^{N} b_{n,j} E\{(a_n - y_n)a_{n-j}^*\}] \qquad (5.43)$$

Using equation (5.43) in (5.40) and noting that

(i) $E\{(a_n - y_n)a_{n-i}^* + \sum_{j=1}^{N} b_{n,j} E(a_{n-i}^* a_{n-j}^*) = E\{e_n a_{n-i}^*\}$,

(ii) $E\{(a_n - y_n)^2\} + \sum_{j=1}^{N} b_{n,j} E\{(a_n - y_n)a_{n-j}^*\} = E\{v_n e_n\}$,

where $v_n = a_n - y_n$, we obtain

$$\frac{\partial G}{\partial b_{n,i}} = 2\{E(e_n \, a^*_{n-i}) + E(v_n \, e_n) \, \text{Sgn} \, b_{n,i}\} \qquad (5.44)$$

Let the coefficients b_i be computed from the iterative formula

$$b_{n+1,i} = b_{n,i} + \frac{\gamma}{2} \, \frac{\partial G}{\partial b_{n,i}} \, , \quad i = 1, \ldots, N \qquad (5.45)$$

Then, using equation (5.44) in (5.45), we obtain the recursive algorithm

$$b_{n+1,i} = b_{n,i} + \gamma[E(e_n a^*_{n-i}) + E(v_n \, e_n) \, \text{Sgn} \, b_{n,i}] \, . \qquad (5.46)$$

The convergence properties of the recursive algorithm of equation (5.46) are given in Appendix F.4. It is shown there that γ is negative lying in the range

$$0 > \gamma > \frac{-2}{\lambda_{max}}$$

where λ_{max} is the maximum eigenvalue of the matrix with entries

$$(E(a^*_{n-i} \, a^*_{n-j}) + E(v_n \, a^*_{n-i}) \, \text{Sgn} \, b_{n,i}).$$

5.5.2 Recursive Formula for the Reference Tap Gain of the Complete Equalizer

Replacing a^*_n by y_n in equation (5.17), the output of the non-recursive section is given by

$$y_n = \sum_{j=-M}^{M} W_{n,j}(a) \, x_j + \delta W_{n,0}(a) \eta_n \qquad (5.47)$$

The mean square error of the complete equalizer is given by equation (5.39).

Substituting (5.47) in (5.39) and taking the first partial derivative with respect to $W_{n,j}(a)$, we get

$$\frac{\partial E\{e_n^2\}}{\partial W_{n,j}(a)} = -2E\{x_j \, a_n\} + 2 \sum_{i=-M}^{M} W_{n,i}(a) \, E(x_i \, x_j) + 2\delta W_{n,0}(a)E\{\eta_n x_j\}$$

$$- 2 \sum_{i=1}^{N} b_{n,i} \, E\{x_j \, a_{n-i}^*\} \tag{5.48}$$

Factoring out x_j, we may rewrite (5.48) as

$$\frac{\partial E\{e_n^2\}}{\partial W_{n,j}(a)} = -2E\{(a_n - \sum_{i=-M}^{M} W_{n,i}(a)x_i - \delta W_{n,0}(a) \, \eta_n + \sum_{i=1}^{N} b_{n,i}a_{n-i}^*)x_j\}$$

$$= -2E\{e_n \, x_j\} \tag{5.49}$$

where

$$e_n = a_n - (\sum_{i=-M}^{M} W_{n,i}(a)x_i + \delta W_{n,0}(a)\eta_n - \sum_{i=1}^{N} b_{n,i}a_{n-i}^*)$$

$$= a_n - (y_n - \sum_{i=1}^{N} b_{n,i} \, a_{n-i}^*)$$

$$= a_n - a_n^* \tag{5.50}$$

Equation (5.49) evaluated at j=0 is identical to equation (5.24) with the exception that the error is given by (5.50) rather than by (5.24a). Except for the above modification the iterative formula for the reference weight is, therefore, given by equation (5.25), as in the non-recursive equalizer case. The iterative formula for the weights in the learning loop remains the same, as given by equation (5.22). Using unbiased estimates in the manner shown in equations (5.26) and (5.27), a tapped
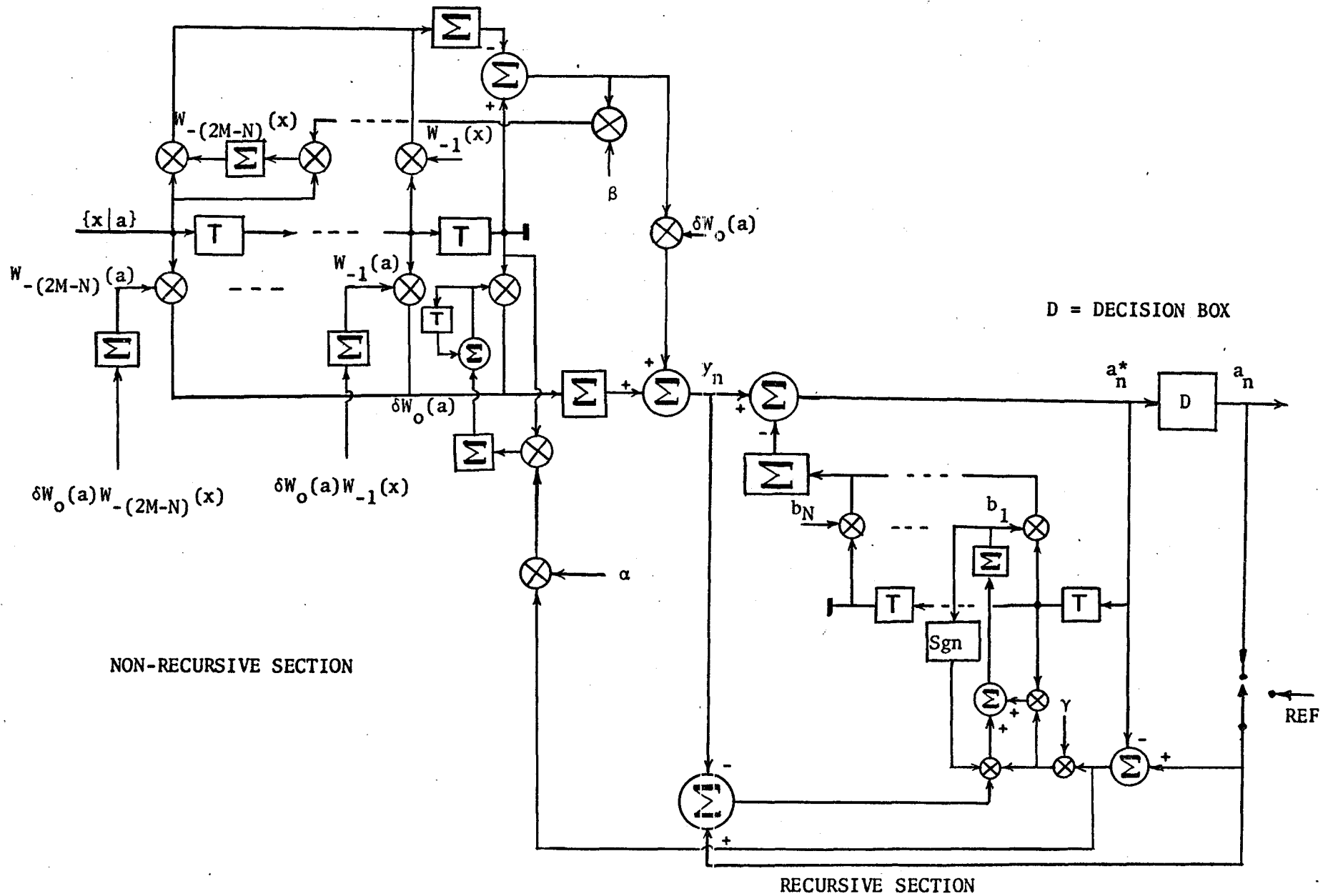
Figure 5.5   The Constrained Adaptive Equalizer

delay line implementation of the constrained recursive equalizer is shown in Figure 5.5.

5.5.3 Unconstrained Optimization

When no stability constraint is imposed in the optimization of the recursive equalizer, the objective function is simply given by the mean square error:

$$G = E\{e_n^2\}$$

The gradient with respect to $b_{n,i}$ is then given by

$$\frac{\partial G}{\partial b_{n,i}} = 2E\{e_n \, a^*_{n-1}\}$$

so that the iterative formula for the recursive tap gains is given by

$$b_{n+1,i} = b_{n,i} + \gamma E\{e_n \, a^*_{n-i}\} \tag{5.51}$$

Equation (4.51) is simply (5.46) with the constraining component, $\gamma E\{v_n \, e_n\} \, \text{Sgn} \, b_{n,i}$, suppressed. The unconstrained recursive equalizer is depicted in Figure 5.6. It is seen that the unconstrained recursive equalizer is much simpler to implement than the constrained one.

5.6 Summary

It has been shown that the complete adaptive equalizer consists of a non-recursive and a recursive section in cascade. The principal results of this Chapter are:

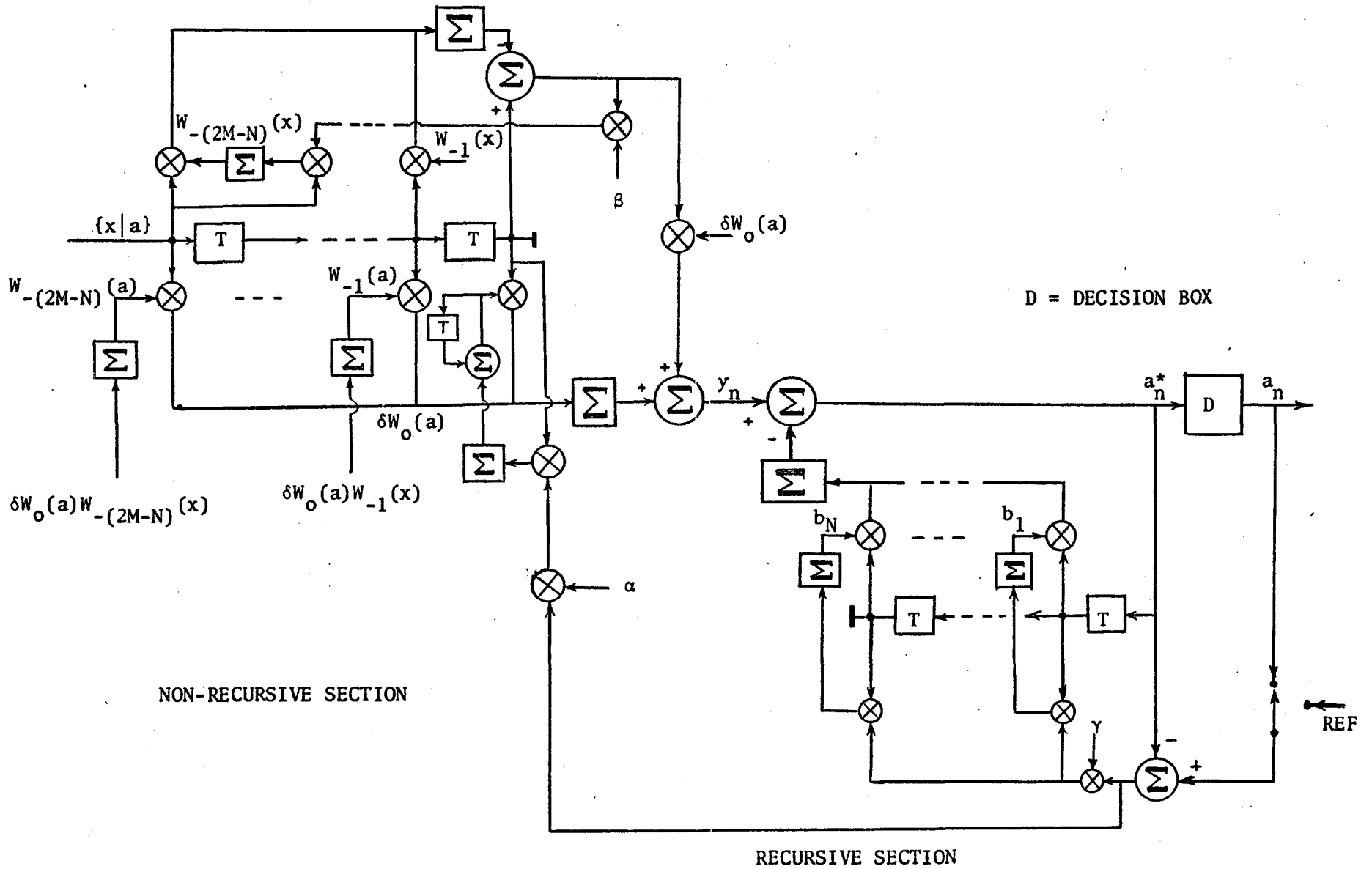(i)   There is provision for the non-recursive section to track its

Figure 5.6   The Unconstrained Adaptive Equalizer

own frame of reference.

(ii)   An adaptive algorithm for the recursive section of the equalizer, with system linearity maintained, has been derived.

(iii)   The learning loop of the equalizer helps speed up the convergence during the adaptation mode.

Without the self-synchronizing capability every tap in the non-recursive equalizer, in its random walk during the adaptation mode, is equally likely to be a frame of reference. If all the tap gains were set to zero initially (Proakis and Miller, 1969) it is possible that the system may exhibit the behaviour of a filter rather than that of an equalizer.

CHAPTER 6

PERFORMANCE EVALUATION OF THE ADAPTIVE SYSTEM

6.1 Introduction

In Chapters 2 through 5 we introduced the structure of an adaptive receiver for PAM signaling through fading dispersive channels. The feasibility of the synchronous demodulation scheme has been demonstrated with some results given in section 2.5. In this Chapter we shall discuss the significance and the implications of the adaptive signal processor (i.e., the adaptive recursive filter and the adaptive equalizer connected in cascade) and evaluate its performance by means of Monte Carlo Simulations[†]. In this thesis we are mainly concerned with a single reception problem. Although extension to diversity reception is easily done, diversity reception is not discussed. Nevertheless we do recognize the fact that diversity reception can improve the system performance.

The overall communications system is simulated and its performance evaluated in a CDC 6400 digital computer. As a test signal we chose a binary M-sequence for the following reasons:

. (1)   It can be generated rather easily, both in the computer and in the laboratory.

(2)   It is a deterministic periodic code and hence it offers the possibility of correlation decoding.

[†]Monte-Carlo simulations of the overall communications system are described in Appendix H.

122

The binary M-sequence is used to effect phase reversal modulation, which is equivalent to a double sideband suppressed carrier amplitude modulation. Since both side bands are transmitted, this type of modulation provides the transmitter with maximum efficiency. The transmitted waveform is a train of pulses the form of which is determined by a pulse shaping network. The pulses are either positive or negative as governed by the binary M-sequence. The binary signals are antipolarity, hence the term antipodal signals. The correlation coefficient, ρ, given by expression (2.28), is equal to -1.

Although we centre our discussions on digital communications, in actual fact the transmitted and received signals are continuous. The observed continuous waveform is often digitized by means of sampling as governed by the Sampling Theorem introduced by Nyquist (1928). The Sampling Theorem states that, in order to recover the information, the sampling rate must at least be twice the highest frequency content of the signal. Provided the Sampling Theorem is satisfied and the system is properly synchronized, it suffices to consider discrete data at the sampling instants. For a properly synchronized digital communication system, it is necessary and sufficient to sample the received signal once per baud. If synchronization is lacking, that is, the arrival time is unknown, it then becomes necessary to develop a synchronization scheme. A rather simple technique for searching the signal is to sample the incoming signal at a much higher rate, i.e., many samples per baud. An analysis of average power loss as a function of the number of samples per baud for the type of signaling under consideration has been described

elsewhere (Mark and Hicks, 1966). If s is the number of samples per baud, the signal processing device, e.g., the equalizer, will require s times as many memory cells as that which is needed for a properly synchronized system. However, the amount of control circuitry remains the same, but the logics are required to operate s times faster. On the other hand, if analog tapped-delay lines were employed, exactly the same amount of components is required for both, except that the logics for the latter case have to be s times as fast. Thus, over-sampling the input waveform provides a means for searching the signal. A price to be paid is the requirement of faster logics and more (digital) memory for storage. In this chapter we assume the arrival time is known and consider sampling the received waveform once per baud only.

In a discrete communication system the probability that an estimate a^* equals the true value a approaches unity as the system performance improves. Hence, the probability of error, P_e, may be used as a measure of 'goodness' in system performance. On the other hand, in the continuous case the probability of $a^*(t)=a(t)$ is, in general, zero, since any small deviations in $a^*(t)$ may not correspond to small deviations in $a(t)$. Also, simulations using a digital computer necessarily restrict all signals to assume a discrete form, whether or not quantization has been applied. Thus, error probabilities are a meaningful measure of goodness in the performance of a digital communication system. In what follows we assume demodulation has taken place so that the input to the Signal Processor is a baseband signal.

6.2   Performance of the Adaptive Recursive Filter

To refresh our memory, briefly, the structure of the Recursive Filter derived in Chapter 4 was obtained through repeated application of the projection and decomposition theorems. A formula for the filter gain, as a function of covariances, was obtained through minimization of the mean square error, where the mean square error, as a function of the filter gains, is convex and hence possesses a unique minimum. Because of the convexity property, the unique minimum may be approached by a steepest descent method. Thus, the filter gains were approximated by an iterative formula with the updating term given by a gradient function of the mean square error with respect to the filter gains. The performance of the adaptive recursive filter was examined by comparing it with that of a matched filter. We employed a raised cosine pulse and a pulse given by an RC response to a rectangular pulse (here after referred to as the RC response pulse) as test signals. The raised cosine pulse was approximated by 19 samples while the RC response pulse was approximated by 20 samples. These pulses were separately imbedded in Gaussian noise (500 samples) and subsequently detected by (19-tap and 20-tap) matched filtering and (5-tap) recursive filtering. Typical traces for a 2 dB signal-to-noise ratio are shown in Figures 6.1 and 6.2, where input signal-to-noise is defined as:

$$SNR_{in} \triangleq \frac{\text{Average Signal Power}}{\text{Noise Variance}} \qquad (6.1)$$

It is readily observed that the raised cosine pulse has better immunity against noise than the RC response pulse. As a further comparison

waveforms showing the detection of an RC response pulse in 6 dB signal-to-noise ratio are given in Figure 6.3. While the detection of the RC response pulse in 2 dB signal-to-noise is only marginal, the 6 dB case gives a clear indication of the noise rejection capability of the recursive filter.

The output signal-to-noise ratio is defined as

$$SNR_o \triangleq \frac{[\text{Peak Value - Noise Mean Value}]^2}{\text{Noise Variance}} \qquad (6.2)$$

Plots of output signal-to-noise ratio vs input signal-to-noise ratio for a 19-sample approximation, a 9-sample approximation and a 5-sample approximation of the raised cosine pulse are shown in Figures 6.4, 6.5 and 6.6, respectively. Each family of curves is upper bounded by the calculated curve for matched filter detection, with the assumption of zero mean white Gaussian noise. The computed curves are obtained by computing the sample means and the sample variances over a population of 500 noise samples and substituting in the output signal-to-noise ratio definition of equation (6.2). In Figures 6.4 to 6.6, the symbol MF refers to Matched Filter and RF refers to Recursive Filter. Examination of Figures 6.1 through 6.6 affords the following observations:

(i) Noise immunity for a particular pulse is a monotonic function of the pulse energy. In discrete systems this implies that the more samples per pulse are taken the better is the noise immunity. This phenomenon is conceptually pleasing.

(ii) The recursive filter has a large effective memory (or time constant) or, equivalently, a narrow bandwidth; it is a function
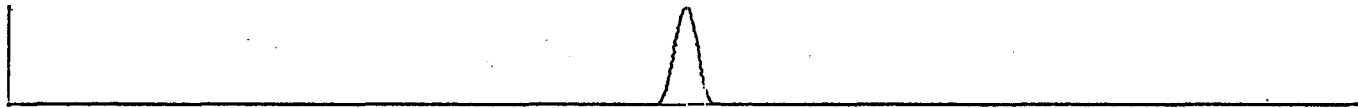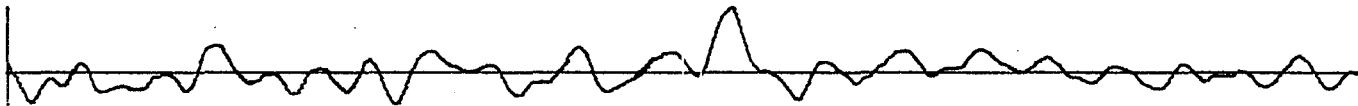
(a) 19-SAMPLE APPROXIMATION OF A RAISED COSINE PULSE

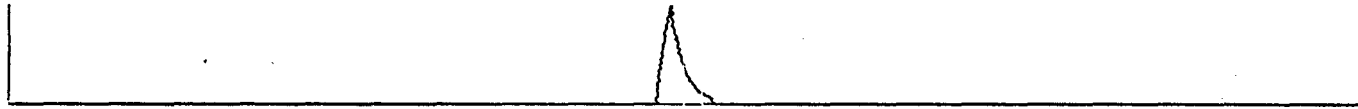(b) RAISED COSINE PULSE OF (a) IMBEDDED IN GAUSSIAN NOISE

(c) 19-TAP MATCHED FILTER OUTPUT
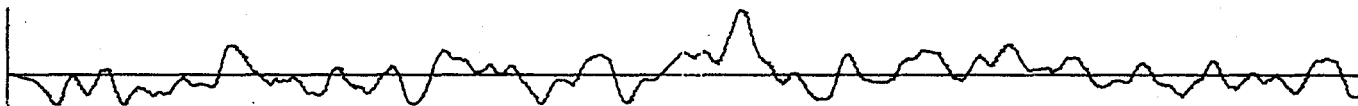
(d) 5-TAP RECURSIVE FILTER OUTPUT

Figure 6.1   Matched Filter and Recursive Filter Detection of A Raised Cosine Pulse
in 2 dB SNR Gaussian Noise

(a) 20-SAMPLE APPROXIMATION OF AN RC RESPONSE TO A RECTANGULAR PULSE

(b) PULSE OF (a) IMBEDDED IN GAUSSIAN NOISE

(c) 20-TAP MATCHED FILTER OUTPUT

(d) 5-TAP RECURSIVE FILTER OUTPUT

Figure 6.2   Matched Filter and Recursive Filter Detection of Pulse of (a)
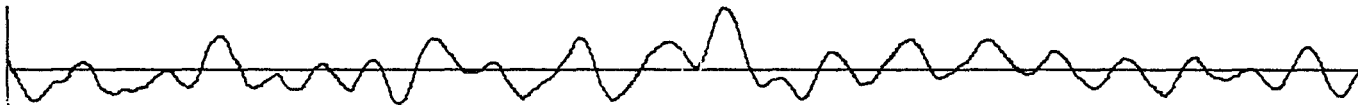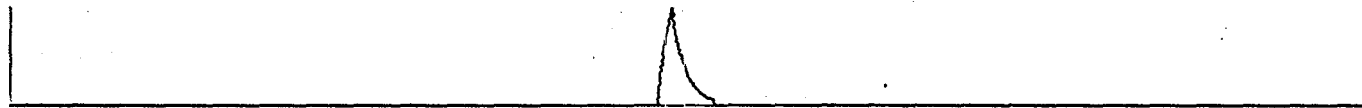in 2 dB SNR Gaussian Noise

(a) 20-SAMPLE APPROXIMATION OF AN RC RESPONSE TO A RECTANGULAR PULSE

(b) PULSE OF (a) IMBEDDED IN GAUSSIAN NOISE

(c) 20-TAP MATCHED FILTER OUTPUT

(d) 5-TAP RECURSIVE FILTER OUTPUT

Figure 6.3   Matched Filter and Recursive Filter Detection of Pulse of (a)
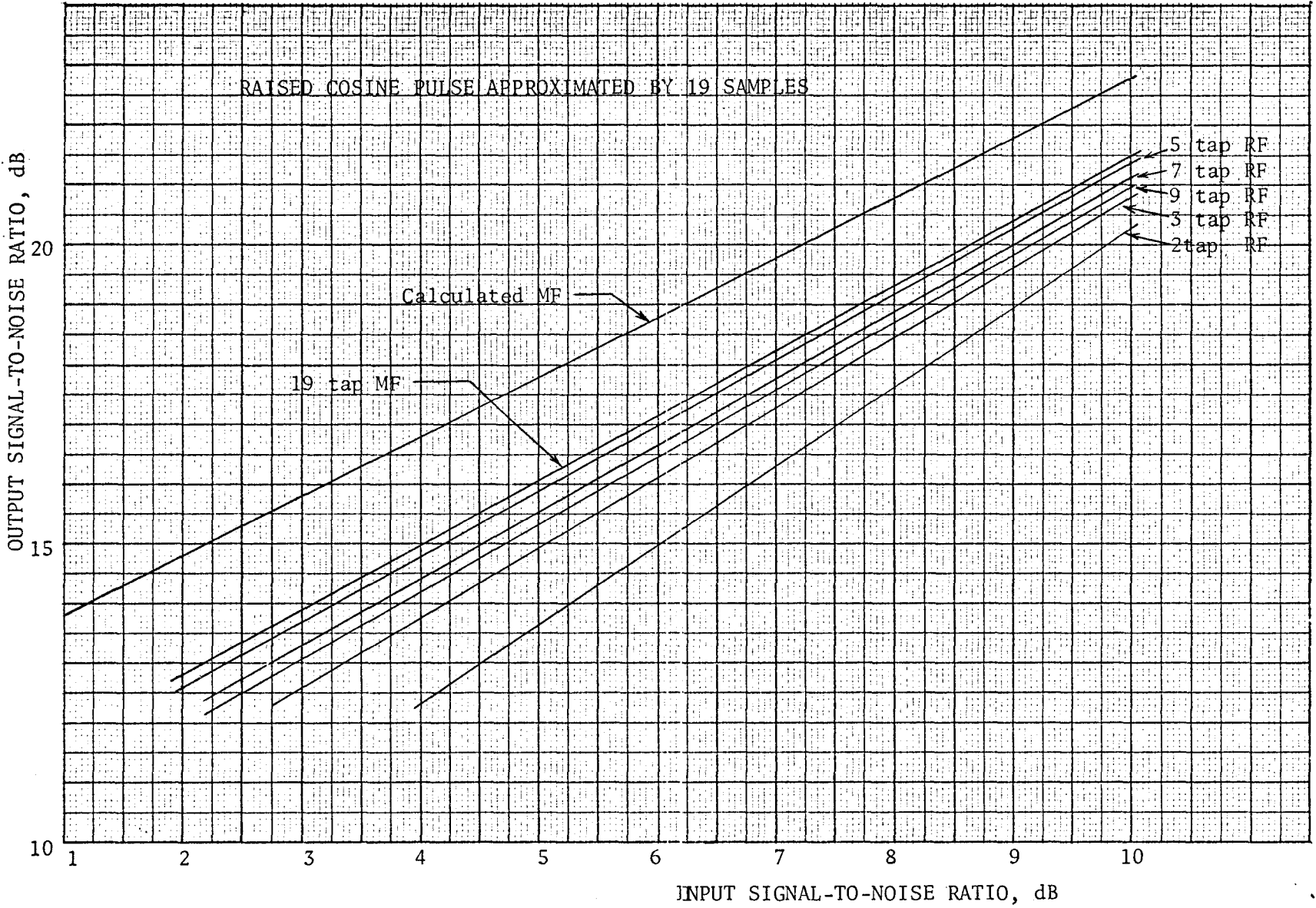in 6 dB SNR Gaussian Noise

Figure 6.4   Output Signal-to-noise Ratio for reception of a Raised Cosine Pulse in Gaussian Noise
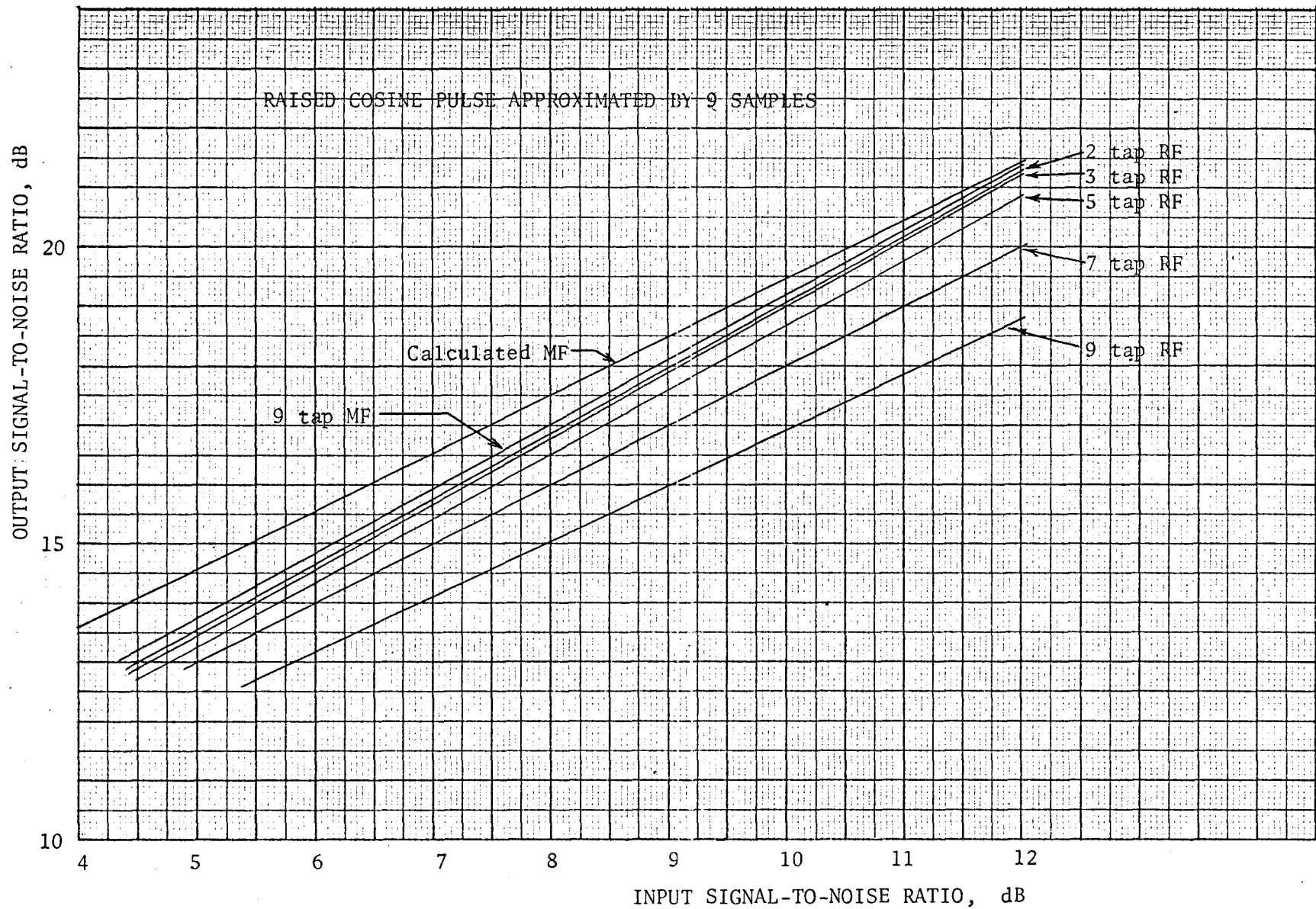
Figure 6.5   Output Signal-to-noise Ratio for Reception of a Raised Cosine Pulse in Gaussian Noise
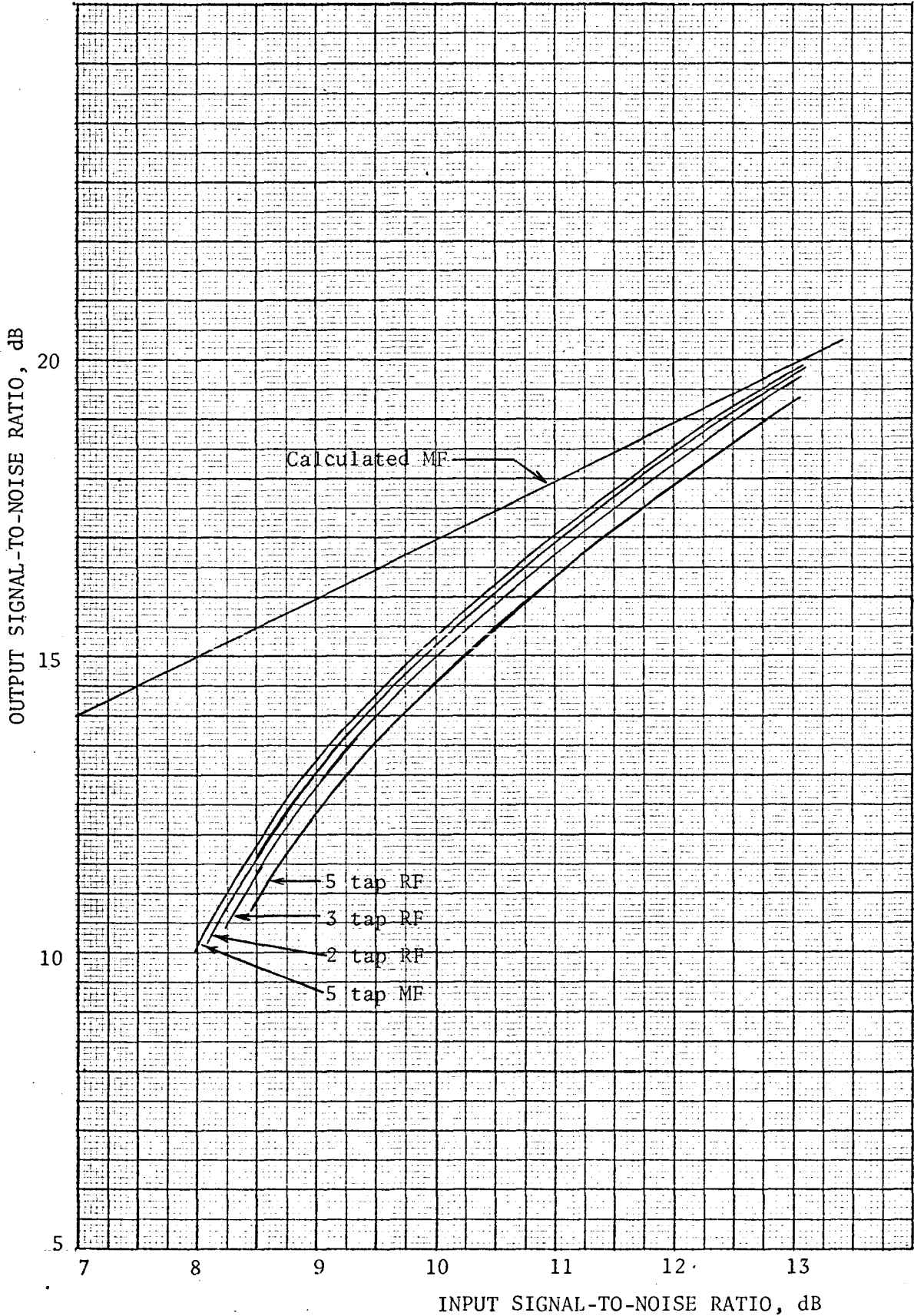
Figure 6.6   Output Signal-to-noise Ratio for Reception of a Raised
             Cosine Pulse in Gaussian Noise (5 Sample Approx.)

of the number of elements (memory cells) used. If the number of elements
is too large the effective bandwidth may be so narrow that it rejects
signal as well as noise. For example, when the raised cosine pulse is
approximated by 19 samples, the 5-tap recursive filter offers the best
performance.

(iii) The performance of an optimized recursive filter is
only a fraction of a dB worse than that of the matched filter. In an
unknown situation where one has no knowledge of the received signal
shape so that matched filtering is not practical, the adaptive recursive
filter becomes a more practical alternative. In fact, since the recur-
sive filter was derived without any assumption as to the noise distribu-
tion, it is better equipped to cope with nonstationary noise than the
matched filter.

6.3 Performance of the Adaptive Equalizer

The new equalizer derived in Chapter 5 was tested by trans-
mitting rectangular pulses with guard spacing equal to the memory of
the channel impulse response. A 20% threshold is applied to the
equalizer output, that is, if the absolute value of the equalizer output
is less than 0.2 (since the signal is normalized to unit height) the
decision is zero, otherwise the decision is either +1 or -1. The
input/output waveforms of the decision directed unconstrained equalizer
(Figure 5.6) for two different channel impulse responses are shown in
Figures 6.7 and 6.8. It is observed that it is much easier to equalize
a channel with impulse response given by Figure 6.7(a) than that of
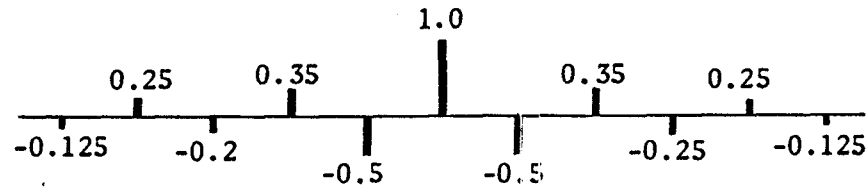
(a) CHANNEL IMPULSE RESPONSE
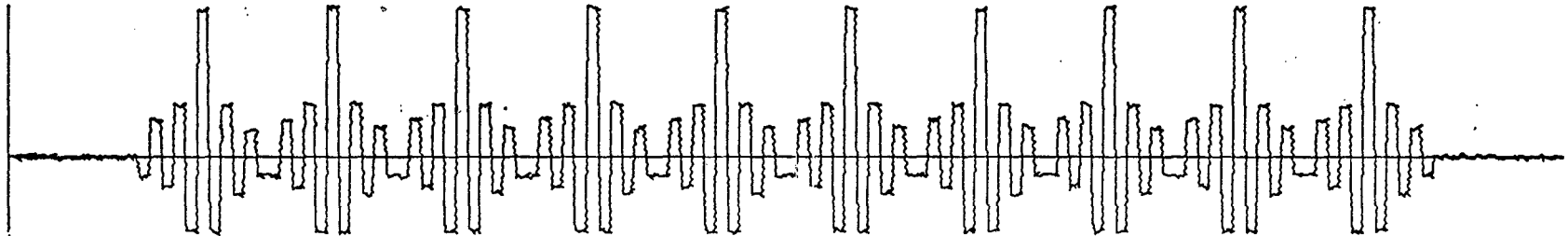
(b) RECTANGULAR PULSES WITH GUARD SPACING EQUAL TO CHANNEL MEMORY
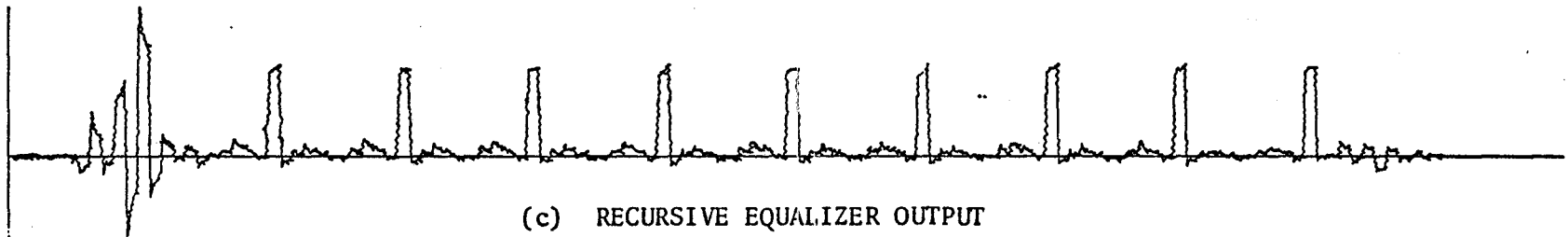
(5 SAMPLES PER PULSE)

(c) RECURSIVE EQUALIZER OUTPUT

Figure 6.7 Equalization of Non-overlapping pulse with 20% Threshold (SNR = 40 dB)

134

1.0

0.5

0.125 0.2 0.25 0.35 0.5 0.5 0.35 0.25 0.2 0.125

(a) CHANNEL IMPULSE RESPONSE

(b) RECTANGULAR PULSES WITH GUARD SPACING EQUAL TO CHANNEL MEMORY

(5 SAMPLES PER PULSE)

(c) RECURSIVE EQUALIZER OUTPUT

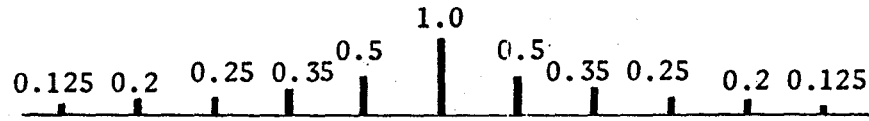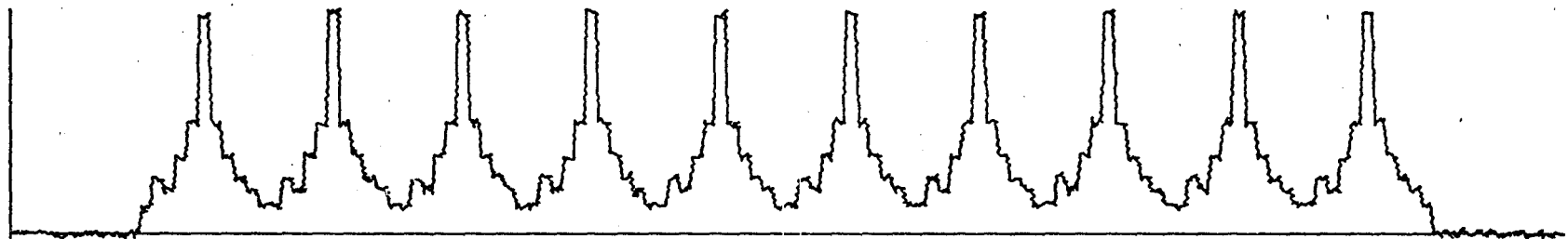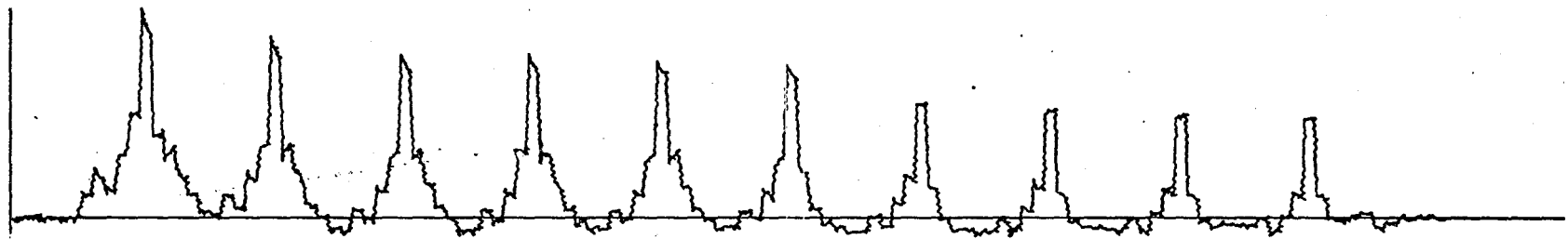Figure 6.8   Equalization of Non-overlapping Pulse with 20% Threshold (SNR = 40 dB)

135

Figure 6.8(a). This is conceptually satisfying, since the sidelobes of Figure 6.7(a) are much more random. In both cases the equalizer starts at its quiescent value, i.e., the reference tap gain equals 1 while all others equal zero. Under the conditions specified above, for the channel impulse response of Figure 6.7(a), the equalizer attains convergence in approximately 45 samples. For the channel impulse response given by Figure 6.8(a) and under similar conditions, convergence is approached only after receiving 550 samples. This is so because the initial errors in the latter case are non-random. The adjustment of the equalizer tap gains favours a random error (hence the term random walk). As the equalizer tap gains acquire finite values, randomness is gradually forced into the error function. Corresponding cases for the non-recursive equalizer are not shown because the convergence of the non-recursive equalizer is extremely slow compared to the recursive one.

To evaluate the convergence properties of the various equalizer structures for different types of channels, repeated transmission of a 127-digit periodic binary M-sequence is used as a test signal. The digit duration is taken to be the same as the pulse separation, that is, $T_o = T_s$. Convergence curves (averaged over 10 runs) for the various equalizers are shown in Figures 6.9 through 6.12, where MS denotes the mean square error gradient algorithm and HYB denotes the hybrid mean square error gradient algorithm. The latter is obtained using the sign of the error rather than the true error. From the implementation point of view the hybrid algorithm is simpler, since multiplications

are reduced to sign switching (or chopping) operations. The non-recursive equalizer, with a capability for tracking its own frame of reference, has been referred to as the modified non-recursive equalizer. We note that the HYB algorithm converges somewhat slower than the MS algorithm, but it converges to approximately the same minimum value of error. In this thesis our main interest lies in introducing a better equalizer than the state-of-the-art. Discussions on the implementation techniques of various convergence algorithms are available in the literature (see, for example, Hirsch and Wolf, 1970; Gersho, 1969). With this remark we employ the MS algorithm in all subsequent performance evaluations. Inspection of Figures 6.9 to 6.12 reveals the following points:

(i) The unconstrained recursive equalizer offers the fastest convergence. The conventional non-recursive equalizer has the slowest convergence.

(ii) In the case of the unconstrained recursive equalizer, the binary eye was open after having received less than 200 samples (see Figure 6.12).

(iii) As was revealed by Figures 6.7 and 6.8, the channel impulse response with the most random sidelobe structure is the easiest to equalize.

(iv) As expected the recursive equalizer is much more superior to the non-recursive equalizer.

Also, during the course of conducting the computer simulations the following points were observed:

(v) Provided the frame of reference is maintained, the uncon-
strained recursive equalizer will operate in a stable mode.

(vi) The recursive equalizer is more robust than the non-
recursive equalizer in that it can withstand much larger gradient
constants, i.e., α, β and γ. Range of values of α, β and γ used are
tabulated in TABLE VI-1.

(vii) The constraining action of the constrained recursive
equalizer accounts for its slow convergence (as compared to the uncon-
strained one).

(viii) In the case of the recursive equalizer it is immaterial
whether or not a reference signal is used, as the decision directed mode
is just as good as the one with an ideal reference. The non-recursive
equalizer, on the other hand, requires an ideal reference, at least to
open the binary eye. The curves for the non-recursive equalizers were
obtained using an ideal reference.

(ix) The non-recursive equalizer, especially the conventional
one, is very sensitive to changes in the values of the gradient constants.
If the gradient constant, α, is slightly too small, the convergence is
extremely slow; if it is slightly too large, for the periodic adjustment
case, the tap gains may walk past the optimum values and the system
starts to degenerate.

(x) The robust operation of the recursive equalizer implies
that it has a much better noise immunity than the non-recursive equalizer;
this may be explained by recognizing that the recursive structure exhibits
negative feedback properties.

TABLE VI-1   RANGE OF GRADIENT CONSTANTS FOR BEST CONVERGENCE

GRADIENT CONSTANTS	RECURSIVE EQUALIZER	MODIFIED NON-RECURSIVE EQUALIZER	CONVENTIONAL NON-RECURSIVE EQUALIZER
α (Reference Tap)	-0.001 to -0.004	-0.00007 to -0.00015	-0.00002 to -0.00005
β (Learning Loop)	-0.01 to -0.04	-0.0001 to -0.0002	
γ (Recursive Loop)	-0.002 to -0.005		

Figure 6.9   Comparison of Convergence of Conventional Non-recursive, Modified Non-recursive and Recursive Equalizers

Figure 6.10 Comparison of Convergence of Conventional Non-recursive,
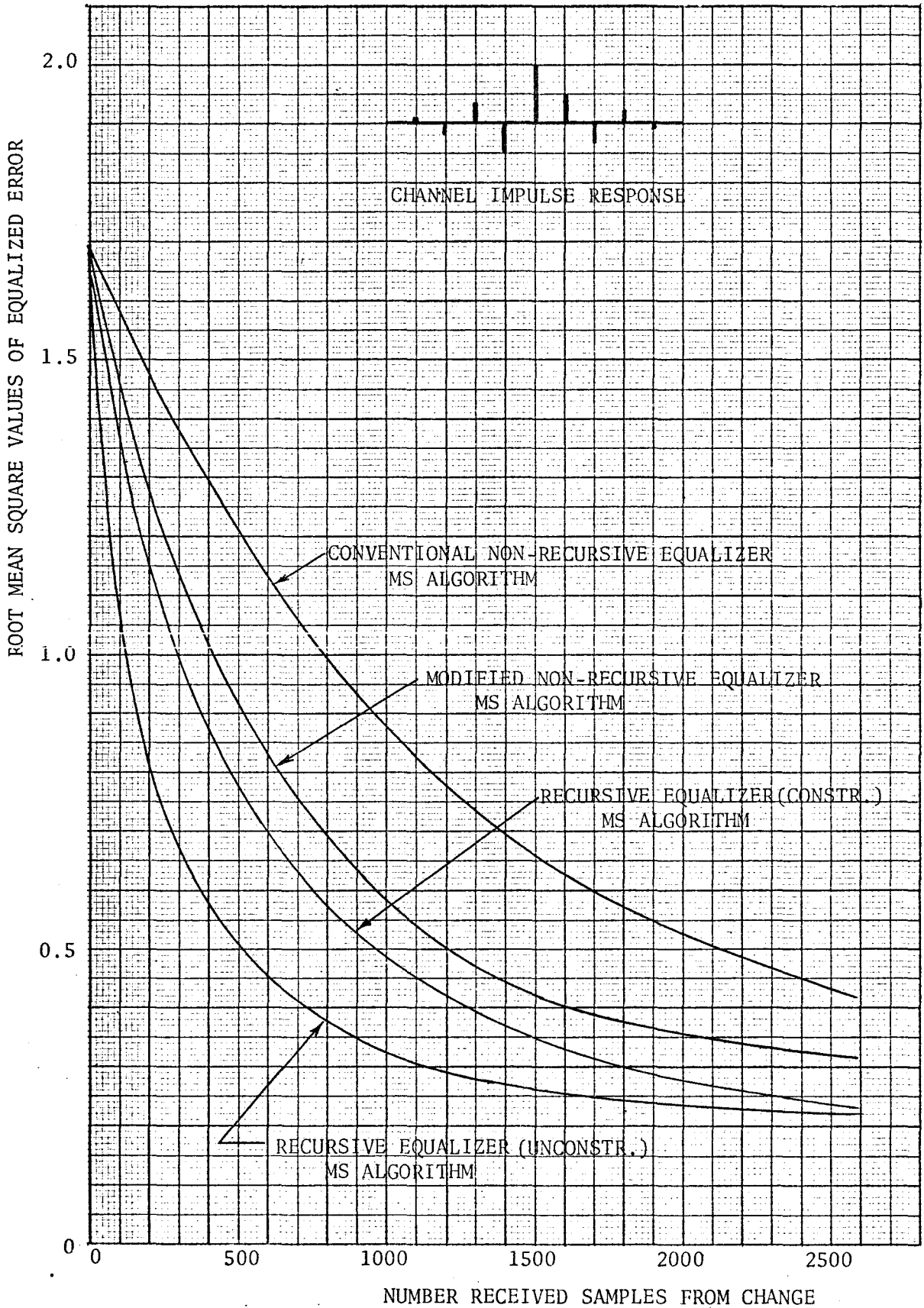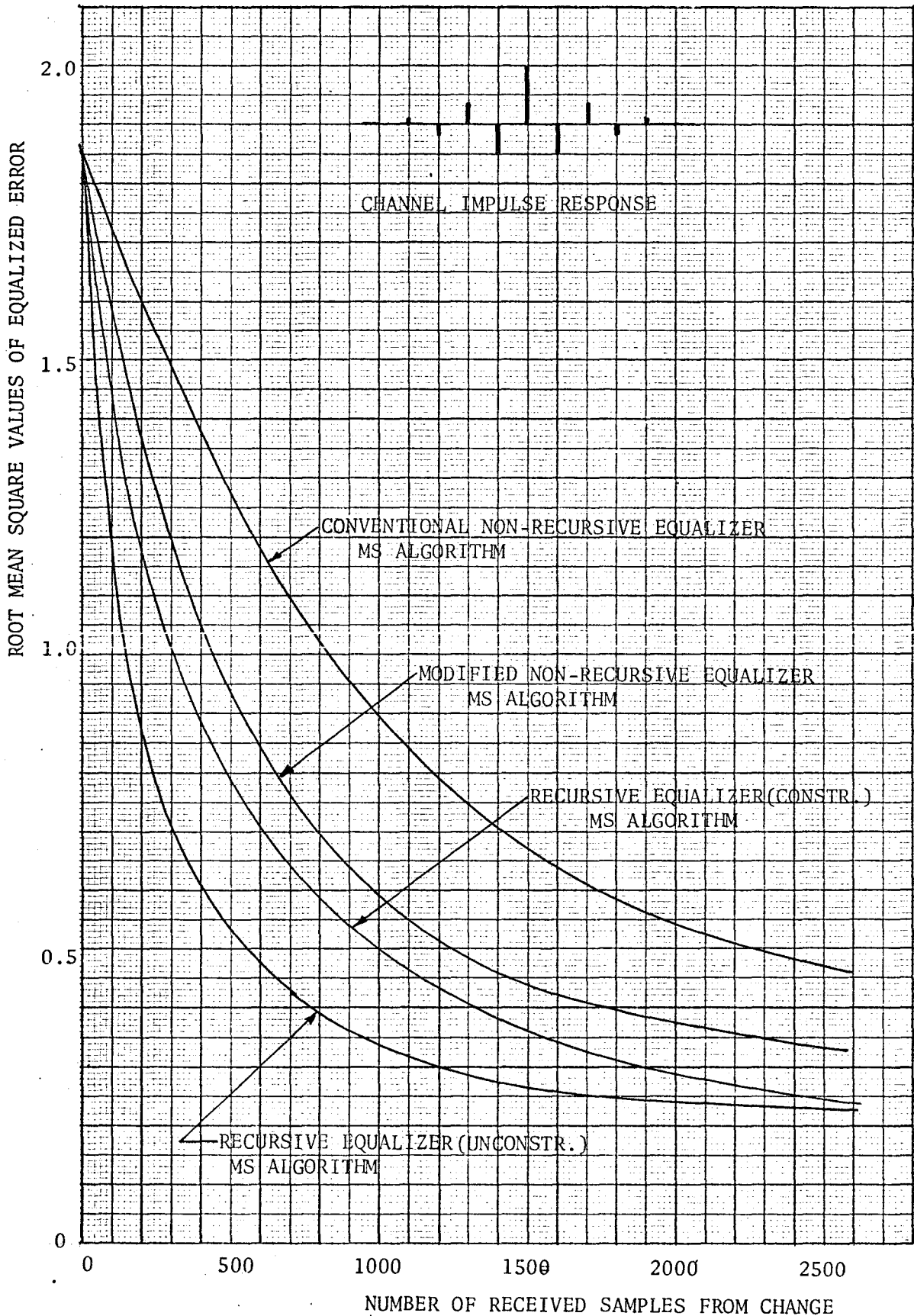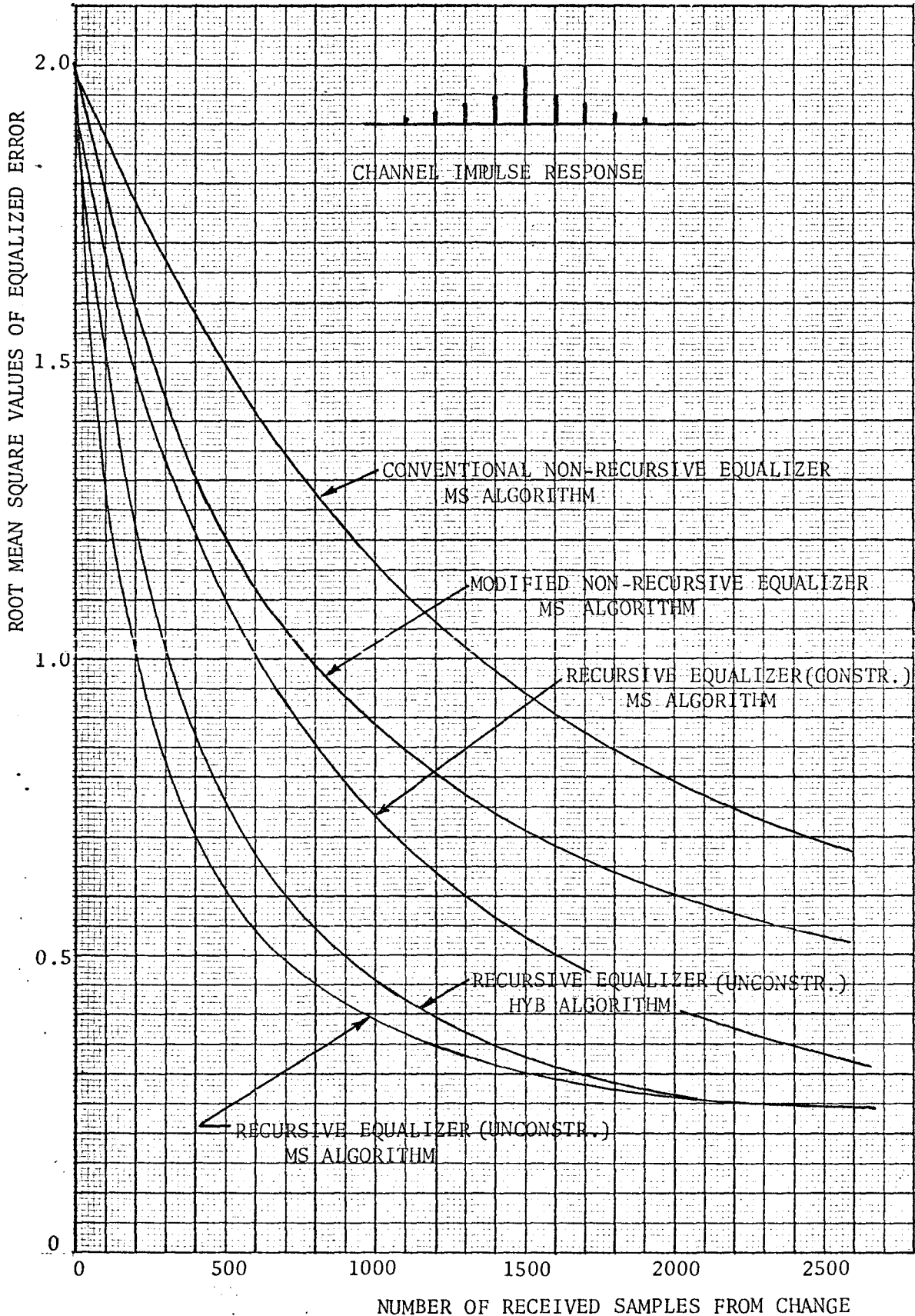Modified Non-recursive and the Recursive Equalizers

Figure 6.11   Comparison of Convergence of Conventional Non-recursive
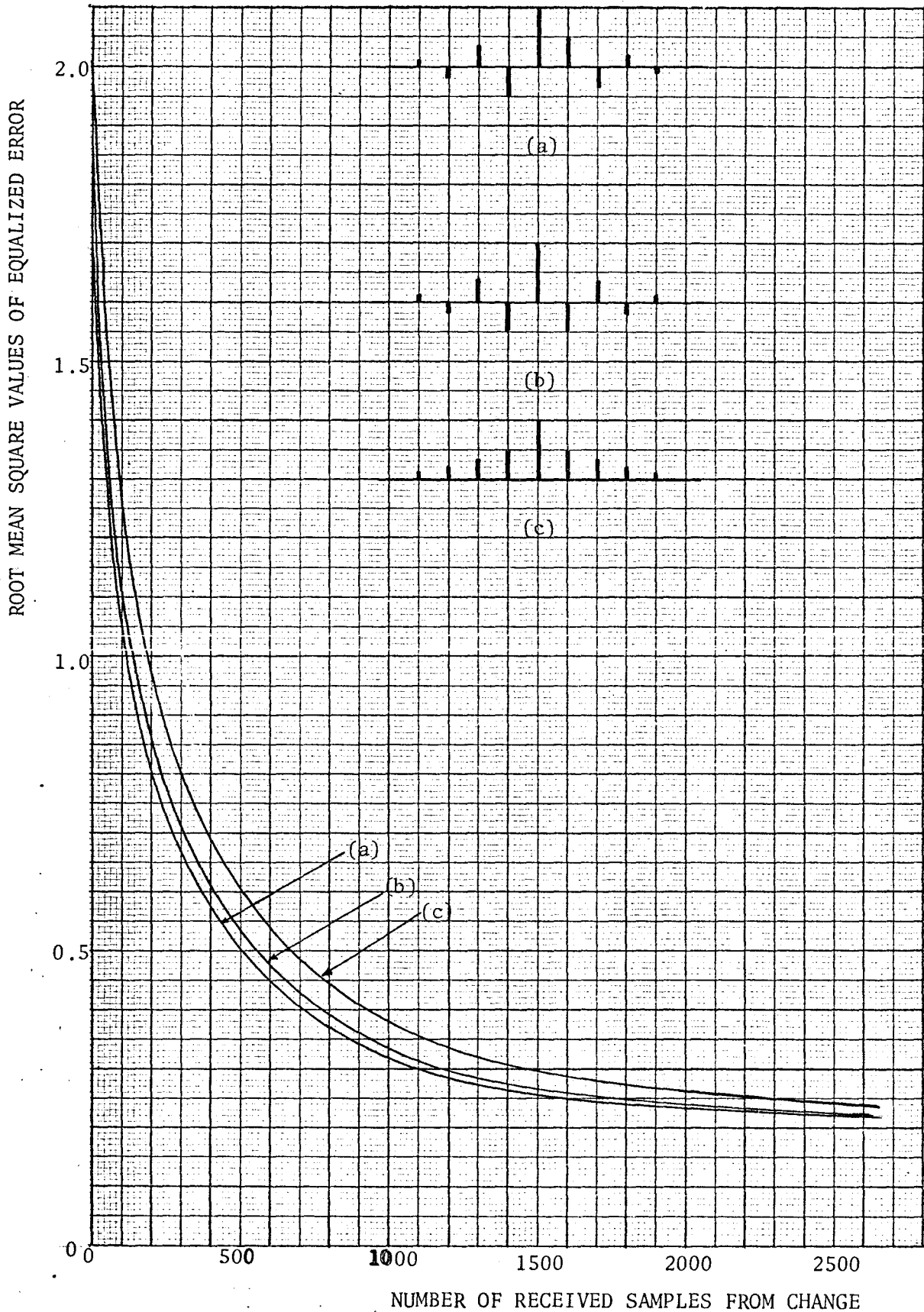Modified Non-recursive and Recursive Equalizers

Figure 6.12 Comparison of Convergence of the Recursive Equalizer(unconstr.) for different types of Channel Impulse Responses

6.4 Performance of the Adaptive Signal Processor

The equalizer is quite sensitive to impulsive noise. For best performance it is necessary to filter the received signal before applying equalization. The optimum filter is that which is matched to the channel output (George, 1965). Since we are concerned with unknown channels, we employ the adaptive recursive filter derived in Chapter 4. A cascade connection of the filter and the equalizer is referred to as the signal processor. In this section we discuss the performance of the signal processor by displaying typical input/output waveforms and probability of error curves[†]. We concentrate our effort in evaluating the performances of the unconstrained recursive equalizer (here after referred to simply as the recursive equalizer) and the modified non-recursive equalizer (here after referred to simply as the non-recursive equalizer).

The transmitted signal is a succession of the 127-digit periodic binary M-sequence. The pulse shaping network is assumed to have a rectangular impulse response. Each binary symbol is approximated by 5 samples on transmission. The three different types of channel impulse responses mentioned in the preceding section are being tested. The Signal Simulator (see Appendix H) is equipped with the capability for changing the channel impulse response. For the cases under consideration, the deterministic channel impulse response is aged randomly by 5% both in amplitude and in phase at the end of one period of the M-sequence.

[†]The results obtained by Monte-Carlo simulation are in actual fact error rates that are dependent on when the counting starts.

With reference to Appendix H, briefly, the signal flow is as follows: The output of the Signal Simulator is the received perturbed signal, which is passed through a 3-tap adaptive recursive filter, the output of which is sampled once per baud and then applied to the adaptive equalizer. A decision is then made on the equalizer output. The 'Decision Box' (see Figure 5.6) is a zero crossing detector, so that the final output is a sequence of +1's and -1's. Typical input/output waveforms for a decision directed recursive equalization system, which corresponds to the channel with impulse response shown in Figure 6.13 a(i), are displayed in Figures 6.13 and 6.14. In each case one period of the 127-digit M-sequence is plotted after having received 635 (5 x 127) samples, 1270 (10 x 127) samples and 2540 (20 x 127) samples. Figures 6.13 a, b and c are good indications of the convergence properties of the decision directed recursive equalization system.

The autocorrelation function of a periodic 127-digit binary M-sequence is a train of periodic pulses of 127 units in height occuring at a periodicity of 127 digits and -1 unit everywhere else. (See, for example, Golomb et al, 1964.) Correlation decoding is the process of cross-correlating the decisions with an ideal reference sequence. When there are no errors in the decisions, the cross-correlation process becomes an autocorrelation operation. Thus, the correlation decoder output provides a measure of the degree of accuracy in the decisions. We know that exact decisions have been made when the correlation decoder output is identical to the autocorrelation function of the periodic M-sequence, as is shown in Figure 6.13 c(vi). The wave-

(i)   CHANNEL IMPULSE RESPONSE

(ii)   TRANSMITTED 127-DIGIT BINARY M-SEQUENCE

(iii)   RECEIVED PERTURBED SIGNAL

(iv)   RECURSIVE FILTER OUTPUT

(v)   RECURSIVE EQUALIZER OUTPUT

(vi)   DECISION BOX OUTPUT

Figure 6.13 a   Reception of a 127-Digit Binary M-sequence after having received
635 Samples, SNR = 1.0 dB

(vii)   CORRELATION DECODER OUTPUT

Figure 6.13 a(vii)   3 Periods of the Correlation Decoder Output, Correlation between (ii) and (vi).

147

(i)   TRANSMITTED 127-DIGIT BINARY M-SEQUENCE

(ii)   RECEIVED PERTURBED SIGNAL

(iii)   RECURSIVE FILTER OUTPUT

(iv)   RECURSIVE EQUALIZER OUTPUT

(v)   DECISION BOX OUTPUT

Figure 6.13 b   Reception of a 127-Digit Binary M-sequence after having received
1270 Samples, SNR = 1.0 dB

148

(vi)   CORRELATION DECODER OUTPUT

Figure 6.13 b(vi)   3 Periods of the Correlation Decoder Output, Correlation between (i) and (v)
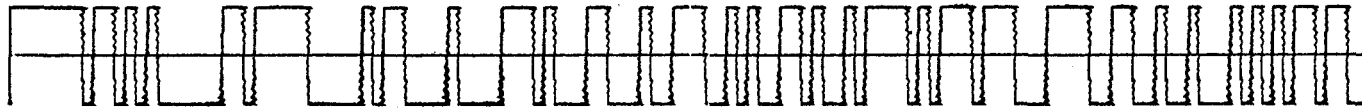
(i)   TRANSMITTED 127-DIGIT BINARY M-SEQUENCE
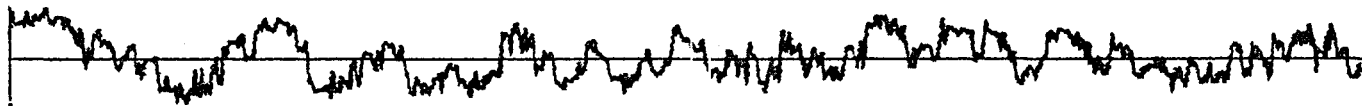
(ii)   RECEIVED PERTURBED SIGNAL

(iii) RECURSIVE FILTER OUTPUT

(iv)   RECURSIVE EQUALIZER OUTPUT
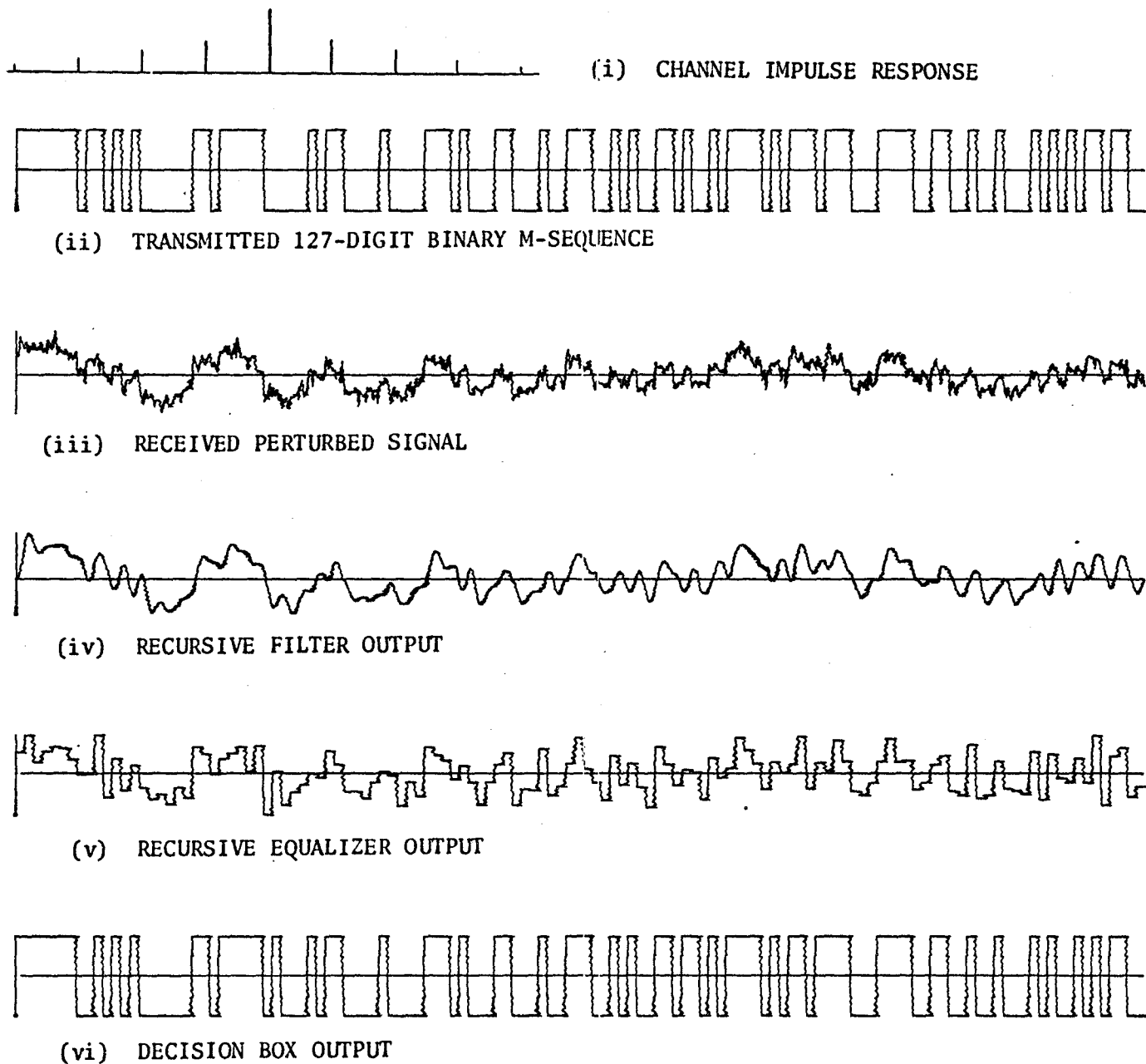
(v)   DECISION BOX OUTPUT

Figure 6.13 c   Reception of a 127-Digit Binary M-sequence after having received
2540 Samples, SNR = 1.0 dB

(vi)   CORRELATION DECODER OUTPUT

Figure 6.13 c(vi)   3 Periods of the Correlation Decoder Output, Correlation between (i) and (v)

151

(i) CHANNEL IMPULSE RESPONSE

(ii)   TRANSMITTED 127-DIGIT BINARY M-SEQUENCE

(iii)   RECEIVED PERTURBED SIGNAL, SNR = -3.0 dB

(iv)   RECURSIVE FILTER OUTPUT

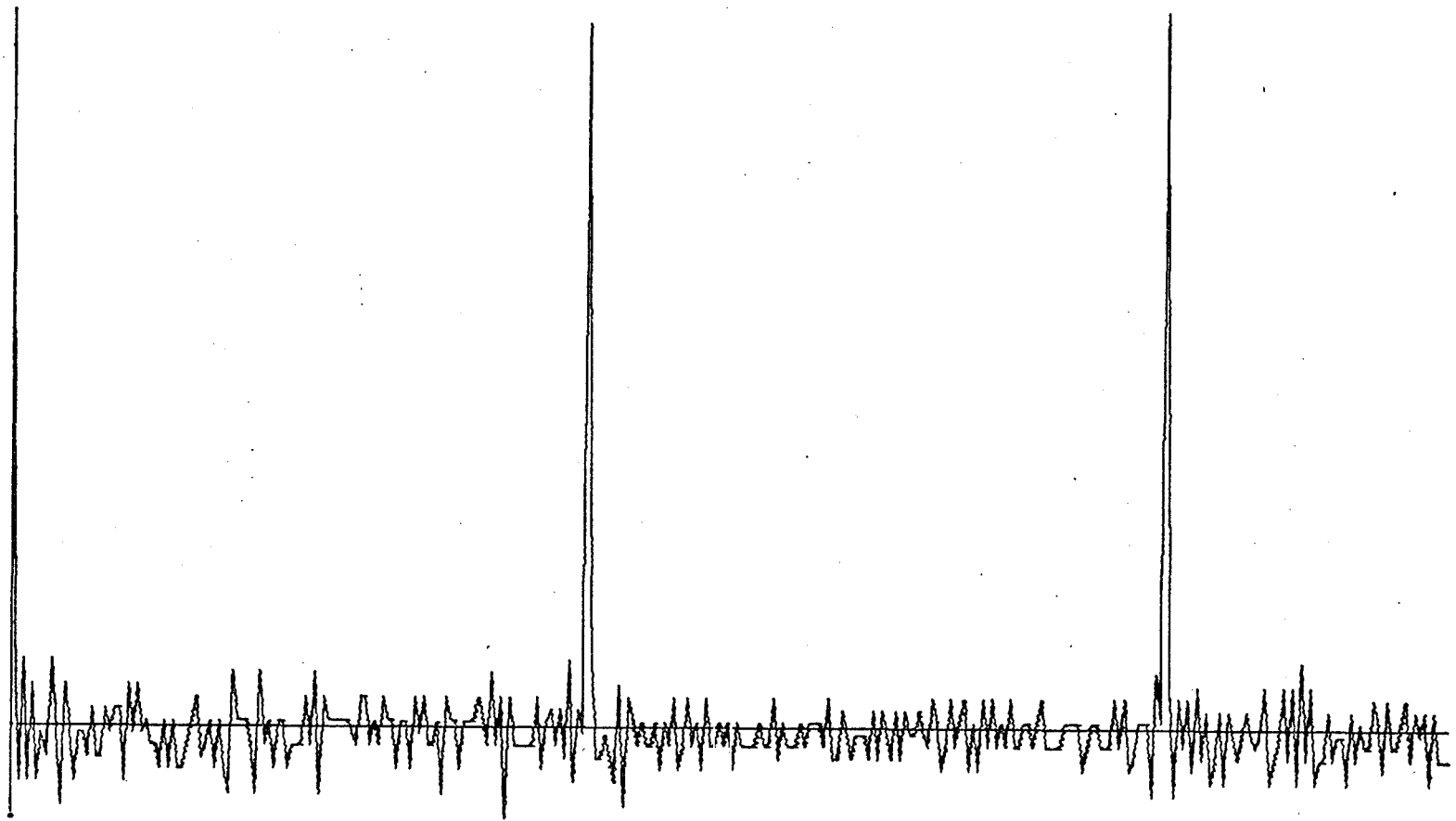(v)   RECURSIVE EQUALIZER OUTPUT

(vi)   DECISION BOX OUTPUT
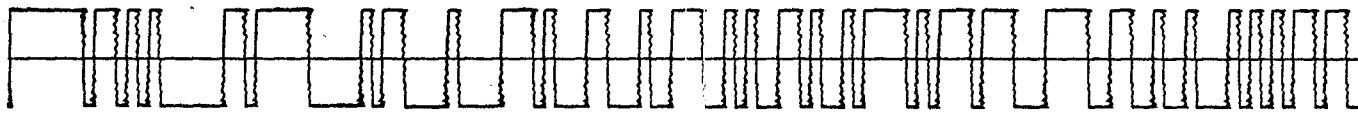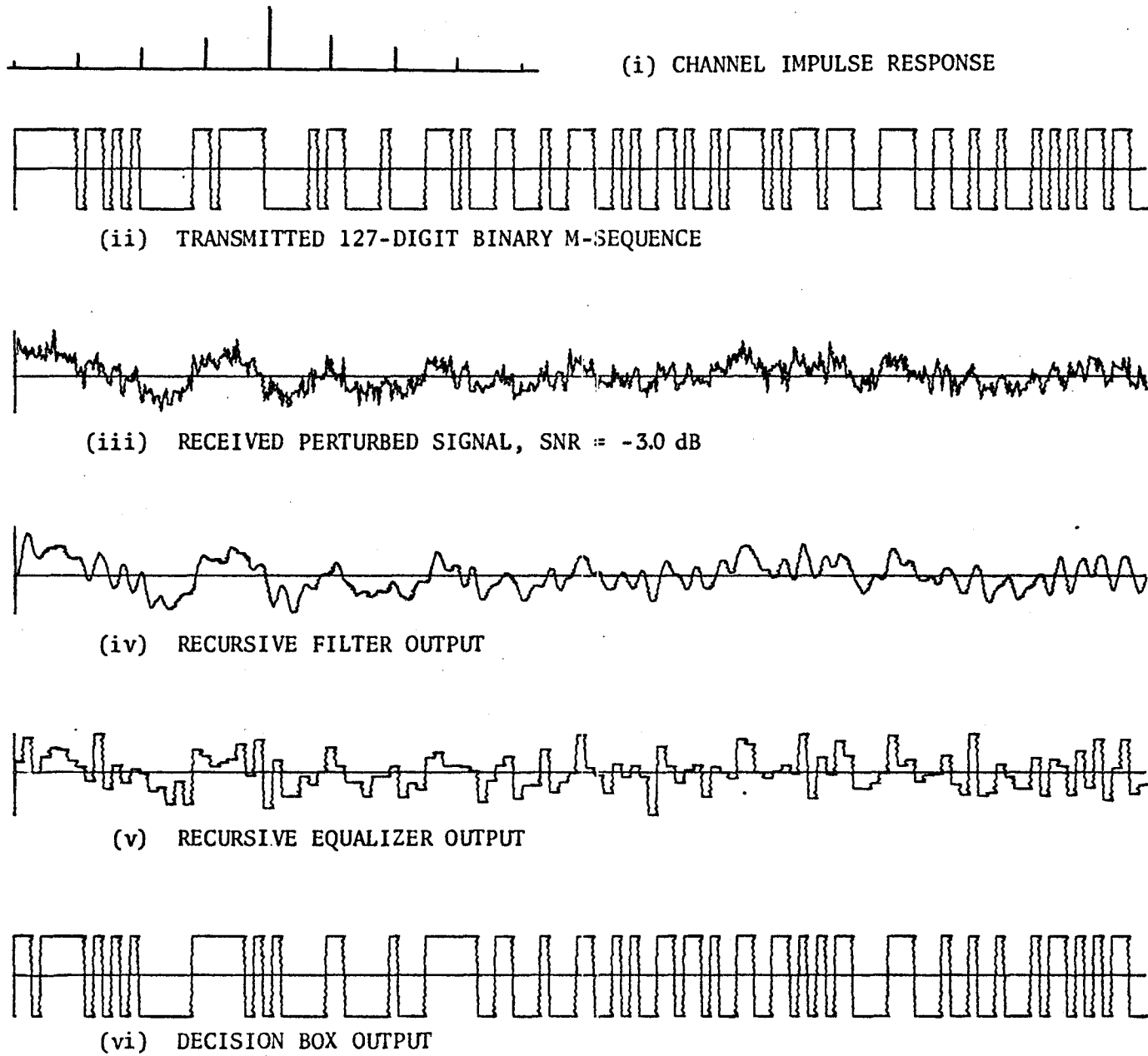
Figure 6.14 a   Reception of a 127-Digit M-sequence after having received
635 Samples, SNR = -3.0 dB
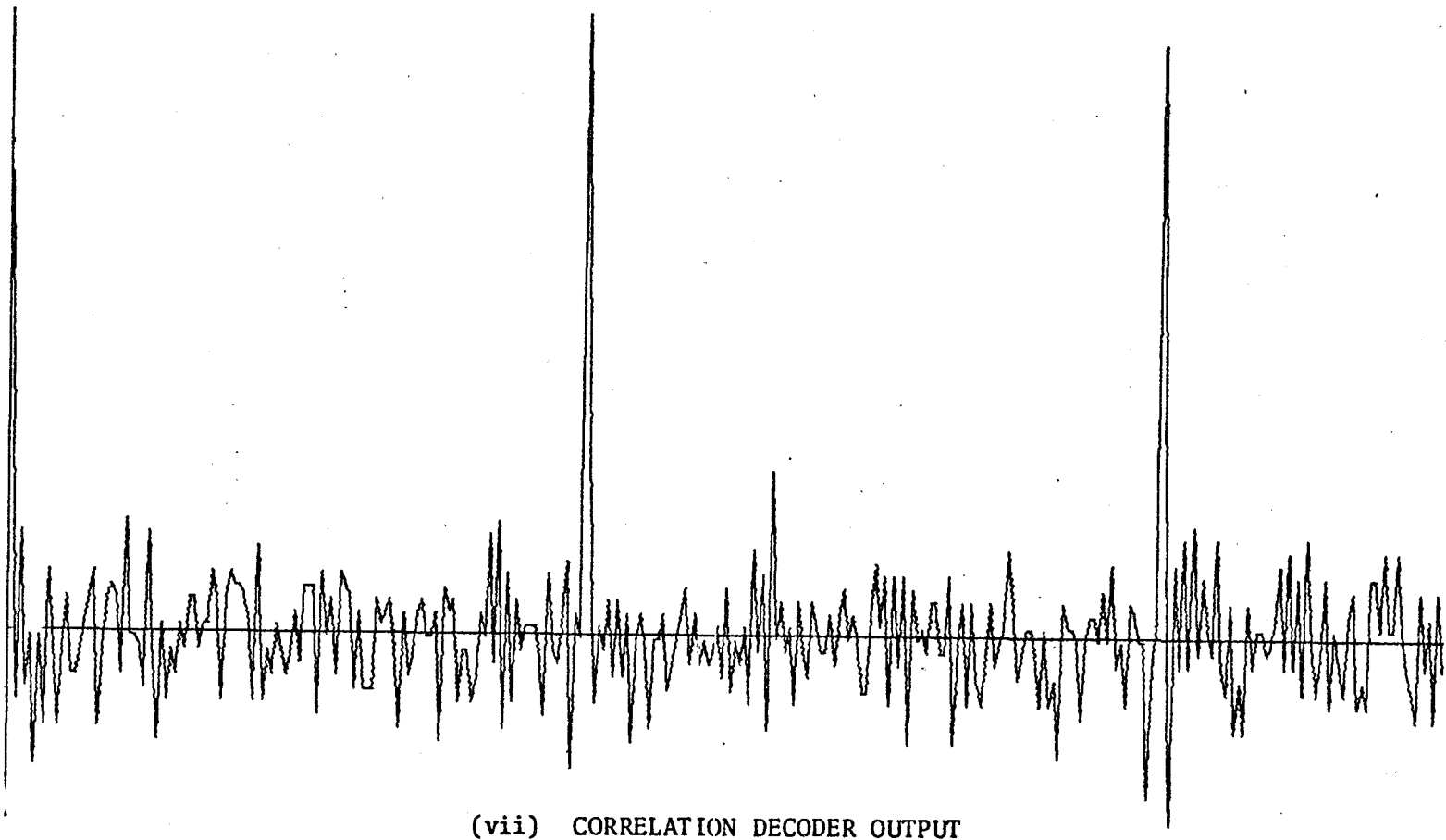
(vii)   CORRELATION DECODER OUTPUT

Figure 6.14 a(vii)   3 Periods of Correlation Decoder Output, Correlation between (ii) and (vi)
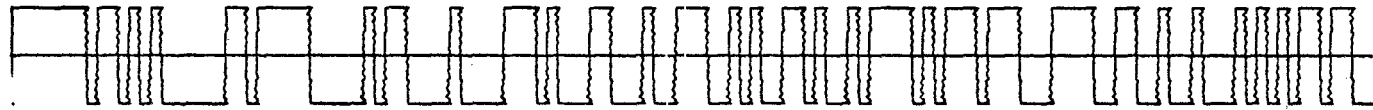
(i)   TRANSMITTED 127-DIGIT BINARY M-SEQUENCE
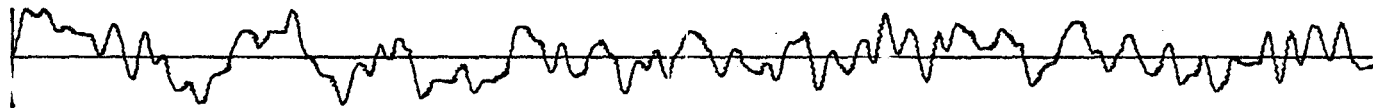
(ii) RECEIVED PERTURBED SIGNAL, SNR = -3.0 dB

(iii) RECURSIVE FILTER OUTPUT
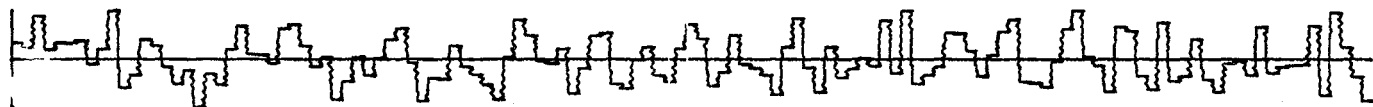
(iv) RECURSIVE EQUALIZER OUTPUT
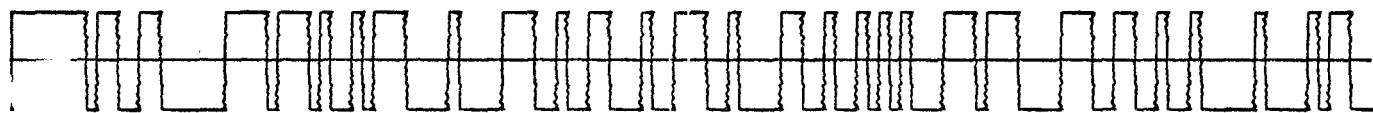
(v)   DECISION BOX OUTPUT

Figure 6.14 b   Reception of a 127-Digit Binary M-sequence after having received
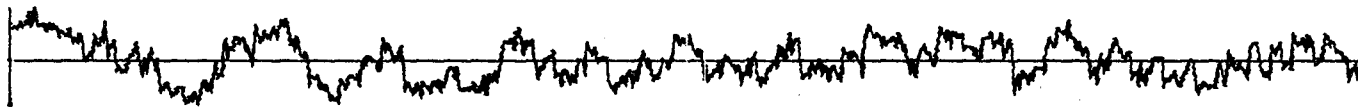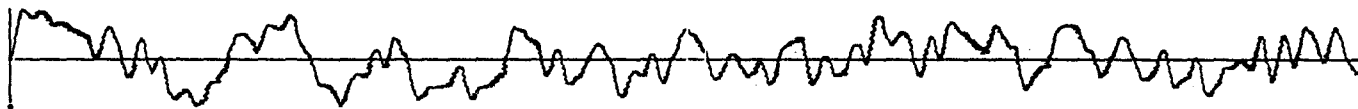1270 Samples, SNR = -3.0 dB
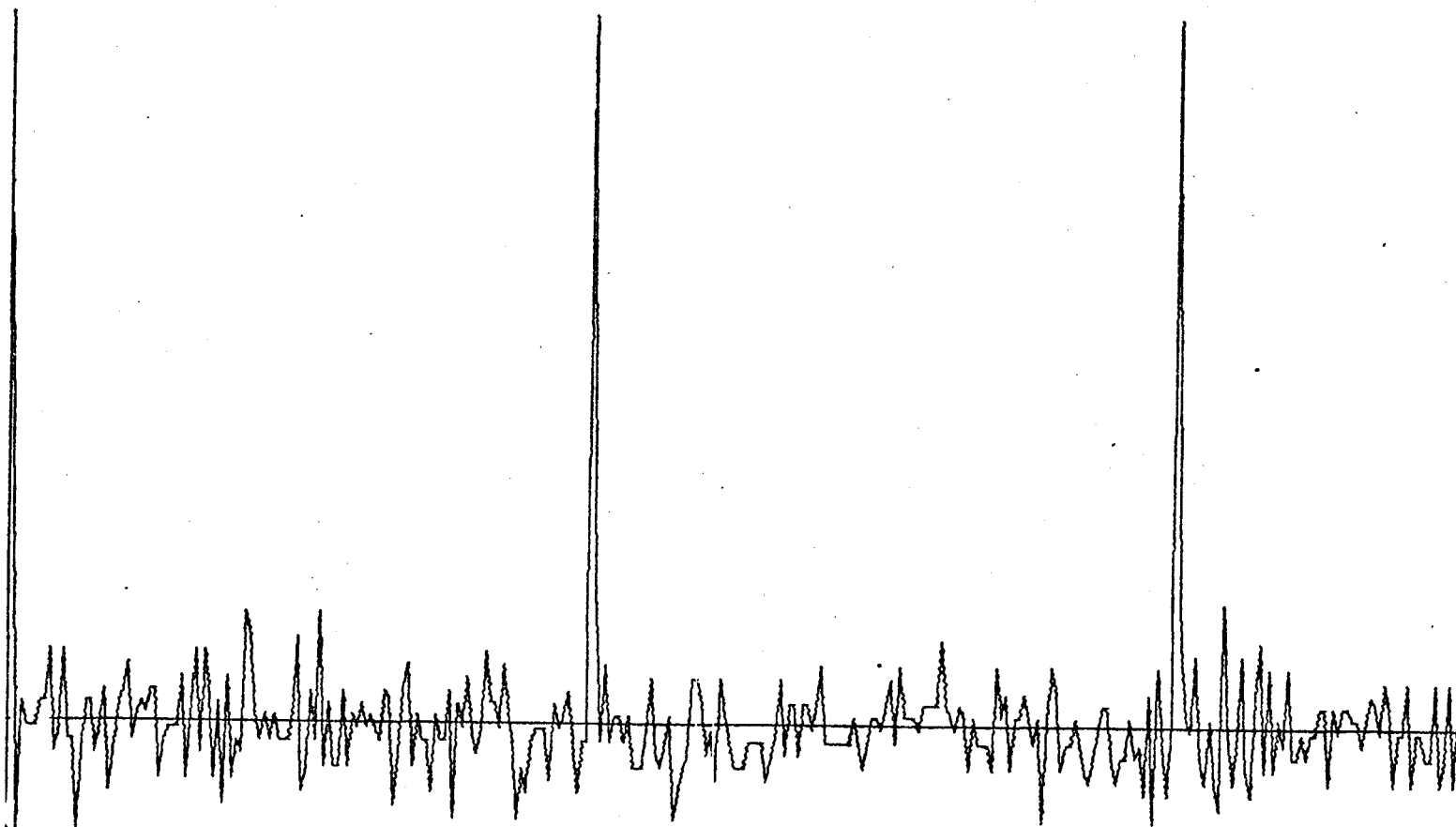
(vi) CORRELATION DECODER OUTPUT

Figure 6.14 b(vi)   3 Periods of Correlation Decoder Output, Correlation between (i) and (v)
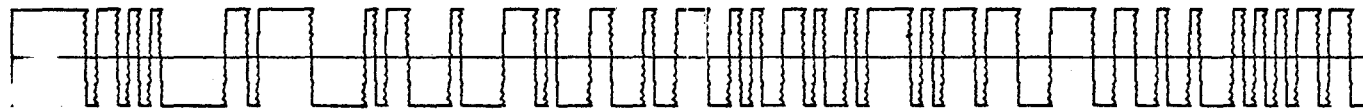
(i) TRANSMITTED 127-DIGIT BINARY M-SEQUENCE
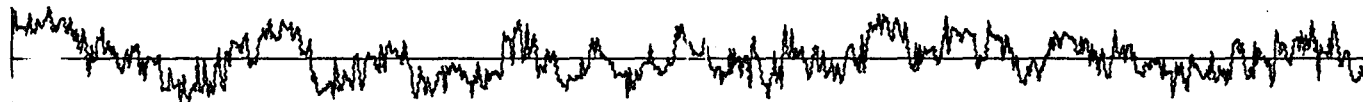
(ii) RECEIVED PERTURBED SIGNAL, SNR = -3.0 dB
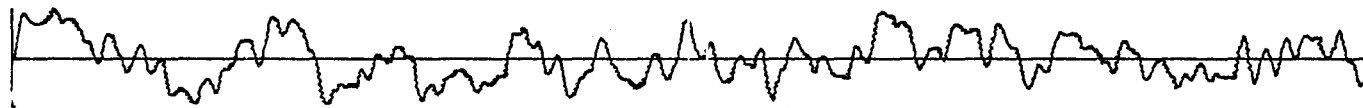
(iii) RECURSIVE FILTER OUTPUT
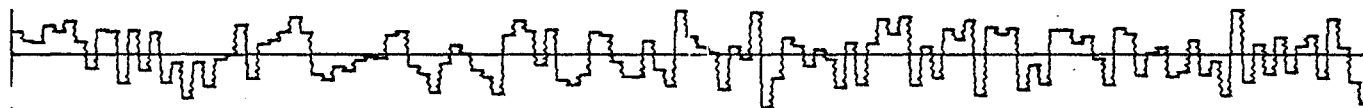
(iv) RECURSIVE EQUALIZER OUTPUT

(v) DECISION BOX OUTPUT

Figure 6.14 c   Reception of a 127-Digit Binary M-sequence after having received
2540 Samples, SNR = -3.0 dB
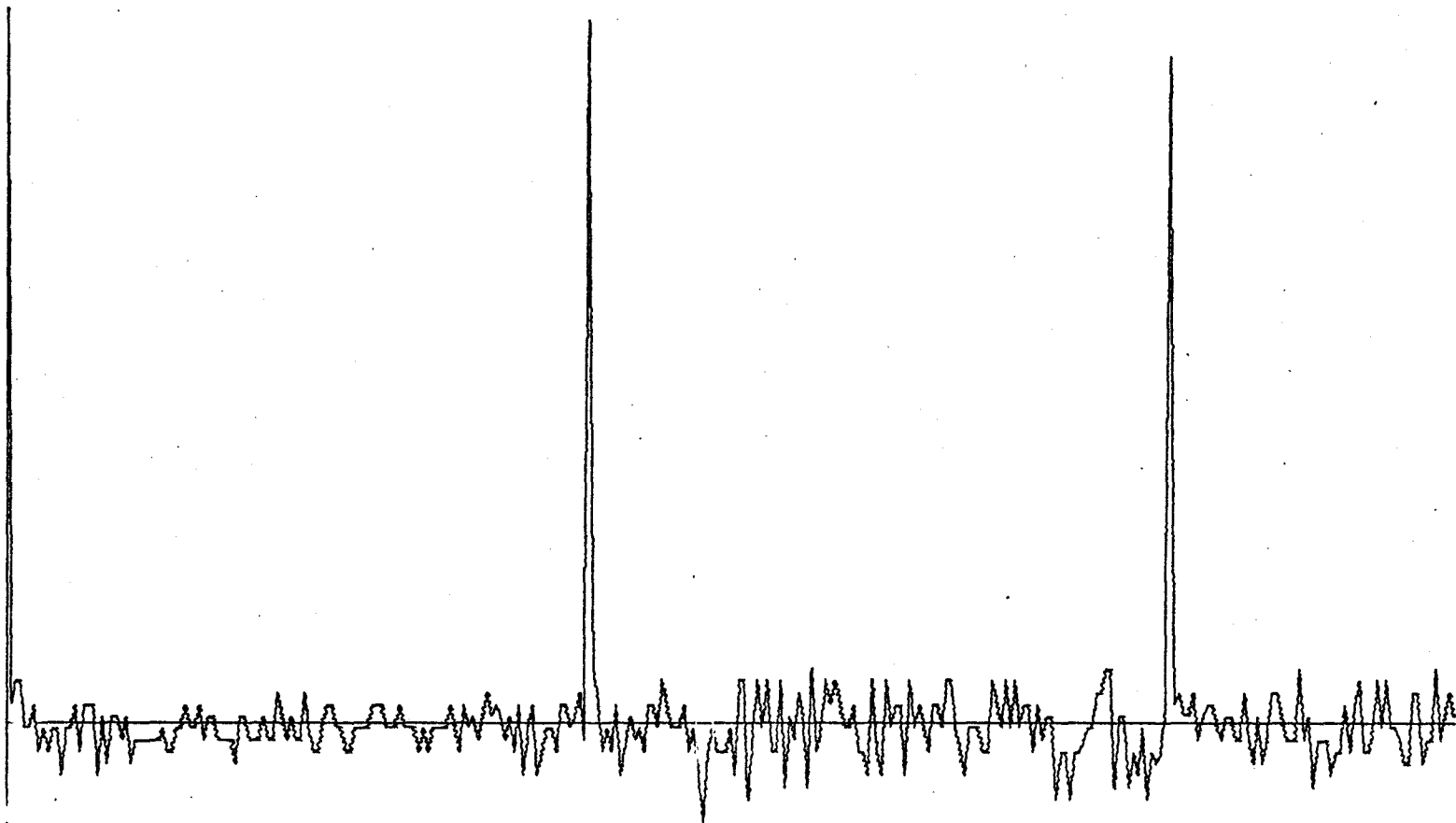
(vi)   CORRELATION DECODER OUTPUT

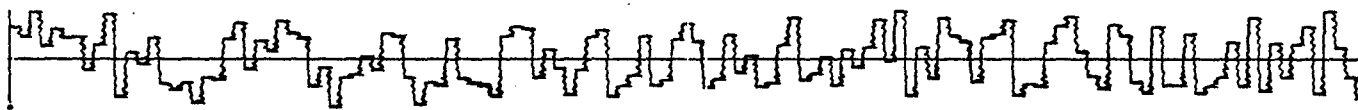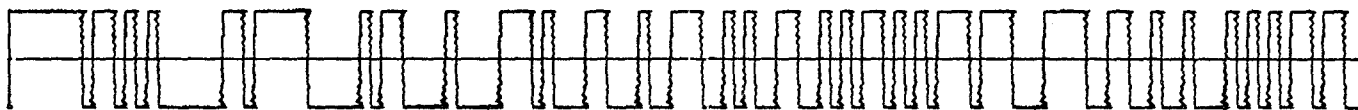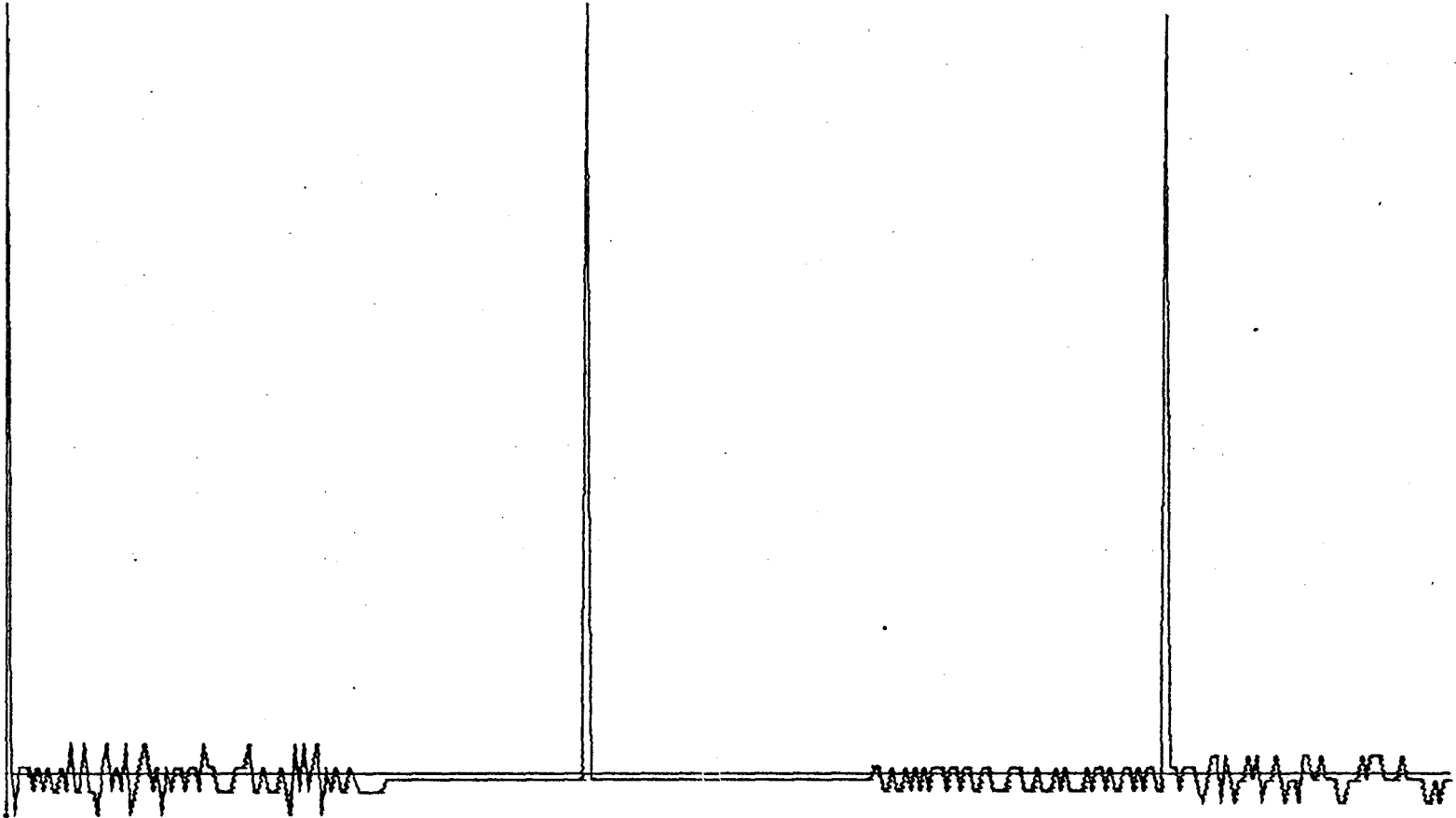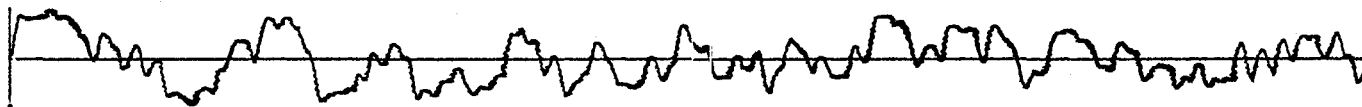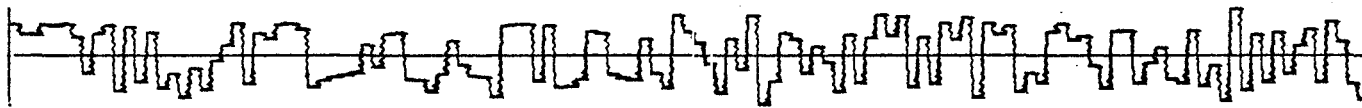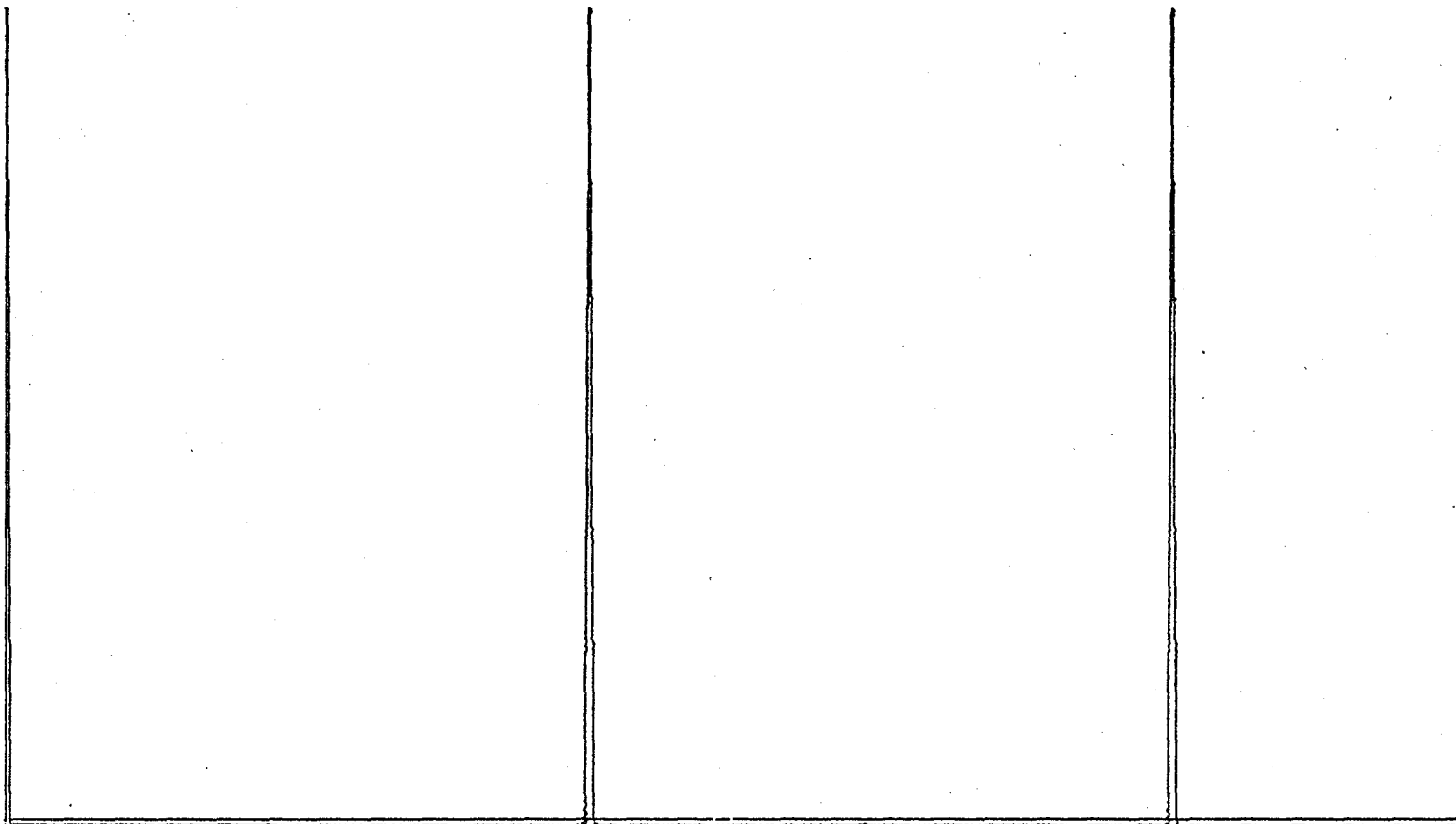Figure 6.14 c(vi)   3 Periods of Correlation Decoder Output, Correlation between (i) and (v)

forms of Figure 6.13 correspond to the case of 1.0 dB signal-to-noise ratio, while those of Figure 6.14 correspond to -3.0 dB signal-to-noise ratio. It is observed that for small variations (5%) in the channel and at moderate signal-to-noise ratio, e.g., 1.0 dB or higher, the decision directed recursive equalizer can acquire and track the channel status to yield very accurate decisions after having received approximately 2540 samples. At low signal-to-noise ratios, e.g., -3.0 dB, the error is rather high, as shown by Figures 6.14 a, b and c. For small channel variations and given sufficient time, it is conceivable that, even at -3.0 dB signal-to-noise ratio, reasonable accuracy is achievable.

It is difficult to compute output signal-to-noise ratio on a per symbol basis. We therefore resort to computing signal-to-interference ratios at the correlation decoder output. Since the receiver is linear, we may define the correlation decoder output signal-to-interference ratio by

$$SIR_{cd} \triangleq \frac{[peak\ value\ -\ mean]^2}{1\ +\ sample\ variance} \tag{6.3}$$

where
        mean = 1 + sample mean.

The sample mean and sample variance are computed from one period of the correlation decoder output, excluding the peak value. When the decisions are exact, the peak value of the correlation decoder output equals 127 units, the sample mean equals -1 and the sample variance equals zero. The signal-to-interference ratio in dB, therefore, becomes

$$SIR_{cd} = 10 \, \log_{10} \, [\frac{(127)^2}{1}]$$

$$\doteq 42 \, dB \qquad\qquad (6.4)$$

Thus, an upper bound for the SIR_{cd} is approximately 42 dB. Signal-to-interference ratio as a function of input signal-to-noise ratio has been computed in accordance with equation (6.3) and plotted in Figure 6.15. The results of Figure 6.15 were obtained after having received 2540 samples. Suppose data are transmitted at a rate of 3600 symbols per second; then the instant of time under consideration is approximately 2/3 of a second from the quiescent condition. In this particular situation the signal processing gain of the recursive equalizer is approximately 6.5 dB. Conceivably, this can improve with time, that is to say, as the 'communication channel' approaches an all pass condition, the output of the equalizer approaches a replica of the transmitted sequence.

Thus far in this section, we have presented results for a recursive equalization system only. At the instant of time under consideration (i.e., approximately 2540 samples from quiescent condition) similar results obtained for a non-recursive equalization system are not very meaningful, because the non-recursive equalizer is still in a transient state. This can be appreciated readily by examining the convergence curves of Figures 6.9, 6.10 and 6.11.
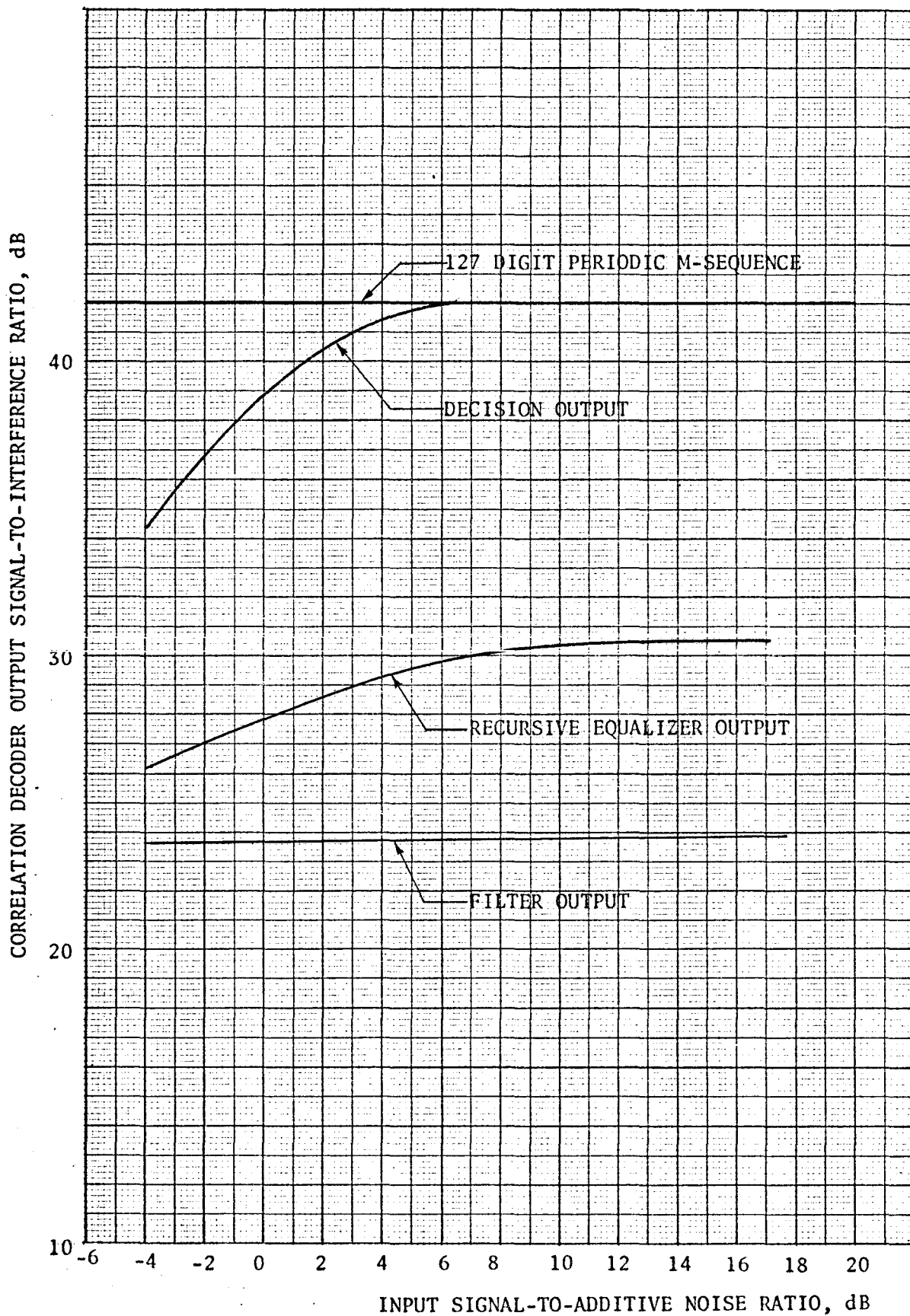
Figure 6.15   Output Signal-to-interference Ratio for Correlation
Decoding of a 127 Digit Periodic Binary M-Sequence
(all computations done after 2540 samples have been received)

As stipulated at the end of section 6.1, the probability of error provides a quantitative measure for system performance. In the remainder of this section we present system performance in terms of probabilities of error. Although all results on error probabilities have been obtained by Monte-Carlo simulation on a digital computer, in what follows we first discuss the analytical aspect of error probability. Through tedious algebraic manipulations, the equalizer output, a_n^*, as given by equation (5.17) or equation (5.37), may be expressed as a function of the transmitted data, the channel impulse response, the additive noise and the equalizer tap gains. For our purpose, however, it is convenient to represent the equalizer output by

$$a_n^* = a_n - d_n - n_n \qquad\qquad (6.5)$$

where

a_n = the true symbol,

d_n = the residual distortion, and

n_n = the noise component at the equalizer output.

The probability of error for a binary symbol is given by

$$P(e \mid d_n) = P(d_n + n_n > a_n) \quad .$$

We may assign a decision boundary by equating the right member of (6.5) to zero:

$$a_n - d_n - n_n = 0 \qquad\qquad (6.6)$$

Since n_n is Gaussian distributed with variance σ_n^2, the error probability for a binary symbol is describable by the conditional probability: (cf. equation (2.30) for $\rho = -1$)

$$P(e|d_n) = \frac{1}{\sqrt{2\pi}} \int_{\frac{a_n - d_n}{\sigma_n}}^{\infty} \exp(-\frac{x^2}{2}) dx \qquad\qquad (6.7)$$

with the proviso that $|d_n| < |a_n|$. The average probability of error is obtained by averaging the conditional probabilities over all possible symbols:

$$P_e = \sum_{n \in I} P(e|d_n) \, P(a_n)$$

where I represents the set of binary symbols and $P(a_n)$, the probability of occurrence for the symbol a_n. For statistically independent, equally likely binary information symbols, $P(a_n) = 2^{-I}$.

Consider transmission of an isolated positive valued symbol, a_0, so that in the absence of additive noise the equalizer output is a train of pulses $(a_{-L}^*, \ a_{-L+1}^*, \ldots, a_0^*, \ldots, a_{L-1}^*, \ a_L^*)$. If the 'communications channel' attains the status of an all pass system, we have

$$a_i^* \equiv \begin{cases} a_0 & \text{for } i = 0 \\ \\ 0 & \text{for } i \neq 0 \end{cases}$$

For serial transmission of data, the set $\{a_i^*\}$ will interfere with the symbols which occur before and after the $i = 0$ instant. If we define

the distortion to be

$$d_0' = \sum_{i=-L}^{L}{}' \; |a_i^*| \quad ,$$

where the prime denotes the absence of the $i = 0$ term, the probability of error is upper bounded by

$$P(e|d_n) < \frac{1}{\sqrt{2\pi}} \int_{\frac{a_0 - d_0'}{\sigma_n}}^{\infty} \exp(-\frac{x^2}{2})dx \qquad (6.8)$$

provided $a_0 > d_n'$. An upper bound of the form

$$P(e|d_n) < \exp\left[-\frac{(a_0 - d_0')^2}{2(\sigma_n^2 + d_0'')}\right]$$

where

$$d_0' = \sum_{i \in K} |a_i^*| \text{ is the larger distortion, and}$$

$$d_0'' = \sum_{i \notin K} |a_i^*|^2 \text{ is the smaller distortion,}$$

has been published by Saltzberg (1968). If the set K is taken to contain the entire distortion, the Saltzberg upper bound becomes a boundary value of inequality (6.8).

The error probability formulae, such as equation (6.7), provide an analytical feel for system performance only. Unless separate measurements of d_n and σ_n can be made, the probability of error cannot be evaluated explicitly. The probability of error curves given in Figures 6.16 through 6.20 have been obtained by Monte-Carlo simulation on the CDC 6400 digital computer. The no intersymbol interference lower bound is also shown in each case. The transmitted binary stream is again

repetitions of a 127-digit binary M-sequence with a 100% duty cycle.
The curves for the recursive equalizer were obtained using a decision-
directed mode; those for the non-recursive equalizer have been obtained
using, initially, 7 periods (889 samples) of the transmitted sequence
as reference. For the recursive equalization system, the error count
started at the 382nd (after 3 periods) sample from quiescent condition;
that for the non-recursive equalization system started at the 1271st
(after 10 periods) sample from quiescent condition. During the course
of simulation the following points have been observed:

(i) A 21-tap recursive equalizer offers no noticeable improve-
ment over a 15-tap recursive equalizer. On the other hand, increasing
the number of taps from 15 to 21 in the non-recursive equalizer definitely
gives an improvement in system performance, as is indicated by Figure
6.20.

(ii) The curves for the recursive equalizer have been obtained
using one typical set of values for the gradient constants (i.e., $\alpha=-0.002$,
$\beta=-0.025$ and $\gamma=-0.003$); those for the non-recursive equalizer were
obtained by optimizing the gradient constants corresponding to the
particular signal-to-noise ratio and a particular channel impulse
response. Needless to say, obtaining error probability curves for the
recursive equalization system was relatively easy compared to getting
the non-recursive equalization curves.

(iii) Any subjective comparison between the performances of
the recursive and the non-recursive equalization systems, as shown by
Figures 6.16 through 6.19, should be made only after taking into account

the conditions under which measurements were made and the comments of (ii).

(iv) The curves of Figures 6.16 to 6.20 again indicate that the channel impulse response with all positive sidelobes is the hardest to cope with. This is especially so for the non-recursive equalizer case, as the curves corresponding to the all positive sidelobe channel exhibit a bottoming effect (Figure 6.20)

(v) Even if a comparison between the results of the recursive and the non-recursive equalization receivers were taken at their face values, as shown by Figures 6.16 to 6.18, the recursive equalizer case is about 4.0 dB superior to the non-recursive equalizer case at high signal-to-noise ratios (e.g., 12 dB).

6.5 Summary

A quantitative and subjective performance evaluation of the adaptive recursive filter, of the adaptive equalizer and of the complete adaptive receiver has been made by means of Monte-Carlo simulation on the CDC 6400 digital computer. The adaptive recursive filter has been shown to be only a fraction of a dB worse than the matched filter, yet the recursive filter requires fewer elements (taps).

A receiver with a recursive equalizer not only converges much faster and yields better results than one with a non-recursive equalizer, but also offers a much more robust operating capability in a purely decision directed mode. This latter feature is really important since it enables the adaptive receiver to operate under a wider range of

channel conditions. The same number of taps (or memory cells) can be assigned to both the recursive and the non-recursive equalizers, so that, from an implementation viewpoint, no extra expenditure is incurred. The modified non-recursive equalizer, with a capability for tracking its own frame of reference, does not require extra memory, but more multipliers are needed. Thus, the new recursive equalizer would cost slightly more to implement than the conventional non-recursive equalizer, but it appears that the improvement offered by the former far outweighs the additional complexity.
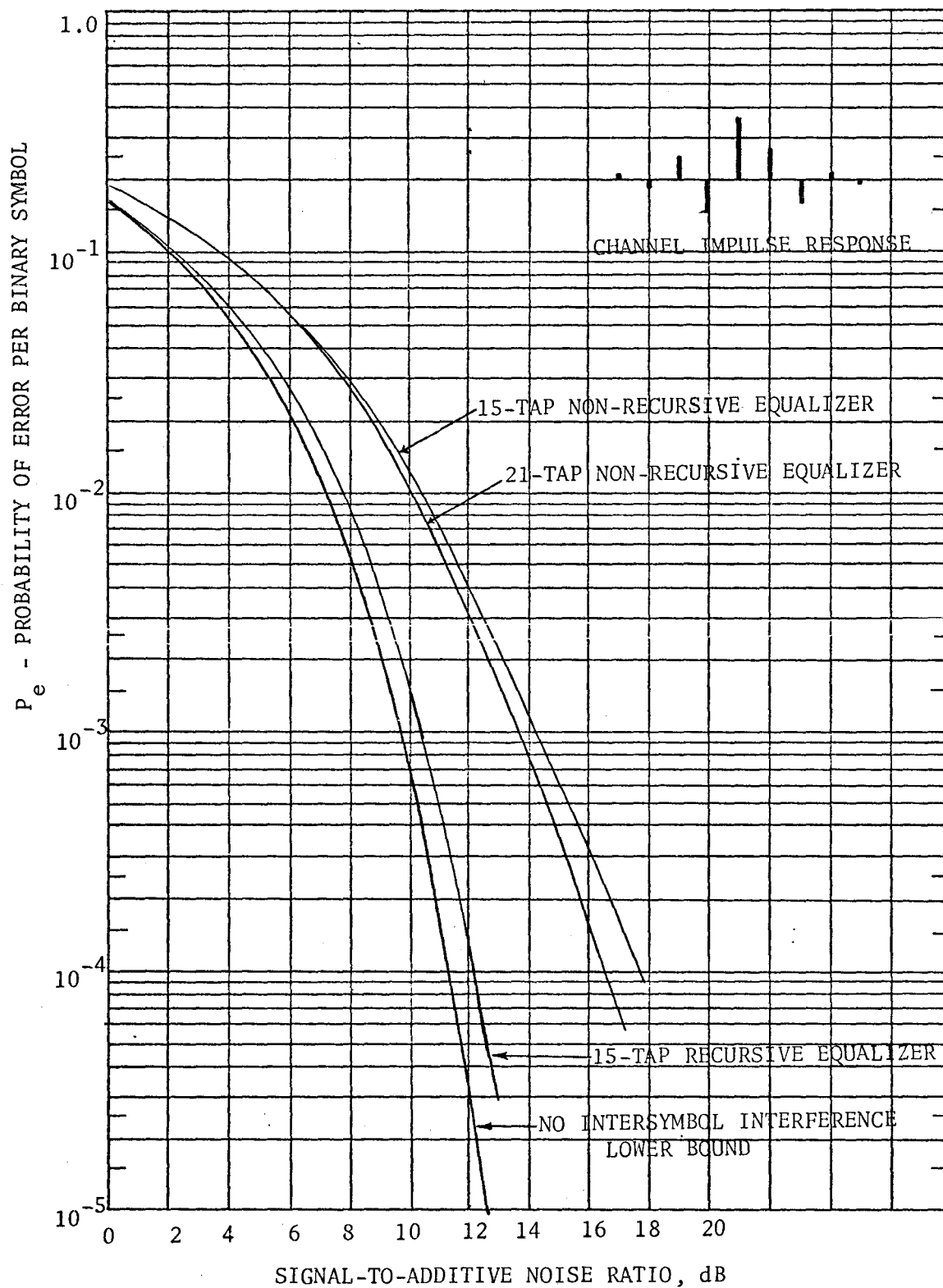
Figure 6.16   Probability of Error of Recursive and Non-recursive
Equalizers for Channel Impulse Response shown
(Equalizer preceded by Adaptive Filter)
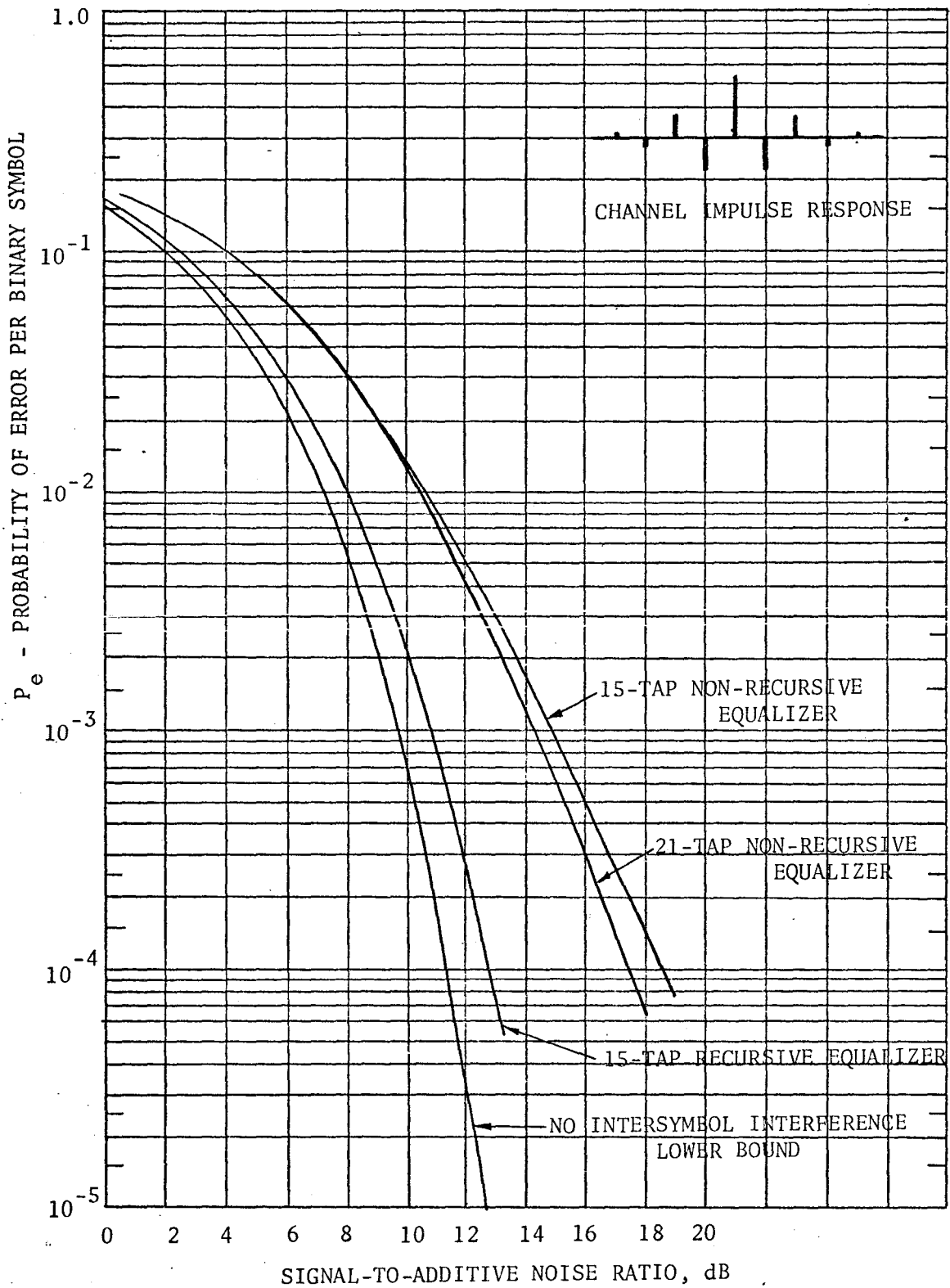
Figure 6.17 Probability of Error of Recursive and Non-recursive
Equalizers for Channel Impulse Response shown
(Equalizer preceded by Adaptive Filter)
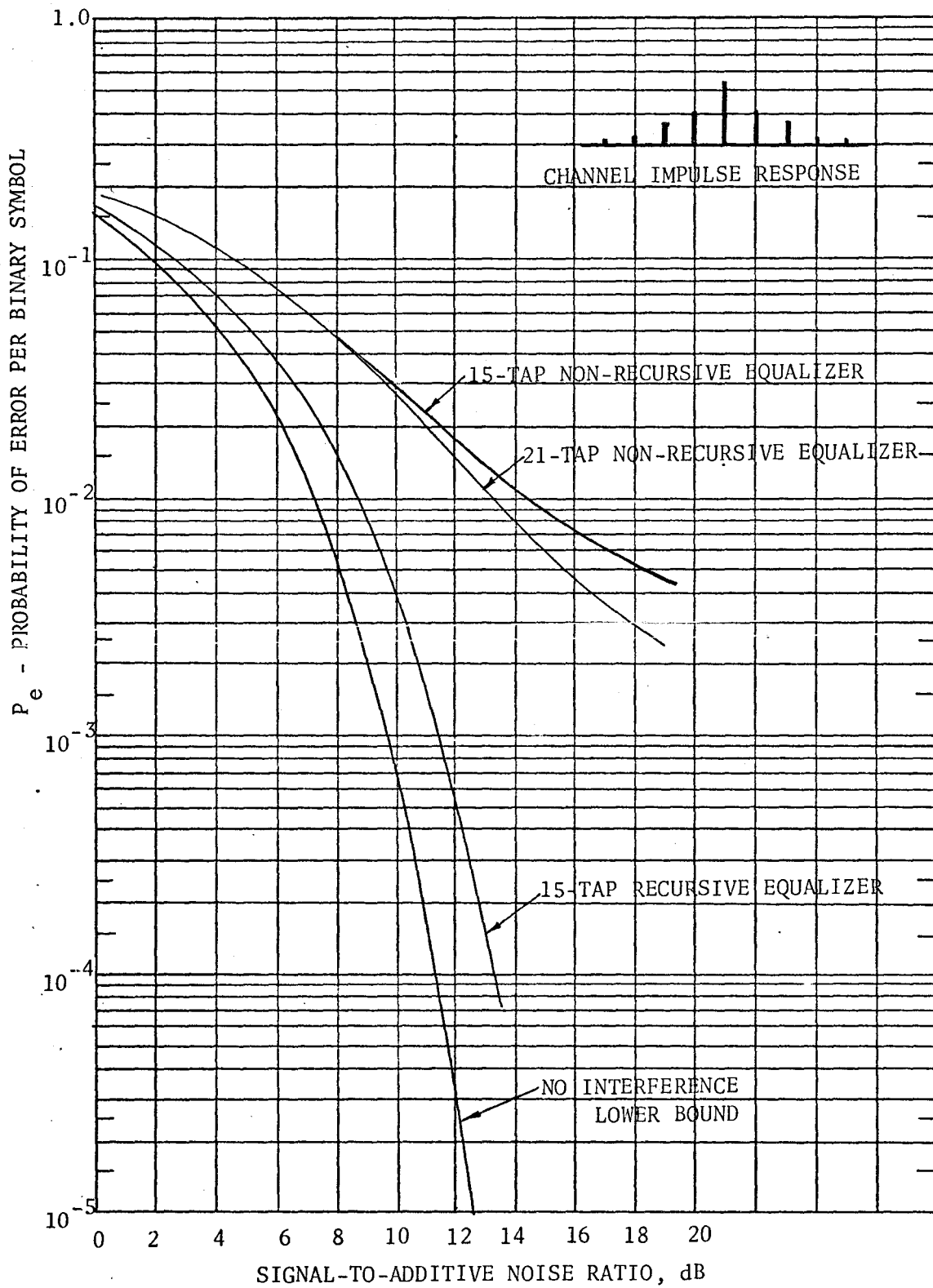
Figure 6.18   Probability of Error of Recursive and Non-recursive
Equalizers for Channel Impulse Response shown
(Equalizer preceded by Adaptive Filter)
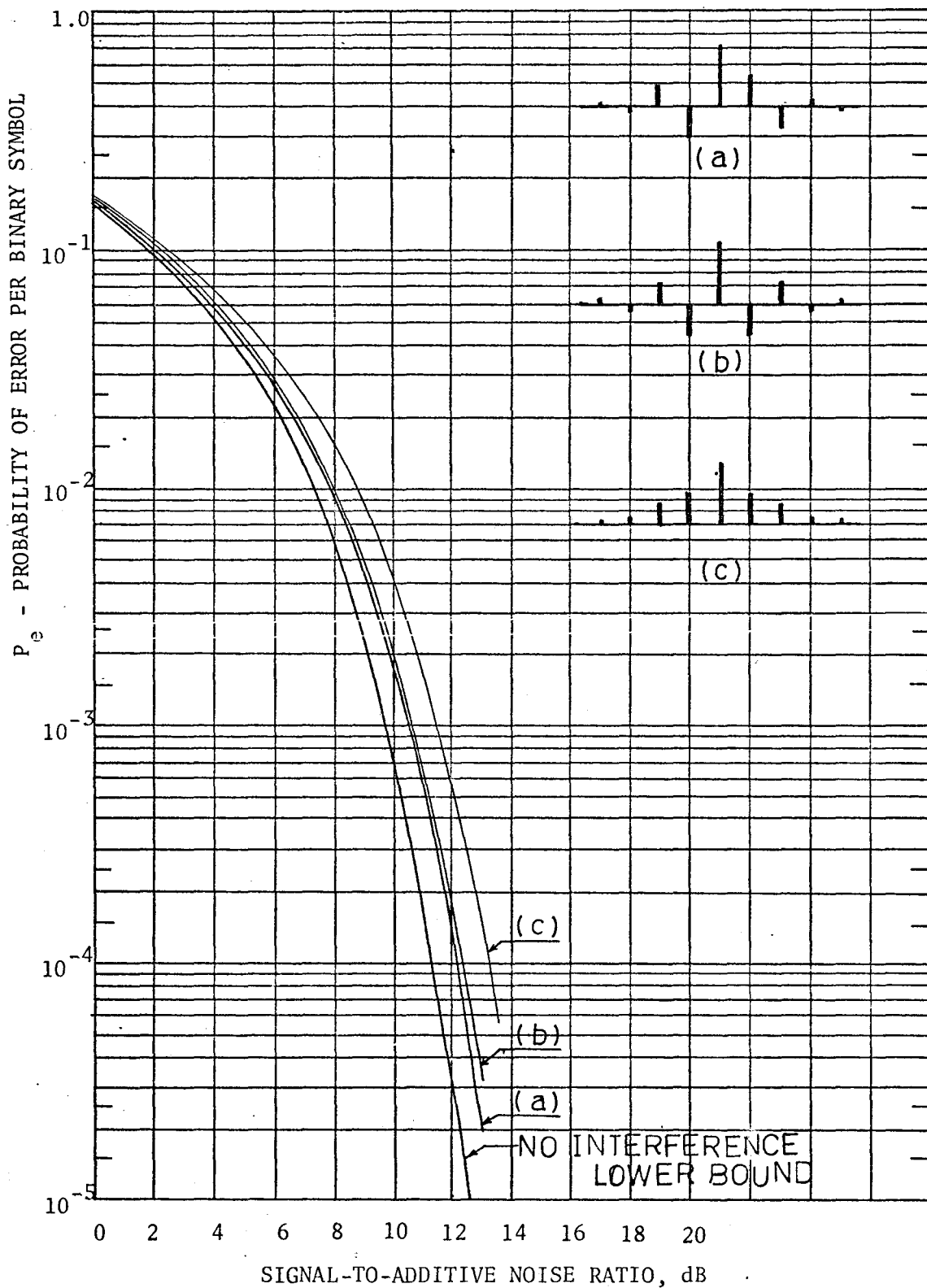
Figure 6.19 Probability of Error of 15-tap Recursive Equalizer
for different Channel Impulse Responses shown
(Equalizer preceded by Adaptive Filter)
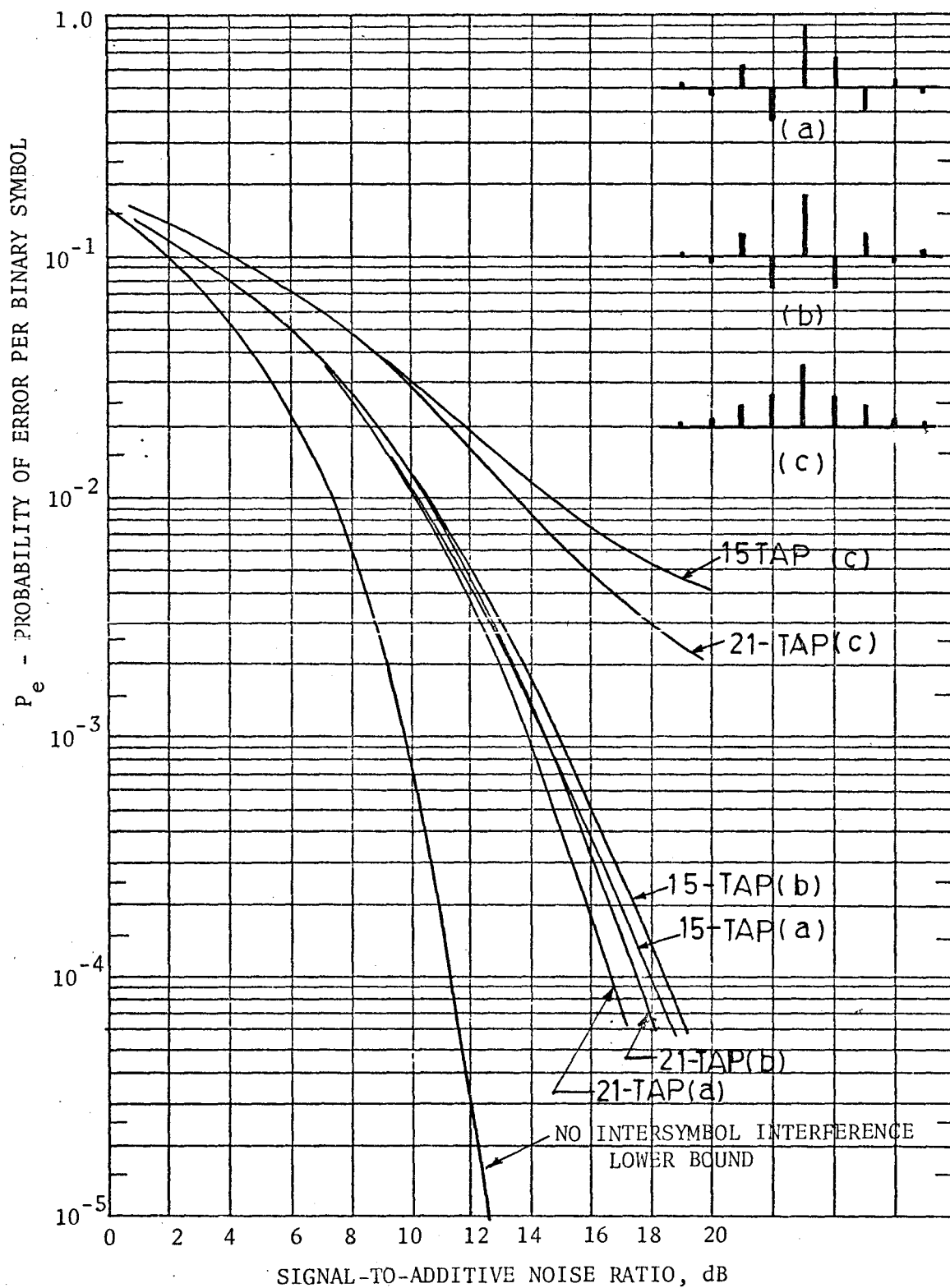
Figure 6.20 Probability of Error of Non-recursive Equalizer
for different Channel Impulse Responses shown
(Equalizer preceded by Adaptive Filter)

CHAPTER 7

CONCLUSIONS AND FUTURE STUDIES

7.1 Conclusions

A general adaptive recursive filter and an adaptive recursive equalizer, for use in digital communications over dispersive unknown channels, have been derived. The major contribution of this research effort has been the introduction of an improved adaptive signal processing technique that should lead to improved digital communications in the future. Performance evaluations for the adaptive system have been undertaken by means of Monte-Carlo simulations on a digital computer.

The following contributions to the field of digital communications have been made by the research described in this thesis:

(1) A synchronous demodulation scheme to facilitate coherent reception of AM signals has been proposed and its feasibility demonstrated.

(2) An adaptive recursive filter exhibiting a performance only a fraction of a dB worse than that of a matched filter has been derived using a combination of Hilbert Space method and a mean square error minimization technique. The adaptive recursive filter is capable of tracking a time-variant signal in stationary or non-stationary noise.

(3) The conventional non-recursive equalizer has been modified by the introduction of an auxiliary function. The final form of the modified non-recursive equalizer contains a learning loop in addition to the conventional non-recursive equalizer structure. This learning loop provides the modified non-recursive equalizer with a capability

to track its own frame of reference. Also, the presence of the learning loop enables the adaptive equalizer to take on larger values for the gradient constants, thereby helping to speed the convergence.

(4) The adaptive equalizer has been realized as the cascade connection of a non-recursive and a recursive structure. Because of the feedback properties of the recursive structure, the recursive equalizer could become unstable during operation. Through the introduction of a sufficient but not necessary stability condition, a constrained recursive equalizer has been derived. Computer simulations have indicated that, under identical conditions, the constrained recursive equalizer converges much slower than an unconstrained one.

(5) The recursive equalizer has been shown to have a superior performance to the non-recursive equalizer.

7.2 Future Studies

The design of a reliable communication system normally consists of three phases; namely, the theoretical study, the feasibility evaluation via simulations on a digital computer, and the experimental verification of the results. The research effort undertaken in this thesis has demonstrated the viability of the first two. A carefully controlled implementation of the adaptive receiver would provide confirmation for the theoretical and computed results reported in this thesis.

The demodulator-estimator aspect of the adaptive recursive filter, briefly discussed in section 4.5, warrants further studies both theoretically and experimentally.

APPENDIX A

MATCHED FILTER RECEPTION OF AN ISOLATED PULSE IN

WHITE GAUSSIAN NOISE

Let $p(t)$ be the transmitted pulse, $0 \leq t \leq T$,

$c(t)$ be the channel impulse response, $0 \leq t \leq T'$,

$q(t)$ be the channel output in response to the excitation $p(t)$.

Then

$$q(t) = p(t) \circledast c(t), \quad 0 \leq t \leq T'' = T + T'. \tag{A.1}$$

where $\circledast$ denotes convolution. The received signal is given by

$$r(t) = q(t) + n(t), \tag{A.2}$$

where

$n(t)$ is white Gaussian noise with one-sided spectral density

N_0 watts per Hz.

The signal energy is given by

$$E_p = \int_0^T p^2(t) dt. \tag{A.3}$$

Consider operating on the observed signal with a linear time-invariant operator, $h(t)$. The output due to the signal at time T'' is a deterministic function:

$$p_0(T'') = \int_0^{T''} h(t) n(T''-t) dt, \tag{A.4}$$

and that due to noise is a random variable:

$$n_0(T'') = \int_0^{T''} h(t)n(T''-t)dt. \tag{A.5}$$

Our criterion for signal detectability is the output signal-to-noise ratio defined as:

$$(S/N)_0 \triangleq \frac{P_0^2(T'')}{E\{n_0^2(T'')\}}$$

$$= \frac{[\int_0^{T''} h(t)q(T''-t)dt]^2}{E\{\int_0^{T''} h(t)n(T''-t)dt \cdot \int_0^{T''} h(y)n(T''-y)dy\}}$$

By interchanging the order of expectation and integration, we get for the output signal-to-noise ratio:

$$(S/N)_0 = \frac{[\int_0^{T''} h(t)q(T''-t)dt]^2}{N_0/2[\int_0^{T''} h(t)dt]^2} \tag{A.6}$$

To find an optimum operator $h_0(t)$, we maximize the output signal-to-noise ratio by taking the first partial derivative of equation (A.6) with respect to $h(t)$ and equating the result to zero:

$$\frac{\partial}{\partial h(t)}(S/N)_0 =$$

$$\frac{N_0[\int_0^{T''} h(t)dt]^2\int_0^{T''} h(t)q(T''-t)dt\int_0^{T''} q(T''-t)dt-[\int_0^{T''} h(t)q(T''-t)dt]^2 N_0\int_0^{T''} h(t)dt\}\int_0^{T''} dt}{[\frac{N_0}{2}[\int_0^{T''} h(t)dt]^2]^2}$$

$$= 0$$

Simplifying, we get

$$\int_0^{T''} h_o(t)dt \cdot \int_0^{T''} q(T''-t)dt = \int_0^{T''} h_o(t)q(T''-t)dt \cdot \int_0^{T''} dt \qquad (A.7)$$

Equation (A.7) is an identity if, and only if,

$$h_o(t) = q(T''-t). \qquad (A.8)$$

Equation (A.8) is a mathematical representation of a matched filter,
i.e., matched in characteristic to the signal component of the received
signal. The output signal-to-noise ratio of the matched filter is
obtained by substituting equation (A.8) in (A.6):

$$(S/N)_o = \frac{\int_0^{T''} q^2(T''-t)dt}{N_o/2} \qquad (A.9)$$

If the channel is non-time-dispersive with a constant gain C, then
equation (A.9) reduces to

$$(S/N)_o = \frac{2E_p C^2}{N_o} \quad , \qquad (A.10)$$

and the matched filter, within an arbitrary gain factor, is given by

$$h_o(t) = p(T-t). \qquad (A.11)$$

APPENDIX B

CHANNEL MODEL

This appendix is intended to provide a summary of the work that has appeared in the literature on channel modelling. In dealing with the analytical modelling of the channel it is convenient to use complex variable representations. As a preparation we introduce the following mathematical preliminaries:

Let $A = e^{j\theta_a}$ and $B = e^{j\theta_b}$ be two complex valued quantities. We than have

$$\text{Re}\{A\} = \cos \theta_a$$

$$\text{Im}\{A\} = \sin \theta_a$$

$$\text{Re}\{B\} = \cos \theta_b$$

$$\text{Im}\{B\} = \sin \theta_b .$$

Using the above, we have

$$\text{Re}\{A\} \cdot \text{Re}\{B\} = \cos \theta_a \cos \theta_b$$

$$= \tfrac{1}{2}[\cos(\theta_a - \theta_b) + \cos(\theta_a + \theta_b)]$$

$$= \tfrac{1}{2}[\text{Re}\{AB^c\} + \text{Re}\{AB\}] \qquad (B.1)$$

$$\text{Im}\{A\} \cdot \text{Im}\{B\} = \tfrac{1}{2}[\text{Re}\{AB^c\} - \text{Re}\{AB\}] \qquad (B.2)$$

$$\text{Re}\{A\} \cdot \text{Im}\{B\} = \tfrac{1}{2}[-\text{Im}\{AB^c\} + \text{Im}\{AB\}] \qquad (B.3)$$

$$\text{Im}\{A\} \cdot \text{Re}\{B\} = \tfrac{1}{2}[\text{Im}\{AB^c\} + \text{Im}\{AB\}] \qquad (B.4)$$

where the superscript c denotes complex conjugate. From (B.1) and (B.2) we have

$$\text{Re}\{A\} \cdot \text{Re}\{B\} + \text{Im}\{A\} \cdot \text{Im}\{B\} = \text{Re}\{AB^c\} \qquad (B.5)$$

177

Equation (B.5) indicates that in order to make full utilization of the complex signal, we need to transmit two real signals in quadrature.

Consider the transmitted signal impinging on the ith scatterer in the propagation path. The motion of the ith scatterer gives rise to an uncertainty in range as well as in frequency. Since time delay is proportional to range, a range uncertainty may be viewed as a delay uncertainty. We shall define a delay rate denoted by δ_i. The range of the ith scatterer may be represented by

$$r_i(t) = r_i + \dot{r}_i t \qquad\qquad (B.6)$$

where r_i = nominal range, and

$\dot{r}_i t$ = range uncertainty.

In terms of delay, we then have

$$\tau_i(\tau) = \tau_i + \delta_i t \qquad\qquad (B.7)$$

where τ_i = nominal delay, and

$\delta_i t$ = delay uncertainty.

The nominal delay is seldom known precisely; we may, therefore, express it in terms of a 'mean' value plus an increment by

$$\tau_i = \tau_{io} + \theta_i/\omega_o, \qquad\qquad (B.8)$$

where ω_o is the carrier frequency of the transmitted signal. That is, imprecise knowledge of the delay variable may be considered as a phase uncertainty, θ_i, lying in the interval $-\pi \leq \theta_i \leq \pi$. We thus have a delay uncertainty due to the motion of the scatterer and a phase

uncertainty due to imprecise knowledge of its range. It can be shown that the delay rate about the nominal delay, τ_i, is given by (Mark, 1968)

$$\delta_i = \frac{\dot{r}_i/c}{1 + \dot{r}_i/c} \tag{B.9}$$

where c is the velocity of propagation.

We note that for $|c| >> |\dot{r}_i|$, $|\delta_i| << 1$.

Let

$$s(t, a(t)) = \text{Re}\{a(t)e^{j\omega_0 t}\} \tag{B.10}$$

be the transmitted signal, where $a(t)$ is the modulating signal and ω_0 is the carrier frequency. For narrow-band signaling, the bandwidth of $a(t)$ is much less than ω_0. The received signal is then given by

$$z_i(t) = s(t - \tau_i(t), \gamma_i)$$

$$= \text{Re}\{\gamma_i\ a(t - \tau_i - \delta_i t)\ \exp j[\omega_0(t - \tau_i - \delta_i t)]\}$$

$$= \text{Re}\{\gamma_i\ a(t - \tau_{io} - \theta_i/\omega_0 - \delta_i t)$$

$$\cdot \exp j[(\omega_0 - \delta_i\omega_0)t - \omega_0\tau_{io} - \theta_i]\} \tag{B.11}$$

where $\gamma_i e^{-j\theta_i}$ is the complex strength of the ith scatterer,

$\delta_i\omega_0$ is the doppler frequency due to the ith scatterer,

and $\delta_i t$ represents a compression or expansion on the envelope of the signal.

For variations in $\delta_i t$ and θ_i/ω_0 much less than the reciprocal of the

bandwidth of $a(t)$, we may make the following approximation

$$a(t - \tau_{io} - \theta_i/\omega_o - \delta_i t) \approx a(t - \tau_{io}) \qquad (B.12)$$

Then equation (B.11) may be rewritten as

$$z_i(t) = \text{Re}\{\gamma_i a(t-\tau_{io})\exp j[(\omega_o-\delta_i\omega_o)(t-\tau_{io})-\theta_i]\} \qquad (B.13)$$

The received signal, given by the total contribution of all scatterers, is obtained by summing over all i:

$$z(t) = \sum_{i\in I} z_i(t)$$

$$= \text{Re}\{\sum_{i\in I} \gamma_i a(t-\tau_{io})\exp j[(\omega_o-\delta_i\omega_o)t-\omega_o\tau_{io}-\theta_i]\}. \qquad (B.14)$$

Imprecise knowledge about any parameter implies that parameter is a random variable. That is, γ_i, θ_i and δ_i are random variables. As such the received signal as represented by equation (B.14) is also a random process, which only can be described statistically. That is, we may attach to each of the above random variables a probability density such as $p_i(\gamma_i)$, $p_i(\theta_i)$ and $p_i(\delta_i)$. The received signal, $z(t)$, can then be described in terms of probability moments:

(1) The first moment of $z(t)$ is given by

$$E[z(t)] = \text{Re}\{\sum_{i\in I} E[\rho_i]a(t-\tau_{io})\exp j[\omega_o-\delta_i\omega_o)t-\omega_o\tau_{io}]\} \qquad (B.15)$$

where $\rho_i = \gamma_i e^{-j\theta_i}$ is the complex strength of the ith scatterer.

(2) The second-order moment, or the correlation function, is given by

$$R_z(t,\tau) = E\{z(t)\ z(y)\}$$

$$= \tfrac{1}{2}[Re\{z(t)z^c(y)\} + Re\{z(t)z(y)\}]$$

Using equation (B.14) in the above and taking into consideration the properties of the autocorrelation function together with the comment given to equation (B.5), we may write

$$R_z(t,\tau) = \tfrac{1}{2}Re\{\sum_i \sum_k E[\rho_i\rho_k^c]a(t-\tau_{io})a^c(y-\tau_{ko})$$

$$\cdot expj[(\omega_o-\delta_i\omega_o)t-(\omega_o-\delta_k\omega_o)y-\omega_o(\tau_{io}-\tau_{ko})-(\theta_i-\theta_k)]\}$$

$$\ldots \text{(B.16)}$$

Assumptions:

(i) If γ_i, θ_i and δ_i are statistically independent of each other, then

$$E[\rho_i] = E[\gamma_i]E[e^{-j\theta_i}]$$

(ii) If the parameters γ_i, θ_i and δ_i are themselves statistically independent, then

$$E[\rho_i\rho_k^c] = E[\gamma_i\gamma_k] = \begin{cases} E[\gamma_i^2] & \text{for } i = k \\ \\ 0 & \text{for } i \neq k \end{cases}$$

Then equations (B.15) and (B.16) reduce, respectively, to

$$E[z(t)] = Re\{\sum_i E[\gamma_i]a(t-\tau_{io})expj[(\omega_o-\delta_i\omega_o)t - \omega_o\tau_{io} - \theta_i]\}\ , \qquad \text{(B.17)}$$

and

$$R_z(t,y) = \tfrac{1}{2}Re\{\sum_i E[\gamma_i^2]a(t-\tau_{io})a^c(y-\tau_{io})expj[(\omega_o-\delta_i\omega_o)(t-y)]\}\ . \qquad \text{(B.18)}$$

(iii) Let

$$\gamma_i e^{-j\theta} = \gamma_i \cos\theta_i - j\gamma_i \sin\theta_i$$

$$= \gamma_{ic} + j\gamma_{is} \ .$$

Then, if

$$E[\gamma_{ic}] = E[\gamma_{is}] = 0,$$

$$E[z(t)] = 0 \ . \qquad\qquad (B.19)$$

Channels whose responses are completely described by equations (B.18) and (B.19) are called wide-sense stationary uncorrelated, or Gaussian, channels. The amplitude has a Rayleigh density function given by

$$p_i(\gamma_i) = \begin{cases} \dfrac{\gamma_i}{\sigma_i^2} \, e^{-\dfrac{\gamma_i^2}{2\sigma_i^2}} \ , & 0 < \gamma_i < \infty \\[3mm] 0 \ , & \text{elsewhere} \end{cases} \qquad (B.20)$$

The phase is uniformly distributed with a probability density given by:

$$p_i(\theta_i) = \frac{1}{2\pi} \ , \qquad\qquad -\pi \leq \theta_i \leq \pi \ . \qquad (B.21)$$

The statistical mean and variance of γ_i can be shown to be

$$E[\gamma_i] = \int_o^\infty \gamma_i \, p_i(\gamma_i) d\gamma_i$$

$$= \sqrt{\frac{\pi\sigma_i^2}{2}}$$

and

$$E[\gamma_i^2] = \sigma_i^2$$

Channels whose responses are partially described by equations (B.15) and (B.16) are extremely complex; higher moments are necessary to give a reasonable description.

If the complex strength of the scatterer has a nonzero mean value, then the first moment is given by equation (B.17). The complex strength is then expressible by

$$\gamma_i e^{-j\theta_i} = \alpha_i e^{-j\phi_i} + \beta_i e^{-j\psi_i} \tag{B.22}$$

where

$$\alpha_i e^{-j\phi_i} = \text{a deterministic component, and}$$

$$\beta_i e^{-j\psi_i} = \text{a random component.}$$

Both ϕ_i and ψ_i are uniformly distributed over the interval $[-\pi, \pi]$ and β_i is Rayleigh distributed with a density function of the form (B.20). It can be shown that the joint probability density of γ_i and θ_i is given by

$$p_i(\gamma_i, \theta_i) = \begin{cases} \dfrac{\gamma_i}{2\pi\sigma_i^2} \exp\left(-\dfrac{\gamma_i^2 + \alpha_i^2 - 2\gamma_i\alpha_i \cos(\theta_i - \phi_i)}{2\sigma_i^2} \right), & \begin{array}{l} 0 < \gamma_i < \infty \\ -\pi \leq \theta_i - \phi_i \leq \pi \end{array} \\[2ex] 0, & \text{elsewhere} \end{cases} \tag{B.23}$$

The amplitude density function is given by

$$p_i(\gamma_i) = \begin{cases} \dfrac{\gamma_i}{\sigma_i^2} \exp\left(-\dfrac{\gamma_i^2 + \alpha_i^2}{2\sigma_i^2}\right) I_0\left(\dfrac{\alpha_i\gamma_i}{\sigma_i^2}\right), & 0 < \gamma_i < \infty \\[2ex] 0, & \text{elsewhere} \end{cases} \tag{B.24}$$

where $I_o(x)$ is the zeroth order modified Bessel function of the first kind given by equation (2.32). The phase density function is given by

$$p_i(\theta_i) = \exp[\frac{\gamma_i \alpha_i}{\sigma_i^2} \cos(\theta_i - \phi_i)]/2\pi \, I_o(\frac{\gamma_i \alpha_i}{\sigma_i^2}) \quad . \qquad (B.25)$$

A plot of the phase density function of equation (B.25) can be found in Van Trees (1968, p. 363). It is noted that as $\alpha_i \to 0$, $p_i(\theta_i)$ approaches a uniform distribution.

Thus far, the channel model has been described in terms of a discrete or point function. In actual fact only the gross or macroscopic effect of all the scatterers that matters. To this end we introduce a density function, $\tilde{\sigma}(\tau,f)d\tau \, df$, associated with a pair of delay and doppler frequency variables through the transformations

$$\tau_{io} \to \tau \quad ,$$

$$\delta_i \omega_o/2\pi \to f \quad ,$$

and

$$\sum_i E[\gamma_i^2] \to \tilde{\sigma}(\tau,f).$$

Using the above density function, equation (B.18) may be rewritten as

$$R_z(t,y) = \tfrac{1}{2}\text{Re}\{ \int\!\!\int_{-\infty}^{\infty} \tilde{\sigma}(\tau,f) a(t-\tau) a^*(y-\tau)$$

$$\cdot \exp j[(\omega_o - \omega)(t-y)]d\tau \, df\} \qquad (B.26)$$

where

$$\omega = 2\pi f \quad .$$

The quantity $\tilde{\sigma}(\tau,f)$ describes the average power or, in radar terminology, the average cross section, attributed to all the scatterers. A normalized quantity, termed the 'channel scattering function' (Bello, 1963, 1969; Kailath, 1962, 1963) is defined as

$$\sigma(\tau,f) \triangleq \frac{\tilde{\sigma}(\tau,f)}{\displaystyle\iint_{-\infty}^{\infty} \tilde{\sigma}(\tau,f)\,d\tau\ df} \qquad\qquad (B.27)$$

The channel scattering function is reminiscent of Woodward's ambiguity function and the energy enclosed is unity, i.e.,

$$\iint_{-\infty}^{\infty} \sigma(\tau,f)\,d\tau\ df = 1$$

APPENDIX C

ABSTRACT VECTOR SPACE

The purpose of this appendix is to state concisely the properties governing the Hilbert Space Theory. More thorough and rigorous treatment of this subject can be found elsewhere (see, for example, Vulikh, 1963). Except for notational differences the complex Hilbert space has similar concepts as the real Hilbert space. For the sake of simplified notations we define the real Hilbert space in the following:

Definitions

(i) Let S be a linear system. S is a linear vector space if and only if for any vectors $\underline{x}$ and $\underline{y}$ in S, and real number c, there exist vectors $\underline{x} + \underline{y}$ and $c\underline{x}$ respectively which satisfy the usual properties of addition and multiplication. There must also exist in S a null vector $\underline{0}$.

(ii) S is an inner product space if and only if to every pair of vectors $\underline{x}$ and $\underline{y}$ in S there corresponds a real number, denoted $(\underline{x},\underline{y})$, which is called the inner product of $\underline{x}$ and $\underline{y}$. The inner product must possess the following properties: for all $\underline{x}$, $\underline{y}$, $\underline{z} \in S$ and real number c,

   (a) $(\underline{x},\underline{y}) = (\underline{y},\underline{x})$;

   (b) $(\underline{x} + \underline{y}, \underline{z}) = (\underline{x},\underline{z}) + (\underline{y},\underline{z})$;

   (c) $(c\underline{x},\underline{y}) = c(\underline{x},\underline{y})$;

   (d) $(\underline{x},\underline{x}) \geqslant 0$ for any $\underline{x} \in S$, moreover

   $(\underline{x},\underline{x}) = 0$ if and only if $\underline{x} = \underline{0}$.

(iii) The norm of a vector $\underline{x}$, denoted $||\underline{x}||$, in an inner produce space

186

S is defined as follows:

$$||\underline{x}|| \triangleq (\underline{x},\underline{x})^{\frac{1}{2}}$$

(iv) S is a complete metric space (under the norm of (iii)) if and only if for any sequence of vectors $\{\underline{x}_n\}$ in S such that $||\underline{x}_m - \underline{x}_n|| \rightarrow \underline{0}$ as m, n $\rightarrow \infty$; then there exists a vector $\underline{x} \in S$ such that $||\underline{x}_n - \underline{x}||^2 \rightarrow \underline{0}$ as n $\rightarrow \infty$, i.e., $\{\underline{x}_n\}$ is a Cauchy sequence.

(v) S is an abstract Hilbert space if and only if it possesses properties (i) to (iv).

(vi) The inner product in a Hilbert space is defined as follows: for all random variables (vector valued) $\underline{x}$, $\underline{y} \in S$

$$(\underline{x},\underline{y}) \triangleq E\{\underline{x}^t\underline{y}\}$$

where $E\{\cdot\}$ is the expectation operator and t denotes transposition.

Projection Theorem

Let Ω be a vector space, S be a vector subspace of Ω, and $\hat{\underline{x}}$ be a vector in S. A necessary and sufficient condition that $\hat{\underline{x}}$ is the unique vector in S satisfying the minimization property

$$||\underline{x} - \hat{\underline{x}}||^2 = \min_{\underline{v} \in S} ||\underline{x} - \underline{v}||^2$$

is that, for all $\underline{v} \in S$,

$$(\underline{x} - \hat{\underline{x}}, \underline{v}) = \underline{0},$$

which is the orthogonality property. The vector $\hat{\underline{x}}$ is called the perpendicular projection of $\underline{x}$ onto S.

Decomposition Theorem

Let S and Γ be two subspaces of a Hilbert space Ω such that every vector in S is orthogonal to every vector in Γ. Let $\underline{x}$ and $\underline{y}$ be vectors in the Hilbert space Ω and their projections onto the subspace S be $\underline{\hat{x}}$ and $\underline{\hat{y}}$, respectively. By the projection theorem

$$\underline{\tilde{x}} = \underline{x} - \underline{\hat{x}}$$

and

$$\underline{\tilde{y}} = \underline{y} - \underline{\hat{y}}$$

are vectors in the subspace Γ. If

$$\underline{x} = \underline{y} ,$$

then

$$\underline{\hat{x}} + \underline{\tilde{x}} = \underline{\hat{y}} + \underline{\tilde{y}}$$
$$\underline{\hat{x}} - \underline{\hat{y}} = \underline{\tilde{y}} - \underline{\tilde{x}} .$$

But $(\underline{\hat{x}} - \underline{\hat{y}}) \in S$ and $(\underline{\tilde{y}} - \underline{\tilde{x}}) \in \Gamma$, and since $S \perp \Gamma$, the above equality holds if

$$\underline{\hat{x}} - \underline{\hat{y}} = \underline{\tilde{y}} - \underline{\tilde{x}} \equiv \underline{0} ,$$

which implies

$$\underline{\hat{x}} = \underline{\hat{y}} \quad \text{and} \quad \underline{\tilde{y}} = \underline{\tilde{x}} .$$

APPENDIX D

DERIVATION OF THE GAIN MATRIX G(n,n)

The gain matrix $G(n,n)$ is derived in this Appendix by minimizing the trace of the covariance matrix incurred due to errors in making the best estimate. Our starting point is the covariance matrix given by equation (4.26) repeated below:

$$P(n|n) = P(n|n-1) - [G(n|n)V(n)D(n)]^c P(n|n-1) - P(n|n-1)[G(n,n)V(n)D(n)]^t$$

$$+ [G(n,n)V(n)D(n)]^c [P(n|n-1) + K_{\underline{m}}(n|n-1) + K_{\underline{n}}(n|n-1)]$$

$$\cdot [G(n,n)V(n)D(n)]^t \qquad (4.26)$$

Let

$$K(n|n-1) = P(n|n-1) + K_{\underline{m}}(n|n-1) + K_{\underline{n}}(n|n-1) \qquad (D.1)$$

Since $P(n|n-1)$, $K_{\underline{m}}(n|n-1)$ and $K_{\underline{n}}(n|n-1)$ are Hermitian matrices, it follows that $K(n|n-1)$ is also Hermitian. Let Q be a unity matrix. Then a linear unitary transformation of $K(n|n-1)$ yields a diagonal matrix. We have

$$[Q^c]^{-1} = [Q^c]^t = Q^+, \text{ and}$$

$$\Lambda_K = [Q^c]^{-1} K(n|n-1) \ Q$$

$$= Q^+ \ K(n|n-1) \ Q \ .$$

Hence

$$K(n|n-1) = Q\Lambda_K Q^+ \qquad (D.2)$$

Substituting equation (D.1) into (4.26) and making the orthogonal transformation indicated in equation (D.2), we have

$$P(n|n) = P(n|n-1) - [G(n,n)V(n)D(n)]^C P(n|n-1)$$

$$- P(n|n-1)[G(n,n)V(n)D(n)]^t$$

$$+ [G(n,n)V(n)D(n)]^C Q\Lambda_K Q^+ [G(n,n)V(n)D(n)]^t$$

$$= P(n|n-1) - [G(n,n)V(n)D(n)]^C P(n|n-1) - P(n|n-1)[G(n,n)V(n)D(n)]^t$$

$$+ [G(n,n)V(n)D(n)Q^C\Lambda_K^{\frac{1}{2}}]^C [G(n,n)V(n)D(n)Q^C\Lambda_K^{\frac{1}{2}}]^t \qquad \text{(D.3)}$$

To isolate the gain matrix G(n,n), complete the square of the right-hand-side of equation (D.3):

$$P(n|n) = P(n|n-1) + [[G(n,n)V(n)D(n)Q^C\Lambda_K^{\frac{1}{2}}]^C - P(n|n-1)[[Q\Lambda_K^{\frac{1}{2}}]^{-1}]^+]$$

$$\cdot [[G(n,n)V(n)D(n)Q^C\Lambda_K^{\frac{1}{2}}]^C - P(n|n-1)[[Q\Lambda_K^{\frac{1}{2}}]^{-1}]^+]^+$$

$$- [P(n|n-1)[[Q\Lambda_K^{\frac{1}{2}}]^{-1}]^+][P(n|n-1)[[Q\Lambda^{\frac{1}{2}}]^{-1}]^+]^+ \quad , \qquad \text{(D.4)}$$

where we have used the fact that P(n|n-1) is Hermitian, i.e.,

$$P(n|n-1) = [P(n|n-1)]^+.$$

To simplify notation let

$$B = [G(n,n)V(n)D(n)Q^C\Lambda_K^{\frac{1}{2}}]^C \quad , \qquad \text{(D.5)}$$

and

$$A = P(n|n-1)[[Q\Lambda_K^{\frac{1}{2}}]^{-1}]^+ \quad . \qquad \text{(D.6)}$$

Then equation (D.4) may be written as

$$P(n|n) = P(n|n-1) + [B - A][B - A]^+ - AA^+ \qquad (D.7)$$

The $P(n|n)$ is Hermitian. Let M be a normalizing unitary matrix such that $[M^c]^{-1} = M^+$. We then have the unitary transformation

$$\Lambda_{P(n|n)} = M^+ P(n|n)M$$

Using the above unitary transformation in equation (D.7), we get

$$\Lambda_{P(n|n)} = M^+ P(n|n-1)M + M^+ (B-A)(B-A)^+ M - M^+ AA^+ M \qquad (D.8)$$

Let $\underline{W}$ be a unit vector, i.e.,

$$\underline{W} = \begin{bmatrix} 1 \\ 1 \\ \cdot \\ \cdot \\ 1 \end{bmatrix}$$

Premultiplying both sides of equation (D.8) by $\underline{W}^t$ and postmultiplying by $\underline{W}$, we have

$$\begin{aligned}
\underline{W}^t \Lambda_{P(n|n)} \underline{W} &= \underline{W}^t M^+ P(n|n-1) M\underline{W} \\
&\quad + \underline{W}^t [M^+(B-A)][M^+(B-A)]^+ \underline{W} \\
&\quad - \underline{W}^t [M^+ A][M^+ A]^+ \underline{W} \\
&= [M\underline{W}]^+ P(n|n-1) [M\underline{W}] \\
&\quad + [\underline{W}^t M^+ (B-A)][\underline{W}^t M^+ (B-A)]^+ \\
&\quad - [\underline{W}^t M^+ A][\underline{W}^t M^+ A]^+ \qquad (D.9)
\end{aligned}$$

Now, $[\underline{W}^t M^+(B-A)$ and $[\underline{W}^t M^+ A]$ are row vectors and $[M\underline{W}]$ is a column vector. Let

$$\underline{R}^+ = \underline{W}^t M^+(B-A) \ ,$$

$$\underline{J}^+ = \underline{W}^t M^+ A \ ,$$

and

$$\underline{\Delta} = M\underline{W} \ ,$$

then equation (D.9) becomes

$$\underline{W}^t \Lambda_{P(n|n)}\underline{W} = \underline{\Delta}^+ P(n|n-1) \ \underline{\Delta} + \underline{R}^+ \ \underline{R} - \underline{J}^+ \ \underline{J} \tag{D.10}$$

Using the trace identity of equation (4.6) we obtain

$$tr[\underline{W} \ \underline{W}^t \ \Lambda_{P(n|n)}]= tr[\underline{\Delta} \ \underline{\Delta}^+ P(n|n-1)]$$

$$+ \ \underline{R}^+ \ \underline{R} - \underline{J}^+ \ \underline{J} \tag{D.11}$$

But

$$tr[\underline{W} \ \underline{W}^t \ \Lambda_{P(n|n)}] = tr[\Lambda_{P(n|n)}] = tr[P(n|n)],$$

since $\underline{W}$ is a unit vector. Therefore equation (D.11) becomes

$$tr[P(n|n)] = tr[\underline{\Delta} \ \underline{\Delta}^+ P(n|n-1)] + \underline{R}^+ \ \underline{R} - \underline{J}^+ \ \underline{J} \tag{D.12}$$

From equation (D.12) we note that

(1) $tr[P(n|n)]$ is real and positive unless $\underline{\tilde{m}}(n|n) \equiv \underline{0}$, in which case $tr[P(n|n)] = 0$.

(2) Both $\underline{R}^+ \ \underline{R}$ and $\underline{J}^+ \ \underline{J}$ are real quantities $\geqslant 0$.

(3) Properties (1) and (2) above imply that $tr[\underline{\Delta} \ \underline{\Delta}^+ P(n|n-1)]$ is also real $\geqslant 0$.

(4)   The Gain matrix $G(n,n)$ appears only in the vector $\underline{R}$. With the above observations we maintain that $\text{tr}[P(n|n)]$ attains its minimum when $\underline{R}^{+} \underline{R}$ vanishes. This requires

$$\underline{R}^{+} = \underline{W}^{t} M^{+} [B - A] = \underline{0}^{t},$$

from which we get

$$B = A \ .$$

Using the defining equations (D.5) and (D.6) we have

$$[G(n,n)V(n)D(n)Q^{c}\Lambda_{K}^{\frac{1}{2}}]^{c} = P(n|n-1)[[Q\Lambda_{K}^{\frac{1}{2}}]^{-1}]^{+}. \tag{D.13}$$

But,

$$[[Q\Lambda_{K}^{\frac{1}{2}}]^{-1}]^{+} = [[Q\Lambda_{K}^{\frac{1}{2}}]^{+}]^{-1}.$$

Postmultiplying both sides of (D.13) by $[Q\Lambda_{K}^{\frac{1}{2}}]^{+}$ yields

$$[G(n,n)V(n)D(n)]^{c}Q\Lambda_{K}^{\frac{1}{2}} \ \Lambda^{\frac{1}{2}} \ Q^{+} = P(n|n-1)$$

or

$$G(n,n) = P(n|n-1) \ [V(n)D(n)K(n|n-1)]^{-1}. \tag{D.14}$$

Recalling

$$K(n|n-1) = Q\Lambda_{K}Q^{+}$$

$$= P(n|n-1) + K_{\underline{m}}(n|n-1) + K_{\underline{n}}(n|n-1) \quad ,$$

our final result is

$$G(n,n) = P(n|n-1) \ [V(n)D(n)[P(n|n-1) + K_{\underline{m}}(n|n-1) + K_{\underline{n}}(n|n-1)]]^{-1} \tag{D.15}$$

APPENDIX E

POSITIVE DEFINITENESS OF THE COVARIANCE MATRIX

Consider the correlation matrix $K = [k(x_j, x_i)]$ where the $k(x_j, x_i)$'s are finite. Let $\{c_j\}$ be a set of arbitrary real positive coefficients[†]. Then

$$\sum_{j,i} c_j k(x_j, x_i) c_i = \sum_{j,i} c_j E(x_j \cdot x_i) c_i \qquad (E.1)$$

Since $E(x_j x_i)$ is finite it is permissible to interchange the order of summation and expectation. Thus, equation (E.1) becomes

$$\sum_{j,i} c_j k(x_j, x_i) c_i = E[\sum_{j,i} c_j c_i x_j \cdot x_i]$$

$$= E\{|\sum_j c_j x_j|^2\} \qquad (E.2)$$

Now let $\quad x_j = \bar{x} + y_j \qquad (E.3)$

where $\quad \bar{x}$ = mean value of x_j,

y_j has zero mean .

Substituting equation (E.3) into equation (E.2) we have

$$\sum_{j,i} c_j k(x_j, x_i) c_i = E\{|\sum_j c_j \bar{x} + \sum_j c_j y_j|^2\}$$

$$= E\{|\sum_j c_j \bar{x}|^2\} + E\{|\sum_j c_j y_j|^2\} \qquad (E.4)$$

[†]If $\{c_j\}$ were complex, complex conjugation must be used throughout the analysis.

194

Now, for $\bar{x} \neq 0$

$$E\{|\sum_j c_j \cdot \bar{x}|^2\} > 0 \qquad\qquad (E.5)$$

and

$$E\{|\sum_j c_j y_j|^2\} \geqslant 0 \qquad\qquad (E.6)$$

Therefore the correlation matrix $[k(x_j, x_i)]$ is positive definite unless $\{x_j\}$ contains no coherent component. Even then, equality in equation (E.6) holds only if $\sum_j c_j y_j = 0$.

APPENDIX F

CONVERGENCE PROPERTIES OF THE RECURSIVE ALGORITHM

This Appendix describes the convergence properties of the tap gain recursive formulae used in the adaptive implementation of the signal processor. Section F.1 is concerned with the adaptive filter derived in Chapter 4 while Sections F.2 to F.4 are devoted to the convergence analyses of the adaptive equalizer derived in Chapter 5.

F.1 The Adaptive Filter

The gain formula for the adaptive filter is given by equation (4.47) repeated below:

$$g_{n+1,j} = g_{n,j} - \alpha \, E\{\overset{\vee}{m}_n \, y_{n,j}\} \tag{4.47}$$

where

$$\overset{\vee}{m}_n = m_d - m_n^*$$

$y_{n,j} = (u_n - m_{n-1}^*)_j$ is the differential signal between the the observables and the estimates.

Equation (4.47) may be expanded to yield

$$g_{n+1,j} = g_{n,j} + \alpha \sum_{i=1}^{M} d_i \, E\{\hat{m}_{n,i} \, y_{n,j}\} - \alpha \, E\{m_d \, y_{n,j}\}$$

$$= g_{n,j} + \alpha \sum_{i=1}^{M} d_i \, g_{n,i} \, E\{y_{n,i} \, y_{n,j}\}$$

$$+ \alpha \sum_{i=1}^{M} d_i \, E\{m_{n-1,i}^* \, y_{n,j}\} - \alpha \, E\{m_d \, y_{n,j}\} \tag{F.1}$$

196

For the purpose of analyzing the stability of the gain function, $g_{n,j}$, the last two terms in (F.1) may be ignored. For this purpose (F.1) may be rewritten, in vector notation, as

$$g_{n+1} = [I - \alpha K_{i,j}]g_n \qquad \text{(F.2)}$$

where

$K_{i,j}$ = the second order moment matrix with entries $E\{y_{n,i} \; y_{n,j}\}$, that is, the correlations of the differential signal between the observables and the estimates,

d_i has been chosen to be 1/M and incorporated in the constant α,

and   I is an identity matrix.

The system of Equation (F.2) will be stable if α is positive lying in the range

$$0 < \alpha < \frac{2}{\lambda_{max}} \qquad \text{(F.3)}$$

where λ_{max} is the maximum eigenvalue of the matrix $K_{i,j}$ (see Section F.2 for a more elaborate treatment). If the gain function is given by Equation (4.48):

$$g_{n+1,j} = g_{n,j} - \alpha \; E\{\tilde{m}_j \; y_{n,j}\} \qquad \text{(4.48)}$$

where

$$\tilde{m}_j = m^* - \hat{m}_j,$$

it can be shown that α is negative lying in the range

$$0 > \alpha > \frac{-2}{\lambda_{max}} \;. \qquad \text{(F.4)}$$

F.2 The Non-recursive Equalizer

From Section 5.4 the recursive algorithm for the reference weight, at $i = 0$, of the estimation loop is given by equation (5.25) repeated below:

$$W_{n+1,0}(a) = W_{n,0}(a) - \alpha^n E(e_n \ x_n) \qquad (5.25)$$

where

$$E(e_n \ x_n) = -[\sum_{i=-M}^{M} W_{n,i}(a) \ K(x_{n-i}, \ x_{n-j}) + \delta W_{n,0}(a) \ K(n_n, x_{n-j})$$

$$-K(a, \ x_{n-j})]\Big|_{j=0}$$

Equation (5.25) above may be extended to cover the range $-M \leqslant j \leqslant M$. Consequently, in vector notation, the recursive algorithm has the following form:

$$\underline{W}_{n+1}(a) = \underline{W}_n(a) - \alpha \underline{P}_n$$

$$= \underline{W}_n(a) - \delta \underline{W}_n(a) \qquad (F.5)$$

where

$$\underline{P}_n = -[K_{ij}]\underline{W}_n(a) - \delta W(a) \ \underline{K}_\eta + \underline{K}_\alpha \ , \qquad (F.6)$$

$[K_{ij}]$ = second order moment matrix with entries $K(x_{n-i}, x_{n-j})$,

$\underline{K}_\eta$ = a column vector with elements $K(n_n, \ x_{n-j})$,

$\underline{K}_\alpha$ = a column vector with elements $K(\alpha_n, \ x_{n-j})$,

j, i = $-M, \ldots, -1, 0, 1, \ldots, M$.

From equation (F.5) we get

$$\delta \underline{W}_{-n}(a) = \alpha \underline{P}_{-n}$$

$$= -\alpha [K_{ij}] \underline{W}_{-n}(a) - \alpha \delta W_{n,0}(a) \underline{K}_{-\eta} + \alpha \underline{K}_{-a}$$

or

$$[\delta \underline{W}_{-n}(a) + \alpha \delta W_{n,0}(a) \underline{K}_{-\eta}] = -\alpha [K_{ij}] \underline{W}_{-n}(a) + \alpha \underline{K}_{-a} . \qquad (F.7)$$

The identity

$$\delta W_{n,0}(a) \underline{K}_{-\eta} = [K(\eta_{n-i}, x_{n-j})] \delta \underline{W}_{-n}(a) \qquad (F.8)$$

holds if

$$[K(\eta_{n-i}, x_{n-j})] = \begin{bmatrix} 0 \ldots 0 & K(\eta_n, x_{n+M}) & 0 \ldots 0 \\ \vdots & \vdots & \vdots \\ \vdots & \vdots & \vdots \\ \vdots & \vdots & \vdots \\ 0 \ldots 0 & K(\eta_n, x_n) & 0 \ldots 0 \\ \vdots & \vdots & \vdots \\ \vdots & \vdots & \vdots \\ \vdots & \vdots & \vdots \\ 0 \ldots 0 & K(\eta_n, x_{n-M}) & 0 \ldots 0 \end{bmatrix} ,$$

that is

$$\eta_{n-i} = \begin{cases} \eta_n , & i=0 \\ \\ 0 , & i \neq 0. \end{cases}$$

Using identity (F.8) in equation (F.7) we have

$$[I + \alpha [K(\eta_{n-i}, x_{n-j})]] \delta \underline{W}_{-n}(a) = -\alpha [K_{ij}] \underline{W}_{-n}(a) + \alpha \underline{K}_{-a} \qquad (F.9)$$

With respect to equation (F.9) we make the following observations:

(i)   The identity matrix I is positive definite.

(ii)   The second order moment matrix $[K(\eta_{n-i}, x_{n-j})]$ is positive semi-definite.

(iii)   Properties (i) and (ii) assure the existence of an inverse for the sum matrix $[I + \alpha[K(\eta_{n-i}, x_{n-j})]]$.

(iv)   The last term on the right-hand-side of (F.9) has no influence on the stability of the recursive algorithm. Therefore, for stability considerations the last term of (F.9) may be neglected to simplify the algebra.

Observations (i) to (iv) enable us to rewrite equation (F.9) as

$$\delta \underline{W}_n(a) = -\alpha[I + \alpha[K(\eta_{n-i}, x_{n-j})]]^{-1} [K_{ij}] \underline{W}_n(a)$$

$$= -\alpha[R_{ij}] \underline{W}_n(a) \tag{F.10}$$

where

$$[R_{ij}] = [I + \alpha[K(\eta_{n-i}, x_{n-j})]]^{-1} [K_{ij}] . \tag{F.11}$$

Substituting equation (F.10) into (F.5) we have

$$\underline{W}_{n+1}(a) = \underline{W}_n(a) + \alpha[R_{ij}] \underline{W}_n(a) = [I + \alpha[R_{ij}]] \underline{W}_n(a) . \tag{F.12}$$

The system of equation (F.12) will be stable if

$$|I + \alpha[R_{ij}]| < 1$$

Let [Q] be a normalized model matrix. Then the following hold (Pierre, 1966)

$$[Q]^T = [Q]^{-1} ,$$

$$[Q]^T[Q] = I$$

and

$$[R_{ij}] = [Q]^T[\Lambda] [Q], \tag{F.13}$$

where $[\Lambda]$ is a diagonal matrix, the non-zero elements of which are the eigenvalues of the matrix $[R_{ij}]$. The canonical linear orthogonal transformation of equation (F.13) holds whether or not the eigenvalues are distinct. If there are multiple eigenvalues, $[\Lambda]$ is a Jordan canonical form. Using the canonical transformation of equation (F.13) in (F.12) we obtain

$$\underline{W}_{n+1}(\alpha) = [Q]^T [I + \alpha[\Lambda]] [Q] \underline{W}_n(\alpha)$$

or

$$[Q] \underline{W}_{n+1}(\alpha) = [I + \alpha[\Lambda]] [Q] \underline{W}_n(\alpha) . \tag{F.14}$$

Writing

$$\underline{W}_{t,n+1}(\alpha) = [Q] \underline{W}_{n+1}(\alpha)$$

and

$$\underline{W}_{t,n}(\alpha) = [Q] \underline{W}_n(\alpha),$$

equation (F.14) becomes

$$\underline{W}_{t,n+1}(\alpha) = [I + \alpha[\Lambda] \underline{W}_{t,n}(\alpha) . \tag{F.15}$$

The stability condition then becomes

$$|I + \alpha[\Lambda]| < 1$$

or

$$|I + \alpha\lambda_j| < 1 . \tag{F.16}$$

By virtue of observations (i) to (iii) above and,

(v) $[K_{ij}]$ is positive definite

$[R_{ij}]$ is positive definite too. Hence, $\lambda_j > 0$. In order that inequality (F.16) holds α must be negative lying in the range

$$0 > \alpha > \frac{-2}{\lambda_{max}} \qquad (\text{F.17a})$$

But $\lambda_{max} < \Sigma \lambda_j =$ trace of $[R_{ij}]$, the bound of (F.17a) may be tightened by

$$0 > \alpha > \frac{-2}{\text{tr}[R_{ij}]} \qquad (\text{F.17b})$$

F.3   The Learning Loop

The quantity $E(\eta_n x_{n-j})$ has the following expansion:

$$E(\eta_n x_{n-j}) = E\{[x_n - \sum_i W_{n,i}(x_n) x_{n-i}] x_{n-j}\}$$

$$= E(x_n - x_{n-j}) - \sum_i W_{n,i}(x_n) E(x_{n-i}x_{n-j})$$

Using the above in equation (5.22), we get

$$W_{n+1,j}(x_n) = W_{n,j}(x_n) + \beta \sum_i W_{n,i}(x_n)E(x_n x_{n,j}) - \beta E(x_n x_{n,j}) \qquad (\text{F.18})$$

In vector notation (F.18) becomes

$$\underline{W}_{n+1}(x_n) = \underline{W}_n(x_n) + \beta K_{ij} \underline{W}_n(x_n) - \beta \underline{K}_{0,j} \ , \qquad (\text{F.19})$$

where

$$K_{ij} = [E(x_{n-i}x_{n-j})],$$

$$\underline{K}_{0,j} = \underline{E(x_n x_{n-j})} \ .$$

The last term in equation (F.19) does not depend on $\underline{W}(x_n)$, hence has no influence on the stability of the recursive equation for $\underline{W}(x_n)$ and may, therefore, be ignored in evaluating the stability condition. We rewrite (F.19) as

$$\underline{W}_{n+1}(x_n) = \underline{W}_n(x_n) + \beta \, K_{ij} \, \underline{W}_n(x_n)$$

$$= (I + \beta \, K_{ij}) \underline{W}_n(x_n)$$

Using the same procedure as in (F.13) through (F.15), we find that β must lie in the range

$$0 > \beta > \frac{-2}{\lambda_{max}}$$

or

$$0 > \beta > \frac{-2}{tr[K_{ij}]} \quad ,$$

where λ_{max} is the maximum eigenvalue of the matrix $K_{i,j}$.

F.4 The Recursive Equalizer

F.4.1. The Constrained Case

The quantity $[E(e_n \, a^*_{n-i}) + E(\nu_n \, e_n)Sgn(b_{n,i})]$ has the following expansion:

$$E(e_n \, a^*_{n-i}) + E(\nu_n \, e_n)Sgn \, b_{n,i}$$

$$= E\{(\nu_n + \sum_j b_{n,j}a^*_{n-j})a^*_{n-i}\} + E\{\nu_n[\,\nu_n + \sum_j b_{n,j}a^*_{n-j}]\} \, Sgn \, b_{n,i}$$

$$= E\{\nu_n \, a^*_{n-i}\} + \sum_j b_{n,j} \, E(a^*_{n-j}a^*_{n-i})$$

$$+ [E[\nu_n^2] + \sum_j b_{n,j} \, E(\nu_n \, a^*_{n-j})] \, Sgn \, b_{n,i} \quad .$$

Substituting the above in equation (5.46), we get

$$b_{n+1,i} = b_{n,i} + \gamma \sum_j b_{n,j} E(a^*_{n-j} a^*_{n-i}) + \gamma Sgn \; b_{n,i} \sum_j b_{n,j} E(\nu_n \; a^*_{n-j})$$

$$+ \gamma \; E(\nu_n a^*_{n-i}) + \gamma \; E[\nu_n^2] \; Sgn \; b_{n,i}$$

Writing the above in vector notation and ignoring the last two terms, which do not depend on $\underline{b}$, we have

$$\underline{b}_{n+1} = \underline{b}_n + \gamma K_{a*} \; \underline{b}_n + \gamma \; Sgn \; \underline{b} \; K^t_{\nu a*} \; \underline{b}_n$$

where

$$K_{a*} = [E(a^*_{n-i} \; a^*_{n-j})] \;,$$

$$\underline{K}_{\nu a*} = \underline{E(\nu_n - a^*_{n-j})} \;\;.$$

We know that K_{a*} is a positive definite matrix (see Appendix E), but we are not sure about the matrix $B = [Sgn(\underline{b}) K^t_{\nu a*}]$. We consider the following cases:

(1) If B is positive definite, then, using the procedure (F.13) through (F.15), we find γ lies in the range

$$0 > \gamma > \frac{-2}{\lambda_{max}} \tag{F.20a}$$

or

$$0 > \gamma > \frac{-2}{tr[K_{a*} + B]} \;\;. \tag{F.20b}$$

where λ_{max} is the maximum eigenvalue of the sum matrix $[K_{a*} + B]$.

(2) If B is negative definite, then the sum matrix $[K_{a*}+B]$ may be positive or negative definite. If $[K_{a*}+B]$ is positive definite, then (F.20) is satisfactory. If, on the other hand, $[K_{a*}+B]$ is negative definite, then γ should be positive lying in the range

$$0 < \gamma < \frac{2}{\lambda_{max}} \qquad \text{(F.21a)}$$

or

$$0 < \gamma < \frac{2}{\text{tr}[K_{a*} + B]} \; . \qquad \text{(F.21b)}$$

We note that the trace operator is linear:

$$\text{tr}[K_{a*} + B] = \text{tr}[K_{a*}] + \text{tr}[B]$$

$$= \sum_j \lambda_{a*j} + \sum_j \lambda_{bj} \; .$$

If B is negative definite, all λ_{bj}'s are negative and hence $\sum_j \lambda_{bj} = \text{tr}[B]$ is also negative. If we let the magnitude of γ be upper bounded by $|\gamma| < \frac{2}{\text{tr}[K_{a*}+B]}$, for B positive definite, we may make the simple test of comparing the trace of K_{a*} with that of B and decide whether (F.20b) or (F.21b) is to be used. In this case we only need to change the sign of γ.

F.4.2. The Unconstrained Case

For the unconstrained recursive equalizer the gain formula of the recursive section is given by equation (5.51):

$$b_{n+1,i} = b_{n,i} + \gamma \, E\{e_n \, a^*_{n-i}\} \qquad \text{(5.51)}$$

In vector notation (5.51) may be written as

$$\underline{b}_{n+1} = [I + \gamma K_{a*}]\underline{b}_n + \gamma E(\nu_n \ a^*_{n-i}) \qquad \text{(F.22)}$$

where the last term of (F.22) does not depend on $\underline{b}$. It can easily be shown that the system of (F.22) will be stable if γ is negative lying in the range

$$0 > \gamma > \frac{-2}{\lambda_{max}} \qquad \text{(F.23a)}$$

or

$$0 > \gamma > \frac{-2}{tr[K_{a*}]} \qquad \text{(F.23b)}$$

where λ_{max} is the maximum eigenvalue of the matrix K_{a*} .

APPENDIX G

STABILITY CONDITION FOR THE RECURSIVE EQUALIZER

In z-transform notation an Nth order normalized recursive equalizer may be expressed as

$$H_2(z) = \frac{1}{1 + \sum\limits_{i=1}^{N} b_i z^{-i}} \tag{G.1}$$

The output is then

$$a^*(z) = H_2(z) \, y(z)$$

or

$$a^*(z)[1 + \sum\limits_{i=1}^{N} b_i z^{-i}] = y(z) \tag{G.2}$$

where $y(z)$ is the excitation. The inverse transform of (G.2) is the following difference equation:

$$a_n^* + \sum\limits_{i=1}^{N} b_{n,i} \, a_{n-i}^* = y_n$$

or

$$a_n^* = y_n - \sum\limits_{i=1}^{N} b_{n,i} \, a_{n-i}^* \quad . \tag{G.3}$$

The system of (G.1) will be stable if a_n^* is upper bounded for a unit step excitation, i.e., $y_j = 1$ for all j. Using the triangle inequality we note that the magnitude of a_n^* is upper bounded by

$$|a_n^*| \leq |y_n| + |\sum\limits_{i=1}^{N} b_{n,i} \, a_{n-i}^*| \quad . \tag{G.4}$$

Also

$$|\sum\limits_{i=1}^{N} b_{n,i} \, a_{n-i}^*| \leq \sum\limits_{i=1}^{N} |b_{n,i} \, a_{n-i}^*| = \sum\limits_{i=1}^{N} |b_{n,i}||a_{n-i}^*| \tag{G.5}$$

where

$$|a^*_{n-i}| \le |y_{n-1}| + \sum_{i=1}^{N} |b_{n-1,i}||a^*_{n-1,i}| \tag{G.6}$$

etc.

Let $k_n = \sum_{i=1}^{N} |b_{n,i}|$ lie in the range $0 \le k_n < 1$. Then, for a unit step excitation, using (G.5) and (G.6) in (G.4) and expanding, we have

$$|a^*_n| \le 1 + k_n + k_n k_{n-1} + k_n k_{n-1} k_{n-2} + \cdots$$

Let the maximum value of $\{k_j\}$ be k_{max} where $0 \le k_{max} < 1$. Then $|a^*_n|$ is upper bounded by the geometric sum

$$|a^*_n| \le 1 + k_{max} + k^2_{max} + k^3_{max} + \cdots$$

$$\le \frac{1}{1 - k_{max}} \tag{G.8}$$

Therefore, the system of (G.1) will be stable subject to the constraint

$$k = \sum_{i=1}^{N} |b_i| < 1 . \tag{5.35}$$

The inequality constraint of (5.35) is a sufficient but not necessary stability condition; the poles of $H_2(z)$ will be restricted to lie within an ellipse, which is a subset of the unit circle in the z-plane. This is sketched in Figure (G.1).
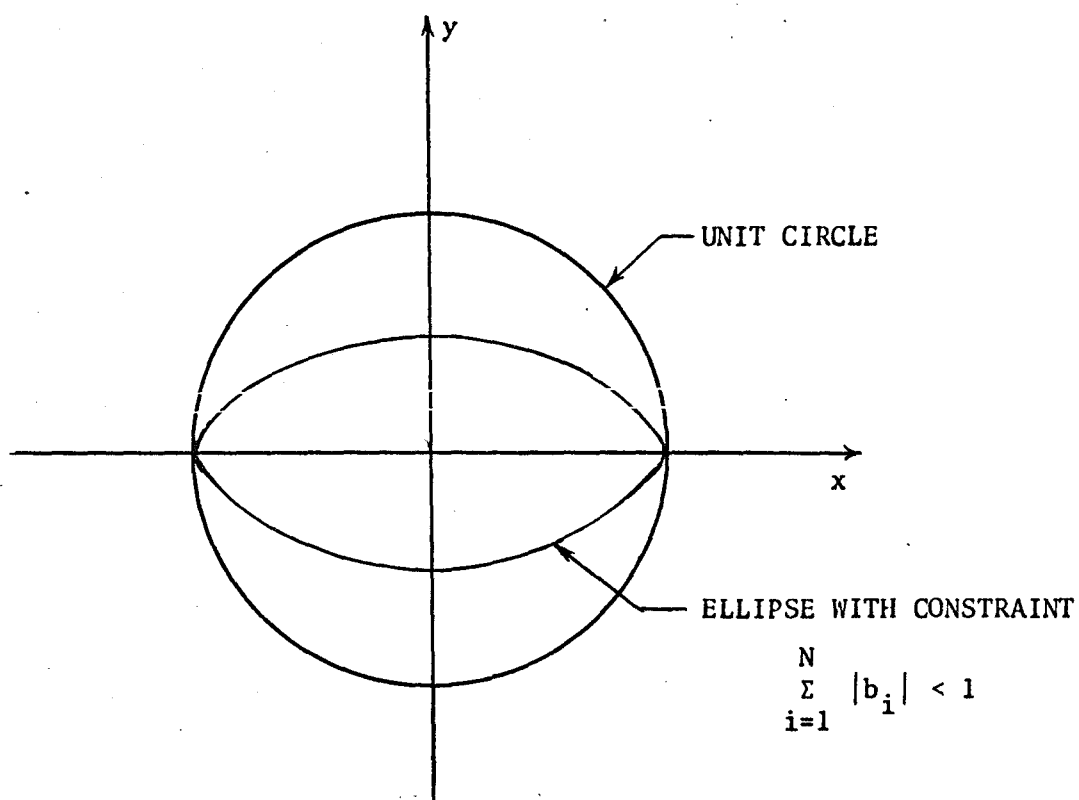
Figure G.1   Stability Condition (z-plane)
              for Recursive Equalizer

APPENDIX H

MONTE CARLO SIMULATIONS

The channel model to be simulated is that which is depicted in Figure 3.6. To probe the channel we transmit two real signals that are the Hilbert transforms of each other. Let the complex (analytic) signal be represented by

$$s(t) = \sum_{i=1}^{N} a_i \, f(t - iT_s) e^{j(\omega_o t + \theta)} \qquad (H.1)$$

where

$\{a_i\}$ is a binary M-sequence,

T_s is the pulse separation, and

N is the code length.

Each symbol a_i has an effective duration of T_o sec. The total signal duration is $T = NT_s$. We simulate the random and the deterministic branches of the channel separately. The complex signal, $s(t)$, may be decomposed into a real and an imaginary part as follows:

$$s(t) = \xi(t) + j \, \hat{\xi}(t) \qquad (H.2)$$

where $\xi(t)$ is real function and $\hat{\xi}(t)$ is the Hilbert transform of $\xi(t)$. That is,

$$\hat{\xi}(t) = H[\xi(t)] = \frac{1}{\pi} \int_{-\infty}^{\infty} \frac{\xi(\tau)}{t - \tau} \, d\tau \qquad (H.3)$$

Suppose

$$\xi(t) = \cos \omega t \ .$$

Then

$$\hat{\xi}(t) = \frac{1}{\pi} \int_{-\infty}^{\infty} \frac{\cos \omega\tau}{t - \tau} \, d\tau$$

$$= \frac{1}{\pi} \int_{-\infty}^{\infty} \frac{\cos[\omega t - \omega(t-\tau)]}{t - \tau} \, d\tau$$

$$= \frac{\cos \omega t}{\pi} \int_{-\infty}^{\infty} \frac{\cos \omega(t-\tau)}{t - \tau} \, d\tau + \frac{\sin \omega t}{\pi} \int_{-\infty}^{\infty} \frac{\sin \omega(t-\tau)}{t - \tau} \, d\tau$$

The first integral is zero since its integrand is odd about τ=t; the second integral is π if ω > 0, which we can assume since cosine is an even function, and we have sinωt as the Hilbert transform of cosωt. Thus, Hilbert transformation corresponds to a 90° phase shift, i.e.,

$$\hat{\xi}(t) = \cos(\omega t - 90°)$$

$$= \sin\omega t \, .$$

Similarly, if

$$\xi(t) = Re\{s(t)\}$$

$$= \sum_{i=1}^{N} a_i \, f(t-iT_s)\cos(\omega_0 t + \theta)$$

$$= Re\{a(t)e^{j(\omega_0 t+\theta)}\} \, ,$$

then

$$\hat{\xi}(t) = \sum_{i=1}^{N} a_i \, f(t-iT_s) \sin(\omega_0 t + \theta) \, ,$$

both of which are real functions. Transmitting the real part of a complex signal is equivalent to transmitting half of the signal energy. Thus, to make full utilization of the transmitter efficiency, we transmit

two real signals so that the total energy is given by

$$E_t = E_c + E_s$$

$$= [\int_{-\infty}^{\infty} [\xi(t)]^2 dt + \int_{-\infty}^{\infty} [\hat{\xi}(t)]^2 dt]$$

$$= \int_{-\infty}^{\infty} [\sum_{i=1}^{N} a_i f(t - iT_s)]^2 dt$$

$$= \int a^2(t) dt \qquad\qquad 0 \leqslant t \leqslant T$$

The per digit energy is given by

$$E_b = \int a^2(t) dt . \qquad\qquad 0 \leqslant t \leqslant T_o$$

The Random Branch

The memory of the random branch is assumed to be essentially zero compared to the baud length, T_o. The impulse response of the random branch is characterized by

$$c_r(t) = \sum_{i \in I} \beta_i(t) e^{-j\psi_i(t)} \qquad\qquad (H.4)$$

where

$\beta_i(t)$ is the amplitude of the ith scatterer,

$\psi_i(t)$ is the phase of the ith scatterer, and

I is a set representing the total number of scatterers.

As described in Appendix B, $\beta(t)$ has a Rayleigh density function and $\psi(t)$ is uniformly distributed in the primary interval $[-\pi, \pi]$. Let $r(t)$ represent the real part of $c_r(t)$. Then, equation (H.4) may be written as

$$c_r(t) = r(t) + j\,\hat{r}(t)$$

$$= \sum_{i\epsilon I} \beta_i(t) \cos \psi_i(t) + j \sum_{i\epsilon I} \beta_i(t) \sin \psi_i(t).$$

The random branch acting on the transmitted signal produces as output a superposition of a myriad of point target echoes. The output of the random branch may be written as

$$z_r(t) = \xi(t) \cdot r(t) + \hat{\xi}(t) \cdot \hat{r}(t)$$

$$= \sum_{i=1}^{N} a_i\, f(t-iT_s) \cos(\omega_o t+\theta) \sum_j \beta_j(t) \cos \psi_j(t)$$

$$+ \sum_{i=1}^{N} a_i\, f(t-iT_s) \sin(\omega_o t+\theta) \sum_j \beta_j(t) \sin \psi_j(t)$$

$$= \sum_{i=1}^{N} a_i\, f(t-iT_s) \sum_j \beta_j(t) \cos(\omega_o t + \theta - \psi_j(t)), \qquad (H.5)$$

which is a real signal.

The Deterministic Branch

Let the time dispersion be L and the frequency dispersion be B, as given by equations (3.23) and (3.24), respectively. The mean value of the doppler dispersion shall be taken to be the effective discrete doppler shift, i.e., $f_d = \bar{f}$, as given by equation (3.17). Then we may represent the impulse response of the deterministic branch by

$$c_d(t) = \sum_{i=-L}^{L} \alpha(t-iT_s) e^{-j[\omega_d t + \phi_i(t)]},$$

where

$$-2\pi B \leq \frac{d\phi_i(t)}{dt} \leq 2\pi B.$$

We write

$$c_d(t) = d(t) + j \, \hat{d}(t)$$

$$= \sum_{i=-L}^{L} \alpha(t-iT_s) \cos[\omega_d t + \phi_i(t)]$$

$$+ j \sum_{i=-L}^{L} \alpha(t-iT_s) \sin[\omega_d t + \phi(t)] \quad .$$

The deterministic branch acting on the transmitted signal produces as output a dispersed signal given by

$$z_d(t) = \xi(t) \cdot d(t) + \hat{\xi}(t) \cdot \hat{d}(t)$$

$$= \sum_{i=1}^{N} a_i \, f(t-iT_s) \cos(\omega_o t + \theta)$$

$$\cdot \sum_{j=-L}^{L} \alpha(t-jT_s) \cos(\omega_d t + \phi_j(t))$$

$$+ \sum_{i=1}^{N} a_i \, f(t-iT_s) \sin(\omega_o t + \theta)$$

$$\cdot \sum_{j=-L}^{L} \alpha(t-jT_s) \sin(\omega_o t + \theta)$$

$$= \sum_{i=1}^{N} a_i \, f(t-iT_s) \sum_{j=-L}^{L} \alpha(t-jT_s)$$

$$\cdot \cos[\omega_o t + \theta - \omega_d t - \phi_j(t)] \quad . \qquad (H.6)$$

The overall channel output is obtained by summing equations (H.5) and (H.6):

$$z(t) = z_d(t) + z_{\hat{r}}(t)$$

$$= \sum_{i=1}^{N} a_i \, f(t - iT_s) \sum_{j=-L}^{L} \alpha(t - jT_s) \cos[\omega_0 t + \theta - \omega_d t - \phi_j(t)]$$

$$+ \sum_{i=1}^{N} a_i \, f(t - iT_s) \sum_j \beta_j(t) \cos[\omega_0 t + \theta - \psi_j(t)] \, . \qquad (H.7)$$

The channel output represented by equation (H.7) is further corrupted by an additive noise, so that the received signal is given by

$$x(t) = z(t) + n(t)$$

$$= \sum_{i=1}^{N} a_i \, f(t - iT_s) \sum_{j=-L}^{L} \alpha(t - jT_s) \cos[\omega_0 t + \theta - \omega_d t - \phi_j(t)]$$

$$+ \sum_{i=1}^{N} a_i \, f(t - iT_s) \sum_j \beta_j(t) \cos[\omega_0 t + \theta - \psi_j(t)]$$

$$+ n(t) \qquad (H.8)$$

The received signal as represented by (H.8) is functionally depicted in Figure H.1. For the case of testing the signal processor alone, we let ω_0, and hence ω_d, equal zero, and the signal $x(t)$ becomes a baseband signal.

Simulation Procedures

(1) The random channel impulse response, $r(n)$ and $\hat{r}(n)$, are first generated and stored in memory. The amplitudes $\{\beta_i\}$ are obtained from a Gaussian sequence generator and the phase $\{\psi_i\}$ are obtained from a random number generator which has been normalized to 2π.

(2)   The impulse response of the deterministic branch is set
to some initial values which are then allowed to vary slowly by modifying
the magnitudes and phase in accordance with perturbations obtained from
the Gaussian sequence generator and the normalized (to 2π) random
number generator, respectively.

(3)   The additive noise is obtained from the Gaussian sequence
generator.

(4)   The Gaussian sequence generator and the random number
generator are library routines provided by the McMaster Computer Centre.
These are called RANGAU and FRANDN, respectively.

The entire communication system is simulated in subroutine form, with
a main routine controlling the central command, as shown in Figure H.2.
Gross flow-charts for the signal simulator, the adaptive equalizer and
the error rate computer are given in Figures H.3, H.4 and H.5, respectively.
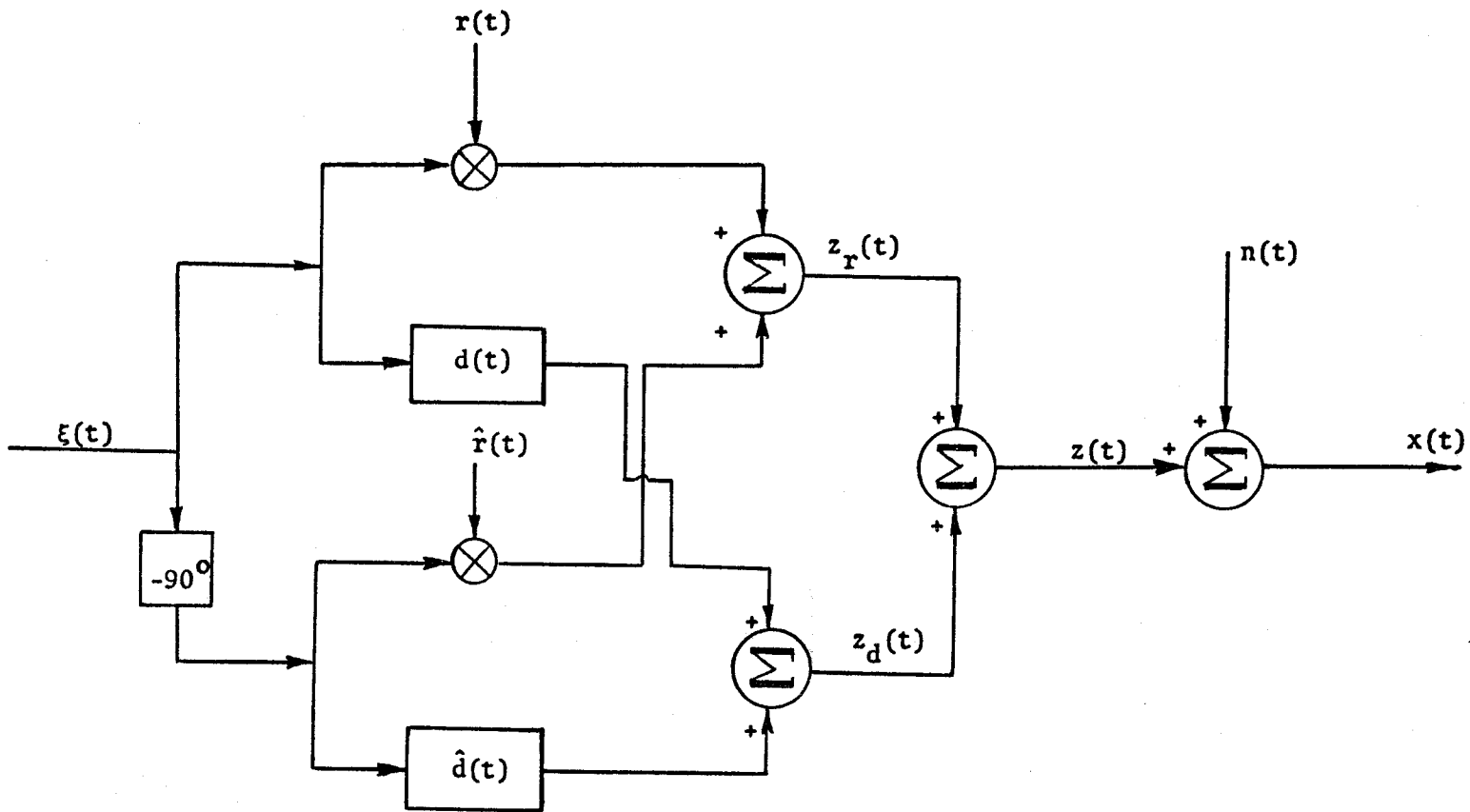
Figure H.1   Channel Model for Simulation
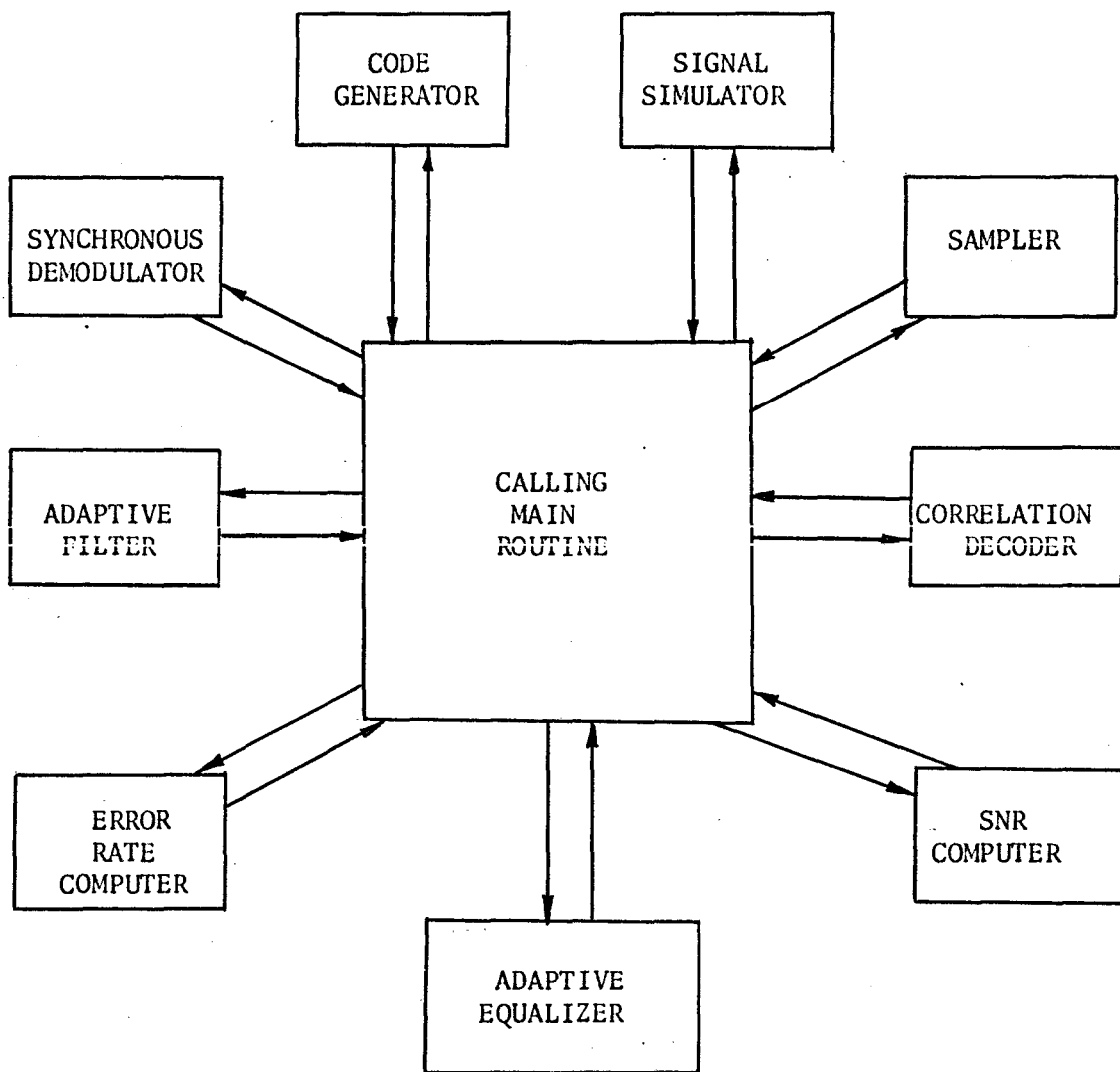
Figure H.2   Hierarchy of Subroutines for System Simulations

```
┌─────────────────────────────────────┐
│  SET INITIAL TAP VALUES OF CHANNEL   │
│  IMPULSE RESPONSE, CHANNEL MEMORY,   │
│  ADDITIVE NOISE VARIANCE, MULTIPLI-  │
│       CATIVE NOISE VARIANCE          │
└─────────────────────────────────────┘
                  │
                  ▼
          ┌──────────────┐
          │   GENERATE   │
          │ 127-DIGIT BINARY │
          │  M-SEQUENCE  │
          └──────────────┘
                  │
                  ▼
            ┌────────────┐
            │ SET BUFFER │
            └────────────┘
```

RANDOM ⟵ WHICH CHANNEL ?

DETERMINISTIC

CREATE RANDOM CHANNEL

CHANNEL AGING REQ'D ? YES ⟶ AGE TAP VALUES OF CHANNEL IMPULSE RESPONSE

NO

MULTIPLY TRANSMITTED SEQUENCE WITH CHANNEL IMPULSE RESPONSE

CONVOLVE TRANSMITTED SEQUENCE WITH CHANNEL IMPULSE RESPONSE

ADD DETERMINISTIC AND RANDOM COMPONENTS

ADD ADDITIVE NOISE

RETURN COMMAND TO CALLING ROUTINE ⟵ YES ⟵ IS BUFFER FULL ? ⟶ NO

Figure H.3   Gross Flow Chart for Signal Simulator

Figure H.4   Gross Flow Chart for Adaptive Equalizer

Figure H.4 Cont'd.

Figure H.5   Gross Flow Chart for Error Rate Computer

BIBLIOGRAPHY

Aaron, M.R. and D.W. Tufts (Jan. 1966). Intersymbol Interference and
    Error Probability. IEEE Trans. on Information Theory, vol. IT-12,
    No. 1, pp. 26-34.

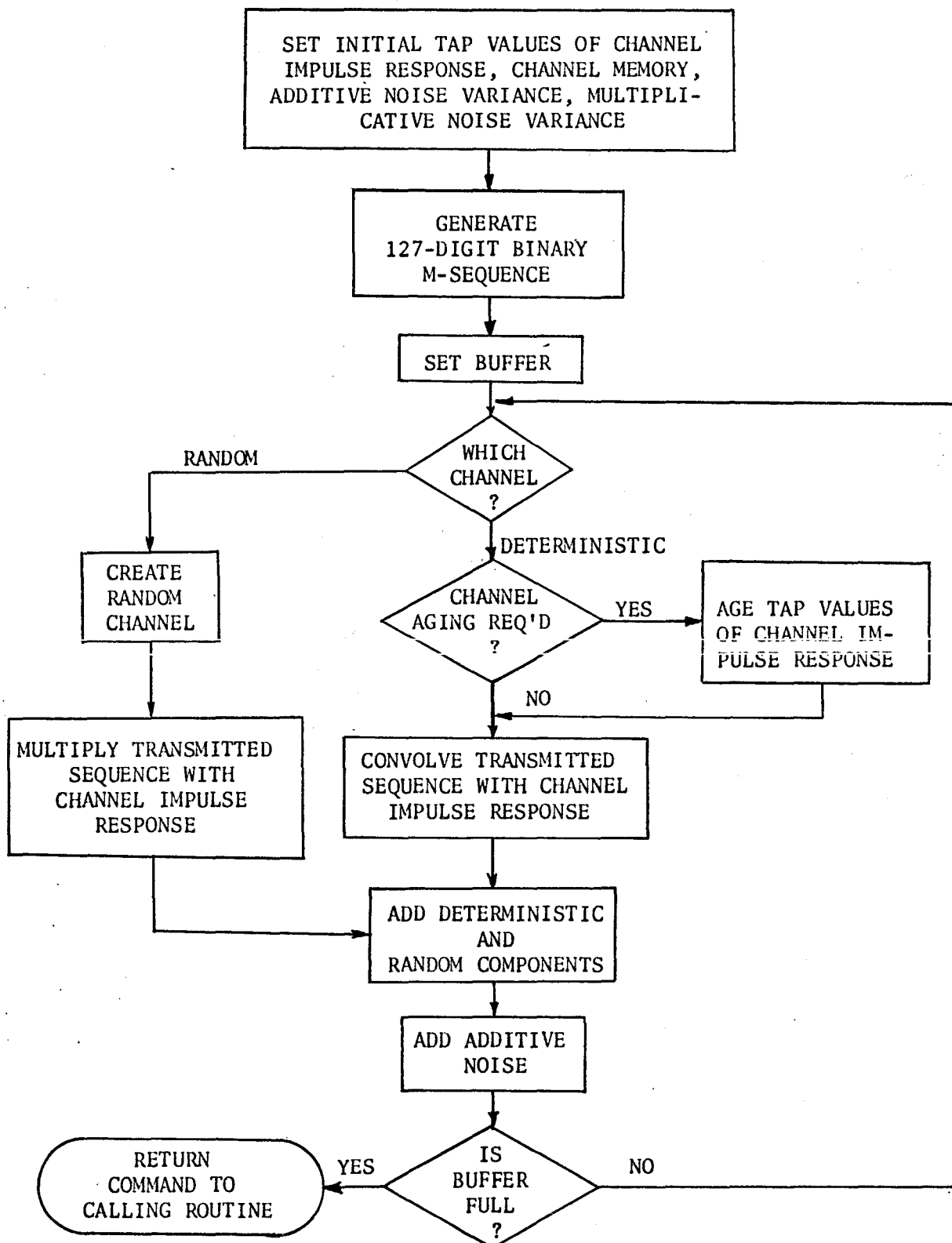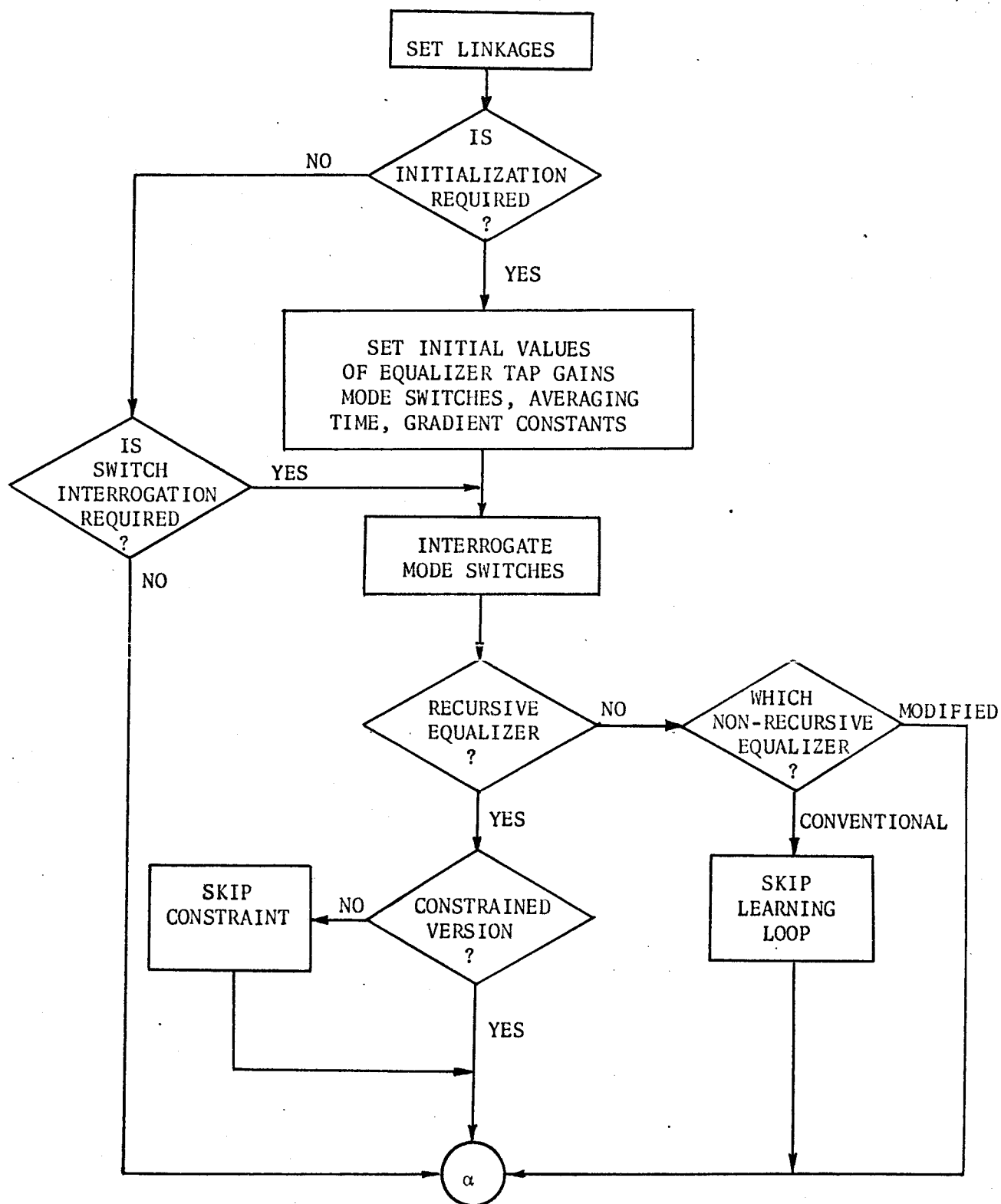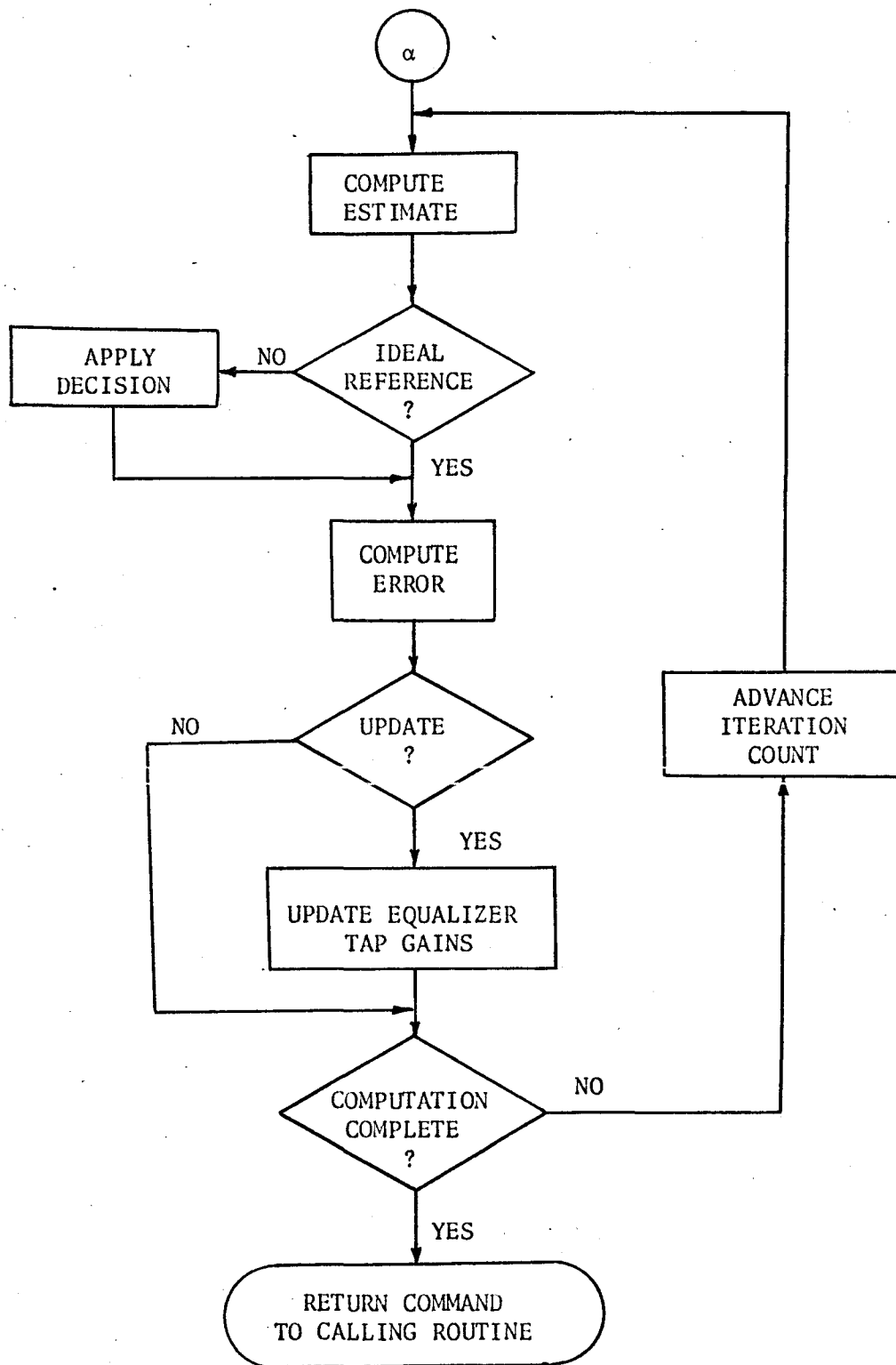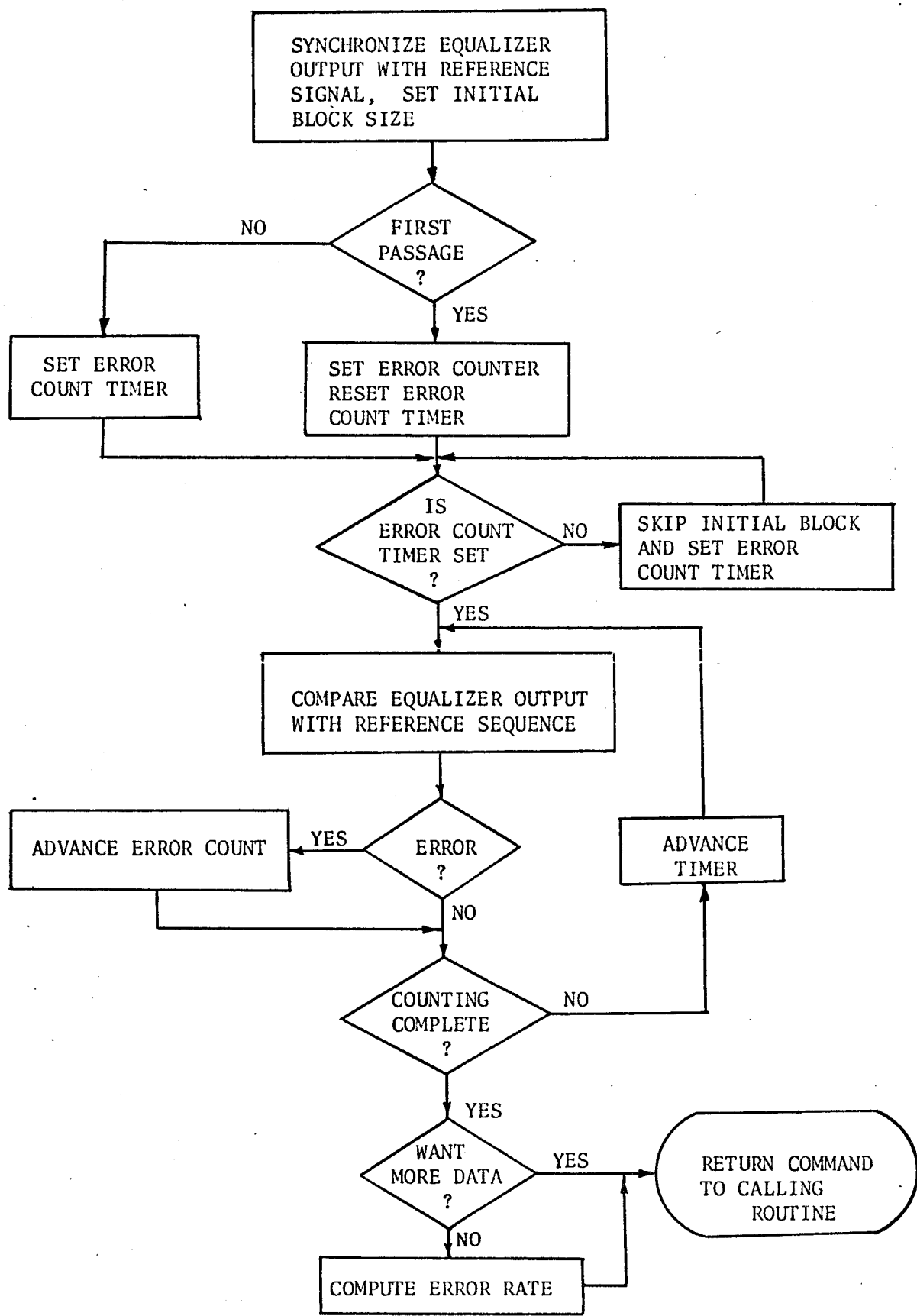Aein, J.M. and J.C. Hancock (July, 1963). Reducing the Effects of Inter-
    symbol Interference with Correlation Receivers. IEEE Trans. on
    Information Theory, vol. IT-9, No. 3, pp. 167-175.

Athans, M. and P.L. Falb (1966). Optimal Control. McGraw-Hill, New
    York.

Austin, M.E. (August, 1967). Decision Feedback Equalization for Digital
    Communication Over Dispersive Channels. M.I.T. Lincoln Lab.,
    Lexington, Mass., Tech. Rept. 437.

Baghadady, E. (Editor)(1961). Lectures on Communication System Theory.
    McGraw-Hill, New York.

Balakrishnan, A.V. (Editor)(1968). Communication Theory. McGraw-Hill,
    New York.

Bellman, R. (Editor)(1963). Mathematical Optimization Techniques.
    Berkeley, Calif., University of California Press.

Bello, P.A. (June, 1962). The Influence of Fading Spectrum on the Binary
    Error Probabilities of Incoherent and Differentially Coherent
    Matched Filter Receivers, IRE Trans. Comm. Systems, pp. 160-168.

        (December, 1963). Characterization of Randomly Time-variant
    Linear Channels. IEEE Trans. on Comm. Systems. CS-11, No. 4,
    pp. 360-390.

        (Jan. 1964). Time-Frequency Duality. IEEE Trans. Information
    Theory. pp. 18-33.

        (June, 1965). On the Instantanious Real-time Measurement of
    Multi-path & Doppler Spread. IEEE Comm. Cov. Conf. Rec., pp. 725-
    729.

        (Apr. 1969). A Troposcatter Channel Model. IEEE Trans. Comm.
    Tech. Vol. Com-17, No. 12, pp. 130-137.

Bello, P.A. and B.D. Nelin (June, 1962). The Influence of Fading Spectrum on the Binary Error Probabilities of Incoherent and Differentially Coherent Matched Filter Receivers. IRE Trans. on Comm. Systems.

———————— (June, 1963). The Effect on Frequency Delective Fading on the Binary Error Probabilities of Incoherent and Differentially Coherent Matched Filter Receivers. IRE Trans. on Comm. Systems.

Chang, S.S.L. and B. Harris (May 1962). An Optimum Self-Synchronized Communication System. Proc. AIEE, pp. 110-116.

Coll, D.C. (December, 1966). A System for the Optimum Utilization of Pulse Communication Channels. Defence Research Telecommunications Establishment, Ottawa, Canada. DRTE Rept. No. 1168.

Coll, D.C. and D.A. George (June, 1965). A Receiver for Time Dispersed Pulses. IEEE Comm. Conv. Conf. Rec., pp. 753-758.

Costas, J.P. (December, 1956). Synchronous Communication. Proc. IRE. Vol. 44, pp. 1713-1718.

Davenport, W.B. Jr. (June, 1953). Signal-to-Noise Ratios in Bandpass Limiters. Journal of Applied Physics. Vol. 24, No. 6, pp. 720-727.

Davenport, W.B. Jr. and W.L. Root (1958). An Introduction to the Theory of Random Signals and Noise. McGraw-Hill, New York.

Davisson, L.D. (Apr. 1966). A Theory of Adaptive Filtering. IEEE Trans. Information Theory. Vol. IT-12, pp. 97-102.

Di Toro, M.J. (June, 1965). A New Method of High-Speed Adaptive Serial Communication Through any Time-Variable and Dispersive Transmission Medium. IEEE Comm. Conv. Conf. Rec., pp. 763-768.

———————— (October, 1968). Communication in Time-Frequency Spread Media Using Adaptive Equalization. Proc. IEEE vol. 56, No. 10, pp. 1653-1679.

Di Toro, M.J., J. Hannlec and B. Goldberg (June, 1965). Design and Performance of a New Adaptive Serial Data Modem on a Simulated Time-Variable Multipath HF link. IEEE Ann. Comm. Conv. Conf. Rec., pp. 769-773.

Freeman, H. (1965). Discrete-Time Systems. Wiley & Sons, New York.

Gabor, D. (1946). Theory of Communication. J. IEE,Vol. 93(III), pp. 429-457.

Gallager, R.G. (1968). Information Theory and Reliable Communication. Wiley & Sons, New York.

George, D.A. (Jan., 1965). Matched Filters for Interfering Symbols. IEEE Trans. on Information Theory, Vol. IT-11, No. 1 (corresp) pp. 153-154.

George, D.A. and D.C. Coll (June, 1965). The Reception of Time Dispersed Pulses. IEEE Comm. Conv. Conf. Rec., pp. 749-752.

George, D.A. et al (Sept. 1969). Channel Equalization for Data Transmission. Presented at IEC Conference, Vancouver, B.C., Canada.

Gersho, A. (Jan., 1969). Adaptive Equalization of Highly Dispersive Channels for Data Transmission. BSTJ., 48, No. 1, pp. 55-69.

(1969). Linear Adaptation. Presented at Polytechnique Institute of Brooklyn Symposium on Computer Processing in Communication.

Glaser, E.M. (Apr., 1961). Signal Detection by Adaptive Filters. IRE Trans. Vol. IT-7, pp. 87-98.

Golomb, S.W. et al (1964). Digital Communications with Space Applications. Prentice-Hall, Englewood Cliffs, N.J.

Gonslaves, R.A. and D.W. Tufts (June, 1968). Data Transmission Through a Random Noisy Channel by PAM. IEEE Trans. Comm. Tech. Vol. Com-16, No. 3, pp. 375-379.

Gorog, E. (June, 1965). A New Approach to Time Domain Equalization with Simplified Procedures. IEEE Comm. Conv. Conf. Rec., pp. 207-212.

Harman, W.W. (1963). Principles of the Statistical Theory of Communications. McGraw-Hill, New York.

Helstrom, C.W. (1968). Statistical Theory of Signal Detection. 2nd Edition, McGraw-Hill, New York.

Hirsch, D. and W.J. Wolf (Feb., 1970). A Simple Adaptive Equalizer for Efficient Data Transmission. IEEE Trans. on Comm. Tech., Vol. Com-18, No. 1, pp. 5-11.

Kailath, T. (Sept., 1962). Measurements on Time-Variant Communication Channels. IEEE Trans. Information Theory, pp. 229-236.

        (Oct. 1963). Time-variant Communication Channels. IEEE Trans. Information Theory, pp. 233-237.

Kalman, R.E. (March, 1960). A New Approach to Linear Filtering and Prediction Problems. Trans. ASME J. Basic Engrg. Ser. D., Vol. 82, pp. 35-45.

Kalman, R.E. and R.S. Bucy (March, 1961). New Results in Linear Filtering and Prediction Theory. Trans. ASME J. Basic Engrg. Ser. D., Vol. 83, pp. 95-108.

Kaye, A.R. (April, 1968). Reception of Digital Signals over Randomly Time Variant Dispersive Channels. Ph.D. Thesis, Carleton University.

Kennedy, R.S. (1969). Fading Dispersive Communication Channels. Wiley & Sons.

Kimball, C.V. (1968). Intersymbol Interference in Binary Communication Systems. Ph.D. Thesis, University of Michigan.

Lindsey, W.C. (Oct. 1965). Error Probability for Incoherent Diversity Reception. IEEE Trans. Information Theory, pp. 491-499.

Lucky, R.W. (April, 1965). Automatic Equalization for Digital Communications. BSTJ., 44, No. 4, pp. 547-588.

        (February, 1966). Techniques for Adaptive Equalization of Digital Communication Systems. BSTJ., 45, No. 2., pp. 255-286.

        (April, 1968). Adaptive Redundancy Removal in Data Transmission. BSTJ., 47, No. 4, pp. 549-573.

Lucky, R.W. and H.R. Rudin (Nov., 1967). An Automatic Equalizer for General-Purpose Communication Channels. BSTJ., 46, No. 9, pp. 2179-2208.

Lucky, R.W., J. Salz and E.J. Weldon (1968). Principles of Data Communication. McGraw-Hill, New York.

Lytle, D.W. (Oct., 1968). Convergence Criteria for Transversal Equalizers. BSTJ., Vol. 47, pp. 1775-1801.

Magill, D.T. (Dec., 1963). Optimal Adaptive Estimation of Sampled Stochastic Processes. Stanford Electronics Lab. TR No. 6302-2, Stanford University.

Marcum, J.I., (Apr., 1960). A Statistical Theory of Target Detection by Pulsed Radar. IRE Trans. Information Theory, Vol. IT-6, pp. 59-267. (Also Rand Corp. Memos RM-753, July 1948 and RM-754, Dec. 1947).

Mark, J.W. (March, 1968). Optimal Detection and Estimation for Echo Ranging in a Randomly Fading Environment. M.Eng. Thesis, Dept. of Electrical Engineering, McMaster University, Hamilton, Canada.

     (Nov. 1968). Optimal Detection for Echo Ranging in a Randomly Fading Environment. Presented at the IEEE Can. Sym. on Comm. Montreal, Canada. (Also Canadian Westinghouse Tech. Rept. R. 413-476, Canadian Westinghouse Co. Ltd., Hamilton, Canada).

     (Nov. 1970). An Adaptive Receiver for Digital Signaling over Unknown Channels. To be presented at the IEEE Canadian Symposium on Communications, Montreal, Canada.

Mark, J.W. and G.J.G. Hicks (Oct., 1966). On the Detection of a Coded Signal in a Gaussian Environment. Presented at IEEE 4th Can. Symposium on Comm., Montreal, Canada. (Also Canadian Westinghouse Technical Report.)

Mark, J.W. and S.S. Haykim (1970). A General Formulation of the Adaptive Equalizer for Digital Communication Through Dispersive Channels. Submitted for publication.

Middleton, D. (1960). Introduction to Statistical Communication Theory. McGraw-Hill, New York.

North, D.O. (June, 1943). An Analysis of the Factors which Determine Signal/Noise Discrimination in Pulsed-Carrier Systems. RCA Lab. Report PTR-6C. (Also Proc. IEEE, July 1963, pp. 1915-1027).

Nuttall, A.H., (July, 1962). Error Probabilities for Equicorrelated M-ary Signals Under Phase-Coherent and Phase-Incoherent Reception. IRE Trans. Information Theory, Vol. IT-8, pp. 305-314.

Nyquist, H. (1928). Certain Topics in Telegraph Transmission Theory. Trans. AIEE, Vol. 47, pp. 617-644.

Papoulis, A. (1965). Probability, Random Variables, and Stochastic Processes. McGraw-Hill, New York.

     (1962). The Fourier Integral and Its Applications. McGraw-Hill, New York.

Peterson, W.W. (1961). Error Correcting Codes. MIT Press. Wiley, New York.

Pierre, D.A. (1969). Optimization Theory with Applications. Wiley & Sons, New York.

Price, R. (Sept., 1954). The Detection of Signals Perturbed by Scatter and Noise. IRE Trans. Information Theory, pp. 163-170.

        (Dec. 1956). Optimum Detection of Random Signals in Noise, with Application to Scatter-Multipath Communication, I. IRE Trans. Information Theory, pp. 125-135.

Price, R. and E.M. Hofstetter (April, 1965). Bounds on the Volume and Height Distributions of the Ambiguity Function. IEEE Trans. on Information Theory, Vol. IT-11, No. 2, pp. 207-214.

Pierce, J.N. (May, 1958). Theoretical Diversity Improvement in Frequency-shift Keying. Proc. IRE, pp. 903-910.

Proakis, J.G. and J.H. Miller (July, 1969). An Adaptive Receiver for Digital Signaling Through Channels with Intersymbol Interference. IEEE Trans. on Information Theory, Vol. IT-15, No. 4, pp. 484-497.

Reiger, S. (May, 1958). Error Rates in Data Transmission. Proc. IRE, Vol. 46, p. 919.

Richters, J.S. (Nov., 1967). Communication Over Fading Dispersive Channels. MIT Research Laboratory of Electronics, Cambridge, Massachusetts. Tech. Rept. 464.

Sakrison, D.J. et al (Dec. 1969). An Adaptive Receiver Implementation for the Gaussian Scatter Channel. IEEE Trans. on Com. Tech. Vol. Com-17, No. 6, pp. 640-647.

Saltzberg, B.R. (July, 1968). Intersymbol Interference Error Bounds with Application to Ideal Bandlimited Signaling. IEEE Trans. on Information Theory, Vol. IT-14, pp. 563-568.

Schwartz, M. (July, 1966). Abstract Vector Spaces Applied to Problems in Detection and Estimation Theory. IEEE Trans. in Information Theory, Vol. IT-12, pp. 327-336.

Schwartz, M., W.R. Bennett and S. Stein (1966). Communication Systems and Techniques. McGraw-Hill, New York.

Shannon, C.E. (1948). A Mathematical Theory of Communication. Bell System Tech. J., Vol. 27, pp. 379-623.

Smith, J.W. (Dec. 1965). The Joint Optimization of Transmitted Signal and Receiving Filter for Data Transmission Systems. BSTJ, Vol. 44, pp. 2363-2392.

        (June, 1969). A Simple Approximation of Data System Error Rate. IEEE Trans. on Com. Tech., Vol. Com-17, No. 3, pp. 415-417.

Stein, S. (Jan. 1964). Unified Analysis of Certain Coherent and Non-coherent Binary Communications Systems. IEEE Trans. Information Theory, Vol. IT-10, pp. 43-51.

Tufts, D.W. (July, 1961). Matched Filters and Intersymbol Interference. Cruft Lab., Harvard University, Cambridge, Mass., Tech. Rept. 345.

        (March, 1965). Nyquist's Problem - The Joint Optimization of Transmitter and Receiver in Pulse Amplitude Modulation. Proc. IEEE, Vol. 53, pp. 248-259.

Turin, G.L. (1956). Communication Through Noisy Random-Multipath Channels. IRE Conv. Rec., Pt. 4, pp. 154-166.

        (Sept., 1958). Error Probabilities for Binary Symmetric Ideal Reception Through Nonselective Slow Fading and Noise. Proc. IRE, pp. 1603-1619.

        (June, 1960). An Introduction to Matched Filters. IRE Trans. on Information Theory, Vol. IT-6, No. 3, pp. 311-329.

        (July, 1961). On Optimal Diversity Reception. IRE Trans. Information Theory, pp. 154-166.

        (March, 1962). On Optimal Diversity Reception, II. IRE Trans. Communication Systems, pp. 22-31.

Van Trees, H.L. (Jan., 1966). Analog Communication Over Randomly-Time-Varying Channels. IEEE Trans. on Information Theory, Vol. IT-12, pp. 51-63.

        (1968). Detection, Estimation and Modulation Theory, Part I. Wiley & Sons, New York.

Viterbi, A. (1966). Principal of Coherent Communication. McGraw-Hill, New York.

Vulikh, B.Z. (1963). Introduction to Functional Analysis for Scientists and Technologists. Pergamon Press. (1968, Addison-Wesley)

Weaver, C.S. (Sept., 1962). Adaptive Communication Filtering. IEEE Trans. Information Theory, Vol. IT-8, pp. S169-S178.

Widrow, B. (Dec., 1966). Adaptive Filters I: Fundamentals. Stanford Systems Theory Lab., Stanford University, Stanford, Calif., Tech. Rept. 6764-6.

Wiener, N. (Feb., 1942). The Extrapolation, Interpolation and Smoothing of Stationary Time Series. Report of the Services 19, Research Project DIC-6037, M.I.T. (Also 1949, New York: Wiley)

Wilks, S.S. (1962). Mathematical Statistics. New York: Wiley & Sons.

Woodward, P.M. (1953). Probability and Information Theory, with Applications to Radar. McGraw-Hill, New York.

Wozencraft, J.M. and I.M. Jacobs (1965). Principles of Communication Engineering. Wiley & Sons, New York.

Zadeh, L.A. and J.R. Ragazzini (July, 1950). An Extension of Wiener's Theory of Prediction. Jour. Appl. Phys., Vol. 21, pp. 645-655.

Detection of Signals in Noise. Proc. IRE, Vol. 40, pp. 1223-1231.